

TECHNISCHE UNIVERSITÄT MÜNCHEN

Lehrstuhl für Experimentelle Genetik

Epigenetic and transcriptional regulation of early mouse development

Silvia Engert

Vollständiger Abdruck der von der Fakultät Wissenschaftszentrum Weihenstephan für Ernährung, Landnutzung und Umwelt der Technischen Universität München zur Erlangung des akademischen Grades eines

Doktors der Naturwissenschaften

genehmigten Dissertation.

Vorsitzender: Univ.-Prof. Dr. D. Langosch
Prüfer der Dissertation: 1. Univ.-Prof. Dr. M. Hrabě de Angelis
2. Univ.-Prof. Dr. H. Lickert
3. Priv.-Doz. Dr. T. Floss

Die Dissertation wurde am 05.12.2013 bei der Technischen Universität München eingereicht und durch die Fakultät Wissenschaftszentrum Weihenstephan für Ernährung, Landnutzung und Umwelt am 28.07.2014 angenommen.

Parts of this dissertation were recently published in the peer-reviewed journals *Development* and *Genesis*. Incorporation of these publications is in agreement with the journals and the supervisors of the dissertation.

Engert S, Burtscher I, Liao WP, Dulev S, Schotta G, Lickert H

Wnt/ β -catenin signalling regulates Sox17 expression and is essential for organizer and endoderm formation in the mouse. *Development*. 2013 Aug;140(15):3128-38

Engert S, Burtscher I, Kalali B, Gerhard M, Lickert H

The Sox17CreERT2 knock-in mouse line displays spatiotemporal activation of Cre recombinase in distinct Sox17 lineage progenitors. *Genesis*. 2013 Aug 26

Content

1	Summary	1
2	Zusammenfassung	3
3	Introduction	5
3.1	Preamble	5
3.2	Early mouse development	5
3.3	Formation of the mouse body axis	6
3.4	Formation of the endoderm	9
3.5	<i>In vitro</i> model of germ layer formation	10
3.6	The Wnt pathway	11
3.7	Epigenetic regulation of gene expression.....	12
3.8	DNA methylation: maintenance and <i>de novo</i> methylation	13
3.9	DNA demethylation during embryonic development	15
3.10	Mechanisms of active DNA demethylation	16
3.11	Structure of the Elongator complex.....	18
3.12	Diverse functions of the Elongator complex	19
3.13	Transcriptional regulation of gene expression	20
3.14	The Sry-related HMG-box gene Sox17	21
3.15	Aims of the study	22
4	Results	23
4.1	The function of the Elongator complex during gastrulation.....	23
4.1.1	Deletion of Elongator protein 4 leads to early embryonic lethality.....	23
4.1.2	Embryos mutant for <i>Elp4</i> are patterned but show developmental delay	26
4.1.3	Transcriptome analysis of <i>Elp4</i> mutant embryos displays genome-wide effects...	30
4.1.4	Stem cell identity of <i>Elp4</i> mutant ESCs is affected	31

4.1.5	Impaired differentiation capacity of <i>Elp4</i> mutant ESCs	34
4.2	Wnt/ β -catenin signaling regulates Sox17 expression and is essential for organizer and endoderm formation in the mouse	37
4.2.1	Conditional knock-out of β -catenin in the Sox17 ⁺ endoderm and vascular endothelial lineage	37
4.2.2	Lack of β -catenin affects endoderm and organizer formation.....	40
4.2.3	Lack of β -catenin affects VE patterning and DE formation.....	43
4.2.4	Tetraploid rescue reveals cell-autonomous and non-autonomous function of β -catenin in organizer and DE formation.....	45
4.2.5	Wnt/ β -catenin activates Sox17 via Tcf4-binding sites in the promoter and regulatory region	50
4.2.6	PVE induces gastrula organizer genes in the epiblast in a Wnt/ β -catenin-dependent manner	52
4.3	Generation and application of the hormone-inducible <i>Sox17^{CreERT2}</i> knock-in mouse line.....	57
4.3.1	The advantage of inducible Cre-driver lines.....	57
4.3.2	Generation of the <i>Sox17^{CreERT2}</i> knock-in mouse line.....	59
4.3.3	Characterization of recombination properties of the <i>Sox17^{CreERT2}</i> mouse line	61
4.3.4	Activation of Cre in specific Sox17 ⁺ progenitor populations labels their progeny.	64
4.3.5	<i>Sox17^{CreERT2}</i> enables lineage tracing of visceral endoderm cells during formation of the primitive gut tube.....	68
4.3.6	Sox17 ⁺ ventral pancreas progenitors contribute to the exocrine cell-lineage of the ventral pancreas	70
4.3.7	Is Sox17 a marker for angioblast progenitors?.....	71
5	Discussion	73
5.1	Summary of results.....	73
5.2	The <i>Sox17^{CreERT2}</i> knock-in mouse line displays spatio-temporal activation of Cre recombinase in distinct Sox17 lineage progenitors.....	75
5.2.1	Effects of allelic combinations for <i>Sox17^{CreERT2}</i> and Cre reporters	75
5.2.2	The inducible <i>Sox17^{CreERT2}</i> mouse line allows lineage-restricted cell fate analysis and genetic modifications.....	77

5.2.3	Using <i>Sox17^{CreERT2}</i> to investigate VE cell fate.....	78
5.2.4	Using <i>Sox17^{CreERT2}</i> to investigate the pancreatic composition.....	79
5.2.5	Using <i>Sox17^{CreERT2}</i> to investigate hemangioblast specification	81
5.3	Wnt/ β -catenin signalling regulates <i>Sox17</i> expression and is essential for organizer and endoderm formation in the mouse	83
5.3.1	Conditional knock-out of β -catenin in the <i>Sox17</i> lineage.....	83
5.3.2	Wnt/ β -catenin signalling is essential for head and tail organizer formation.....	84
5.3.3	Wnt/ β -catenin signalling via <i>Sox17</i> is required for DE formation.....	86
5.3.4	Wnt/ β -catenin is required for epithelia formation of endoderm-derived organs .	86
5.4	The Elongator complex is required for proper differentiation of the early mouse embryo	87
5.4.1	The function of the Elongator complex during early mouse embryogenesis	87
5.4.2	Loss of <i>Elp4</i> leads to embryonic delay and reduced body size.....	89
5.4.3	<i>Elp4</i> -deficient ESCs reveal abnormalities during maintenance and differentiation...	92
6	Material and methods.....	95
6.1	Material.....	95
6.1.1	Equipment.....	95
6.1.2	Consumables.....	98
6.1.3	Kits	99
6.1.4	Chemicals.....	100
6.1.5	Buffer and solutions.....	104
6.1.6	Enzymes.....	109
6.1.7	Antibodies and Sera	110
6.1.8	Vectors and BACs	111
6.1.9	Oligonucleotides.....	112
6.1.10	Molecular weight markers	114
6.1.11	Bacteria and culture media.....	114

6.1.12	Cell lines.....	114
6.1.13	Culture media	115
6.1.14	Solutions for cell culture	115
6.1.15	Mouse lines.....	116
6.2	Methoden.....	116
6.2.1	Cell culture.....	116
6.2.2	Generation of the Sox17 ^{CreERT2} targeting vector	122
6.2.3	Identification of TBE binding elements	122
6.2.4	Chromatin immunoprecipitation (ChIP) assays.....	123
6.2.5	Endoderm differentiation.....	124
6.2.6	Generation of expression vectors.....	125
6.2.7	Generation of fluorescent β -catenin CKO and control ESCs cell lines.....	125
6.2.8	Molecular biology.....	126
6.2.9	Methods in protein biochemistry.....	138
6.2.10	Embryology	143
6.2.11	Histology.....	150
7	References	153
8	List of abbreviations	170
9	Appendix	175
9.1	Curriculum Vitae.....	175
9.2	List of publications and conference contributions	176
9.2.1	Publications.....	176
9.2.2	Conference contributions	176
9.3	Danksagung.....	177

List of figures

Figure 1: Formation of the body axis	8
Figure 2: Formation of the principle germ layers	10
Figure 3: The canonical Wnt pathway	12
Figure 4: Suggested mechanisms of active demethylation.....	17
Figure 5: Schematic overview of the affected regions in the deletions H9 and Tcm2	24
Figure 6: Embryonic lethality of homozygous and compound heterozygous mice	24
Figure 7: mRNA expression of genes located in the deleted region	25
Figure 8: H9/Tcm2 mutant embryos are delayed in development and reduced in size	27
Figure 9: No patterning defects on mRNA level.....	28
Figure 10: Delayed development is reflected by marker expression.....	29
Figure 11: Cluster analysis of mutant and control embryos	30
Figure 12: Transcriptome analysis of deregulated genes at gastrulation.....	31
Figure 13: Ratio of expected and observed genotypes of ESCs.....	32
Figure 14: Pluripotency markers are expressed in mutant ESCs	33
Figure 15: mRNA profiling of mutant (KO) cells versus wild-type (WT) cells	34
Figure 16: Impaired differentiation ability of <i>Elp4</i> deficient ESCs	36
Figure 17: Expression pattern of <i>Sox17</i> in the extra-embryonic and embryonic lineages	38
Figure 18: Conditional knock-out of β -catenin in the <i>Sox17</i> endoderm lineage	39
Figure 19: Cell-autonomous and non- cell autonomous phenotypes in β -catenin CKO embryos.	40
Figure 20: β -catenin is required cell-autonomously for AVE and DE formation.....	41
Figure 21: Proliferation and apoptosis rate are not changed in CKO mutant embryos.....	42
Figure 22: Lack of β -catenin in the endoderm affects AVE formation	44
Figure 23: Lack of β -catenin in the endoderm affects DE formation.....	45
Figure 24: Wild-type VE rescues head and neural tube truncation in aggregation chimera.....	47
Figure 25: RFP ⁺ β -cat CKO cells rarely contribute to DE formation	48

Figure 26: RFP ⁺ β -cat CKO cells rarely contribute to mid- and hindgut formation.....	49
Figure 27: Sox17 is expressed in vascular endothelial cells in β -cat CKO embryos.....	50
Figure 28: β -catenin deletion affects Sox17 maintenance in the endoderm	51
Figure 29: Sox17 is a downstream target gene of Wnt/ β -catenin signalling in the endoderm ...	52
Figure 30: Loss of PVE identity.....	53
Figure 31: PVE induces organizer gene expression in the posterior epiblast	54
Figure 32: Control and β -catenin CKO ESCs contribute to the formation of embryonic organs ...	55
Figure 33: CKO ESCs failed to contribute to the epithelial lining of endodermal organs	57
Figure 34: Operating mode of CreER	58
Figure 35: Generation of the <i>Sox17^{CreERT2}</i> allele	60
Figure 36: Leak tightness and application methods	61
Figure 37: β -galactosidase activity in endoderm and vascular endothelial lineages.....	63
Figure 38: R26R recombination in the DE lineage labels all endoderm-derived organs.....	65
Figure 39: Vascular endothelial cells and ventral pancreas progenitors are lineage-labelled by β -galactosidase using the <i>R26</i> reporter.....	66
Figure 40: The <i>mT/mG</i> reporter labels endothelial, ventral pancreatic and hematopoietic stem cell lineages	68
Figure 41: Contribution of VE cells to DE	69
Figure 42: Recombination in the ventral pancreas lineage labels exocrine acinar cells	71
Figure 43: LacZ expression in the epiblast and germ layers.....	72
Figure 44: Southern Blot setup.....	136

List of tables

Table 1: List of primary antibodies	110
Table 2: List of secondary antibodies	111
Table 3: Oligonucleotides for genotyping.....	113
Table 4: TCF/LEF binding elements.....	123
Table 5: Oligonucleotides for CHIP analysis.....	124

1 Summary

The development of a multicellular organism requires tightly controlled activation and repression of genes, while pluripotent stem cells acquire a lineage-specific fate. Therefore, different mechanisms have evolved especially on the level of DNA and chromatin modification. To investigate whether active DNA demethylation mediated by the recently identified Elongator complex is essential for early embryonic development, the Elongator subunit Elp4 was deleted. This resulted in stunted development and embryonic lethality. Formation of the three principal germ layers indicates that differentiation is initiated but imperfect and thus leads to growth retardation. *In vitro* analysis revealed impaired differentiation and reduced proliferative capacity of mutant embryonic stem cells. Therefore, decreased progenitor recruitment or expansion could result in stunted embryonic development. Transcriptome analysis suggests that the Elongator complex is involved in genome-wide chromatin organisation likely by regulation of DNA methylation of developmental regulators, such as differentiation-associated and imprinted genes. In a second part, the role of canonical Wnt signalling in embryonic patterning and endoderm formation was analysed. Conditional gene deletion of β -catenin in the Sox17⁺ visceral and definitive endoderm resulted in anterior head and posterior neural tube truncations. In the anterior and posterior visceral endoderm, β -catenin is required non-cell autonomously for head and tail organizer formation, respectively. In the definitive endoderm, β -catenin is required cell-autonomously for mid- and hindgut development. Deletion of β -catenin in the endoderm causes loss of *Sox17* expression suggesting its regulation by canonical Wnt signalling. This is supported by accumulation of Tcf4/ β -catenin transactivation complexes on binding elements in the *Sox17* regulatory region upon endoderm differentiation. Taken together, these results indicate that Wnt/ β -catenin activates *Sox17* expression for visceral endoderm patterning and definitive endoderm formation. In a third part, we generated a hormone-inducible Sox17Cre mouse line. Analysis of recombination characteristics of *Sox17^{CreERT2}* demonstrated that Cre-mediated recombination can be selectively induced in extra-embryonic and embryonic endoderm, vascular endothelial cells, hemogenic endothelium and in the ventral pancreas. Thus, this new *Sox17^{CreERT2}* mouse line can be used for tissue-specific genetic lineage tracing as well as for lineage-restricted genetic manipulations to investigate the impact of signalling cascades or factors during later stages of endoderm development.

2 Zusammenfassung

Für die Entwicklung spezialisierter Zelltypen eines vielzelligen Organismus muss die Aktivität von Genen während der Differenzierung streng kontrolliert werden. Hierfür sind vor allem Mechanismen auf Ebene der DNA- und Chromatinumgestaltung entscheidend. Deshalb wurde in dieser Arbeit die Rolle der aktiven DNA-Demethylierung bei der frühen Embryonalentwicklung durch den kürzlich beschriebenen Elongator-Komplex untersucht. Funktionelle Inaktivierung von Elp4 führte zu verzögerter Entwicklung und embryonaler Letalität. Die Keimblätter werden während der Gastrulation ausgebildet, aber die folgende Differenzierung ist verzögert und unvollständig. Die Untersuchung von mutanten embryonalen Stammzellen zeigte, dass Pluripotenz und Differenzierung *in vitro* beeinträchtigt sind. Genomweite mRNA Expressionsanalysen weisen darauf hin, dass der Elongator-Komplex eine generelle Rolle bei der Umorganisation des Chromatins während der Differenzierung spielt. Dies geschieht sehr wahrscheinlich durch die Regulation der DNA-Methylierung und impliziert zum ersten Mal, dass aktive Demethylierung von Genen für die Gastrulation und später für die Differenzierung entscheidend ist.

In einem zweiten Teil dieser Arbeit wurde die Rolle des Wnt-Signalweges auf die Musterbildung und Endodermentwicklung untersucht. Eine konditionelle Inaktivierung von β -Catenin im Sox17-positiven viszeralem und definitivem Endoderm führte zu Verkürzung von anterioren Kopf- und posterioren Neuralrohrstrukturen. Im anterioren und posterioren viszeralem Endoderm ist β -Catenin zur Bildung des anterioren und posterioren Organisators, welche die Ausbildung der Körperachsen regulieren, erforderlich. Im definitivem Endoderm wird β -Catenin für die Entwicklung des Mittel- und Hinterdarms benötigt. Die Anhäufung von Tcf4/ β -Catenin Transaktivierungskomplexen in der regulatorischen Region von Sox17 im Zuge der Endodermdifferenzierung weist darauf hin, dass Sox17 über den Wnt-Signalweg aktiviert wird. Zusammenfassend zeigen diese Ergebnisse, dass der Wnt-Signalweg über die Aktivierung von Sox17 die Musterbildung des Embryos und die Entwicklung des definitiven Endoderms bedingt.

Im dritten Teil dieser Arbeit wurde eine über Hormone induzierbare Sox17Cre-Mauslinie generiert. Diese eignet sich zur Verfolgung Sox17-positiver Vorläuferzellen und deren Nachkommenschaft während der Organentwicklung. Darüber hinaus kann durch gezielte Mutagenese der Einfluss von Signalwegen und Faktoren auf die Differenzierung dieser Zellen in z.B. Lunge, Leber und Pankreas untersucht werden.

3 Introduction

3.1 Preamble

Life begins when sperm fertilises the oocyte and the male and female pronuclei fuse to form an entity. During development, the totipotent zygote gives rise to various cell types and tissues to form a complex and highly structured organism. This is achieved by neighbouring tissue interaction and integration of environmental signals. The cell-to-cell interactions and signals are mediated by regulatory signalling pathways, which in turn lead to the activation of specific genes in order to determine the nature of a cell type or tissue. Misregulation of signalling and gene expression can cause developmental defects, diseases or even embryonic lethality. Understanding how an organism develops, which signals and factors are involved and how they are regulated, does not only reveal fundamental processes of life but also provides chances to prevent, treat or cure a multitude of human disease.

3.2 Early mouse development

Life starts with the union of the sperm and the oocyte. After fertilization, the zygote undergoes a series of cleavage processes, remodelling of cell adhesion proteins and initiation of embryonic gene expression. First lineage segregation events take place, which specify the pluripotent inner cell mass (ICM) and the surrounding trophectoderm (TE). While the TE supports the development of the ICM and contributes to a large extent to the placenta, the ICM undergoes a second lineage segregation event to form the primitive endoderm (PrE) and the epiblast by the end of the implantation period. In the ICM, the transcription factors Sox2, Nanog and Oct4 form the core pluripotency network and are required for proper formation of the epiblast (Avilion et al., 2003; Chambers et al., 2003; Mitsui et al., 2003; Nichols et al., 1998). Segregation of PrE and epiblast cells is initiated by waves of asymmetric cell divisions within the ICM, which already prime the

cells to distinct lineages reflected by mutually exclusive distribution of PrE and epiblast markers (Chazaud and Rossant, 2006; Kurimoto et al., 2006; Morris et al., 2010; Niakan et al., 2010; Plusa et al., 2008). In the second wave of cell internalisation, up-regulation of the transcription factors *Gata6* and *Sox17* determine the PrE fate of ICM cells, which segregate and form the PrE cell layer, confining the ICM versus the blastocoel cavity (Morris et al., 2010; Niakan et al., 2010). The PrE gives rise to the parietal endoderm and the visceral endoderm (VE) while the remaining cells of the ICM form the embryo proper.

3.3 Formation of the mouse body axis

After segregation of the extra-embryonic and embryonic lineages, the ICM extends into the blastocoel cavity and thereby forms the cup-shaped epiblast. The epiblast joins the extra-embryonic ectoderm (ExE), which gives rise to the embryonic component of the placenta. The ExE and the epiblast are surrounded by the VE, which forms the endodermal component of the yolk sac. Interaction of the ExE, VE and epiblast initiates the formation of the proximal-distal (PD) and anterior-posterior (AP) body axis.

At E5.5, BMP signalling from the ExE induces Nodal signalling in the adjacent epiblast in a proximal to distal direction. Nodal-dependent target gene activation leads to the expression of Wnt and Nodal antagonists, including Dickkopf homologue 1 (*Dkk1*), Cerberus-like protein 1 (*Cer1*) and left-right determination factor 1 (*Lefty1*) in the distal visceral endoderm (DVE) (Brennan et al., 2001). The DVE restricts Nodal and Wnt signalling as well as target gene activation to proximal regions of the epiblast thereby generating a PD axis and defining the anterior character of the distal epiblast (Arnold and Robertson, 2009).

Migration of DVE cells to the prospective anterior side of the embryo converts the PD axis into an AP axis between E5.5 and E6.5 (Fig. 1a, b) (Takaoka et al., 2011; Yamamoto et al., 2004). The anterior visceral endoderm (AVE) shares characteristic markers with the DVE and was long thought to directly derive from it. However, a recent study suggested that a

global movement of VE cells initiates the migration of newly formed AVE cells (Takaoka et al., 2011). Although the origin of the AVE is still under investigation, VE which is located in the anterior side of the embryo and expresses AVE markers can be designated as AVE. Marker genes for the AVE include *Dkk1* (Mukhopadhyay et al., 2001), *Hex* (Martinez Barbera et al., 2000), *Hesx1* (Hermesz et al., 1996; Thomas and Beddington, 1996), *Lim1* (Barnes et al., 1994; Shawlot and Behringer, 1995) and *Otx2* (Ang et al., 1994; Simeone et al., 1992; Simeone et al., 1993). Mutations within these genes result in head truncations, reflecting their anterior neuroectoderm induction properties.

Besides its head organizer function, the AVE expresses antagonists of the Nodal/TGF β - and Wnt/ β -catenin signalling pathways restricting their action to the posterior side of the embryo. There, *Wnt3* is expressed in the posterior visceral endoderm (PVE) at E5.5 (Rivera-Perez and Magnuson, 2005). Subsequently, Nodal-dependent BMP4 activity induces *Wnt3* expression in the neighbouring proximal and posterior epiblast at E5.5 to E6.5 (Ben-Haim et al., 2006). The restricted signalling function of Nodal/TGF β and Wnt/ β -catenin to the posterior side of the embryo allows the formation of the primitive streak (PS) and the gastrula organizer (Fig. 1c). In amphibians, accumulation of β -catenin on the dorsal side of the embryo results in the formation of the Nieuwkoop centre. This signalling centre induces the overlying Spemann-Mangold organizer, which organises the neural tube and AP body axis. The notion that the PVE covers the PS region and expresses *Wnt3* suggests that the PVE in mice could have similar induction properties as the Nieuwkoop centre in amphibians (Rivera-Perez and Magnuson, 2005; Tam and Beddington, 1992). However, the role of PVE in organizer gene induction remains to be investigated (Beddington and Robertson, 1999; Liu et al., 1999a; Rivera-Perez and Magnuson, 2005; Tam and Behringer, 1997).

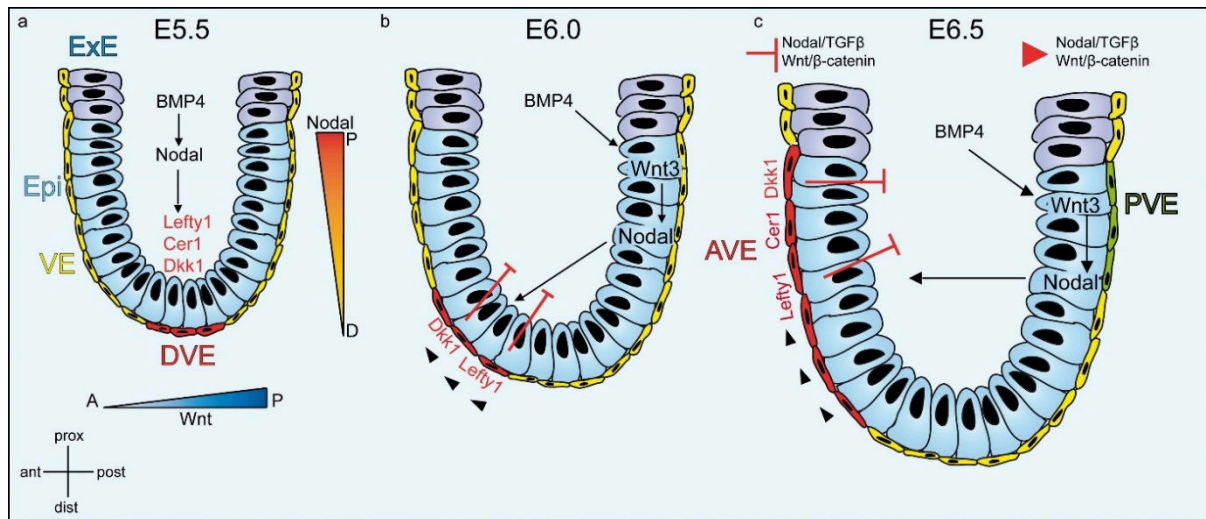


Figure 1: Formation of the body axis

(a) At E5.5 the distal visceral endoderm cells (DVE, red) get specified. (b) Movement (arrowheads) of DVE cells to the prospective anterior side converts the proximal-distal axis into the anterior-posterior axis at E5.5-E6.5. (c) Visceral endoderm cell located at the anterior side form the anterior visceral endoderm (AVE) whereas visceral endoderm cells at the posterior side form the posterior visceral endoderm (PVE, green). At E6.5, expression of Nodal/TGF β and Wnt/ β -catenin inhibitors in the AVE restricts signalling activity to the posterior side of the embryo. Major signalling events and gradients are depicted. Epiblast (Epi) cells are represented in blue, extra-embryonic ectoderm (ExE) in purple visceral endoderm (VE) cells in yellow.

The gastrula organizer consists of a dynamic population of cells that form an early- (EGO), mid- (MGO) and late-gastrula organizer (LGO), which possesses head-, trunk-, and tail-organising activity, respectively (Kinder et al., 2001). Precise mapping of posterior epiblast progenitor cells revealed that these different organizer regions constitute different cell fates. At E6.5, *Gooseoid (Gsc)*- and *Foxa2*-positive cells of the EGO give rise to the anterior definitive endoderm (ADE), prechordal mesoderm and axial mesoderm (Burtscher and Lickert, 2009; Kinder et al., 2001). The ADE and prechordal mesoderm together with the AVE form the head organizer (Arkell and Tam, 2012). The MGO and LGO are defined by expression of *Gsc*, *Foxa2*, *Chordin (Chrd)* and *Noggin (Nog)* (Beddington and Robertson, 1998; Kinder et al., 2001; Takaoka et al., 2011; Thomas and Beddington, 1996) in the posterior epiblast at mid-streak (E7.0) to early-bud stage (E7.75). Precursor cells of both the MGO and LGO give rise to the anterior endoderm, prechordal mesoderm, notochord and node.

3.4 Formation of the endoderm

Formation of the gastrula organizer proceeds alongside with the formation of the three principle germ layers. Interestingly, epiblast cells which give rise to mesoderm and endoderm are already patterned prior to gastrulation. Posterior epiblast cells synthesise the T-box transcription factor brachyury (T) and the forkhead transcription factor *Foxa2* in two intermingled but mutually exclusive cell populations (Burtscher and Lickert, 2009). During PS formation, these two cell populations separate into a T⁺ proximal and a *Foxa2*⁺ distal posterior epiblast domain. While retracting from the primitive streak, both cell populations undergo drastic changes forming the mesoderm and the endoderm. These changes include loss of columnar shape and acquirement of a bottle-shaped morphology, loss of apical-basal polarity, downregulation of junctional and basement membrane proteins and are summarized in a process called epithelial-to-mesenchymal transition (EMT) (Nowotschin and Hadjantonakis, 2010). Three different cell populations can be distinguished in the PS region, the T⁺ posterior mesoderm, the *Foxa2*⁺/T⁺ axial mesoderm and *Foxa2*⁺ VE and DE populations (Burtscher and Lickert, 2009) (Fig. 2).

Shortly before integration of the endoderm progenitors into the surrounding VE, the cells start to express *Sox17* (Burtscher et al., 2012). The now called DE disperses the surrounding VE (Kwon et al., 2008). At E7.5, gastrulation is accomplished. During the next two days the external endoderm will form the primitive gut tube, which gets internalised by turning of the whole embryo. During further development, the foregut gives rise to oesophagus, trachea, lungs, thyroid, stomach, liver, pancreas, and hepatobiliary system. The midgut forms the jejunum, ileum, and the small intestine, whereas the hindgut becomes the large intestine, cloaca, and portions of the urogenital tract (Zorn and Wells, 2009).

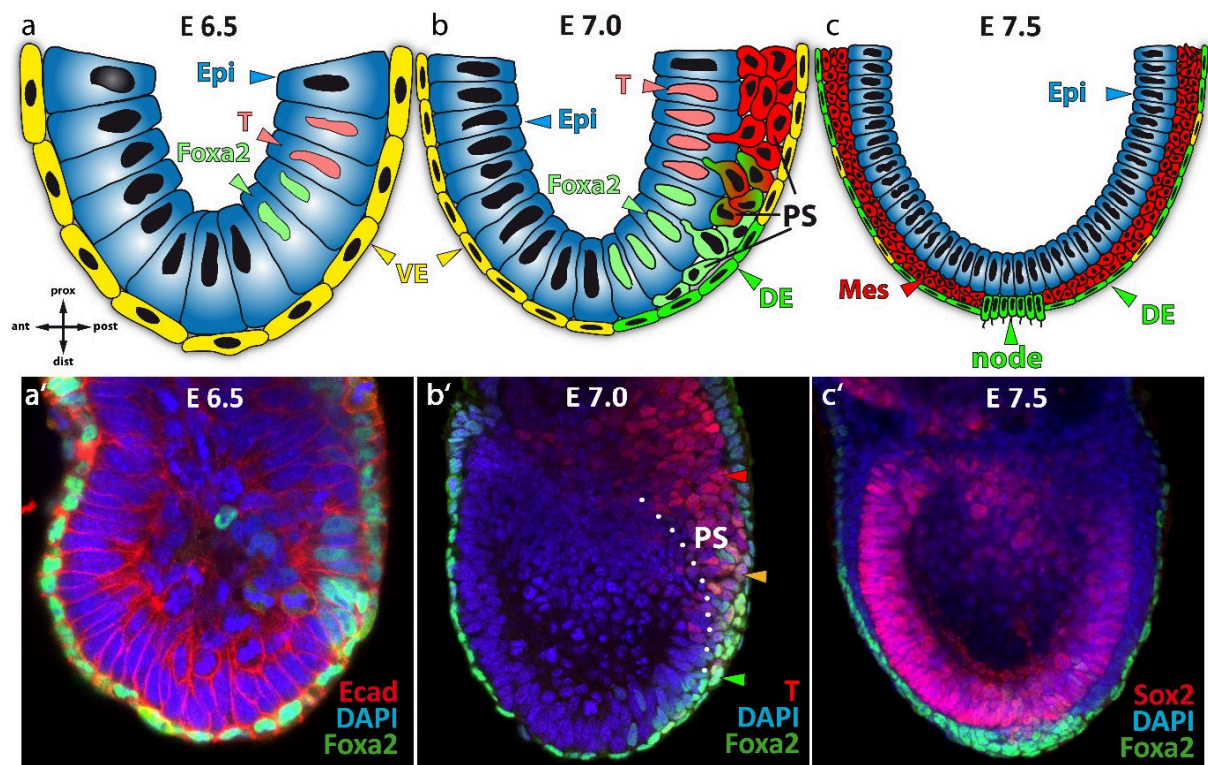


Figure 2: Formation of the principle germ layers

(a) At E6.5, T and Foxa2 are synthesised in a mutually exclusive manner in the epiblast (Epi). (b) During gastrulation, T⁺ and Foxa2⁺ cells undergo epithelial-to-mesenchymal transition and ingress into the primitive streak (PS). (c) After gastrulation is completed, mesoderm (Mes), definitive endoderm (DE) and the node have formed (published in Biospectrum 2011, modified).

3.5 *In vitro* model of germ layer formation

The differentiation of pluripotent epiblast cells into lineage-restricted cell types can be modelled *in vitro*. Embryonic stem cells (ESCs), obtained from cells of the ICM, show expression of pluripotency markers such as *Oct4*, *Nanog*, *Sox2* and *Klf4* and possess self-renewal capacity (Avilion et al., 2003; Boyer et al., 2006; Chambers et al., 2003; Mitsui et al., 2003; Nichols et al., 1998; Niwa, 2007). ESCs can differentiate into ectoderm, mesoderm or endoderm depending on the culture conditions (Gadue et al., 2006; Johansson and Wiles, 1995; Lindsley et al., 2006; Tada et al., 2005). To initiate endoderm differentiation, the addition of Activin and Wnt proteins, which signal via the Nodal (Activin)/TGF β and Wnt/ β -catenin pathway, is required (Gadue 2006). During endoderm

differentiation, the ESCs down-regulate the pluripotency factors and at the same time up-regulate *Foxa2* and *T* (Gadue et al., 2006). From this bipotent mesendoderm state, the cells differentiate into *Foxa2*⁺/*Sox17*⁺ endoderm cells (Ang et al., 1993; D'Amour et al., 2005; Kanai-Azuma et al., 2002; Monaghan et al., 1993; Sasaki and Hogan, 1993). The addition of Activin and Wnt proteins to initiate endoderm formation *in vitro* shows the importance of Nodal (Activin)/TGF β and Wnt/ β -catenin signalling for endoderm development.

3.6 The Wnt pathway

The canonical Wnt pathway is activated upon binding of Wnt ligands to their seven transmembrane receptors of the Frizzled family. LRP5/6, which are members of the low-density lipoprotein receptor-related protein family, act as co-receptors for Wnt ligands (Pinson et al., 2000; Tamai et al., 2000; Wodarz and Nusse, 1998). Wnt antagonists like Cer bind directly to Wnt ligands to inhibit receptor binding while Dkk prevents signalling by blocking the access to the LRP co-receptors (Mao et al., 2001; Piccolo et al., 1999). In the absence of a Wnt ligand, β -catenin levels in the cytoplasm are low due to the action of a degradation complex containing the tumour suppressors axin and adenomatous polyposis coli (APC), and the enzymes protein phosphatase 2A (PP2A) and glycogen synthase kinase 3 β (GSK3 β). Phosphorylation of β -catenin by Gsk3 β triggers its ubiquitinylation and therefore its degradation. Upon binding of Wnt ligands, dishevelled blocks β -catenin degradation. Stabilised β -catenin translocates to the nucleus and interacts with Lymphoid enhancer factor (LEF) and T-cell factor (TCF) transcription factor family providing a transactivation domain for activation of target gene transcription (Fig. 3). In mouse, several β -catenin/TCF target genes were found to regulate mesendoderm induction and specification (Arnold et al., 2000; Lickert et al., 2000; Sawada et al., 2005; Yamaguchi et al., 1999). Genetic deletion of β -catenin in epiblast progenitors results in the formation of ectopic cardiac mesoderm at the expense of DE (Lickert et al., 2002). This observation indicates that Wnt/ β -catenin signalling is

essential for the specification of mesoderm and endoderm from epiblast progenitor cells that are still plastic. The complete knock-out of components of the canonical Wnt pathway such as Wnt3 and β -catenin results in early embryonic lethality prior to primitive streak formation (Huelsenken et al., 2000; Liu et al., 1999b). Therefore, the function of Wnt/ β -catenin signalling in the embryonic patterning and endoderm formation is not known.

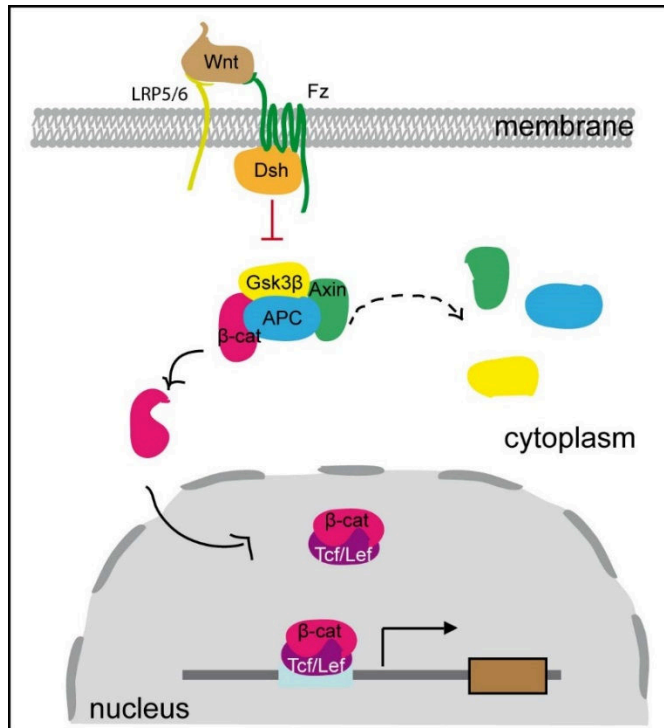


Figure 3: The canonical Wnt pathway

Upon binding of the Wnt ligand to Fizzled (Fz) and the co-receptor LRP5/6, β -catenin is freed from the degradation complex and translocates into the nucleus. In the nucleus, β -catenin interacts with Tcf/Lef to activate gene transcription.

3.7 Epigenetic regulation of gene expression

The development from a single cell to a multicellular complex organism requires a tightly controlled regulation of gene expression. Controlled expression of pluripotency- and differentiation-associated genes allows the formation of distinct cell types within an organism that can differ in their morphology, function and self-renewal capacity. During development most of the cells lose their self-renewal capacity and differentiate to fully specified cell types. However, stem cell identity needs to be retained in a subset of cells within an adult organism to maintain homeostasis and the possibility to replace

differentiated cells. To ensure gene activity in a temporal-spatial manner, several mechanisms have evolved.

Gene expression can be regulated by the accessibility to the genetic information (Phillips and Shaw, 2008). This accessibility is controlled by the arrangement of DNA in solid chromatin and this chromatin state can be maintained during cell divisions. The heritable changes in gene expression that occur without alteration in the DNA sequence are described by the term epigenetics (Goldberg et al., 2007). One way to non-genetically alter DNA accessibility and thus gene expression is based on histone variants and histone modifications such as acetylation, phosphorylation and methylation. Different combinations of these modifications generate a histone code, which promotes either repression or activation of gene transcription. The other major epigenetic modification to control gene expression is methylation of DNA, where a methyl group is added to the 5th position of cytosines. Such DNA methylation enables the transmission of a transcriptional status from one cell to its daughter cells over several generations without losing cell identity.

3.8 DNA methylation: maintenance and *de novo* methylation

DNA methylation enables stable repression of target promoters, silencing of endogenous retrotransposon activity that helps maintaining genomic integrity, X-chromosome inactivation and genomic imprinting (Bird, 2002; Jaenisch and Bird, 2003). In mammals, the methylation is restricted to cytosine residues of CpG dinucleotides. High concentrations of methylated CpG dinucleotides are found in repetitive sequences. However, CpG rich clusters at the 5' end of many genes are generally not methylated with the exception of differentially methylated regions associated with imprinted genes and genes on the inactive X-chromosome (Bird, 2002).

DNA methylation is mediated by DNA methyltransferases, which catalyse the transfer of a methyl group from S-adenosyl-L-methionine to cytosine (Goll and Bestor, 2005).

Inheritance of methylation patterns is accomplished by the maintenance activity of DNA methyltransferase 1 (Dnmt1) (Meissner et al., 2008). Dnmt1 has a preference for hemimethylated DNA and re-establishes the methylation pattern of the newly synthesised DNA strand on basis of the methylated parental strand after DNA replication (Pradhan et al., 1999). Knock-out of Dnmt1 in mice leads to embryonic lethality past mid gestation (Li et al., 1992). Homozygous Dnmt1 $-/-$ embryos are stunt, delayed in their development and exhibit a drastic reduction of genomic 5-methylcytosine (5mC) content. However, Dnmt1 $-/-$ ESCs are viable and contain reduced but stable levels of 5mC and methyltransferase activity (Lei et al., 1996; Li et al., 1992). In addition, *de novo* methylation activity is not affected in the homozygous mutant ESCs (Lei et al., 1996). This observation suggested the existence of other methyltransferases and led to the discovery of the Dnmt3 family (Okano et al., 1998).

The Dnmt3 family members Dnmt3a and Dnmt3b are co-expressed in the embryonic ectoderm in early embryos but show differential expression at later stages of development. Mice deficient for Dnmt3a develop normally until birth, but die at about 4 weeks of age. Embryos deficient for Dnmt3b exhibit growth impairment and neural tube defects and die during development. In contrast, a double knock-out of Dnmt3a and Dnmt3b leads to embryonic lethality before E11.5. Double mutant embryos are smaller in size, lack somites and fail to turn, suggesting an arrest in development shortly after gastrulation (Okano et al., 1999). The double knock-out of Dnmt3a and Dnmt3b inhibits *de novo* methylation of viral DNA in ESCs as well as genome-wide *de novo* methylation during embryonic development. However, the maintenance of existing methylation patterns is not affected suggesting that Dnmt3a and Dnmt3b are essential for *de novo* methylation rather than maintaining methylation patterns (Okano et al., 1999). The lethal phenotype of Dnmt knock-out mice demonstrates the importance of DNA methylation for proper embryonic development and differentiation of distinct cell types.

3.9 DNA demethylation during embryonic development

Removal of methylation marks is just as important as retaining and establishing of methylation patterns. Thus, there are two waves of DNA demethylation during embryonic development, one at the zygote stage and another in the primordial germ cells (PGCs). Prior to PGC migration to the gonads, PGCs exhibit a methylation pattern comparable to somatic cells, demonstrating that methylation imprints are inherited and maintained (Hajkova et al., 2002). At E10.5 to E12.5, when PGC enter the gonads, a rapid demethylation process takes place (Hajkova et al., 2002; Lee et al., 2002). Erasure of acquired methylation marks at CpG clusters of imprinted genes in the germ line is required to reset the imprints and remove acquired epigenetic modifications in order to allow gender-specific re-methylation and return of PGCs to a pluripotent stage (Reik, 2007). This wave of reprogramming also affects non-imprinted genes and repetitive elements. While demethylation of repetitive elements seems to be incomplete, demethylation of imprinted and non-imprinted genes is completed within one day. The rapid loss of methylation marks suggests the involvement of an active demethylation process in epigenetic reprogramming (Hajkova et al., 2002).

A second wave of genome-wide DNA demethylation occurs after fertilization and during pre-implantation development. Here, removal of the 5mC is thought to occur passively in a replication-dependent manner (Rougier et al., 1998). It was suggested that Dnmt1 and the related oocyte-derived Dnmto are preferentially localized in the cytoplasm during the first cleavage stages (Carlson et al., 1992). Thus, demethylation could occur during DNA replication in the absence of maintenance DNA methyltransferases. This passive mechanism was observed in the maternal pronucleus where methylation patterns are lost during the second and third cleavage stage in a replication-dependent manner (Mayer et al., 2000). In contrast, the rapid demethylation of the paternal pronucleus occurs after exchanging protamines (proteins associated with sperm DNA) with histones but before DNA replication, which suggests an active mechanism in the paternal pronucleus (Reik, 2007). Although the activity of DNA methyltransferases is absolutely required for early

embryonic development, it is currently not known if active demethylation plays also a role in these processes.

3.10 Mechanisms of active DNA demethylation

Despite intense research, the mechanism of active demethylation is still not known. Direct removal of the methyl group is energetically unfavoured as the covalent bond between the methyl group and carbon 5 of cytosine is very strong. Therefore an enzymatic reaction is required to erase the methylation mark.

Various mechanisms were suggested for the removal of 5mC (Chen and Riggs, 2011). In *Arabidopsis thaliana*, a subfamily of glycosylases initiate DNA repair mechanisms to remove and replace methylated cytosine (Gehring et al., 2006; Gong et al., 2002). Since mammalian glycosylases exhibit only weak 5mC activity, such a mechanism is unlikely. However, the basic principle of DNA repair mechanisms to replace 5mC is an attractive possibility for DNA demethylation. Deamination of 5mC to thymine coupled to T/G mismatch repair would provide such a possibility. Indeed, the activin-induced deaminase (AID) and the apolipoprotein B RNA-editing catalytic component-1 (ApoBec-1) are able to deaminate 5mC, potentially leading to T/G mismatch (Morgan et al., 2004). The observation that both proteins have 5mC deaminase activity and are expressed in pluripotent tissues led to the hypothesis that demethylation could occur by deamination of 5mC, followed by BER which could be initiated by T/G mismatch glycosylases (Morgan et al., 2004). Additional evidence is provided by the observation that methylation levels in AID $-/-$ PGCs are reduced throughout the genome (Popp et al., 2010). Since the difference in methylation levels is low and no effect on viability and fertility is observed, it is likely that other mechanisms are also involved in the removal of the 5mC group (Popp et al., 2010).

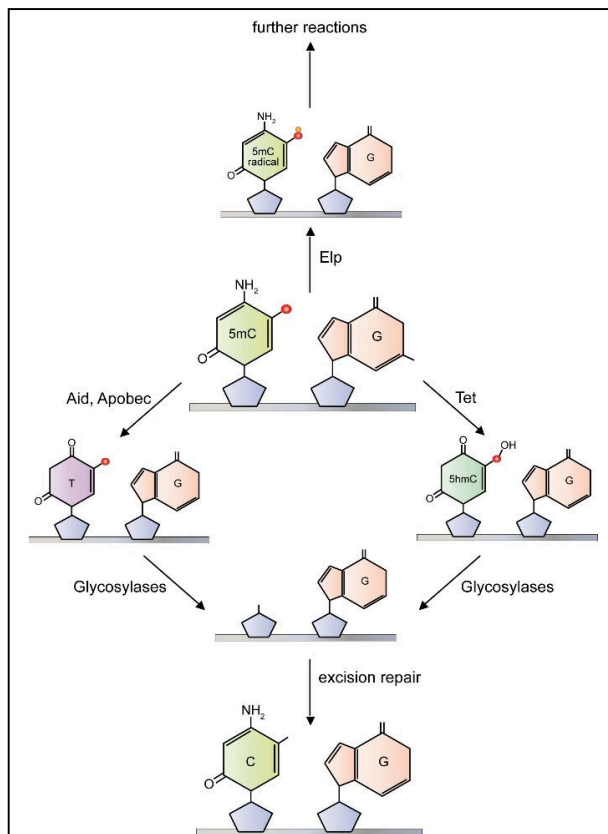


Figure 4: Suggested mechanisms of active demethylation

Demethylation by deamination and excision repair, Tet-mediated oxidation and excision repair or by generating a 5mC radical for subsequent reactions. (5mC = 5-methylcytosine, 5hmC = 5-hydroxymethylcytosine, C = cytosine, T = thymine, G = guanine)

A new hypothesis how 5mC could be modified and replaced by cytosine emerged with the discovery of a new DNA nucleotide, 5-hydroxymethylcytosine (5hmC) (Kriaucionis and Heintz, 2009). The conversion of 5mC to 5hmC by hydroxylation of 5mC was shown to be mediated by TET proteins (Tahiliani et al., 2009). Three members of this so-called ten eleven translocation (TET) family have been identified to date. In addition to hydroxylation of 5mC to 5hmC, Tet proteins can generate 5-formylcytosine (5fC) and 5-carboxycytosine (5caC) from 5mC (Ito et al., 2011).

The observation that Tet1 is present in the one-cell to blastocyst stage as well as in PGCs at E11.5 supports the hypothesis of Tet-mediated active demethylation (Hajkova et al., 2010; Ito et al., 2010). Furthermore, components of the BER machinery were found to be expressed

together with Tet1 in PGCs and in the paternal pronucleus (Hajkova et al., 2010). These results suggest that Tet-mediated oxidation of 5mC to 5hmC, 5fC or 5caC is followed by BER to replace 5mC with cytosine (Fig. 4).

Recently, Okada et al. established a method to screen for factors that might be involved in paternal DNA demethylation in the zygote (Okada et al., 2010). A live cell imaging reporter system coupled with siRNA knock-down of potential factors allowed screening of candidate genes that were selected based on their expression in zygotes, their domain/structure motif and their potential in catalysing DNA demethylation. Using this system,

Elongator protein 3 (Elp3) was shown to have an impact on paternal DNA demethylation. Since knock-down of Elp3, as well as knock-down of Elp1 and Elp4, prevents removal of 5mC in the paternal pronucleus, it was suggested that the whole Elongator complex is required for the demethylation process (Okada et al., 2010).

3.11 Structure of the Elongator complex

The Elongator complex was first identified in yeast as a major component of the elongating RNA polymerase II holoenzyme (Otero et al., 1999). The multimeric Elongator complex presumably consists of six subunits, Elp1-6. Elp1, Elp2 and Elp3 build the core Elongator complex while Elp4, Elp5 and Elp6 form the small Elongator subcomplex (Hawkes et al., 2002; Krogan and Greenblatt, 2001; Li et al., 2001; Winkler et al., 2001). The Elongator proteins are conserved from yeast to humans (Close et al., 2012; Hawkes et al., 2002; Kim et al., 2002). Holo Elongator consists of at least two copies of each subunit (Glatt et al., 2012).

Elp1/IKAP, which is encoded by the *Ikbkap* gene, is the largest protein and is thought to act as a scaffold for all Elongator subunits (Glatt and Muller, 2013; Stirnimann et al., 2010). Although the nuclear localisation of the Elongator subunits is controversial, it was shown that Elp1 contains a nuclear localization signal in its C-terminus (Fichtner et al., 2003; Glatt and Muller, 2013). Elp2, which also contains scaffolding domains is thought to support the function of Elp1 as a scaffold (Fellows et al., 2000). Elp3 represent the catalytic subunit of the complex. The protein contains a radical S-adenosylmethionine (SAM) binding domain and an iron-sulphur cluster (Paraskevopoulou et al., 2006) as well as a histonacetyltransferase (HAT) domain (Wittschieben et al., 1999). The second subcomplex is formed by Elp4, Elp5 and Elp6. The quite recent identification of human Elp5 and Elp6 confirmed that also the small Elongator unit is conserved from yeast to human (Close et al., 2012). Nevertheless, the function of the second subcomplex remains unclear. Resolution of the crystal structure of yeast Elp456 revealed that this complex

forms a hexameric Rec-like ATPase and binds to the anticodon loop of tRNA in an ATP dependent manner (Glatt et al., 2012).

Deletion of any of the six subunits causes identical phenotypes suggesting that the whole Elongator complex is required to fulfill its function. Furthermore, loss of Elongator function leads to similar phenotypes in *Saccharomyces cerevisiae*, *Caenorhabditis elegans*, *Drosophila melanogaster* or *Arabidopsis thaliana* suggesting that not only the structure of Elongator but also its function is conserved among different species (Chen et al., 2009b; Dietrich et al., 2011; Frohloff et al., 2001; Huang et al., 2005; Mehlgarten et al., 2010; Singh et al., 2010; Walker et al., 2011).

3.12 Diverse functions of the Elongator complex

Since RNA immunoprecipitation showed that Elongator is associated with nascent RNA emanating from the elongating form of RNA polymerase II it was proposed that Elongator is involved in transcription elongation (Gilbert et al., 2004). However, loss-of-function experiments rather suggested a function for Elongator in histone acetylation to facilitate transcript elongation (Close et al., 2006).

There is emerging evidence that the main function of Elongator is not transcriptional but translational regulation via modification of tRNAs. It was shown that Elongator is involved in the modification of uridine nucleosides present at the wobble position of several eukaryotic tRNAs (Huang et al., 2005). Overexpression of two RNAs that are modified by Elongator could rescue several phenotypes of yeast mutants deficient for Elongator (Esberg et al., 2006). Moreover, Elongator deletion affects a set of proteins whose translation depend on Elongator modified tRNAs (Bauer and Hermand, 2012; Bauer et al., 2012). Although the function of Elongator in tRNA modification can explain most of the observed phenotypes, additional roles in α -tubulin acetylation, exocytosis, cytoplasmic kinase signalling, meiotic progression as well as paternal DNA demethylation were

suggested (Creppe et al., 2009; Holmberg et al., 2002; Lin et al., 2013; Okada et al., 2010; Rahl et al., 2005).

A potential role for Elongator in active demethylation was based on the observation that knockdown of either Elp3, Elp1 or Elp4 impaired demethylation of the paternal pronucleus in the zygote. Furthermore, it was shown the radical SAM and not the HAT domain is crucial for the demethylation function. Members of the radical SAM superfamily contain an iron-sulphur (Fe-S) cluster and use S-adenosylmethionine (SAM) to catalyse radical reactions (Wang and Frey, 2007). Okada et al. (Okada et al., 2010) suggested a potential demethylation mechanism that involves the generation of an oxidizing agent, 5'-deoxyadenosyl radical, from SAM. The radical could extract a hydrogen atom from the methyl group of 5mC in order to generate a 5mC radical for subsequent reactions (Fig. 4).

3.13 Transcriptional regulation of gene expression

Besides epigenetic mechanisms, gene expression can be also controlled by transcriptional regulation, RNA-processing, RNA transport and localisation, mRNA degradation, translation and protein activity. Although each step is required to ensure cell type-specific gene expression, the initiation of transcription is the most efficient one. Gene transcription can be regulated by the combined action of transcription factors. The unique composition of transcription factors within a cell type allows a tightly controlled activation of target genes. These target genes in turn specify the character of the tissue in which they are expressed. Since it is the composition of transcription factors that specifies a cell type and not the single factors themselves, they can be used in spatio-temporal manner to define the nature of various cell types as in the case of Sox17.

3.14 The Sry-related HMG-box gene Sox17

Sox17 is one of 30 members of the Sry-related high mobility gene (HMG) box gene family. The mammalian testis-determining factor Sry (sex-determining region of Y chromosome) is the archetype of *Sox* genes. The HMG domain of *Sox* proteins share at least 50% amino acid sequence identity with that of Sry (Pevny and Lovell-Badge, 1997). The characteristic of the HMG box domain is its unique interaction with the minor groove of the DNA helix which results in a bend in the DNA molecule (Grosschedl et al., 1994). *Sox* family members have similar DNA-binding specificity and same *Sox* proteins can regulate different sets of target genes in various tissues. The sharp transition in the set of target gene activation can be explained by changes of specific partners or by dynamic expression of the *Sox* genes (Kamachi et al., 2000). Members of the *Sox* family are involved in a variety of developmental processes like testis, endoderm, neural and cardiovascular development (Koopman, 2005; Koopman et al., 1991; Sakamoto et al., 2007; Stolt et al., 2006).

The *Sox* family members are further divided into 10 subgroups, A-J, according to their sequence homology within and outside the HMG box (Bowles et al., 2000). *Sox17* belongs to the subgroup F, together with *Sox7* and *Sox18*. *Sox17* and its splicing variant t-*Sox17*, which lacks the HMG box, were identified in adult testis (Kanai et al., 1996). Whereas there is no evidence for t-*Sox17* function, *Sox17* is crucial for endoderm development. Deletion of *Sox17* results in turning defects and posterior truncations due to defects in mid- and hindgut formation (Kanai-Azuma et al., 2002; Viotti et al., 2012). While *Sox17* expression in the endoderm decreases at E9.0, it is upregulated in the common pancreatobiliary progenitor. Here, *Sox17* is required in lineage choice decision between pancreatic and biliary fate (Spence et al., 2009).

Besides its expression in the endoderm, *Sox17* was also found to be expressed in different lineages of the mesoderm. In the mesodermal lineage, *Sox17* is expressed in endothelial cells of the blood vessels including the dorsal aorta and in hematopoietic stems cells (Burtscher et al., 2012; Choi et al., 2012; Clarke et al., 2013; Engert et al., 2009; Kim et al., 2007; Liao et al., 2009; Matsui et al., 2006; Sakamoto et al., 2007)

3.15 Aims of the study

The formation of an organism requires the interaction of cells and their environment to initiate diverse developmental processes such as the formation and patterning of the three principle germ layers. The interaction is mediated via several signalling cascades but their precise spatio-temporal effectiveness during development remains partially unknown. This is also true for the role of canonical Wnt signalling during embryonic development. The complete knock-out of Wnt3 or β -catenin impaired PS and thus germ layer formation whereas depletion of β -catenin in epiblast progenitors resulted in formation of ectopic cardiac mesoderm instead of endoderm (Huelsken et al., 2000; Lickert et al., 2002; Liu et al., 1999b). This already reveals that Wnt signalling is required in distinct progenitor populations during different embryonic stages for proper development. To investigate the role of Wnt/ β -catenin signalling in lineage formation and patterning, β -catenin was conditionally deleted in the Sox17⁺ visceral and definitive endoderm as well as in vascular endothelial cells.

The observation that *Sox17* is expressed in the endoderm and endothelial cells of the vasculature reflects the dual lineage expression of *Sox17*. To investigate the lineage contribution of distinct Sox17⁺ progenitor cells, it is important to follow their fate in a spatio-temporal manner which is not practicable using currently available constitutive active Sox17Cre lines (Choi et al., 2012; Engert et al., 2009; Liao et al., 2009). To enable lineage-restricted cell fate analysis, a hormone-inducible *Sox17^{CreERT2}* mouse line was generated and its recombination properties were investigated.

Besides regulation of gene expression on the transcriptional level mediated by the action of signalling cascades and transcription factor activity, gene expression is also controlled by epigenetic modifications of the DNA such as methylation. Loss of DNA methyltransferases results in early embryonic lethality demonstrating the importance of DNA methylation for embryonic development (Li et al., 1992; Okano et al., 1999). In contrast, the role of demethylation in embryonic development is currently unknown. To investigate whether active demethylation is involved in patterning and germ layer formation, loss-of-function analysis of the potential demethylase *Elongator* complex were performed.

4 Results

4.1 The function of the Elongator complex during gastrulation

4.1.1 Deletion of Elongator protein 4 leads to early embryonic lethality

It was previously described that the Elongator complex is involved in the erasure of paternal DNA methylation marks at the zygote stage (Okada et al., 2010). To address the role of Elongator in DNA demethylation during development, we performed loss-of-function analysis by deletion of the Elongator complex subunit Elongator protein 4 (*Elp4*).

Since all subunits are required for Elongator complex function (Fichtner and Schaffrath, 2002; Frohloff et al., 2001; Krogan and Greenblatt, 2001; Li et al., 2009), deletion of *Elp4* is sufficient for loss-of-function analysis. Two mouse strains were used to delete the *Elp4* gene. The two mouse strains bear contiguous gene deletions within mouse chromosome 2 in the region homologous to the human WAGR region containing the genes Wilms tumour 1 homolog (*Wt1*), reticulocalbin 1 (*Rcn1*), paired box gene 6 (*Pax6*) and *Elp4* (Favor et al., 2009). These two deletions encompassing the *Pax6* region have been assigned the mutant allele symbols Del(2)*Pax6*^{11Neu}/1Neu and Del(2)*Pax6*^{13Neu}/3Neu (Favor et al., 2009) and will be referred to H9 and Tcm2, respectively. The mutations are schematically depicted in Figure 5. The H9 deletion starts proximal to the *Rcn1* gene, includes the entire *Rcn1* and *Pax6* genes, and ends in intron 9-10 of the *Elp4* gene. As the *Pax6* and *Elp4* genes are oriented tail-to-tail, the deletion within *Elp4* results in loss of the 3' end of intron 9-10 and exon 10 (Favor et al., 2009). The Tcm2 deletion starts within the *Pax6* gene in intron 6-7, includes the entire *Elp4* gene, and ends in intron 2-3 of the IMP1 inner mitochondrial membrane peptidase-like (*Immp1L*) gene (Favor et al., 2009).

RCN proteins act as regulators of calcineurin-mediated signalling pathways (Fuentes et al., 2000; Gorlach et al., 2000; Kingsbury and Cunningham, 2000). Mice deficient for MCIP1, the mouse *Rcn1* homologue, are viable and fertile and exhibit no abnormalities (Vega et al., 2003). *Immp1L* together with *Immp2L* form the mitochondrial inner membrane peptidase (IMP) complex. Effects of IMP complex deficiency is not known but

mice mutant for *Imp2L* develop until adulthood and show impaired gametogenesis and erectile dysfunction (Lu et al., 2008).

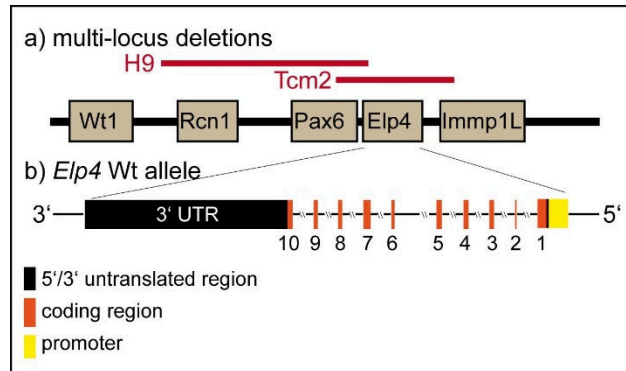


Figure 5: Schematic overview of the affected regions in the deletions H9 and Tcm2

(a) Localization of the *Wt1*, *Rcn1*, *Pax6*, *Elp4* and *Imp1L* genes on mouse chromosome 2. Red bars indicate the *H9* and *Tcm2* deletions. (b) *Elp4* consists of 10 exons and is oriented tail-to-tail with *Pax6*. The black, orange and yellow boxes represent the untranslated region (UTR), coding region and promoter region of *Elp4*, respectively. Exons are numbered (1-10).

Previous quantitative real-time PCR experiments have demonstrated that *Elp4* levels are significantly reduced in H9 and Tcm2 heterozygotes, suggesting that a transcript encoded by the non-deleted portion of *Elp4* in H9 is not produced or is unstable (Favor et al., 2009). Homozygous H9 and Tcm2 deletions or compound heterozygous deletions (H9/Tcm2) lead to early embryonic lethality at E10.5-11.5 (Favor et al., 2009). Closer investigation of mutant embryos showed that homozygous H9 and Tcm2 deletions as well as double heterozygous H9/Tcm2 deletions results in identical phenotypes, i.e. stunted and approximately one day delayed development compared to wild-type littermates (Fig. 6).

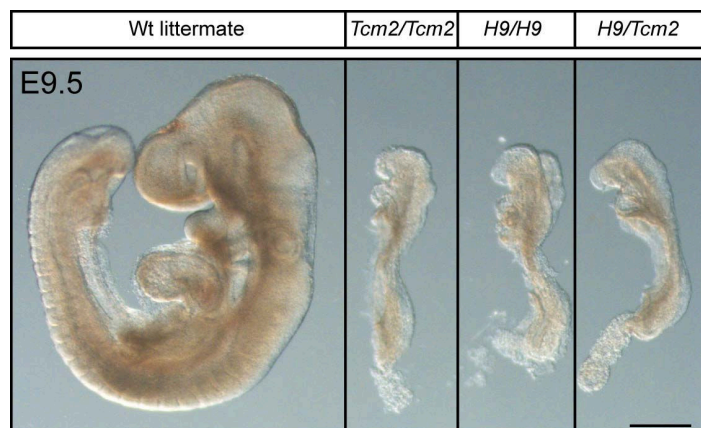


Figure 6: Embryonic lethality of homozygous and compound heterozygous mice

Embryos homozygous for Tcm2 and H9, respectively or double heterozygous for both alleles show the same embryonic lethal phenotype. The mutants are delayed in their development compared to wild-type littermates. Scale bar: 250 μ m.

Since the H9 and Tcm2 deletions do not only affect *Elp4* but also *Pax6* and *Rcn1* or *Imp1L*, it is crucial to exclude effects caused by deletion of these genes. Therefore, we

first investigated if *Pax6*, *Rcn1* and *Immp1L* are expressed at the embryonic stages when the phenotype arises. *In situ* hybridization (ISH) of whole wild-type embryos, as well as on paraffin sections at E7.5-7.75 showed that *Rcn1* is expressed in extra-embryonic and embryonic lineages (DE; Fig. 7a and a'). *Immp1L* is expressed at low levels only in the embryonic compartment (Fig. 8c and c'). *Pax6* is not expressed as early as E7.5-7.75 (Fig. 7b and b') and it was previously shown that mice homozygous for *Pax6* intragenic null mutations die shortly after birth and not during embryonic development (Hogan et al., 1986; Roberts, 1967). This suggests that heterozygous or homozygous deletion of *Pax6* does not contribute to the observed mutant phenotype. Although *Rcn1* and *Immp1L* are expressed at this early stage, it is unlikely that their deletion contribute to the observed phenotype since the KO of *Rcn1* as well as the KO of *Immp1L* family member *Immp2L* does not affect viability (Lu et al., 2008; Vega et al., 2003). Furthermore, embryos homozygous for H9 and Tcm2 as well as the compound heterozygotes, where still one copy of *Rcn1* and *Immp1L* remains intact, showed the same phenotype, strongly suggesting that loss of *Elp4* alone accounts for the observed phenotype. For further analysis we only used compound heterozygous embryos.

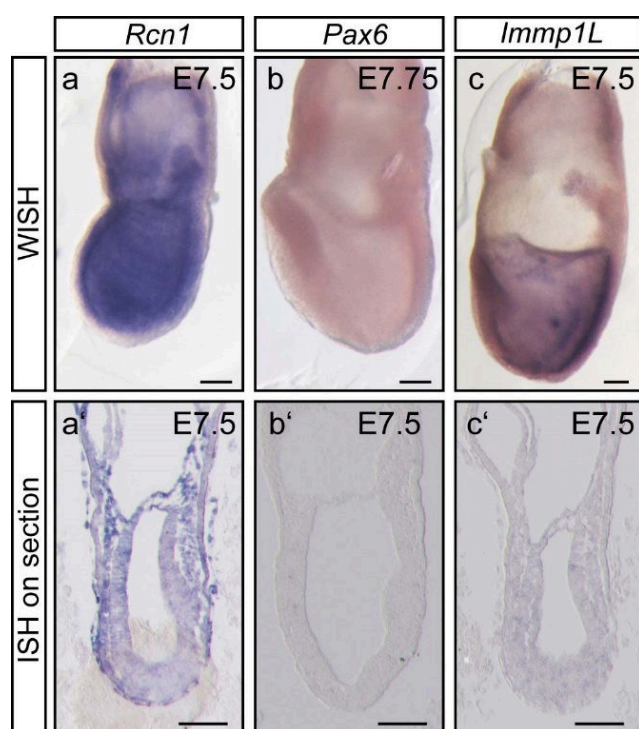


Figure 7: mRNA expression of genes located in the deleted region

(a, a') *Rcn1* is ubiquitously expressed at E7.5, (b, b') *Pax6* is not expressed at E7.5-7.75 and (c, c') *Immp1L* is expressed at low levels within the ectoderm, mesoderm and endoderm. WISH = whole mount *in situ* hybridization, ISH = *in situ* hybridization. Scale bar: 100 μ m.

4.1.2 Embryos mutant for *Elp4* are patterned but show developmental delay

In order to analyse the mutant phenotype in more detail, mice heterozygous for *H9* and *Tcm2* were intercrossed to obtain compound heterozygous embryos. At E8.0, gross morphological analysis showed a slight delay in development of about half-a-day. In addition, the size of the mutant embryos was drastically reduced compared to wild-type littermates (Fig. 8a). At E8.5, the developmental delay was more pronounced. While wild-type embryos have already formed the brain, heart, primitive gut tube and somites, the mutant embryos still remain at the gastrulation stage, suggesting that the initially formed three germ-layers were not able to sufficiently grow and differentiate (Fig. 8b).

At E9.5, the mutant embryos were still delayed in development by one day and showed comparable characteristics of E8.5 wild-type embryos (Fig. 8c). Gross morphology and paraffin section indicated that the neural tube, vascular system, heart, foregut, midgut and hindgut, as well as the somites have formed normally in mutants, indicating that patterning and cell differentiation occurred normally, but at a much slower pace (Fig. 8c-f). To compare mutant embryos to developmental matching wild-types, CD1 embryos were sectioned at E8.5. No differences in the organisation of the ectoderm-, mesoderm- or endoderm-derived tissues could be observed in mutants compared to wild-type embryos, suggesting that the differentiation process was initiated (compare Fig. 8d-f with Fig. 8g-i).

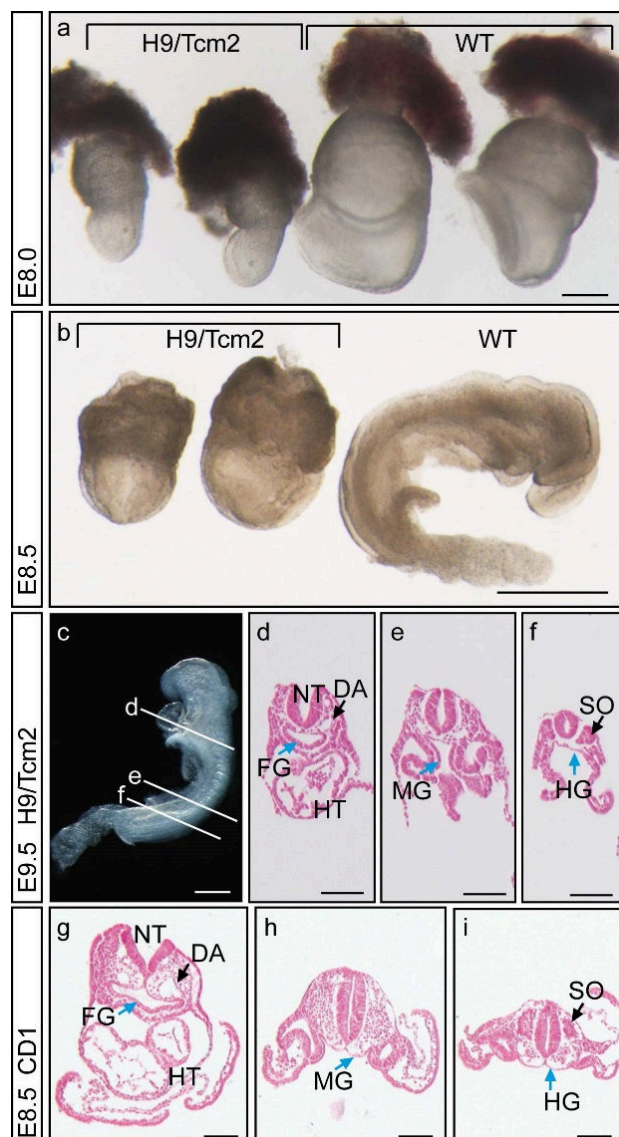


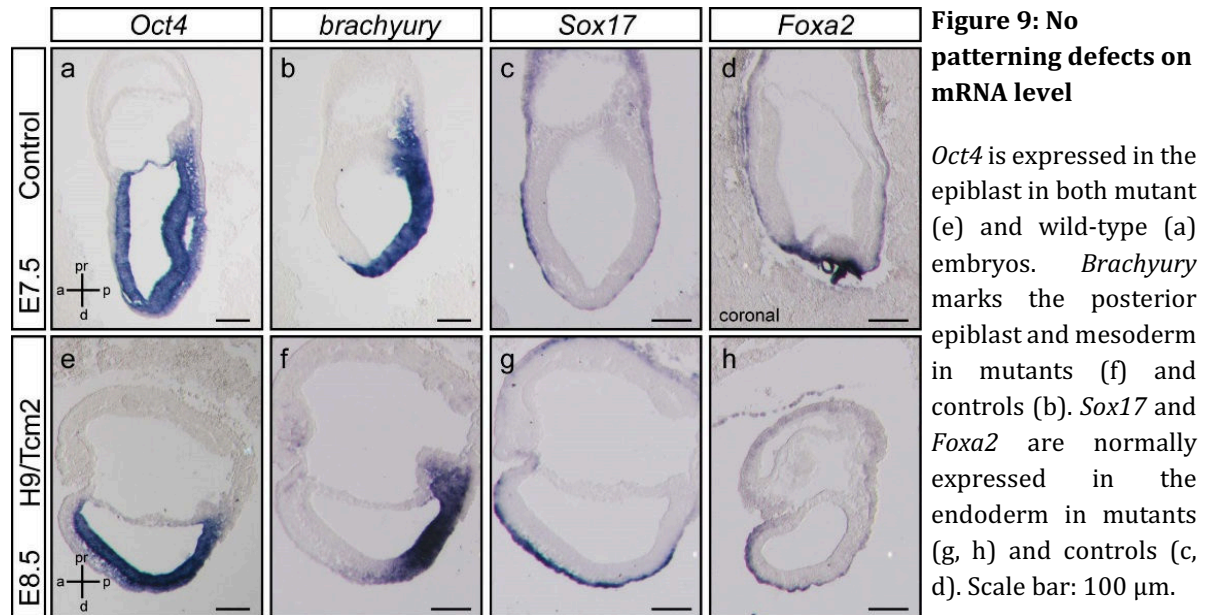
Figure 8: H9/Tcm2 mutant embryos are delayed in development and reduced in size

(a, b) Gross morphology of mutant embryos compared to littermates at E8.0 (a) and E8.5 (b). (c) H9/Tcm2 mutant at E9.5. (d-f) Sections of the embryo shown in (c) at indicated levels. (g-i) Sections of developmentally matching wild-type CD1 embryos at comparable levels to sections in (d-f). DA = dorsal aorta; FG = foregut; HG = hindgut; MG = midgut; NT = neural tube; SO = somites. Scale bar (a-c): 250 μ m, (d-i): 100 μ m.

Although the mutant embryos seemed to be well organized they showed developmental delay and died between E10.5 to E11.5. To analyse the cause of this phenotype more in detail, we investigated gene expression patterns for marker genes between E7.25 and E8.5, a time window when the phenotype becomes apparent. Expression of pluripotency- and differentiation-associated genes were examined on mRNA and protein level by ISH and immunohistochemistry (IHC)

combined with laser scanning microscopy. As the development of the mutants is delayed compared to their littermates, developmentally matched wild-type embryos were used as controls. To investigate the differentiation of pluripotent epiblast cells into different lineages, *Oct4* was used as a marker for pluripotency, *Brachyury* as a marker for mesoderm, and *Foxa2* as well as *Sox17* as markers for the endoderm. ISH on sections of E8.5 H9/Tcm2 mutants showed normal expression of *Oct4* throughout the epiblast when compared to E7.5 control embryos (Fig. 9a, e). *Brachyury* was expressed at comparable levels in the posterior epiblast and mesoderm in both mutants and controls (Fig. 9b, f). Likewise *Foxa2* and *Sox17* showed no difference in expression in the endoderm (Fig. 9c-h). Thus, marker expression on the mRNA level did not exhibit any patterning defects in

the mutants at the gastrulation stage, indicating that all three germ layers formed normally.



Although it was suggested that the Elongator complex is involved in transcriptional elongation (Gilbert et al., 2004; Otero et al., 1999; Wittschieben et al., 1999), mRNA synthesis of the investigated genes was not impaired. This indicates that loss of Elongator function does not affect transcription in general. In addition to transcriptional control, Elongator was shown to regulate gene expression on the translational level by modification of certain tRNAs (Bauer et al., 2012; Esberg et al., 2006; Huang et al., 2005; Mehlgarten et al., 2010).

To exclude impaired translation, the same set of markers was investigated by antibody staining on whole mount embryos. At E7.25, *Oct4* was localised to the epiblast in both control and mutant embryos. *Foxa2* was synthesized in the embryonic VE, the arising DE and the axial mesoderm progenitors in controls (Fig 10a, arrowhead in a'), whereas *Foxa2* was restricted to the posterior epiblast and VE in the mutant (Fig 10b, arrowhead in b'). At six to seven somite stage, *Foxa2* was expressed in the hindgut endoderm, notochord and node in the control embryos (Fig. 10c, e). In the mutants, *Foxa2* was also localised to the notochord and node, but was more restricted to the midgut endoderm than to the

hindgut endoderm (Fig. 10d, f). Likewise, Sox17 was synthesized in the mid- and hindgut endoderm in controls (Fig. 10c), but more restricted to the midgut endoderm in mutants (Fig. 10d). Brachyury marked the notochord and node in both mutant and control embryos (Fig. 10e, f). Except for the shifted localisation of Foxa2 and Sox17 to the midgut rather than to the hindgut region, no overt differences in patterning of the mutant embryos were observed.

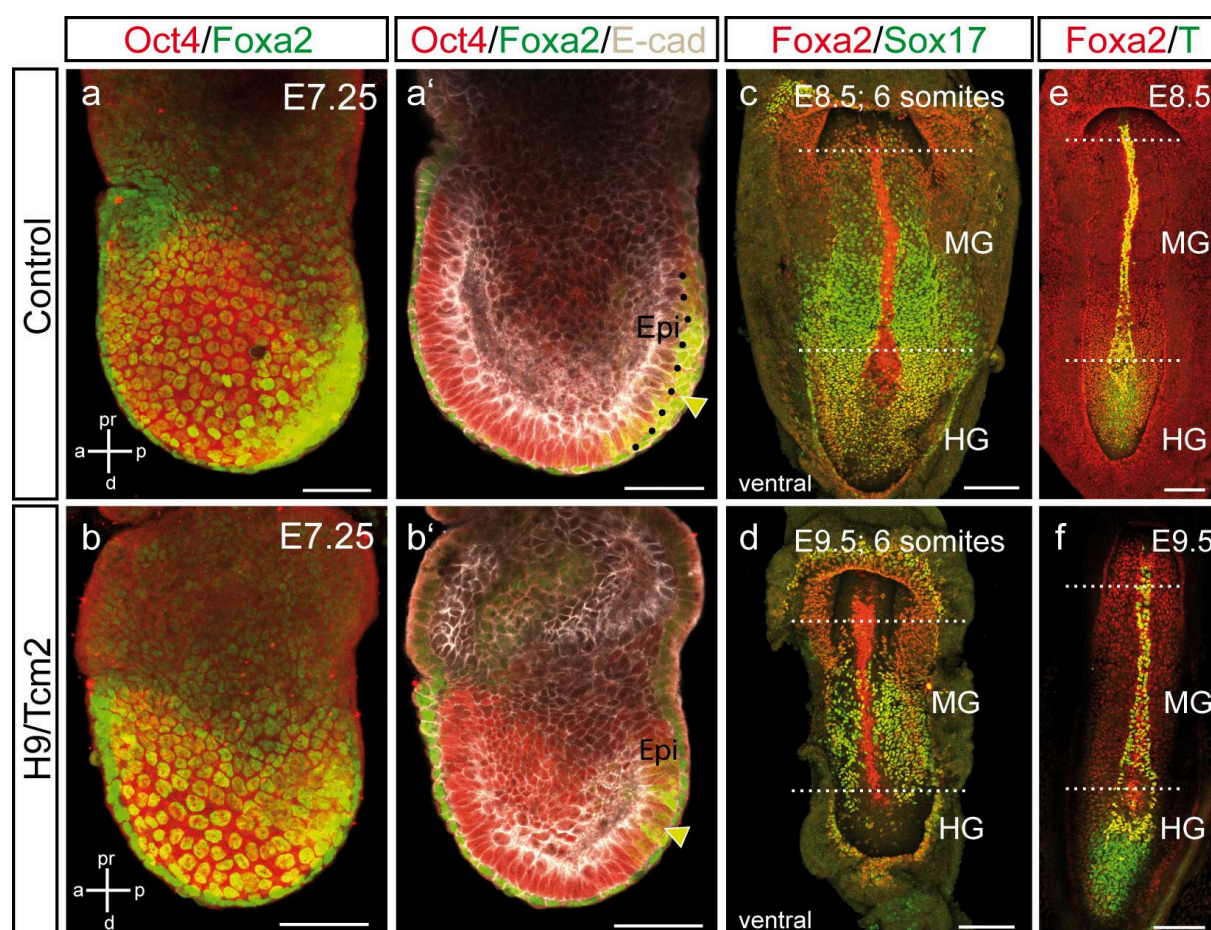


Figure 10: Delayed development is reflected by marker expression

Oct4 is synthesised in the epiblast (Epi) while Foxa2 marks the endoderm and axial mesoderm precursors at E7.25 in mutants (b, b', arrowhead) and controls (a, a', arrowhead). (a') and (b') are optical sections of the embryos depicted in a and b, respectively, and show an additional staining of E-cadherin. Foxa2 and Sox17 localise to the hindgut (HG) region in controls (c, e), but to the midgut (MG) region in mutants (d, f). The notochord and node is positive for Foxa2 and Brachyury in mutants (d, f) and controls (c, e). Scale bars: (a-b): 50 μm , (c-f): 100 μm .

4.1.3 Transcriptome analysis of *Elp4* mutant embryos displays genome-wide effects

Since the analysis of a few selected marker genes on mRNA and protein levels did not reveal any gross abnormality, we wondered if more global subtle changes lead to the observed delay in embryonic development. Thus, mutant embryos were analysed by mRNA profiling using Affymetrix GeneChip analysis (in collaboration with M. Irmeler). To analyse the primary cause of the embryonic phenotype, we extracted the mRNA from the embryonic part of five H9/Tcm2 double heterozygous embryos and six wild-type embryos at developmental stage E7.5, a stage where no obvious morphological phenotype

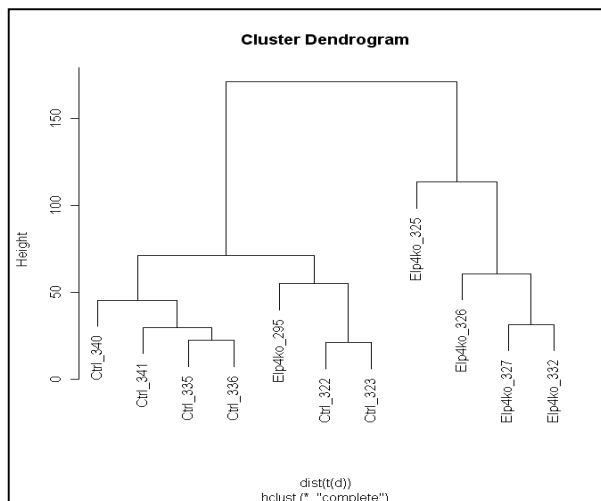


Figure 11: Cluster analysis of mutant and control embryos

Clusters of control (Ctrl) and mutant embryos (Elp4ko).

is visible, and subjected it to genechip analysis. Data mining and cluster analysis using Hclust showed that the mutants cluster separately from the wild-types, except for mutant number 295 (Fig. 11), which we excluded from further analysis. To detect differentially regulated genes in mutant embryos, a ratio of more than 1.1 fold and a false discovery rate of less than 10 % were applied. Analysis of all samples with this approach revealed 5352 deregulated genes. The same analysis was performed excluding the mutant embryo 295, which clustered more to the wild-type controls than to the other mutants. Exclusion of mutant 295 from the statistical analysis led to an increase of deregulated genes up to 8547. To identify the top deregulated genes, a ratio higher than 3 fold was applied, resulting in 902 differentially expressed genes (Fig. 12a, b). Gene ontology (GO) term enrichment analysis linked the deregulated genes to oxoacid metabolic processes, signal transducer and activator of transcription, defence response, interleukin 6, steroid metabolic processes

and inflammatory processes (Fig. 12c). Interesting, several GO terms are associated with chemical reactions and pathway involving organic acids and compounds. It is conceivable, that the profile data already contains information about possible chemical mechanisms that trigger DNA modifications. The observation that deregulated genes are involved in diverse metabolic processes as well as in immune response together with the generally high number of affected genes, suggests that loss of Elongator function has an impact on the whole genome. This is in line with the embryonic analysis, which suggested that not a single germ layer or tissue is affected, but the whole embryo. In addition, it was proposed that the Elongator complex is ubiquitous expressed (Chen et al., 2009b) and therefore loss-of-function likely affects all three germ layers during gastrulation.

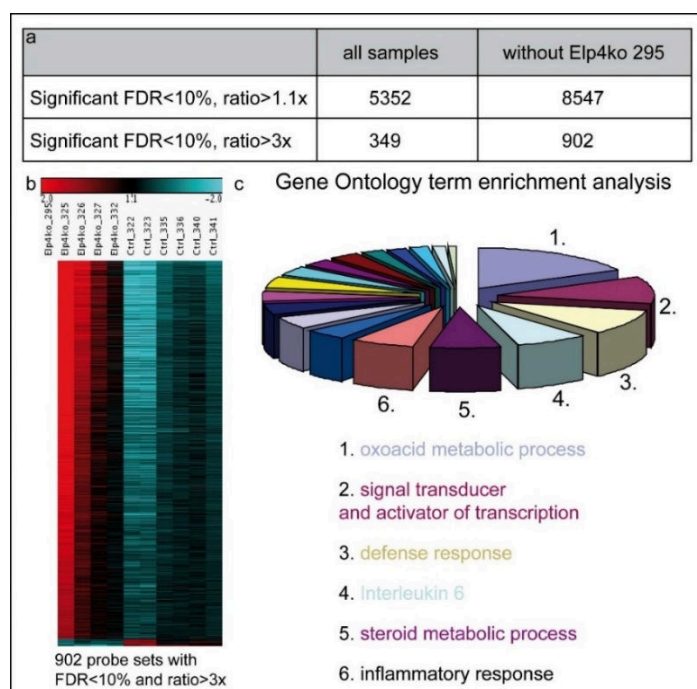


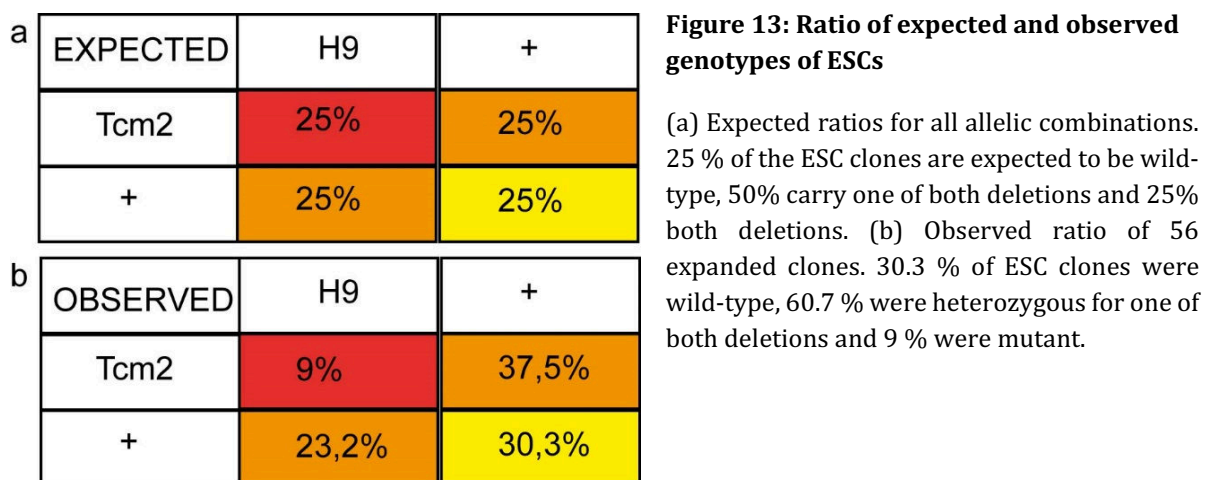
Figure 12: Transcriptome analysis of deregulated genes at gastrulation

(a) Probe set analysis of all samples and without #295. (b) Heat map of deregulated genes with FDR < 10 % and ratio > 3x. (c) GO term analysis of probe sets with FDR < 10 % and ratio > 3x.

4.1.4 Stem cell identity of *Elp4* mutant ESCs is affected

Since the profiling was done on whole embryos that already underwent gastrulation, defects within single germ layers would not be distinguishable. Furthermore, potential pluripotency- and differentiation-associated defects might not be seen, because the

embryos overcame the pluripotent state, although with delay. For these and also for practical reasons such as availability of mutant material, we aimed to generate an ESC line from compound heterozygotes. However, within two rounds of ESC generation no mutant ESC colony could be expanded, but some spontaneously differentiated ESC clones were found to be positive for the H9 and Tcm2 deletions, suggesting that pluripotency or self-renewal of ESCs might be affected. To prevent spontaneous differentiation of mutant ESC colonies, media containing leukemia inhibitory factor (LIF), mitogen-activated protein kinase enzyme MEK1 (MEK1) inhibitor and glycogen synthase kinase 3 β (Gsk3 β) inhibitor, were used for a third round of ESC generation. Using these pluripotency-promoting conditions (Ying et al., 2008), we obtained 5 mutant ESC clones out of 56 clones (Fig. 13).



The generation of the mutant ESCs was only successful when blastocysts were kept and expanded in ES media containing LIF, MEK1 and Gsk3 β . Without these pluripotency-promoting factors spontaneous differentiation of mutant ESC clones was observed, suggesting that the pluripotency network in mutant ES cells is affected.

To investigate the pluripotent state of the generated mutant ESC clones, immunohistochemistry was performed. Using antibodies specific to Oct4, Sox2 and Klf4 revealed that both control and H9/Tcm2 mutant cells expressed pluripotency markers and retained their self-renewal capacity under pluripotency-promoting conditions (Fig. 14).

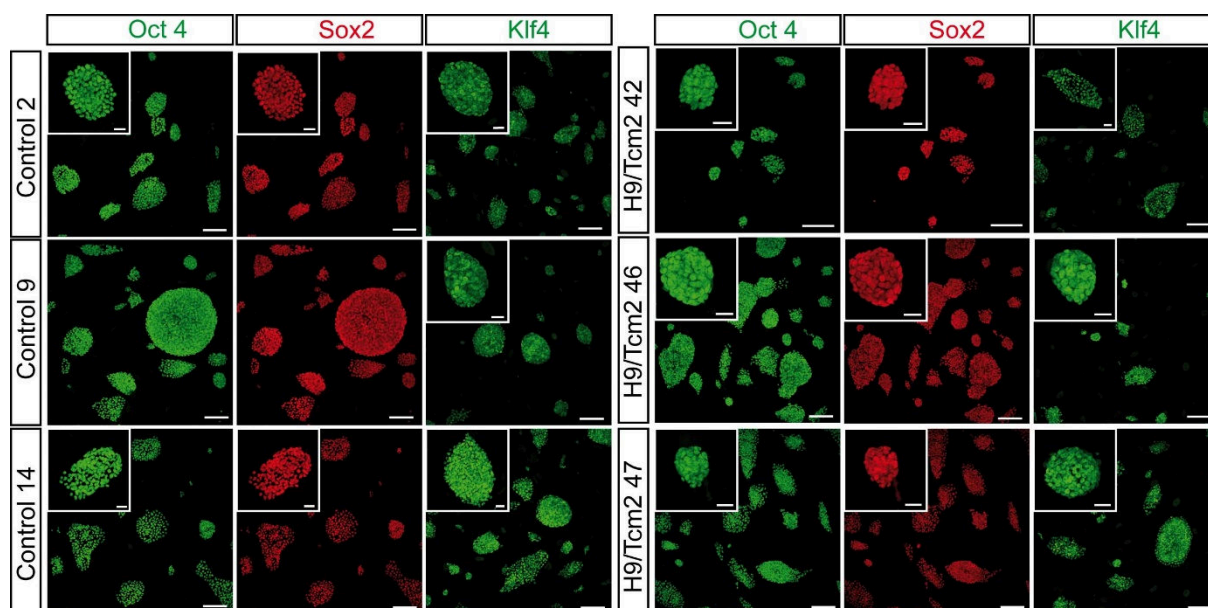


Figure 14: Pluripotency markers are expressed in mutant ESCs

IHC on control and H9/Tcm2 mutant ESCs using α -Oct4, α -Sox2 and α -Klf4 antibodies shows expression of pluripotency genes in both Ctrl and mutant ESC clones. Boxed area shows higher magnification. Scale bar: 100 μ m, boxed area: 25 μ m.

No overt abnormalities of ESCs were observed by IHC, although ESC generation was impaired. To investigate the pluripotent state of these ESCs on a more sensitive and global level, we extracted the mRNA from H9/Tcm2 ESCs under pluripotency conditions and subjected it to genechip analysis. Cluster analysis of the ESC clones revealed that the mutant clone 47 clustered more to wild-type clones (#9 and #14) than to mutants (#42 and #46) (Fig. 15a). For this reason, clone 47 was excluded from further data analysis. The profile was split into top up-regulated and top down-regulated genes (Fig. 15b). GO term enrichment analysis for the top up-regulated genes showed genes involved in cell differentiation, purine ribonucleotide binding and stress response, among others. The fact that especially genes that are involved in cell differentiation are up-regulated in Elp4 mutant ESCs indicates that maintenance even under stringent pluripotency conditions is compromised. Interestingly, GO terms of top down-regulated genes were associated with DNA metabolic processes, DNA binding, chromosome organisation, among others. The accumulation of GO terms for DNA and chromosome points towards an epigenetic function of the Elongator complex.

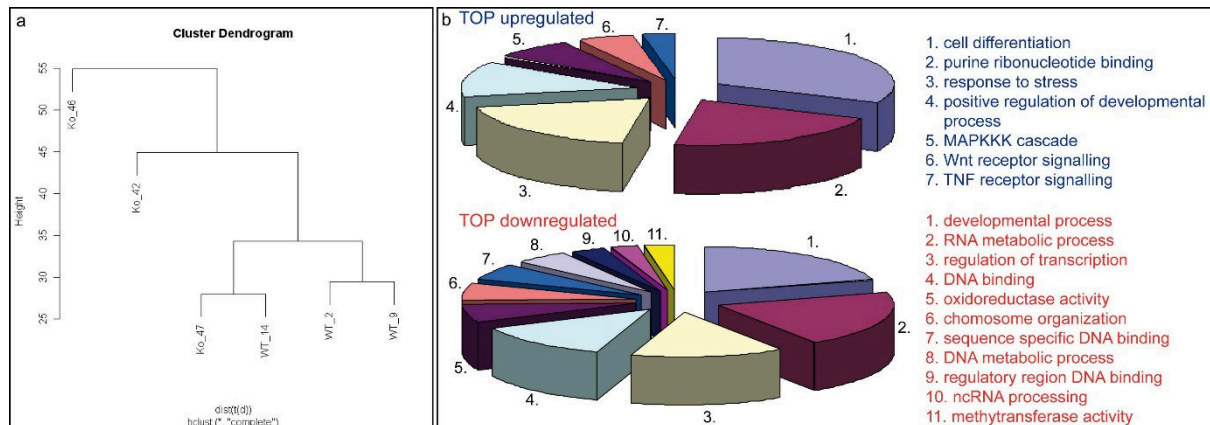


Figure 15: mRNA profiling of mutant (KO) cells versus wild-type (WT) cells

(a) Cluster analysis of mutant and wild-type ESC clones kept under pluripotency-promoting conditions including MEK1 and Gsk3 β inhibitors. (b) GO term enriched analysis for top up- and top-down regulated genes.

4.1.5 Impaired differentiation capacity of *Elp4* mutant ESCs

Although, genechip analysis revealed drastic changes in the mRNA profile, no overt phenotype was observed in ESCs under pluripotency conditions besides reduced growth abilities for some mutant clones. The observation that *Elp4*-deficient ESCs formed colony-like structures and could be maintained over several passages mirrors the *in vivo* results. Mutant embryos are able to overcome the blastocyst stage and develop normally until E6.0 to E6.5. However, further development is delayed and the embryos are significantly smaller. These observations indicate that the ability to exit pluripotency and initiate the differentiation process is affected. In order to understand this in more detail, representative ESC clones were tested in their ability to differentiate into mesendoderm and endoderm. During endoderm differentiation, the Oct4⁺ ESCs pass through a T⁺/Foxa2⁺ double positive mesendoderm stage on day two of endoderm differentiation (Burtscher and Lickert, 2009; Gadue et al., 2006). Whereas the expression of *T* is transient under endoderm-promoting conditions, *Foxa2* becomes strongly up-regulated on day three and additionally expression of *Sox17* is initiated (Fig. 16a)(Ang et al., 1993; D'Amour et al., 2005; Kanai-Azuma et al., 2002; Monaghan et al., 1993; Sasaki and Hogan, 1993).

For differentiation, the control (#9) as well as the H9/Tcm2 mutant clones (#46 and #47) were cultured three days under endoderm-promoting conditions including Wnt3a and Activin A. IHC using antibodies specific to Oct4, T, Foxa2 and Sox17 revealed reduced ability of the mutant clone 46 to differentiate into the endoderm lineage and abnormal differentiation behaviour of the mutant clone 47. In the control, a low proportion of the cells was positive for T whereas a high proportion was positive for Foxa2 and Sox17. Additionally the number of Oct4⁺ cells was decreasing at day 3 of endoderm differentiation. In contrast, the mutant clone 46 showed delayed differentiation into endoderm in general. A low percentage of T⁺ or Foxa2⁺ cells and almost no Foxa2⁺/Sox17⁺ double positive cells were observed, instead more cells retained Oct4. The mutant clone 47 differentiated as efficient as the control but showed a higher amount of T⁺ and Oct4⁺ cells and again a low amount of Foxa2⁺/Sox17⁺ cells at day 3, indicating abnormal differentiation ability (Fig. 16b).

The differentiation from a Oct4⁺ pluripotent state to a Foxa2⁺/Sox17⁺ endoderm state was strongly delayed and less efficient in the mutant clones or abnormal, illustrated by transdifferentiation into T⁺ rather than Foxa2⁺ cells. The retained Oct4 level in the mutant cell clones, as well as the delay in their *in vitro* differentiation ability is in line with the observed *in vivo* phenotype. In addition to the IHC, transcriptome analysis was performed on day 0, day 1 and day 2 of endoderm differentiation. The mRNA profile reflected the observed differentiation behaviour of the mutant ESC clones.

Additionally, the profile revealed up-regulation of pluripotency-associated genes in the mutant clone 46 in contrast to normal expression levels in the mutant clone 47. Interestingly, several imprinted genes were also differentially expressed in mutant ESC clones. We also noticed reduced proliferation abilities of mutant clone 46 compared to clone 47 and control 9. The differences between the mutant ESC clones prompt us to investigate their gender. We found that the mutant clone 46 is female, whereas the mutant clone 47 as well as the control clones 9 and 14 are male. To further investigate gender-dependent cellular behaviour, female control ESC clones need to be included in the *in vitro* analysis.

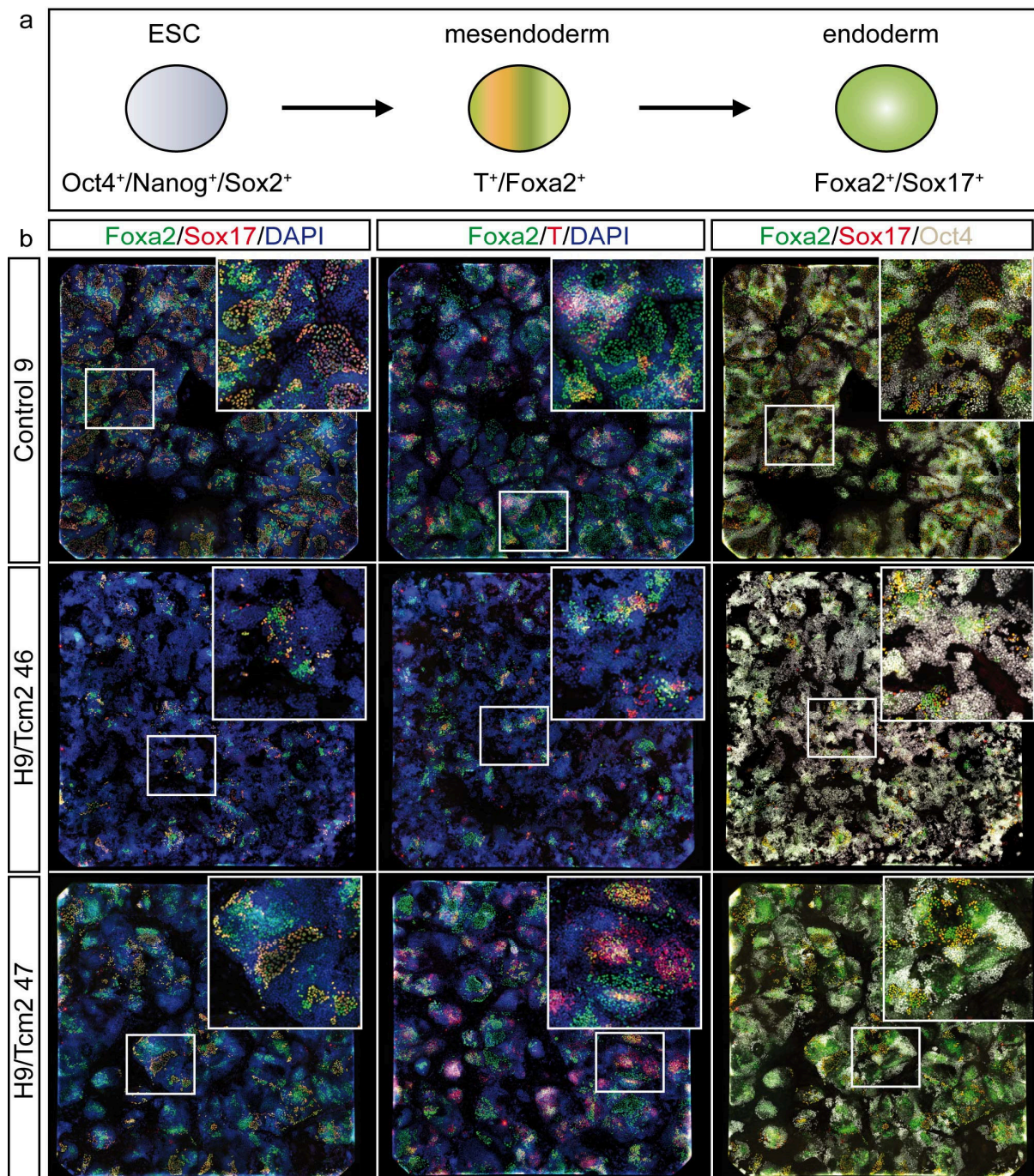


Figure 16: Impaired differentiation ability of *Elp4* deficient ESCs

(a) Scheme of marker gene expression during endoderm differentiation. (b) Control and mutant ES cell clones cultured three days under endoderm differentiation conditions. While the control clone 9 shows high differentiation abilities into Foxa2⁺/Sox17⁺ endoderm, the ability of mutant ESC clones 46 and 47 is reduced or abnormal.

Taken together, loss of Elongator function impairs embryonic development further than E10.5-11.5. Gross morphology revealed that mutant embryos are reduced in size and delayed in their developmental progression. However, ectoderm-, mesoderm- and endoderm-derived structures were formed suggesting that differentiation was initiated but in less extent. *In vitro* analysis revealed reduced ability to exit the pluripotent stage to enter the differentiation process which was confirmed by mRNA profiling. Deregulation of genes involved in chromosome organisation and DNA binding points towards an epigenetic function of Elongator during embryonic development. Chromatinimmunoprecipitation (ChIP) with antibodies specific to 5mC and 5hmC as well as bisulfite sequencing could reveal if aberrant DNA methylation causes the developmental delay *in vivo* and *in vitro* and thus would provide the first evidence for the necessity of epigenetic regulation on DNA level during gastrulation.

4.2 Wnt/ β -catenin signaling regulates Sox17 expression and is essential for organizer and endoderm formation in the mouse

4.2.1 Conditional knock-out of β -catenin in the Sox17⁺ endoderm and vascular endothelial lineage

Wnt/ β -catenin was shown to be crucial for PS formation, mesendoderm specification and organizer induction (Huelsen et al., 2000; Lickert et al., 2002; Liu et al., 1999b). Nevertheless, its role in embryonic and extra-embryonic endoderm lineages remains unknown. To investigate Wnt/ β -catenin function in the endoderm, we aimed to delete β -catenin in the Sox17 lineage. For this purpose, we used the Sox17^{2AiCre} mouse line (Engert et al., 2009) to delete the signalling molecule β -catenin in the extra-embryonic and embryonic endoderm. Since Sox17 is also expressed in the endothelial cells of the vascular system, deletion of β -catenin occurs additionally in the vascular endothelial cells.

Immunohistochemistry (IHC) of fixed embryos reveals that Sox17 is strongly expressed in the extra-embryonic visceral endoderm (exVE), anterior visceral endoderm (AVE) and posterior visceral endoderm (PVE) at E6.5 (Fig. 17a, b) as well as in the definitive endoderm (DE) at E7.5 to E7.75 (Fig. 17c, d). This is consistent with previous findings and suggests that it regulates gene expression in these cell types during endoderm development (Burtscher et al., 2012; Kanai-Azuma et al., 2002).

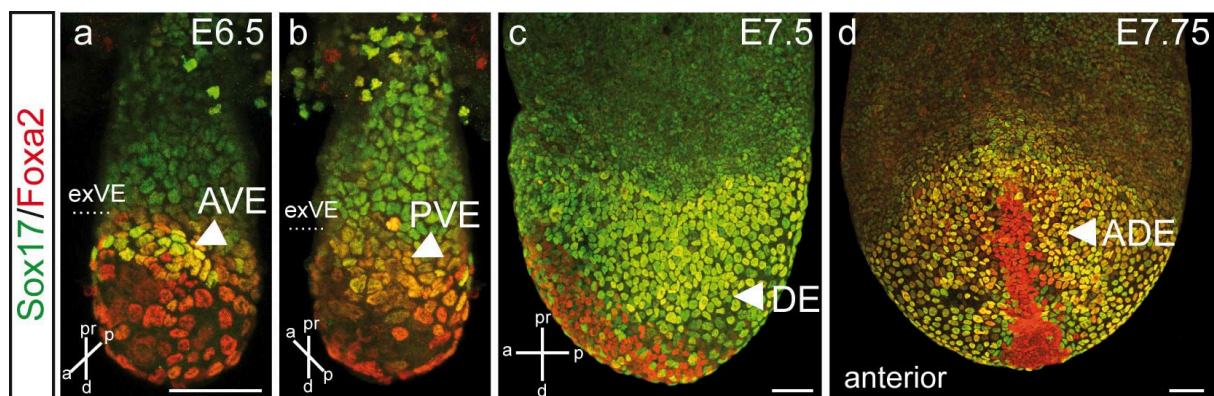


Figure 17: Expression pattern of Sox17 in the extra-embryonic and embryonic lineages

(a-d) IHC using α -Sox17 and α -Foxa2 antibodies on wild-type embryos at E6.5-7.75. Sox17 is localised to the extra-embryonic visceral endoderm (exVE), anterior visceral endoderm (AVE, arrowhead in a) and posterior visceral endoderm (PVE, arrowhead in b), Foxa2 to the embryonic visceral endoderm, AVE and PVE at E6.5 (a-b). At E7.5 Sox17 is synthesised in definitive endoderm (DE, arrowhead in c), while Foxa2 is also apparent in the anterior mesendoderm (AME) (c). Sox17 marks the anterior definitive endoderm (ADE, arrowhead), Foxa2 the ADE and AME at E7.75 (d). Scale bars: 50 μ m.

At E8.5, Sox17 protein is abundant in the mid- and hindgut endoderm and in the endothelial cells of the developing vasculature (Burtscher et al., 2012). To delete β -catenin in the Sox17 lineage, we mated males heterozygous for β -catenin floxed (*FD*) (Brault et al., 2001; Lickert et al., 2002) and *Sox17^{2AiCre}* (Engert et al., 2009) alleles with females homozygous for β -catenin floxed (*F*) and the *R26R* Cre reporter alleles (Fig. 18a, b) (Soriano, 1999). The *R26R* allele allows monitoring Cre-recombination activity. Using this crossing scheme, one quarter of the offspring showed a conditional knock-out (CKO) for β -catenin (β -catenin CKO) by recombination of only one β -catenin floxed allele. Littermates which inherited some, but not all of the alleles served as controls. To confirm β -catenin deletion upon Cre-mediated recombination, we analysed β -catenin localisation

at the cell membrane by IHC. Besides β -catenin's signalling function in the canonical Wnt pathway, β -catenin is a component of the adherens junctions, where it mediates cell-cell adhesion. Since detection of the β -catenin signalling pool in the nucleus is not possible, we investigated total β -catenin levels in the cytoplasm and at the membrane as an indicator for conditional deletion in the Sox17 lineage. By doing so, we confirmed efficient gene deletion in the VE at E5.5 and E6.5, as well as in the DE at E7.5 in CKO embryos (Fig. 18c-j). Whereas β -catenin was localised to E-cadherin⁺ adherens junctions in control embryos, β -catenin was deleted uniformly and specifically in both extra-embryonic and embryonic endoderm lineages in β -catenin CKO embryos.

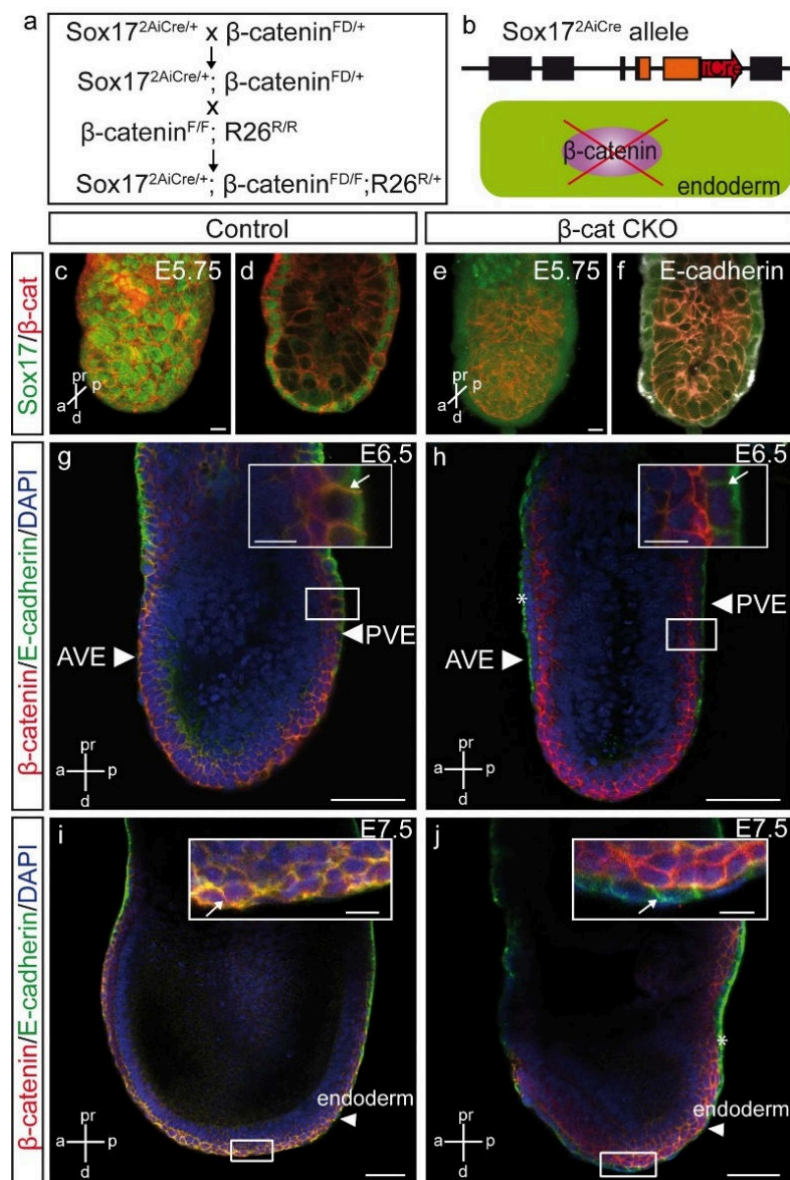


Figure 18: Conditional knock-out of β -catenin in the Sox17 endoderm lineage

(a) Crossing scheme to generate β -catenin CKO embryos containing the *R26R* allele using the *Sox17^{2AiCre}* deleter mouse line (b). (c-f) Antibody staining against Sox17 and β -catenin at E5.5, as well as antibody staining against β -catenin and E-cadherin at E6.5 (g-h) and E7.5 (i-j) confirmed β -catenin deletion in the VE (f, h, arrowheads) and endoderm (j, arrowheads) of CKOs (insets show higher magnification, scale bar: 10 μ m). * unspecific E-cadherin staining. Scale bars: 50 μ m, except c-f: 10 μ m.

Since E-cadherin was still localised to the basolateral membrane compartment in the endoderm of mutant embryos, epithelial integrity seemed to be maintained despite absence of β -catenin. This observation is in line with previous studies demonstrating that β -catenin's homologue plakoglobin can substitute for β -catenin to mediate cell-cell adhesion (Haegel et al., 1995; Huelsken et al., 2000; Lickert et al., 2002).

4.2.2 Lack of β -catenin affects endoderm and organizer formation

Next, we analysed gross morphology and histology of mutant embryos and the fate of wild-type vs mutant cells by using the Sox17-lineage reporter. At E8.5, β -catenin CKO embryos exhibited truncations of the anterior head and posterior neural tube (NT) (Fig. 19a, b, red arrows). The truncation of the anterior head structure can be explained by lack of anterior neural induction due to defects in the head organizer tissues, i.e. AVE, AME and/or ADE. In contrast, the posterior NT truncations were unexpected, as β -catenin was not deleted in the NT but only in the endoderm and vascular endothelial cells, which was monitored by recombination of the *R26R* allele at E8.5 (Fig. 19a, b). These observations suggest that posterior embryonic or extra-embryonic endoderm acts in a paracrine fashion to induce posterior NT structures.

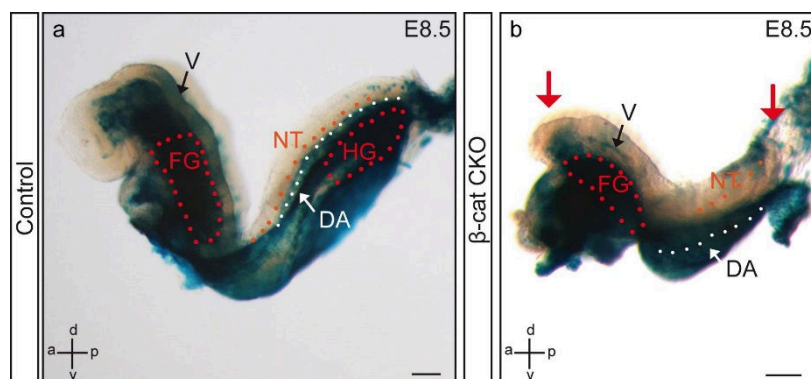


Figure 19: Cell-autonomous and non-cell autonomous phenotypes in β -catenin CKO embryos

(a) Sox17 lacZ⁺ cells contribute to the vascular system (V) including the dorsal aorta (DA, white dots), the foregut (FG), midgut and hindgut (HG) endoderm in controls at E8.5. (b) Mutant embryos show cell non-autonomous head and neural tube (NT) truncations (red arrows) and cell-autonomous loss of hindgut structures. Scale bars: 100 μ m.

To investigate the fate of β -catenin mutant cells in more detail, we analysed embryos during gastrulation and head-fold stage. At E7.5 to E8.0, Sox17⁺ cells were uniformly labelled in the embryonic and extra-embryonic endoderm of control embryos (Fig. 20a-c). On the contrary, β -catenin CKOs exhibited an accumulation of AVE/ADE cells in the anterior region at E7.5 (Fig. 20d, f'), indicating that AVE and/or ADE formation was affected. An accumulation of Sox17 lineage⁺ mutant cells was detected in the PS and anterior region at E7.75 (Fig. 20e), while the lateral and posterior DE region lack Sox17 lineage⁺ cells at E8.0 (Fig. 20f). These results indicate that DE cells were initially specified, but failed to contribute to the lateral and posterior endoderm. Marker analysis revealed some Sox17/ β -catenin double positive cells in the ADE region, but not in the posterior region at E7.75 (Fig. 20g-i), suggesting that the deletion of β -catenin was almost complete using this genetic strategy.

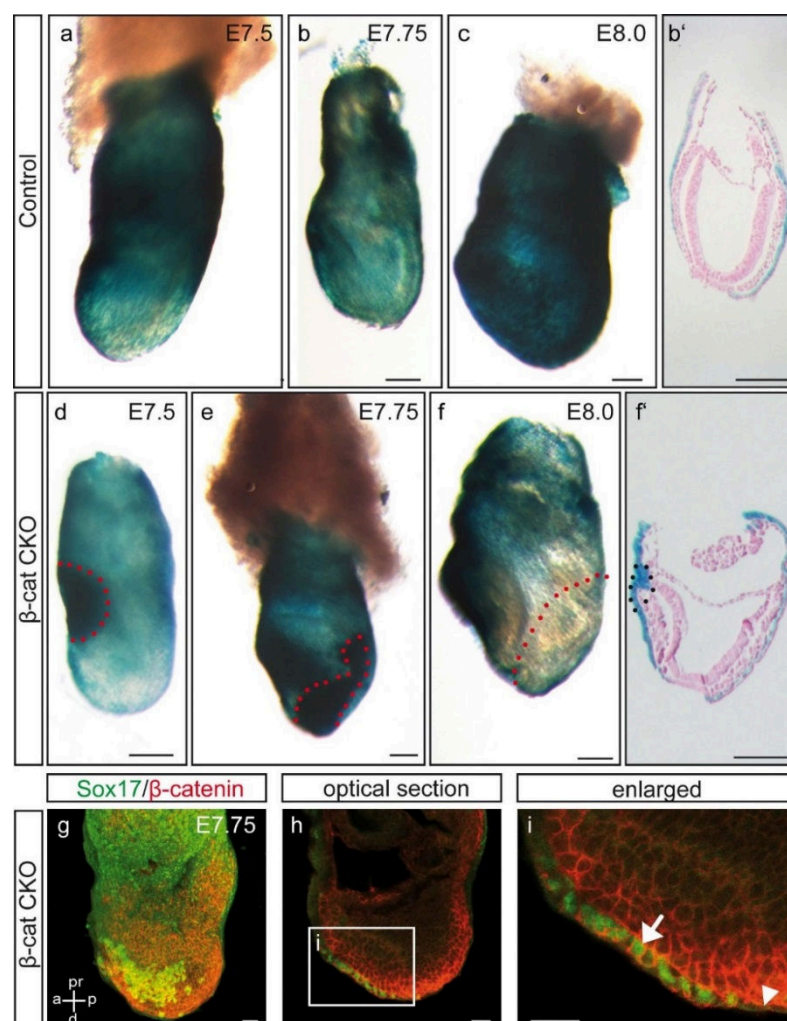


Figure 20: β -catenin is required cell-autonomously for AVE and DE formation

(a-f) LacZ expression in control (a-c) and CKO (d-f) embryos demonstrates an accumulation of Sox17 lineage⁺ cells in the AVE/ADE at E7.5 (d, f', dotted area), PS at E7.75 (e, dotted area) and absence of mutant cells in the posterior region at E8.0 (f, dotted area). (b', f') Sections of b and f. (g-i) IHC shows Sox17⁺/ β -catenin⁺ cells (arrow) in the anterior endoderm of the mutant at E7.75. (g) z-projection, (h) optical section, (i) higher magnification of (h). Scale bars: 100 μ m, except for g-i: 25 μ m. Anterior to the left.

To investigate the fate of Sox17 lineage⁺ cells, which were absent from the posterior endoderm, we analysed apoptosis and proliferation by TUNEL and phosphor histone H3 antibody staining, respectively. However, we did not observe any significant changes in the mutants at E7.5 (Fig. 21a-e). This is in line with previous results obtained with Sox17 KOs (Kanai-Azuma et al., 2002) and suggests that Sox17 lineage⁺ cells die between E7.5 and E8.5. Taken together, these results suggest a cell-autonomous requirement for β -catenin in AVE and DE formation, whereas non-cell autonomous defects lead to head and tail truncations.

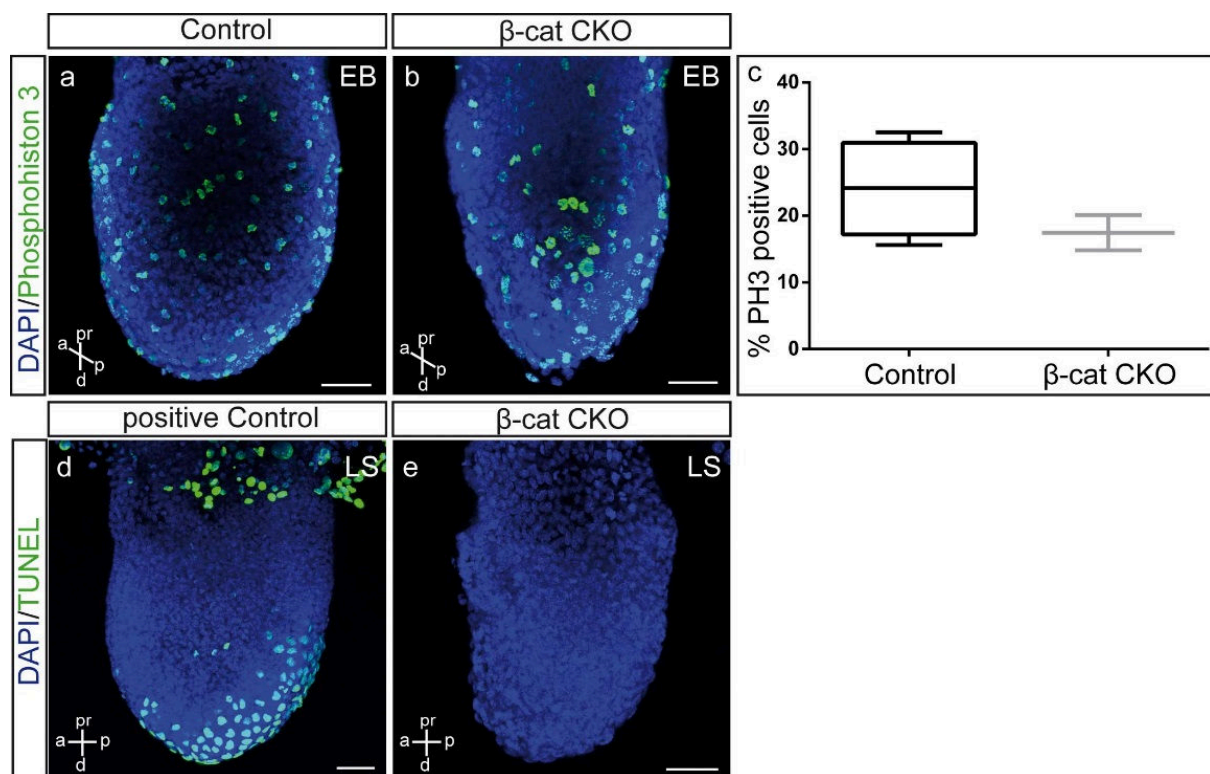


Figure 21: Proliferation and apoptosis rate are not changed in CKO mutant embryos

Cell proliferation depicted by phospho histone H3 (PH3) antibody staining in control (a) and CKO (b) at E7.5. (c) Quantification of PH3⁺ cells reveals no significant change in proliferation. None of the TUNEL positive cells detected in the positive control (d) were detected in CKO (e) at E7.5. Scale bars: 50 μ m.

4.2.3 Lack of β -catenin affects VE patterning and DE formation

To further investigate the defects in AVE formation leading to failure of anterior neural induction, we analysed expression of anterior marker genes by IHC. In mutant embryos, Sox17 was not detected in the AVE region at E6.5 (Fig. 28b, d). In addition, we analysed expression of *Otx2*, which is normally localized in the AVE and anterior epiblast and has been shown to be important for head organizer formation (Beddington and Robertson, 1999). In β -catenin CKO embryos, *Otx2* was detected throughout the VE, but was strongly reduced in the epiblast at E7.0 (Fig. 22a, b). Reduced *Otx2* expression was confirmed by whole mount *in situ* hybridisation (WISH) at E7.5 (Fig. 22c, d). Moreover, expression of *Cer1* and *Hex* in more distal parts of the VE suggests that AVE migration is affected in β -catenin CKO embryos (Fig. 22e-h). The failure of anterior neural induction was confirmed by measuring the distance from the rostral forebrain to the rhombomere 3 and 5 of the caudal hindbrain which was marked by *Krox20* in control and β -catenin CKOs at E8.5 (Fig. 22i, j). This analysis revealed that impaired AVE formation led to defects of the anterior organizer which in term resulted in truncation of the fore- and midbrain.

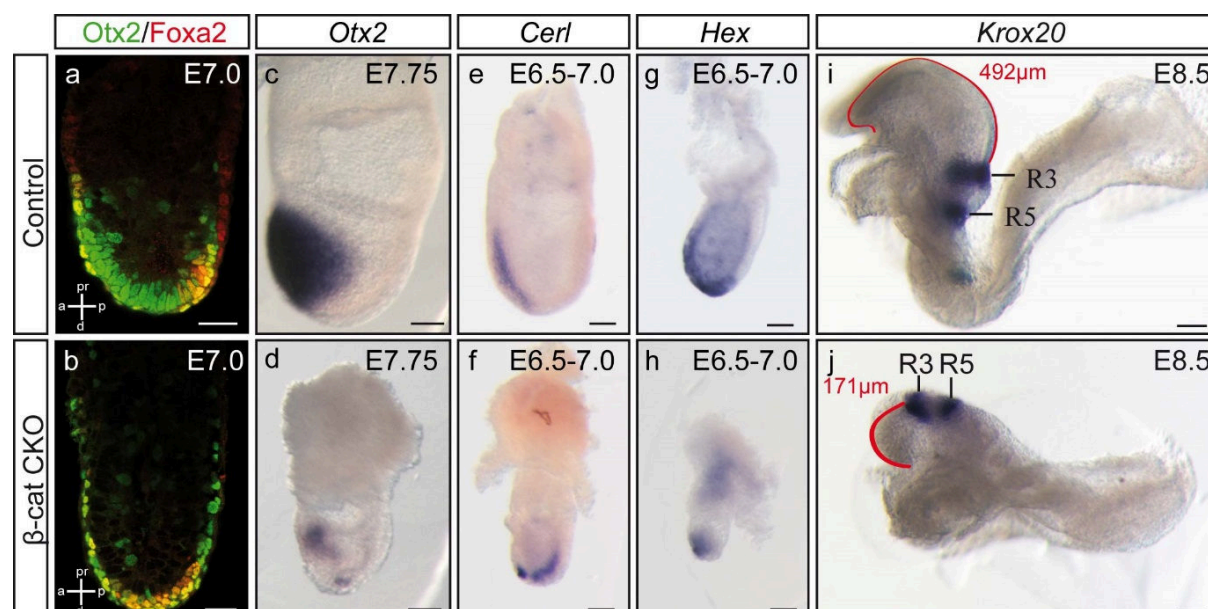


Figure 22: Lack of β -catenin in the endoderm affects AVE formation

Antibody staining against Otx2 (a-b) demonstrates reduced Otx2 levels in the epiblast at E7.0. *Otx2* mRNA is reduced in the anterior epiblast in CKOs (d) compared to controls (c) at E7.75. In CKOs *Cer1* (f) and *Hex* (h) expression remains distally compared to controls (e, g). Lack of anterior structures is shown by reduced distance of forebrain to hindbrain rhombomere R3 in CKO (j) compared to control (i). Scale bars: 100 μ m, except for a-b: 25 μ m. Anterior to the left.

Besides investigation of extra-embryonic endoderm effects, we analysed the consequences of β -catenin deletion in the embryonic endoderm between E7.5 and E8.5. Since it was previously shown that loss of β -catenin in progenitors of the anterior mesendoderm (AME) and DE leads to the formation of ectopic cardiac mesoderm in expense of DE (Lickert et al., 2002), we investigated a potential cell-lineage switch in β -catenin CKOs. Therefore, the expression of the mesendoderm markers T and *Foxa2* were investigated (Burtscher and Lickert, 2009). At E6.5 to E7.5, T marks the posterior epiblast mesendoderm progenitors and their progeny (AME and mesoderm), whereas *Foxa2* marks the anterior epiblast mesendoderm progenitors and their descendants (AME and DE). Whereas T⁺ cells were formed at comparable numbers in the AME and mesoderm in both control and β -catenin CKOs (Fig. 23a-d), *Foxa2*⁺ cells were reduced in numbers in the AME, node, lateral and posterior DE in the mutants at E7.75 (Fig. 23e, f). Failure of DE formation in β -catenin CKOs resulted in the absence of Sox17⁺ mid- and hindgut endoderm, while Sox17 was still abundant in the endothelial cells judged by co-expression with *Pecam1* (Fig. 23g, h). These results support the previous idea that β -catenin is essential for lateral and posterior DE formation. Furthermore, they demonstrate that Sox17⁺ cells are already restricted to the endoderm lineage, because a cell-fate switch to cardiac mesoderm does not occur (Lickert et al., 2002). Since the failure of *Foxa2* induction in epiblast progenitors of the Sox17 lineage was unexpected (Engert et al., 2009), most likely both cell-autonomous and non-autonomous mechanisms contribute to the mutant phenotype.

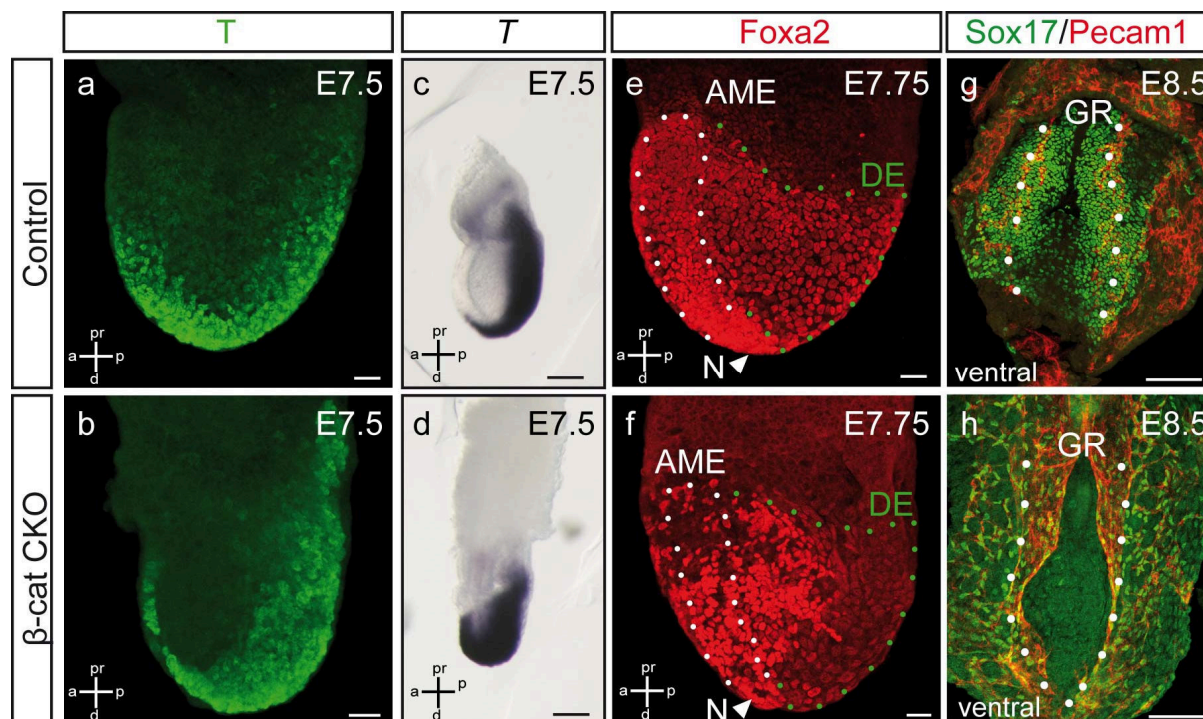


Figure 23: Lack of β -catenin in the endoderm affects DE formation

IHC and ISH against T demonstrate normal T localisation in AME and mesoderm at E7.5 (a-d). Antibody staining against Foxa2 (e-f), Sox17 and Pecam1 (g-h) exhibits reduction of Foxa2 expression in the DE (green dotted area) at E7.75 (e-f, white dotted area indicates AME, N the node) and absence of Sox17 in the gut region (GR, indicated by dotted area) at E8.5 (g-h) in CKO embryos. Scale bars: 25 μ m, except c-d: 100 μ m.

4.2.4 Tetraploid rescue reveals cell-autonomous and non-autonomous function of β -catenin in organizer and DE formation

In order to analyse the cell-autonomous requirement of β -catenin in extra-embryonic and embryonic endoderm, we used tetraploid (4n) embryo \leftrightarrow ESC aggregations to generate ESC-derived embryos (Tam and Rossant, 2003). In the tetraploid complementation assay, the diploid (2n) ESCs can only contribute to the embryonic epiblast which gives rise to the ectoderm, mesoderm and endoderm. In contrast, the tetraploid wild-type cells of the host embryo form the extra-embryonic lineage including ExE and VE. We generated several control and β -catenin conditional mutant ESC lines. The ESC lines were stably transfected with a ubiquitously expressed red fluorescent protein reporter to trace the

contribution of the ESC to chimeric embryos. These control and CKO ESC were aggregated with 4n wild-type embryos, which ubiquitously express yellow fluorescent protein (YFP). The tetraploid complementation assay showed that all 4n WT embryo ↔ CKO ESC aggregation chimera were able to form head structures comparable to that of control embryos at E8.0 to E8.5 (Fig. 24a, f). The rescue of the anterior head truncation phenotype demonstrated that β -catenin is cell-autonomously required in the extra-embryonic AVE for head induction. Furthermore, *Sox17* genetic-lineage tracing using the *R26R* allele of control and CKO ESCs suggests that β -catenin is neither essential for the formation of the vasculature (Fig. 24b, g) nor for the formation of the foregut endoderm in the aggregation chimera (Fig. 24c, h).

In contrary, β -catenin in the embryonic endoderm was crucially important for mid- (Fig. 24d, i) and hindgut formation (Fig. 24e, j). To investigate the gut tube defects in extra-embryonic endoderm rescued chimera in more detail, we analysed the expression of *Pyy* and *Nepn* by WISH. *Pyy* and *Nepn* are expressed in the fore- and midgut endoderm, respectively (McKnight et al., 2010). The marker expression revealed that the foregut is formed in CKO chimera (Fig. 24k, m), whereas the lateral region of the mid- (Fig. 24l, n) and hindgut (Fig. 24e, j) does not develop at E8.5. Although the lateral mid- and hindgut endoderm were almost completely missing, the posterior NT truncation phenotype was rescued in 4n WT embryo ↔ CKO ESC aggregation chimera (compare Fig. 19a, b to Fig. 24a, f and k-n). This rescue was quantified by measurement of the posterior tail region in control, CKO and rescued CKO embryos (Fig. 24o). The observation indicates that WT PVE rescues the tail truncation phenotype in otherwise mid- and hindgut depleted aggregation chimera. This in turn raises the intriguing possibility that PVE cells are crucial for posterior organizer formation in a β -catenin-dependent manner.

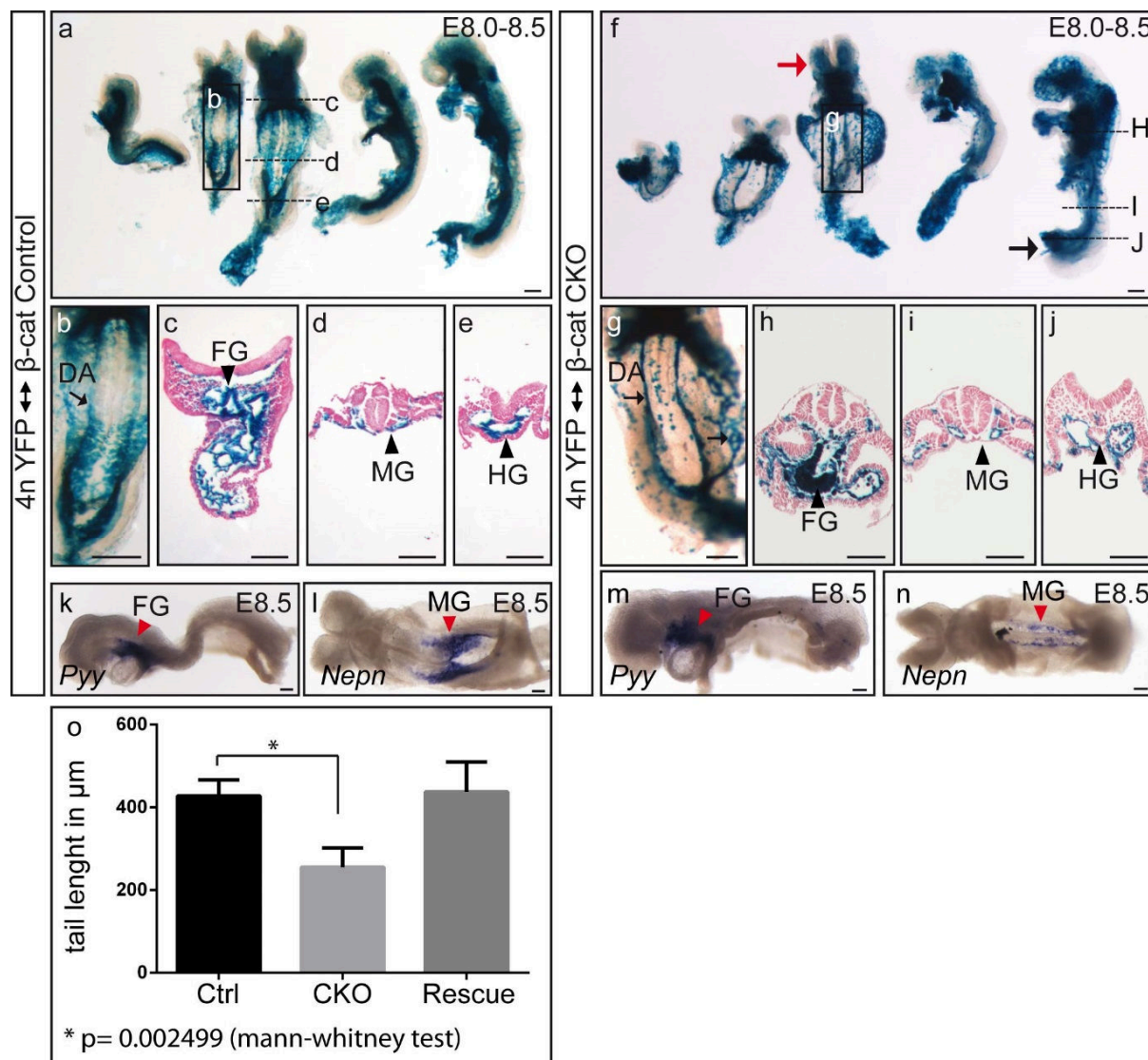


Figure 24: Wild-type VE rescues head and neural tube truncation in aggregation chimera

LacZ stained control (a) and CKO (f) aggregation chimera at E8.0 to E8.5 demonstrate rescue of the head (red arrow) and tail (black arrow) truncation phenotype by WT VE. Vascular endothelial cells, dorsal aorta (DA, arrows) and foregut (FG) are formed in control (b-c) and CKO aggregation chimera (g-h). Midgut (MG) and hindgut (HG) formation of CKO aggregation chimera (i-j) is impaired compared to controls (d-e). (c-e) and (h-j) show sections at indicated levels of embryos depicted in a and f. (o) Quantification of posterior tail length by measuring the distance from the last somite to the end of the tail in control, CKO and rescued CKO chimera at 6-7 somite stage. Tail length is significantly reduced in CKO embryos compared to control embryos and rescued chimera. Scale bars (a-b) and (f-g): 250 μm , (c-e) and (h-n): 100 μm .

To address the role of PVE in posterior organizer formation, we investigated the relative contribution of 4n WT embryo-derived VE (YFP⁺/RFP⁻) and ESC-derived DE (YFP⁻/RFP⁺)

cells in aggregation chimera between E7.5 and E8.5. At E7.5, both control and CKO chimeric embryos showed coherent sheets of 4n YFP⁺ PVE cells above the PS region (Fig 25e-h). While the anterior and lateral VE (YFP⁺/RFP⁻) are dispersed by DE cells (YFP⁻/RFP⁺) in control chimera, VE cells still form coherent sheets in CKO chimera (Fig. 25a-h). This observation confirms that lateral and posterior DE cells are not formed in CKO chimera. The relative contribution of 4n YFP⁺ VE and RFP⁺ DE cells to the endoderm of control and CKO chimera were quantified (Fig. 25i-o). Further evidence that WT PVE cells rescue the axis elongation defect comes from the observation that YFP⁺ VE cells still form an epithelial sheet above the PS region in both control and CKO chimera at E8.0 and E8.5 (Fig. 26a-p).

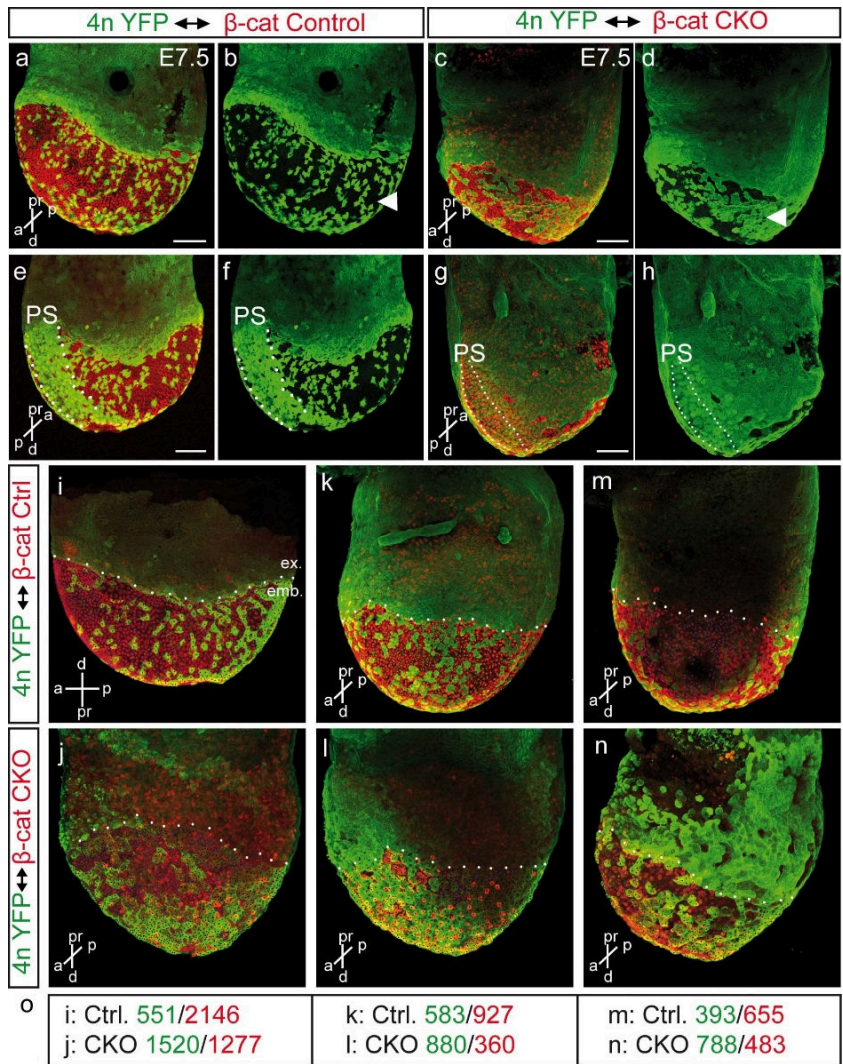


Figure 25: RFP⁺ β-cat CKO cells rarely contribute to DE formation

IHC using α-GFP and α-RFP antibodies to distinguish between 4n YFP⁺ host embryo and RFP⁺ ESC-derived cells, respectively. In contrast to control chimera (a-b), the YFP⁺ VE in CKO aggregation chimera is not replaced by RFP⁺ DE cells at E7.5 (c-d, arrowhead). In both control (e-f) and CKO chimera (g-h), sheets of VE cells underlie the primitive streak region (PS, indicated by dotted area). Quantification of VE and DE cells in individual control (i, k, m) and CKO (j, l, n) chimera. (o) Relative number of VE (green) and DE (red) cells in the embryos depicted in (i-n). White dotted line indicates extra-embryonic/embyonic boundary. Scale bars: 100 μm.

In addition, the tetraploid complementation experiment showed that Sox17⁺ DE cells (YFP⁻/RFP⁺) have replaced almost all VE cells (YFP⁺/RFP⁻) in the mid- and lateral hindgut region in control chimera. However, no Sox17⁺ DE cells but epithelial rupturing and a high contribution of Sox17⁺ VE cells (YFP⁺/RFP⁻) to the endoderm were observed in CKO chimera at E8.5 (Fig. 26j-l, n-p). Interestingly, DE and VE cells were positive for Sox17 in control chimera, whereas the few remaining DE (YFP⁻/RFP⁺) cells in the mid- and hindgut region were Sox17 negative in the CKO chimera and only YFP⁺ VE cells expressed Sox17 (Fig. 26k, o).

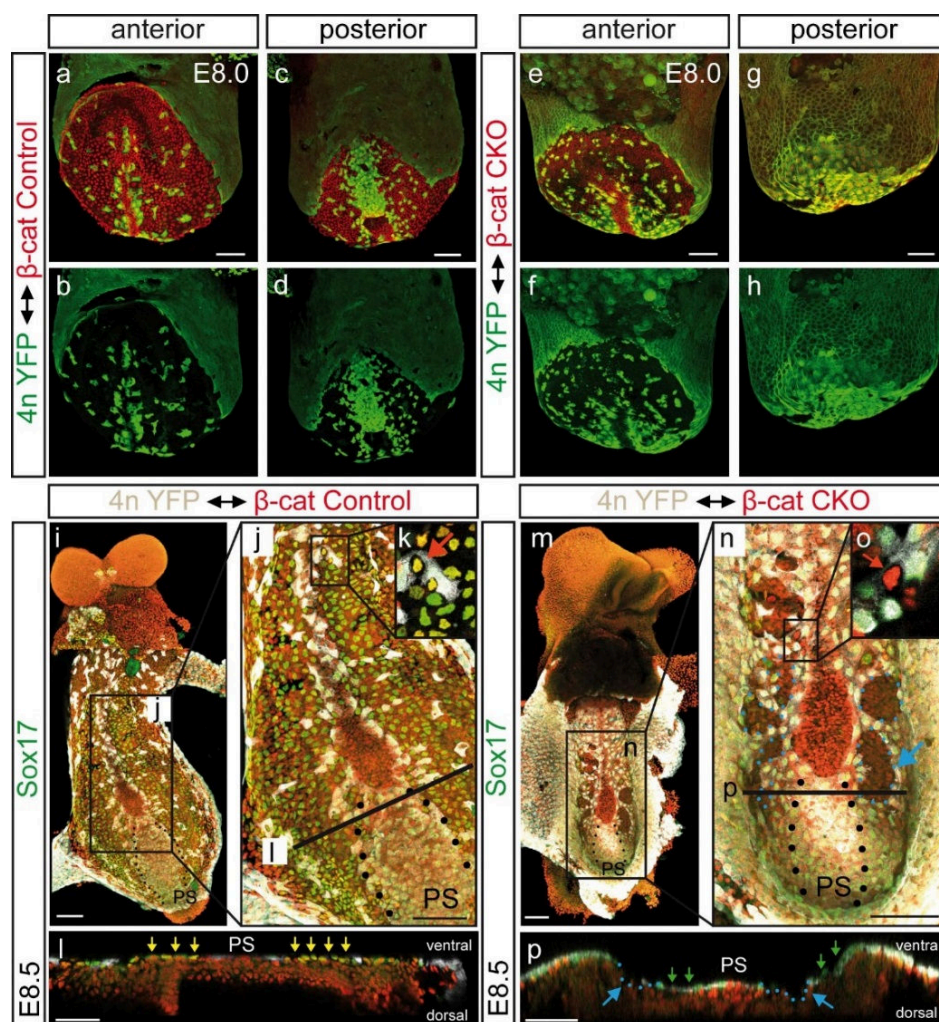


Figure 26: RFP⁺ β -cat CKO cells rarely contribute to mid- and hindgut formation

IHC using α -GFP and α -RFP antibodies to distinguish between 4n YFP⁺ host embryo and RFP⁺ ESC-derived cells, respectively. Comparable numbers of CKO or control ESCs in the anterior (a, b and e, f), but not in the posterior region (c, d and g, h) of chimeric embryos at E8.0. At E8.5, IHC using α -GFP, α -RFP and α -Sox17 antibodies demonstrate that the VE cell layer is not replaced by DE (m-p) and shows rupturing in CKO chimera (n, p, blue dotted area and arrows) compared to controls (j, l). VE cells underlie the PS (indicated by dotted area) in both control and CKO chimera (i-j and m-n). VE cells in the gut of CKO chimera express Sox17 (o and p; green arrows), in contrast to the few DE-like cells (compare o and k; red arrow). In control chimera both the DE and remaining VE cells express Sox17 (k and l; yellow arrows). Scale bars: 100 μ m.

arrows) compared to controls (j, l). VE cells underlie the PS (indicated by dotted area) in both control and CKO chimera (i-j and m-n). VE cells in the gut of CKO chimera express Sox17 (o and p; green arrows), in contrast to the few DE-like cells (compare o and k; red arrow). In control chimera both the DE and remaining VE cells express Sox17 (k and l; yellow arrows). Scale bars: 100 μ m.

These results were confirmed in control and β -catenin CKO embryos derived from natural mating at E8.5. No Sox17 protein was detectable in the mid- and hindgut region but in the developing vasculature in β -catenin CKOs (Fig. 27a, b). These observations raise the possibility that *Sox17* might be a downstream target gene of the Wnt/ β -catenin signalling cascade in the endoderm, but not in the vascular endothelial lineage. Taken together, the results reveal a cell-autonomous requirement of β -catenin for AVE and DE formation. Additionally, both AVE and PVE display head and tail organizer function, respectively.

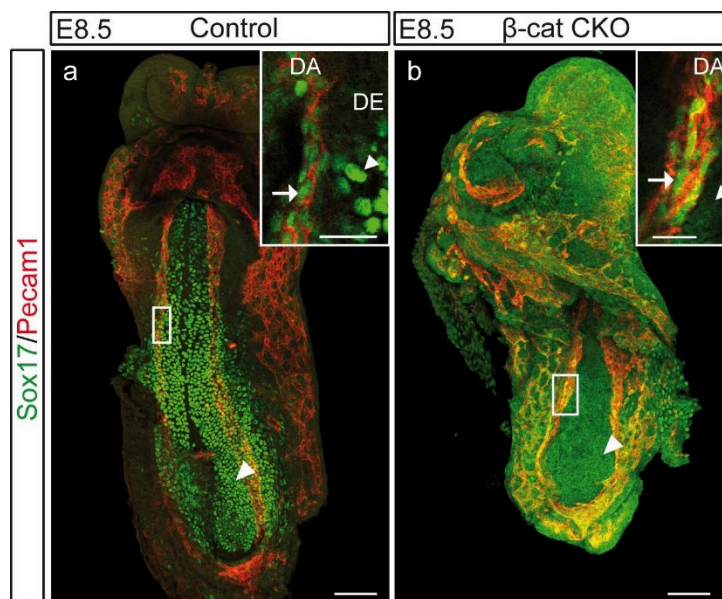


Figure 27: Sox17 is expressed in vascular endothelial cells in β -cat CKO embryos

(a) Sox17 localises to the gut endoderm (arrowhead), and is co-expressed with Pecam1 in the dorsal aorta (DA, arrow) and blood vessels in control embryos as revealed by whole-mount antibody staining at E8.5 (inset). (b) Loss of Sox17 synthesis in the gut endoderm (arrowhead), but not in the endothelial cells of the DA (arrow) and blood vessels in β -catenin CKOs (inset). Scale bars: 100 μ m; inset scale bars: 25 μ m.

4.2.5 Wnt/ β -catenin activates *Sox17* via Tcf4-binding sites in the promoter and regulatory region

In the CKO embryos, β -catenin deletion occurred within the entire VE, which is consistent with the reported *Sox17* expression in PrE at E4.5 (Artus et al., 2010; Burtscher et al., 2012; Morris et al., 2010; Niakan et al., 2010). Deletion throughout the VE coincided with the loss of *Sox17* at E5.5-6.5 (Fig. 28a-d). At E7.25, a few nascent DE cells synthesized *Sox17*, likely due to the delay in Cre-mediated recombination (Fig. 28e-h). The absence or

loss of *Sox17* expression suggests that Wnt/ β -catenin signalling is necessary for maintenance of *Sox17* expression in visceral and definitive endoderm.

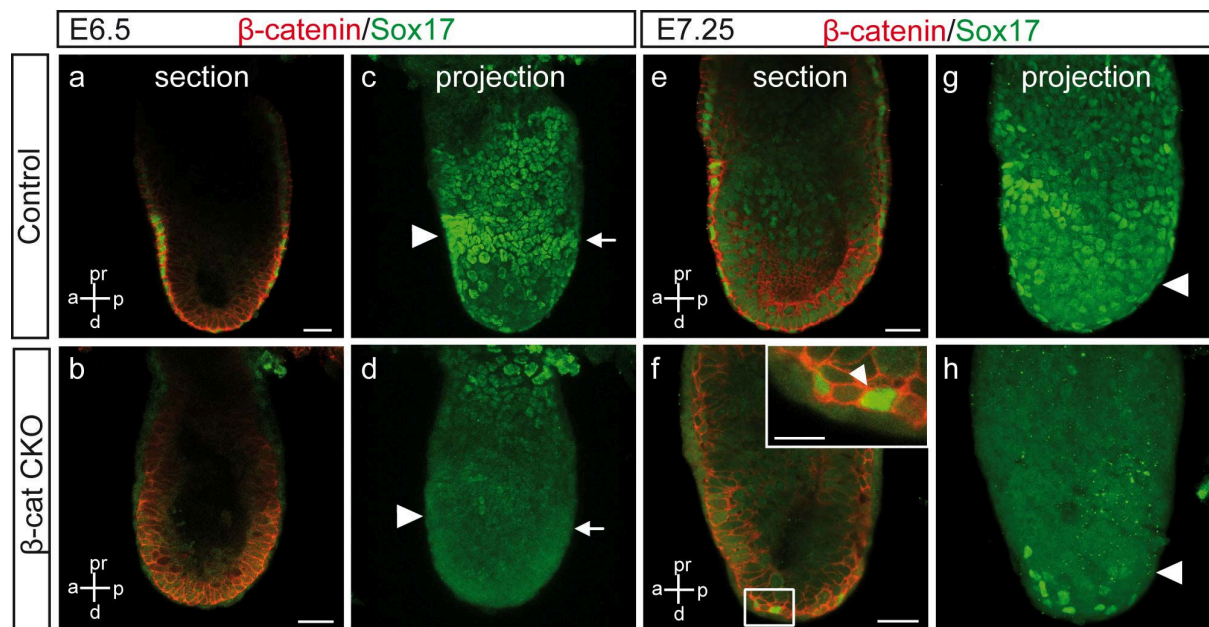


Figure 28: β -catenin deletion affects *Sox17* maintenance in the endoderm

Absence of *Sox17* in the AVE (arrowhead) and PVE (arrow) at E6.5 (b, d) and in the DE (arrowhead) at E7.25 (f, h) in CKOs (a-h). Inset in F shows higher magnification of *Sox17*⁺/ β -catenin⁺ cells (arrowhead).

To support this concept, we examined the *Sox17* up- and downstream regulatory regions for presence of Tcf/Lef-binding elements (TBE; Lickert et al., 2000) using Genomatix software. Thirteen TBEs were identified in an 8945 bp regulatory region, including intron 1 and 2 (Fig. 29a). To test if these TBEs are occupied by Tcf4/ β -catenin transactivation complexes, chromatin immunoprecipitation (ChIP) with Tcf4 and β -catenin specific antibodies was performed and the enrichment on putative TBEs was analysed by quantitative PCR (in collaboration with G. Schotta's laboratory). For this purpose, we used ESCs under pluripotency and endoderm differentiation conditions (Burtscher et al., 2012; Yasunaga et al., 2005). Strikingly, both Tcf4 and β -catenin could be immunoprecipitated in endoderm differentiated ESCs, whereas none of them was bound to the TBEs at the

pluripotent state (Fig. 29b). These results strongly propose that Wnt/ β -catenin signalling regulates *Sox17* via Tcf4/ β -catenin complexes during endoderm formation (Fig. 29c).

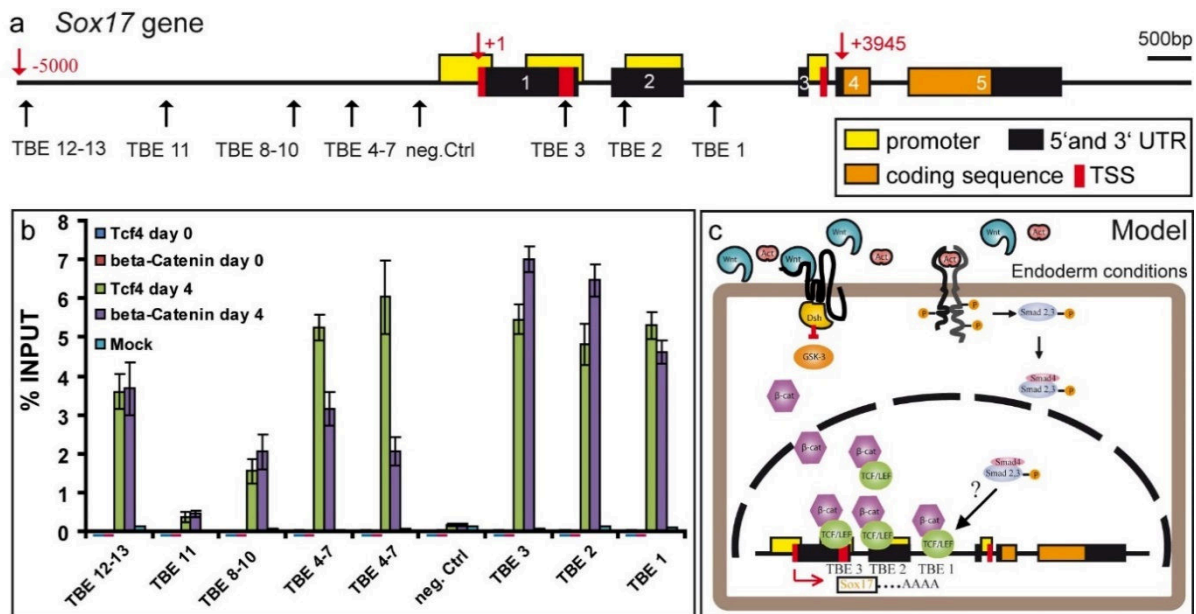


Figure 29: Sox17 is a downstream target gene of Wnt/ β -catenin signalling in the endoderm

(a) *Sox17* gene with indicated Tcf/Lef-binding elements (TBE, black arrows) and regulatory region from -5000 to +3945 bp (red arrow). (b) Chromatin immunoprecipitation with antibodies against β -catenin and Tcf4 on ESCs under pluripotency conditions (d0) or endoderm differentiation conditions (d4) reveals strong accumulation of Tcf4 and β -catenin on TBEs containing fragments during endoderm differentiation. (c) Model: Upon binding of the Wnt ligand to its receptor, the degradation complex is inhibited, β -catenin accumulates in the cytoplasm, translocates to the nucleus and together with Tcf4 activates the expression of *Sox17* in the endoderm. Scale bars: 25 μ m, inset scale bar: 10 μ m. Anterior to the left.

4.2.6 PVE induces gastrula organizer genes in the epiblast in a Wnt/ β -catenin-dependent manner

It was previously shown that Wnt3 expression and Wnt/ β -catenin activity is restricted to the proximal posterior epiblast and PVE at E5.5-6.5 (Ferrer-Vaquero et al., 2010; Rivera-Perez and Magnuson, 2005), where it initiates AP asymmetries and posterior mesendoderm formation (Chazaud and Rossant, 2006; Huelsken et al., 2000; Liu et al.,

1999b; Tortelote et al., 2013). Our analysis suggests that canonical Wnt signalling via Sox17 is essential for VE patterning and posterior axis formation. To further support this notion, we investigated the expression of the Wnt/ β -catenin target gene *Foxa2* (Sawada et al., 2005). *Foxa2* protein could not be detected in the PVE region at E6.0, but in the residual VE cells in CKOs (Fig. 30a-d). This observation indicates that PVE identity was lost upon deletion of β -catenin.

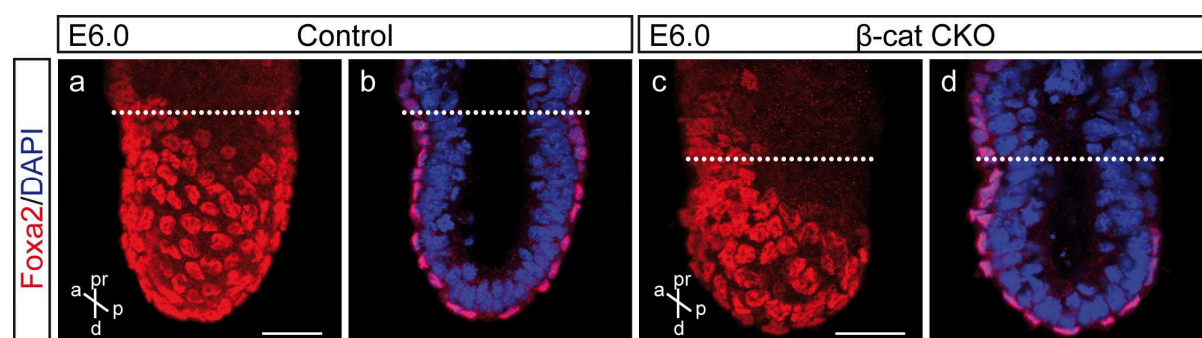


Figure 30: Loss of PVE identity

IHC revealed reduced levels of *Foxa2* in the PVE of mutants at E6.0 (c, d), compared to controls (a, b); white line indicates extra-embryonic/embryonic boundary. Scale bars: 25 μ m.

To investigate whether lack of PVE identity influenced posterior epiblast patterning in a non-cell autonomous fashion, we analysed *Foxa2* expression in CKO and CKO chimeric embryos. At E7.0, *Foxa2* mRNA and protein were not induced to normal levels in the proximal epiblast in CKO embryos. Interestingly, *Foxa2* expression could be rescued by WT VE in CKO aggregation chimera (Fig. 31a-i). Consistently, the gastrula organizer gene *Noggin* was reduced in the node region of β -catenin CKO embryos (Fig. 31j-m). In summary, these results strongly propose that paracrine signals from the PVE induce organizer gene induction in the posterior epiblast in a non-cell autonomous fashion at E6.5 to E7.5 to orchestrate the formation of the tail region.

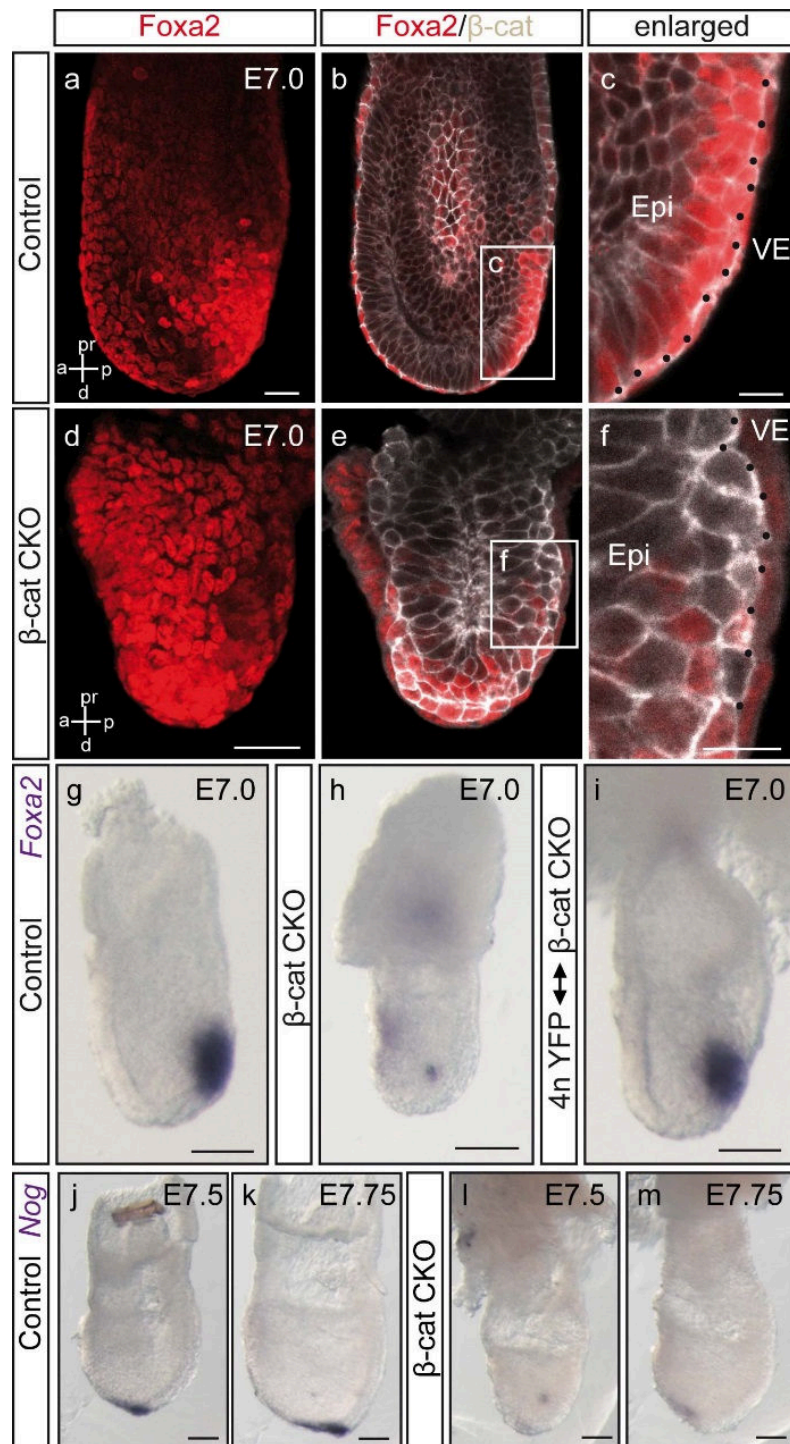


Figure 31: PVE induces organizer gene expression in the posterior epiblast

IHC (a-f) and WISH (g-i) show reduced *Foxa2* expression in the posterior epiblast in CKO (d-f, h) compared to control embryos (a-c, g), which is restored in CKO chimera (i). Mutants show reduced expression of *Noggin* in the node region (l, m) compared to controls (j, k) at E7.5. Insets show higher magnification images. Scale bars (a-b) and (d-e): 25 μm, (c, f): 10 μm, (g-m): 100 μm. Anterior to the left.

Besides the role of Wnt/ β -catenin signalling in endoderm formation and embryonic patterning, the function during endoderm-derived organ formation is far from being understood. Since the CKO of β -catenin resulted in early embryonic lethality, diploid aggregations were performed to overcome lethality and investigate mutant cell behaviour in an otherwise wild-type cell environment. At E15.5, no high percentage CKO chimera was observed. This is in line with the observed embryonic lethality of β -catenin CKO embryos at E9.5. However, low percentage chimera could be obtained. Whereas in control chimera, ESCs contributed to the liver, lung, heart, gut and stomach monitored by lacZ staining (Fig. 32a-e), CKO ESCs only gave rise to a subset of cells in the liver, lung, heart, gut and stomach, respectively (Fig. 32f-j).

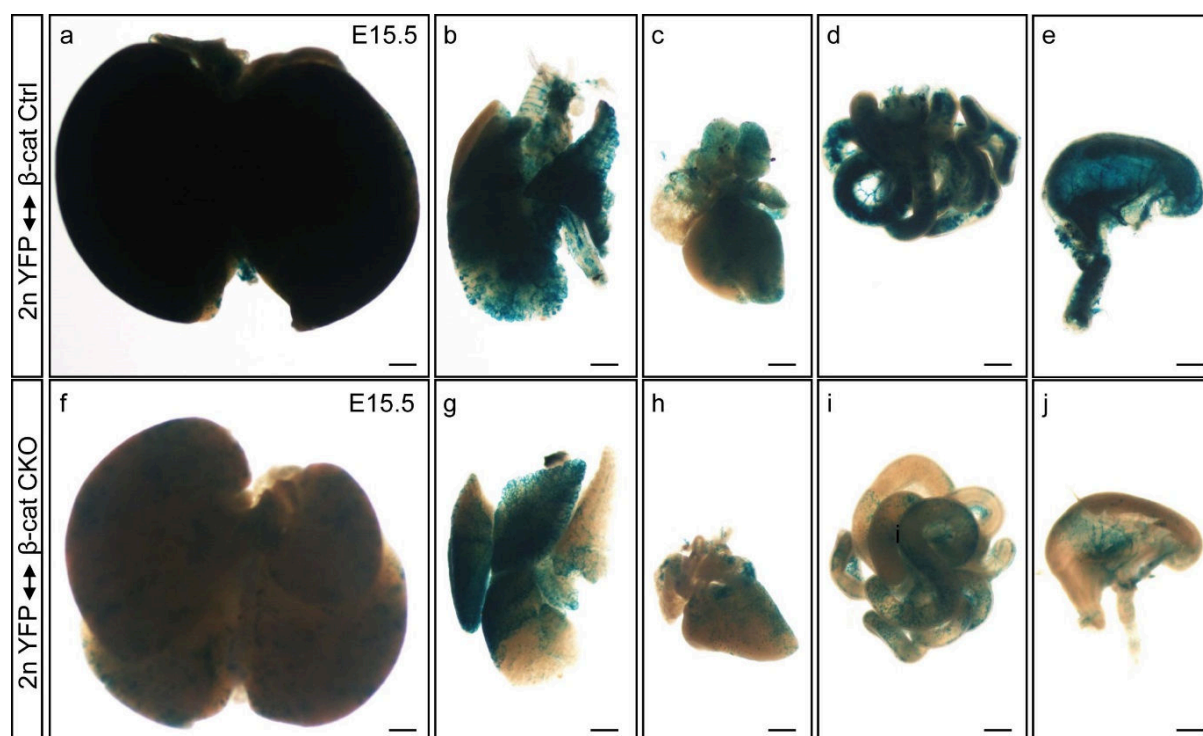


Figure 32: Control and β -catenin CKO ESCs contribute to the formation of embryonic organs

Whole mount lacZ staining of diploid chimera generated from control (a-e) or CKO (f-j) ESCs contribute to the liver (a, f), lung (b, g), heart (c, h), gut (d, i) and stomach (e, j). Scale bars: 500 μ m.

Although both control and CKO ESCs contributed to embryonic organs, the lacZ staining pattern differed between control and CKO embryos. In the control, the ESCs contributed

to the endoderm and vascular endothelial lineage, whereas in the CKO the contribution seemed to be restricted to the endothelial cells. To investigate this in more detail, lacZ stained organs were sectioned and documented (control) or stained with antibodies against GFP (YFP⁺ WT), RFP (CKO) and DAPI. Due to the high contribution of lacZ⁺ cells to the organs in the control and the inability of the antibodies to bind to lacZ-stained tissue, antibody staining of controls could not be performed. However, sections of lacZ-stained control organs demonstrated the ability of control ESCs to form the epithelial lining of the lung, stomach and gut tube, as well as the endothelial cells of the vascular system (Fig. 33a-c). In contrast, CKO ESCs (RFP⁺) failed to contribute to all epithelia of endoderm-derived organs, but contributed to the endothelial lineage (Fig. 33d-f). This observation suggests that during organogenesis Wnt/ β -catenin signalling is required to form the epithelial component of the embryonic organs, which is in line with previous observations within this study. This is in contrast to the endothelial cells of the vasculature, which do not depend on canonical Wnt signalling.

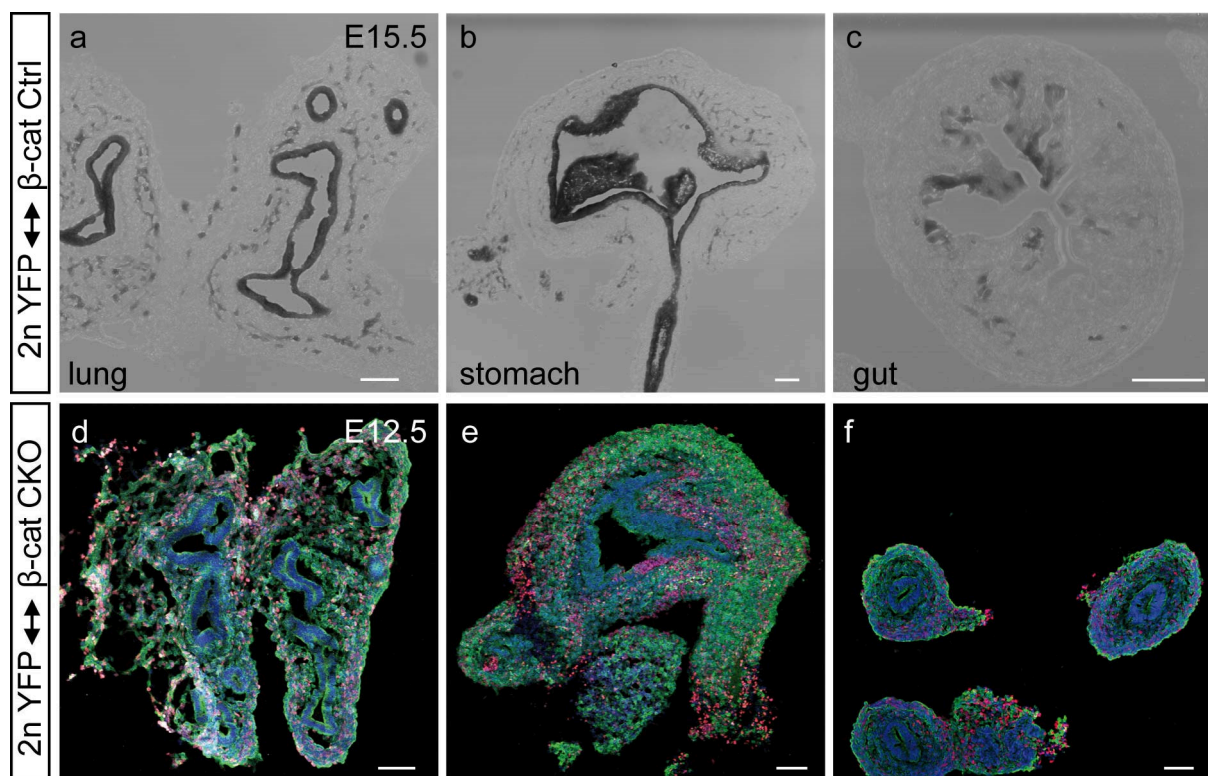


Figure 33: CKO ESCs failed to contribute to the epithelial lining of endodermal organs

Sections of lacZ stained control organs show their capability to form the epithelia of the lung (a), stomach (b) and gut (c) at E15.5. IHC using DAPI (blue) and antibodies against GFP (green, wild-type) and RFP (red, mutant) reveals the disability of CKO cells to form the epithelial lining of the lung (d), stomach (e) and gut (f), while contribution to endothelial cells is not affected. Scale bars: 100 μ m.

Taken together, we showed that deletion of β -catenin in the Sox17⁺ extra-embryonic and embryonic endoderm results in head and tail truncations as well as in absence of mid- and hindgut endoderm. The truncations are caused by impaired Wnt/ β -catenin signalling in the extra-embryonic AVE and PVE which constitute the anterior and posterior organizer, respectively. Loss of signalling function in the embryonic endoderm affects lateral and posterior DE formation which in turn impairs mid- and hindgut as well as epithelia development. Moreover, the canonical Wnt pathway activates Sox17 for endoderm formation and organizer gene induction. Interestingly, formation of the foregut and vascular endothelial cells occurs in absence of Wnt/ β -catenin signalling.

4.3 Generation and application of the hormone-inducible *Sox17^{CreERT2}* knock-in mouse line

4.3.1 The advantage of inducible Cre-driver lines

The conditional deletion of β -catenin in the endoderm and endothelial cells illustrates that usage of constitutive Cre lines such as Sox17Cre lines (Choi, 2012 #773; Engert, 2009 #677; Liao, 2009 #745) is limited as recombination takes place in various Sox17-expressing cell types. Since many signalling cascades and genes are functional during pre- and post-implantation stages, even conditional gene deletion could result in embryonic lethality as demonstrated by the CKO of β -catenin in the Sox17 lineage. The early lethality prevents further analysis of signalling pathways and gene function during later stages of development. For these reasons, an inducible Cre line is required to allow tissue-specific gene deletion. To achieve inducibility of Cre-mediated recombination, Cre can be fused to the ligand-binding domain of the human estrogen receptor (ER), which can be activated

by the synthetic estrogen receptor ligand 4-hydroxytamoxifen (tamoxifen) (Fig. 34). Without tamoxifen, the fusion protein CreER is retained within the cytoplasm by heatshock protein (HSP) 90. Binding of tamoxifen induces a conformational change and thereby releases CreER from HSP90. CreER translocates to the nucleus to become active and perform excision of *loxP* flanked target genes (Fig. 34).

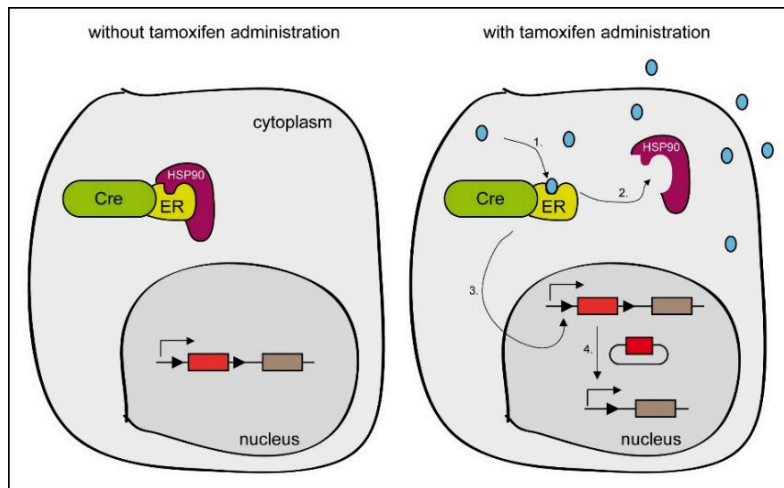


Figure 34: Operating mode of CreER

Without tamoxifen, CreER stays in the cytoplasm and is therefore inactive. Upon tamoxifen application, CreER translocates to the nucleus and activates target genes.

An additional improvement of inducibility can be achieved by reducing the response of CreER to natural estrogen. Modification of the ligand-binding domain of ER by exchange of three amino acids, G400V, M543A and L544A, prevents binding of estrogen to its receptor (Feil et al., 1996; Feil et al., 1997). The now called CreERT2 recombinase is solely inducible by tamoxifen.

By generating a Sox17CreERT2 mouse line, gene function can be investigated in a spatio-temporal resolved fashion. This enables the analysis of gene function in extra-embryonic or embryonic endoderm and during organogenesis of endoderm-derived organs such as lung, liver and pancreas. Furthermore, tissue-restricted reporter recombination allows genetic lineage tracing of endoderm or vascular endothelial progenitor cells at any given time to understand their individual cell fate.

4.3.2 Generation of the *Sox17^{CreERT2}* knock-in mouse line

To generate the hormone-inducible *Sox17^{CreERT2}* line, we used targeted mutagenesis in ESCs to exchange the translational stop codon of *Sox17* with the viral 2A peptide sequence from *Thosea Asigma* virus (Donnelly et al., 2001a). The T2A sequence was followed by the coding region of a codon-optimised CreERT2 recombinase (Feil et al., 1997). The codon-optimisation allows expression of the prokaryotic Cre recombinase in mammalian cells without epigenetic silencing due to the high CpG content. The introduction of the viral T2A sequence results in transcription of a bicistronic mRNA coding for Sox17 and Cre and mediates their co-translational cleavage in an equimolar ratio (Donnelly et al., 2001b). For manipulation of ESCs, we designed a targeting vector containing the T2A sequence followed by *CreERT2* cDNA and a *FRT*-flanked PGK (phospho-glycerate kinase)-driven *neomycin* (neo) resistance gene (Fig. 35a). The neo resistance enables the selection of positive recombined ESC clones. The targeting vector was used for electroporation of IDG3.2 ESCs (Hitz et al., 2007) and 6 neo resistant clones out of 384 selected clones, were confirmed by southern blot using a *Sox17* 5'-probe (Fig. 35b). To obtain chimeric mice, we aggregated confirmed ESCs with CD1 morula (Nagy et al., 1993). High percentage chimera were mated to an ubiquitous Flippase (Flp)-driver line to remove the *FRT*-flanked neo resistance cassette in the germ line to prevent PGK promoter activity. These *Sox17^{CreERT2}* mice were backcrossed two generations into the CD1 background. To distinguish wild-type, heterozygous and homozygous *Sox17^{CreERT2}* mice, we designed a PCR strategy with primers flanking the integrated T2A-CreERT2 sequence and within the sequence (Fig. 35c). Although homozygous mice are underrepresented at weaning age and exhibit reduced fertility, no developmental defects are observed indicating that Sox17 function in the endoderm and vascular endothelial cells as a transcription factor is not affected by the T2A-tag. To confirm the 2A-mediated cleavage of Sox17 and CreERT2 protein, we performed western blot analysis using an antibody against Sox17 protein on lung tissue lysates from six-week-old mice homozygous, heterozygous or wild-type for *Sox17^{CreERT2}* (Fig. 35d). Since the polyclonal Sox17 antibody detects several unspecific bands, an ESC negative control was included to confirm the specificity of the detected Sox17 double band. Two Sox17 isoforms are generated by alternative start codon usage of the

translational machinery. The observed double band in homozygous, heterozygous and wild-type tissue as well as the lack of Sox17-2A-CreERT2 fusion protein with the expected size of 150 kD suggested, that Sox17-2A and CreERT2 were co-translationally cleaved at high efficiency. GAPDH served as a loading control to show that Sox17-2A and wild-type Sox17 protein were synthesized in equimolar amounts.

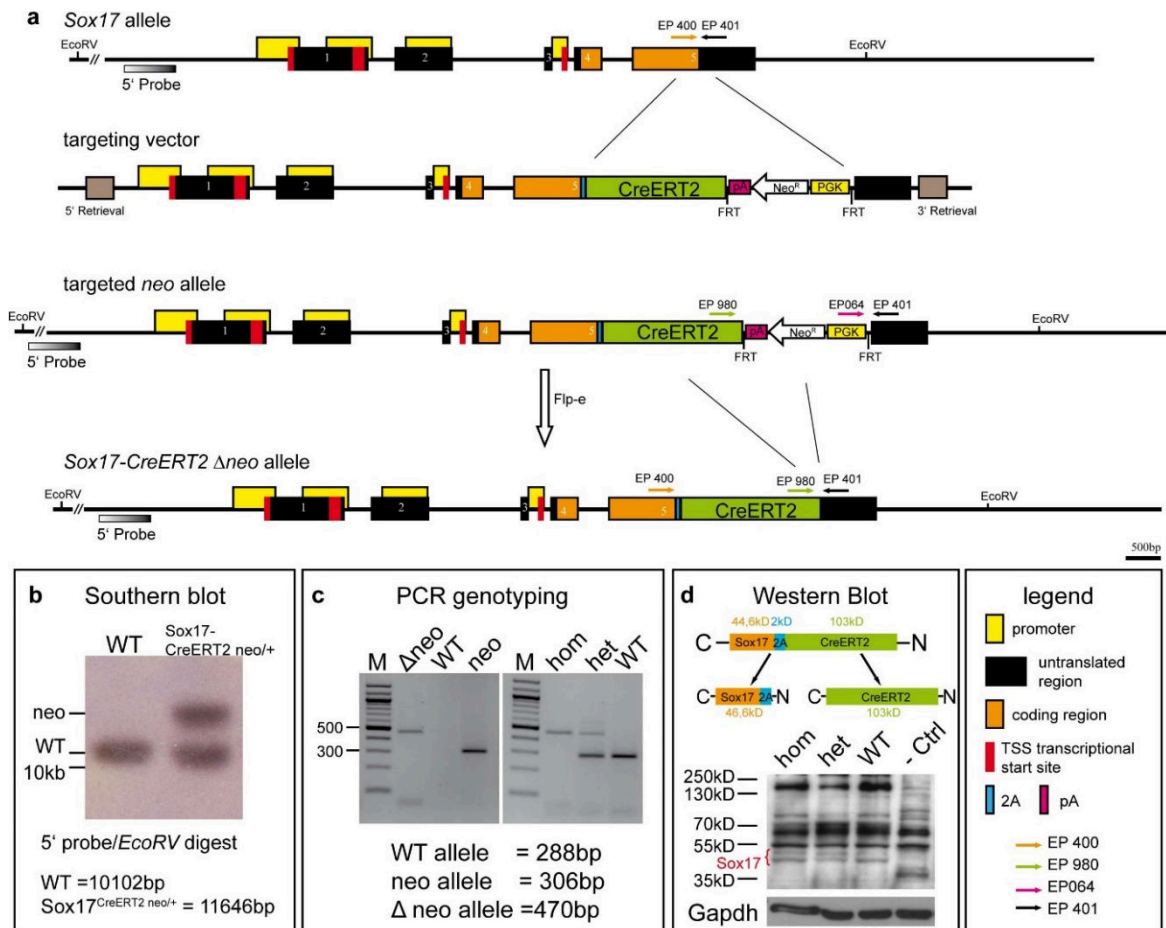


Figure 35: Generation of the Sox17^{CreERT2} allele

(a) Targeting strategy for the Sox17^{CreERT2} allele. A targeting vector was used to introduce the T2A-CreERT2 sequence into exon 5 of the Sox17 gene. The FRT-flanked PGK-driven neomycin resistance cassette (Neo^R) was removed by Flp-mediated excision. Sox17 exons are numbered (1-5). The 5'- and 3'-UTRs are depicted in black, the open reading frame in orange, and the predicted promoter regions in yellow, the transcriptional start sites in red, the T2A tag in blue and the polyA signal in pink. Genotyping primers are designated EP400, EP401, EP980 and EP064. The 5' probe, restriction sites for EcoRV, 5'- and 3'-homology regions (retrieval) are indicated. (b) Southern blot of ESC DNA digested with EcoRV and hybridized with the 5' probe, showing the 10.1 kb wild-type (WT) and 11.6 kb targeted allele (Sox17-CreERT2neo/+).

(c) PCR genotyping of *Sox17^{CreERT2}* mice using the primers EP064, EP401 and EP980 to distinguish the *Sox17^{CreERT2neo}* (neo; 306 bp) and *Sox17^{CreERT2Δneo}* (Δ neo; 470 bp) allele. Homozygous, heterozygous and WT mice were distinguished by using the primers EP400, EP401 and EP980 resulting in a band of 288 bp for the WT and 470 bp for the targeted allele. (d) Western blot analysis using α -Sox17 antibody on adult lung tissue from WT, heterozygous and homozygous *Sox17^{CreERT2}* mice. ESCs served as a negative control. The scheme illustrates the cleavage of the proteins. The double band of Sox17 is indicated. Sox17 (~45 kDa) and Sox17-2A (~47 kDa) can not be distinguished but absence of a Sox17-2A-CreERT2 fusion protein demonstrates the 2A-mediated cleavage of Sox17-2A and CreERT2 protein. Note that the unspecific bands also appear in the WT. α -GAPDH antibody was used to show the equal loading of proteins.

4.3.3 Characterization of recombination properties of the *Sox17^{CreERT2}* mouse line

Next we characterized the recombination properties of our newly developed inducible Cre-driver line using the *Rosa26* reporter (*R26R*) line. The *R26R* line expresses β -galactosidase uniformly and constitutively from the ubiquitously active ROSA26 locus upon Cre-mediated excision of a *loxP*-flanked stop cassette (Soriano, 1999). β -galactosidase converts the substrate X-gal into a blue precipitate thereby labelling the mother and daughter cells. To confirm the inducibility and tissue-specific activity of the CreERT2 line, the heterozygous *Sox17^{CreERT2}* mice were crossed to the *R26R* mice. To exclude leakiness of the CreERT2 system, we stained tamoxifen-induced and non-induced embryos for lacZ (Fig. 36a-c). Tamoxifen was administered by gavage or intraperitoneal injection, but no differences in recombination efficiency was observed between the application methods (Fig. 36b, c).

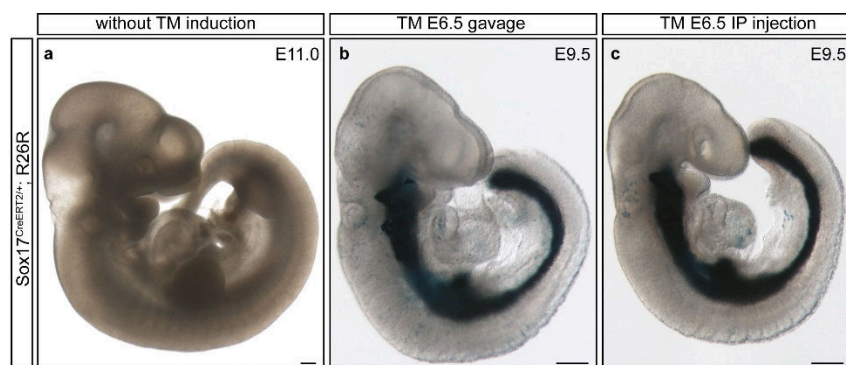


Figure 36: Leak tightness and application methods

(a) No lacZ staining in non-induced embryos. No differences in reporter activity upon tamoxifen administration by gavage (b) compared to intraperitoneal injection (c). Scale bar: 250 μ m.

Tamoxifen was first applied at E6.0 when Sox17 protein is synthesized in the extra-embryonic visceral endoderm. Lineage analysis of *Sox17^{CreERT2/+}* embryos at E7.0 exhibited staining of cells within the visceral endoderm, indicating that Cre activity was restricted to the extra-embryonic lineage (Fig. 37a). In order to label definitive endoderm cells, which arise during gastrulation, tamoxifen was administered at beginning of gastrulation at E6.5. Since most of the definitive endoderm cells at E7.75 exhibited lacZ staining, recombination occurred in early definitive endoderm progenitors (Fig. 37b). Few labelled cells of extra-embryonic origin were observed as *Sox17* is still expressed in VE at the beginning of gastrulation. Induction of Cre-mediated reporter recombination at E7.0 resulted in β -galactosidase expression within the whole gut tube at E8.5 (Fig. 37c). This was confirmed by paraffin sections, which exhibited lacZ staining in the fore-, mid-, and hindgut endoderm (Fig. 37d-f).

Tamoxifen application at E8.0 and lineage analysis at E11.5 revealed staining in the hindgut endoderm reflecting the decreasing Sox17 expression in the fore- and midgut endoderm (Fig. 37h). Additionally, expression was noticed in the developing vasculature (Fig. 37h). As less staining was observed in vascular endothelial cells than expected, we wondered if Cre levels could have an impact on recombination efficiency in the vasculature. Therefore, heterozygous *Sox17^{CreERT2}* mice carrying the *R26R* allele were intercrossed. The lacZ staining of heterozygous and homozygous *Sox17^{CreERT2}* embryos were compared. To focus on β -galactosidase expression in the vascular system, tamoxifen was applied at E9.0 when endodermal expression of *Sox17* is vanished. At E10.5, heterozygous *Sox17^{CreERT2}* embryos revealed staining in a subset of vascular cells and in the region containing the liver and pancreatic anlagen (Fig. 37i). However, in homozygous embryos, a higher percentage of lacZ⁺ cells in the vasculature as well as in the organ anlagen were observed (Fig. 37j).

To analyse the vascular staining pattern in more detail and to identify the lacZ-stained organ, embryos homozygous for *CreERT2* were sectioned. LacZ staining was detected in the dorsal aorta, cardinal vein and additionally in the ventral portion of the pancreas (Fig. 37g), which is in line with previous observations (Choi et al., 2012; Engert et al., 2009; Matsui et al., 2006; Sakamoto et al., 2007; Spence et al., 2009).

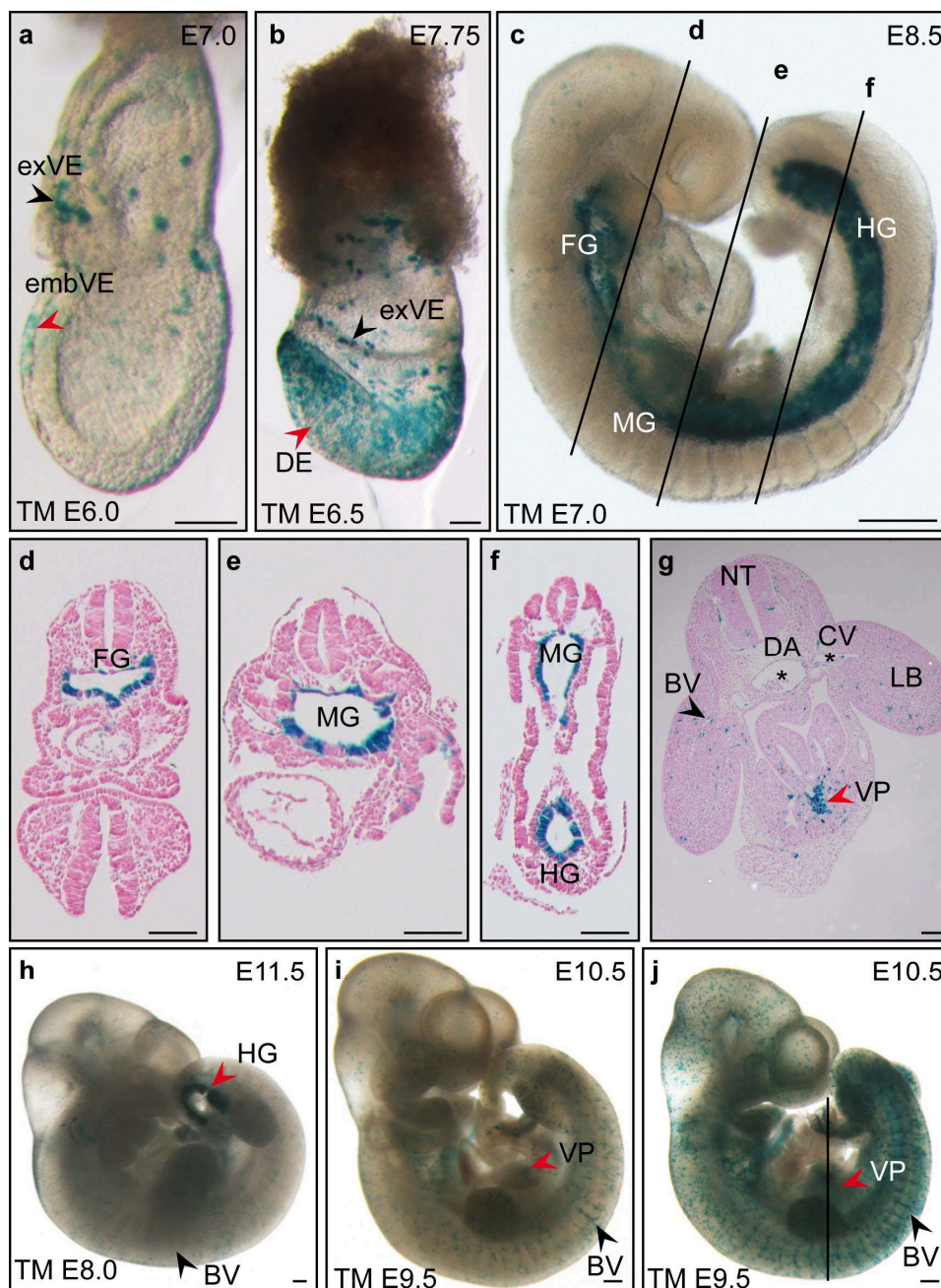


Figure 37: β -galactosidase activity in endoderm and vascular endothelial lineages

Tamoxifen administration and dissection at depicted time points showed recombination in the extra-embryonic (a) and embryonic (b) endoderm and in the primitive gut tube (c). (d-f) Sections of the embryo shown in (c) at indicated levels. LacZ staining is apparent in the hindgut (HG) and blood vessels (BV; h) or in the ventral pancreas (VP) anlagen and blood vessels in heterozygous (i) and homozygous (j) *Sox17^{CreERT2}* embryos. (g) Section of the embryo shown in (j) at indicated level. Asterisks labels the dorsal aorta (da) and cardinal vein (CV). (DE = definitive endoderm; embVE = embryonic visceral endoderm; exVE = extra-embryonic visceral endoderm; FG = foregut; MG = midgut; LB = limb bud; NT = neural tube). Scale bar: (a-b, d-g): 100 μ m), (c, h-j): 250 μ m.

Taken together, early lineage analysis confirmed that CreERT2 is inducible upon tamoxifen treatment and mediates recombination in the expected tissues. Furthermore, we showed that Cre-mediated recombination of the Rosa26 locus is very efficient in the endoderm as almost all cells expressed β -galactosidase. In addition, we found that Cre levels have an impact on the recombination efficiency in the endothelial and ventral pancreas progenitor lineage. The dose-dependant Cre activity should be taken into account for future analysis of the endothelial and ventral pancreatic lineages.

4.3.4 Activation of Cre in specific Sox17⁺ progenitor populations labels their progeny

Next, we aimed to induce Cre-mediated reporter expression in specific progenitor populations to monitor their fate over time. Since our main focus was the generation of an endoderm-specific mouse line, we first analysed contribution of Sox17⁺ cells to the endodermal lineage. Previous lineage tracing analysis showed that the whole gut tube is efficiently labelled when tamoxifen is administered at E7.0 (Fig. 37c). Therefore, tamoxifen was applied at that this stage and recombination patterns were investigated in gut tube-derived organs of homozygous *Sox17^{CreERT2}* embryos at E15.5. All endoderm-derived organs exhibited lacZ staining (Fig. 38a-f). To specify the lacZ⁺ cells within the different organs, we analysed the lacZ expression pattern in paraffin sections. LacZ staining was observed in the epithelial lining of the trachea and bronchi of the lung (Fig. 38g), and in the epithelial lining of the stomach (Fig. 38h) and gut tube (Fig. 38k). In contrast, the mesoderm-derived spleen was not stained (Fig. 38b). Both the dorsal and ventral pancreas showed staining in all cell types besides the mesoderm-derived connective tissue (Fig. 38i-j). In the liver, the staining seemed to be more limited to a specific cell type since not all cells were staining (Fig. 38l). It appeared that the staining was restricted to the hepatic endoderm, called hepatoblast, while the hepatic mesenchyme was devoid of staining due to its mesodermal origin. All cells of the thymus (th) showed lacZ staining, except the connective tissue capsule surrounding the lobe (Fig.

38m). This is consistent with the endodermal origin of the thymus but not of the capsule. Taken together, the restriction of lacZ staining to the endoderm-derived compartments of the organs demonstrates that Cre activity can be selectively activated in endoderm progenitor cells to trace their fate over time.

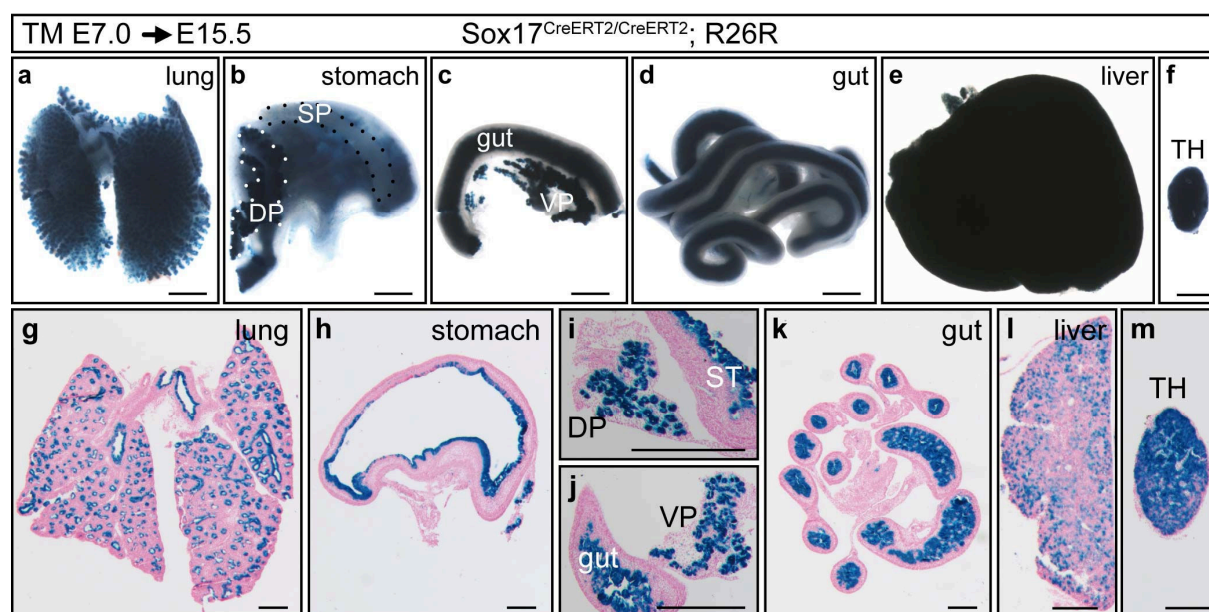


Figure 38: R26R recombination in the DE lineage labels all endoderm-derived organs

Tamoxifen induction at E7.0 and analysis at E15.5. (a-f) LacZ staining of whole mount organs, (g-m) sections of organs depicted in (a-f). β -galactosidase activity is apparent in the epithelial lining of the lung (a, g), stomach (b, h), dorsal (DP; white dotted area in b, i) and ventral pancreas (VP; c, j) and the gut tube (d, k). The majority of cells in the liver (e, l) and thymus (TH; f, m) displays lacZ staining. (SP = spleen, black dotted area) Scale bar: (a-h and k-l): 500 μ m, (i-j and m): 250 μ m.

Beside the endoderm, Sox17⁺ precursors give rise to mesoderm-derived cell types such as the endothelial cells of the vasculature. To constitutively activate Cre-mediated reporter expression in the endothelial lineage, we applied tamoxifen at E9.0 when Sox17 is not longer expressed in the endoderm. At E14.5, all organs isolated from homozygous Sox17^{CreERT2} embryos showed staining in the vasculature (Fig. 39a-h). More precisely, staining was observed in the lobes and trachea of the lung (Fig. 39b), in the stomach (Fig. 39c), in the spleen (Fig. 39c), in the gut (Fig. 39e) and in the dorsal (dp; Fig. 39c) pancreas as well as in the ventral pancreas (vp; Fig. 39d). Furthermore, staining was detected, in the thymus, testis, kidney and heart (Fig. 39a, f, g, h). In the vasculature of the heart,

reporter expression was restricted to the right ventricle and additional expression was apparent in the lining of the aorta and pulmonary trunk (Fig. 39a).

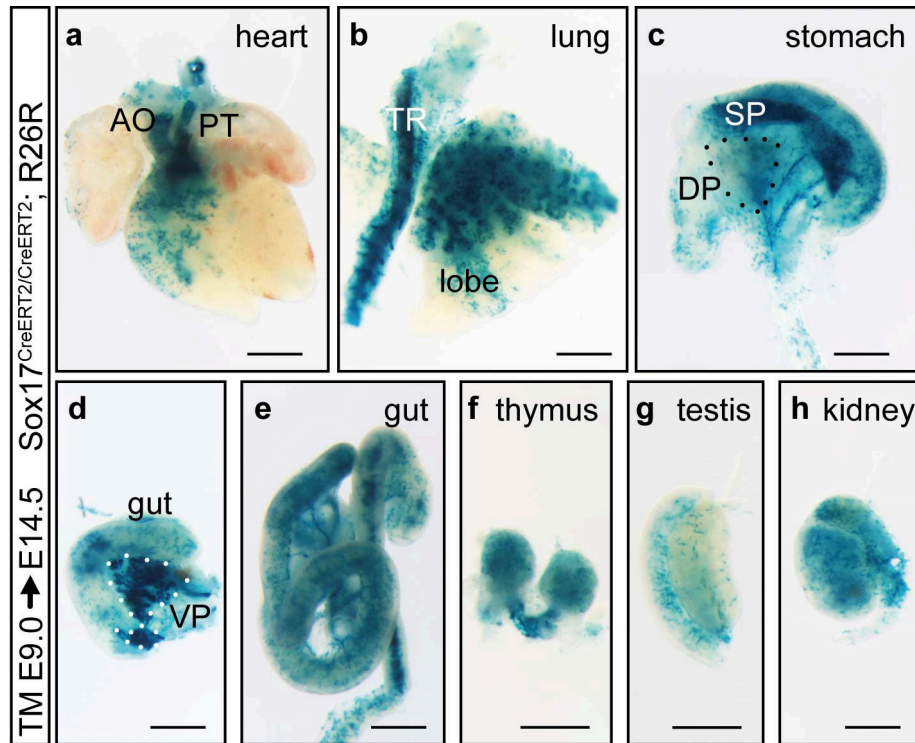


Figure 39: Vascular endothelial cells and ventral pancreas progenitors are lineage-labelled by β -galactosidase using the *R26* reporter

Tamoxifen application at E9.0 and analysis at E14.5 using whole mount lacZ staining, revealed reporter activity in the aorta (AO) and pulmonary trunk (PT) as well as in the vasculature of the right heart chamber (a). β -galactosidase is expressed in the trachea (TR) and lung lobe (b), the stomach, spleen (SP) and slightly in the dorsal pancreas (DP, black dotted area in c), in the gut and broadly in the ventral pancreas (VP, white dotted area in d, e), in the thymus, testis and kidney. Scale bar: 500 μ m.

To investigate the spatial expression pattern of β -galactosidase in more detail, the *Sox17^{CreERT2}* mice were mated to the double-fluorescent Cre *mT/mG* reporter mice (Muzumdar et al., 2007). The *mT/mG* reporter expresses membrane-targeted tandem dimer tomato (mT) preceding Cre-mediated excision and membrane-targeted green fluorescent protein (mG) afterwards. Using the *mT/mG* reporter line allowed us to combine immunohistochemistry with laser scanning microscopy in order to specify the nature of lacZ-stained cells. To confirm the endothelial origin of reporter-expressing cells,

antibodies specific to GFP (mG) labelling the Sox17 lineage and Pecam1 marking endothelial cells were used. GFP was co-localized with Pecam1 in the heart outflow tract (Fig. 40a), the lung lobe (Fig. 40b), the kidney (Fig. 40g), the testis (Fig. 40h), the stomach (Fig. 40i), and the gut (Fig. 40j). In the ventral pancreas, also GFP⁺ single positive cells were observed besides GFP⁺/Pecam1⁺ cells (Fig. 40c). Morphology and lineage analysis strongly suggest that these cells had undergone recombination in the ventral pancreas progenitor region at E9.0 to 9.5 and thus labelled the ventral pancreatic lineage at E14.5. Also, within the thymus (th), only a small fraction of GFP⁺ cells synthesized Pecam1 (Fig. 40d). Since the thymus is a hematopoietic organ, we investigated co-localisation of GFP and CD45, which marks the majority of hematopoietic cells. We found that GFP⁺/Pecam1⁺ cells co-expressed CD45 (Fig. 40e, f). In agreement with previous work, this suggests that the *Sox17^{CreERT2}* line labelled *Sox17*-expressing hemogenic endothelial cells, which give rise to definitive hematopoietic stem cells (Choi et al., 2012; Clarke et al., 2013).

The results show that recombination can be induced in vascular endothelial cells in a spatio-temporal manner alongside activation of Cre in the endoderm. Furthermore, Cre can be activated in the hemogenic endothelium and thereby lineage label definitive HSC. Moreover, Cre activity can be induced specifically in the ventral pancreatic bud.

Taken together, induction of Cre-mediated recombination of reporter lines demonstrated that the *Sox17^{CreERT2}* line is sensitive to tamoxifen. Lineage analysis showed that recombination occurred in the expected lineages during development. In addition, endodermal and mesodermal Sox17⁺ precursor cells could be selectively labelled.

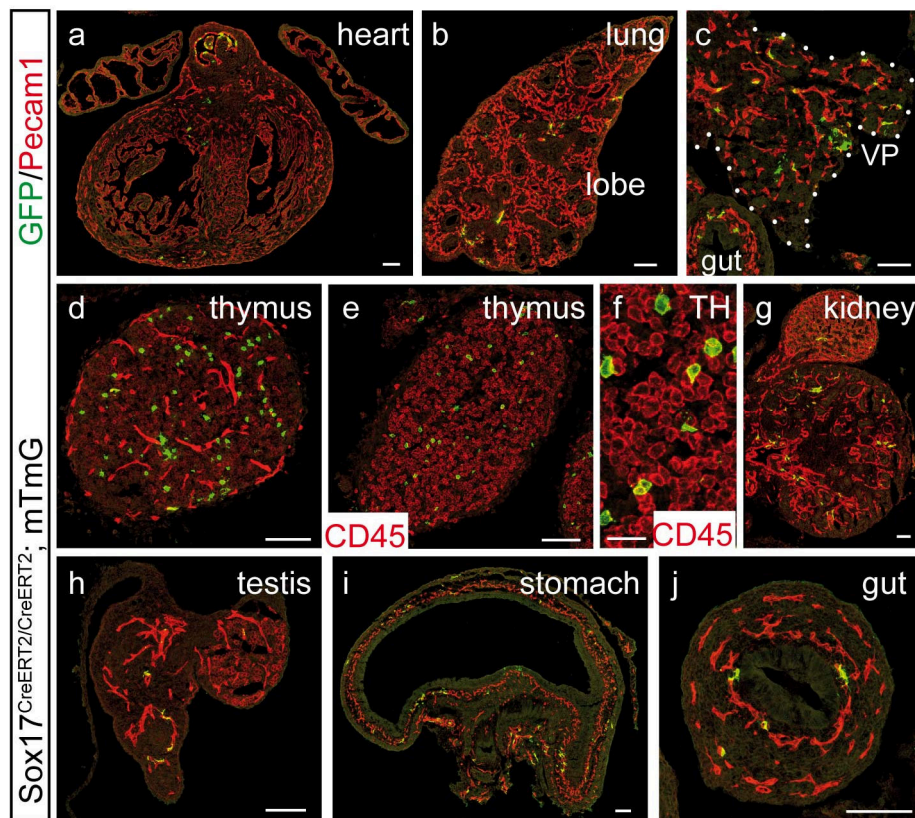


Figure 40: The *mT/mG* reporter labels endothelial, ventral pancreatic and hematopoietic stem cell lineages

IHC on sections with antibodies specific to GFP, Pecam1 and CD45. Cre-mediated recombination is restricted to a subset of vascular endothelial cells in the heart and to the epithelial lining of the aorta and pulmonary trunk (a). β -galactosidase activity is evident in the trachea and the blood vessels of the lung lobes (b), and stomach (i). In the ventral pancreas (VP; dotted area in c), recombination is apparent in some pancreatic cells as well as in the blood vessels. β -galactosidase is active in the vascular endothelial cells of the gut (j), testis (h), kidney (g) and thymus (d). In addition, the reporter is active in the hematopoietic stem cells within the thymus (TH, e) labelled by CD45 antibody. (f) Magnification of boxed area in e. Scale bar: 100 μ m, except for f: 25 μ m.

4.3.5 *Sox17^{CreERT2}* enables lineage tracing of visceral endoderm cells during formation of the primitive gut tube

As previously shown (Burtscher et al., 2012; Engert et al., 2013b; Kanai-Azuma et al., 2002), *Sox17* is expressed in the extra-embryonic endoderm prior to gastrulation. During gastrulation, when DE is formed, the VE cells of the embryonic compartment are

dispersed by DE cells (see also Fig. 25) (Kwon et al., 2008). Since DE and VE cells express the same set of marker genes, these two tissues cannot be distinguished one the molecular level. Therefore the fate of the VE cells during endoderm development is currently unknown. The characterization of recombination abilities of the *Sox17^{CreERT2}* line showed that Cre activity can be selectively activated in the VE (Fig. 37a) and thus provides a valuable tool to investigate VE cell fate during DE and gut development.

To exclude recombination in DE cells, tamoxifen was applied at E5.0. At E8.5, lineage analysis displayed β -galactosidase activity in a subset of cells within the gut endoderm. Most of the lacZ⁺ cells remained in the hindgut (hg, Fig 41a, b), which is in line with previous observations (Kwon et al., 2008). Additionally, lacZ⁺ cells contributed to the fore- and midgut endoderm (Fig. 41b, c). Administration of tamoxifen at E5.0 and restricted β -galactosidase activity to a small proportion of endoderm cells suggest that recombination of the reporter was restricted to VE cells. As lineage analysis showed, the recombined VE cells can be followed over time suggesting that *Sox17^{CreERT2}* line can be used to eventually understand the fate of the VE cells during gut development.

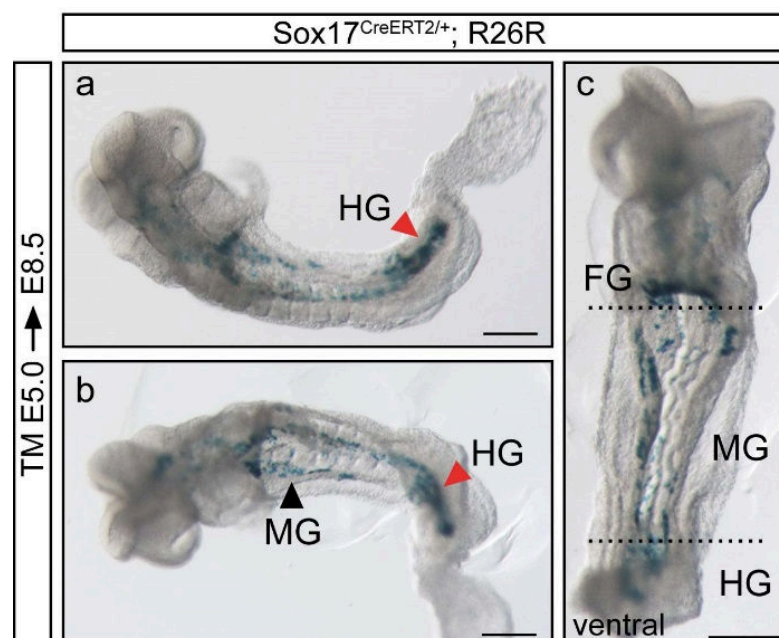


Figure 41: Contribution of VE cells to DE

Administration of tamoxifen at E5.0 and analysis at E8.5 shows that VE cells contribute to the foregut (FG; c), midgut (MG; b, c) and hindgut (HG; a, b) endoderm. (a) Embryo is shown from a lateral view and (b) ventral view. (c) Magnification of (b). Scale bar: 250 μ m.

4.3.6 Sox17⁺ ventral pancreas progenitors contribute to the exocrine cell-lineage of the ventral pancreas

Our Sox17⁺ lineage tracing demonstrated that recombination can be specifically induced in the ventral pancreas anlagen (Fig. 37g). To further investigate the fate of ventral pancreas progenitors during organ formation, tamoxifen was administered at E9.0 and pancreata were analysed at E14.5 and P31. As already shown, at E14.5 the ventral part of the developing pancreas showed strong β -galactosidase activity (Fig. 42a, c), whereas the dorsal part exhibited weak staining within the pancreas (Fig. 42a, b). Paraffin sections revealed that in the dorsal pancreatic bud only few endothelial cells of the vascular system expressed β -galactosidase (Fig. 42d). In comparison, the ventral pancreatic bud showed staining in a subset of pancreatic cells (Fig. 42e, f). At P31, analysis of the pancreas displayed contribution of ventral pancreas progenitors to the head of the pancreas, which is located within the curve of the duodenum. However, whole mount analysis exhibited, that only a small proportion of the pancreatic head derived from Sox17⁺ progenitor cells (Fig. 42g, h). To investigate the nature of the stained cells in more detail, paraffin sections of P31 pancreata were performed. The morphology of lacZ-stained regions suggested that Sox17⁺ progenitor cells gave rise to exocrine acinar cells (Fig. 42i-k), but not to endocrine cells of the islet of Langerhans. This would either suggest, that the ventral pancreatic anlage does not contribute to the endocrine compartment or that *Sox17* is only expressed in exocrine progenitors of the ventral pancreas. These interesting observations have to be analysed in more detail in future experiments.

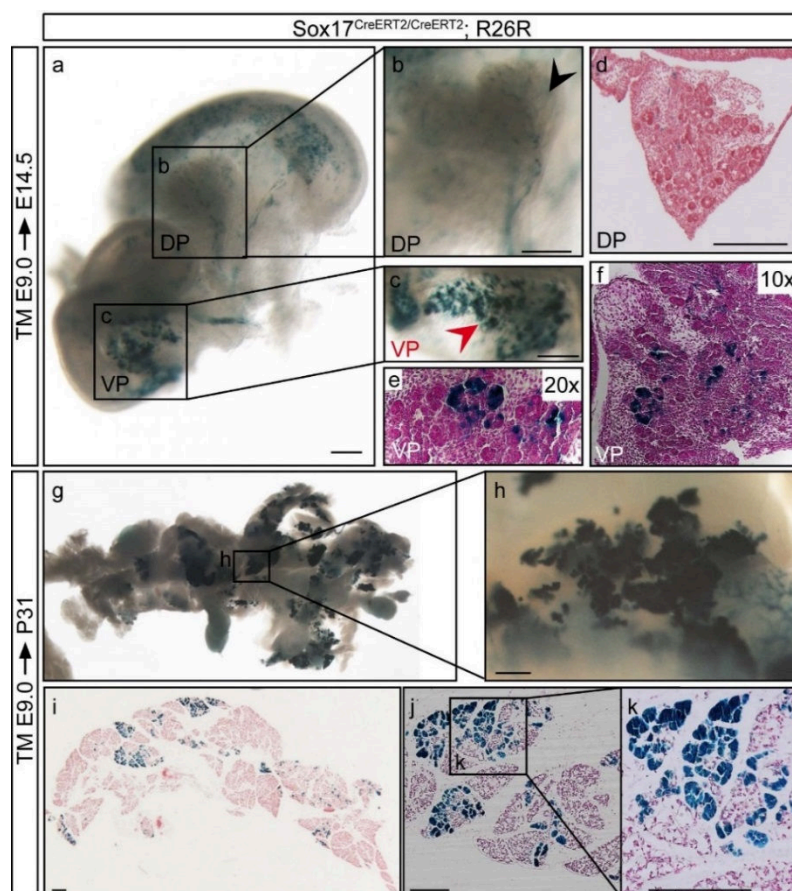


Figure 42: Recombination in the ventral pancreas lineage labels exocrine acinar cells

(a) Tamoxifen administration at E9.0 and whole mount lacZ staining of the ventral (VP) and dorsal pancreas (DP) at E14.5 exhibited expression of β -galactosidase in only the ventral bud. (b, c) Magnification of boxed area in (a). (d) Paraffin section of (b). (f) Paraffin section of (c). (e) Magnification of (f). (g) Tamoxifen application at E9.0 and analysis at P31 showed contribution of Sox17⁺ VP progenitors to the head of the pancreas. (h) Magnification of boxed area in (g). (i-k) Paraffin sections revealed the exocrine nature of the lacZ stained cells. (k) Magnification of boxed area in j. Scale bar: 250 μ m.

4.3.7 Is Sox17 a marker for angioblast progenitors?

Previous Sox17⁺ lineage tracing experiments, which were performed during my diploma thesis, using the *Sox17^{2AiCre}* Cre (Engert et al., 2009) and the *R26* reporter line (Soriano, 1999) revealed β -galactosidase expression in the epiblast in roughly 50% of the obtained *Sox17^{2AiCre/+}* embryos. Single recombined cells were evenly distributed in the epiblast prior to gastrulation (Fig. 43a-b, diploma thesis, modified) and in the germ layers afterwards (Fig. 43c, d). The observed pattern is not described in the literature and raises the question about the cellular fate of lacZ⁺ epiblast cells.

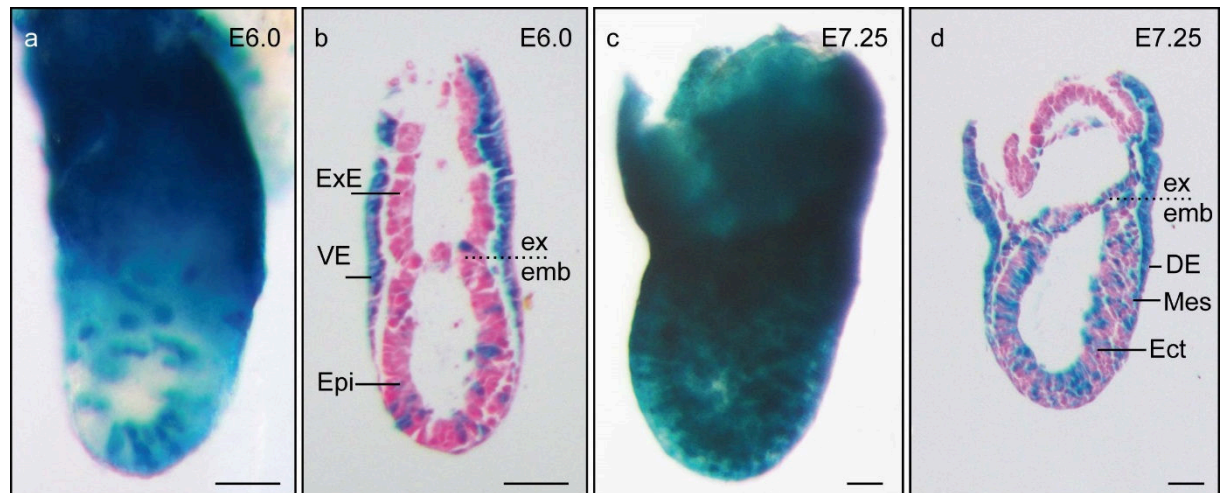


Figure 43: LacZ expression in the epiblast and germ layers

(a) LacZ expression is observed in the visceral endoderm (VE) and in single cells of the epiblast (Epi) at E6.0. (b) Paraffin section of (a). (c) β -galactosidase staining is apparent in the VE and definitive endoderm (DE), the mesoderm (Mes) and the ectoderm (Ect) at E7.25. (d) Paraffin section of (c). The broken line indicates the extra-embryonic (ex)/embryonic (emb) boundary. ExE = extra-embryonic ectoderm. Scale bar: 50 μ m.

As previously shown (Burtscher and Lickert, 2009), the endoderm precursors arise in the posterior epiblast prior to gastrulation and are marked by expression of *Foxa2*. Since the observed lacZ-expression pattern at E6.0 does not mark the territory of the *Foxa2* epiblast progenitors of the endoderm, the intriguing question about the identity of the lineage-labelled epiblast progenitors remains. In addition to the endoderm, *Sox17* is expressed in endothelial cells of the blood vessels and in hematopoietic stem cells (Burtscher et al., 2012; Choi et al., 2012; Clarke et al., 2013; Engert et al., 2009; Kim et al., 2007; Liao et al., 2009; Matsui et al., 2006; Sakamoto et al., 2007). Since an early endoderm precursor fate can be excluded, the lacZ stained epiblast cells might reflect progenitors of the endothelial/hematopoietic lineage. To address this question, we can now use the newly generated *Sox17^{CreERT2}* line and we will perform *Sox17* lineage tracing experiments in the near future.

5 Discussion

5.1 Summary of results

The aim of this study was to investigate the impact of epigenetic regulators and signalling pathways on gastrulation and germ layer formation in mouse. More precisely, we used the Cre/loxP technology to specifically delete β -catenin and therefore suppress canonical Wnt signalling in the Sox17⁺endoderm germ layer. The conditional knock-out of β -catenin in the Sox17 lineage revealed that β -catenin deletion is not restricted to the definitive endoderm but also occurs in the anterior and posterior visceral endoderm (AVE and PVE). Here, deletion of β -catenin leads to anterior head and posterior neural tube truncations. The rescue of these truncations by wild-type VE demonstrates that β -catenin is required non-cell autonomously for anterior and posterior organizer formation. Moreover, the results indicate that impaired migration of AVE cells to the future anterior side led to head organizer defects. In the posterior side of the embryo, Wnt/ β -catenin signalling is essential to establish and/or maintain PVE identity. We showed that the PVE signals to the adjacent epiblast in a paracrine manner to induce gastrula organizer gene expression such as *Foxa2* and *Noggin*. These results demonstrate for the first time that the PVE is crucial for posterior organizer formation as previously suggested (Beddington and Robertson, 1999; Liu et al., 1999a; Rivera-Perez and Magnuson, 2005; Tam and Behringer, 1997).

Deletion of β -catenin in the embryonic endoderm resulted in lack of lateral and posterior endoderm which in turn impaired mid- and hindgut development as well as formation of endoderm-derived epithelia. Although endoderm formation is impaired, the axis elongation defect of the CKO embryos was rescued by wild-type VE. Together with the observation that the PVE remains a coherent epithelial sheet overlying the primitive streak during axis formation and elongation this supports the idea that the PVE displays tail organizer activity.

The canonical Wnt pathway signals via β -catenin to activate target gene transcription. To do so, nuclear β -catenin functions as a transcriptional co-activator for Tcf/lef DNA binding

transcription factors. Strikingly, Tcf4/ β -catenin transactivation complexes accumulate at TBEs in the Sox17 regulator region upon endoderm differentiation *in vitro*. Furthermore, Sox17 protein is absent in the endoderm of β -catenin CKO embryos *in vivo*. This strongly suggests that that Wnt/ β -catenin signalling induces Sox17 expression and thus endoderm formation *in vitro* as well as *in vivo*. Finally, the CKO analysis revealed that neither formation of the foregut nor the formation of vascular endothelial cells depend on canonical Wnt signalling.

Initially, we intended to understand which signalling cascades are involved in the specification of distinct endoderm-derived organs such as lung, liver and pancreas. However, even the conditional inhibition of canonical Wnt signalling caused a phenotype that was too severe to analyse this later aspect of development. Therefore, our newly generated Sox17^{CreERT2} line will be of great help. This hormone-inducible line shows tissue-specific Cre-mediated recombination in the endoderm and vascular endothelial cells. This allows the investigation of extra-embryonic and embryonic endoderm formation as well as endoderm-derived organ formation by induction of Cre activity at different time points during development, e.g. during endoderm pattern formation, organogenesis or in adult endoderm-derived tissues. Moreover, by using the Sox17^{CreERT2} line, we can analyse the cell fate of different Sox17⁺ progenitors e.g. whether Sox17 lineage⁺ epiblast cells give rise to the vasculature; whether Sox17⁺ ventral pancreas cells contribute to the exocrine and/or endocrine lineage and whether extra-embryonic endoderm cells contribute to functional cell types in embryonic and adult tissues. Taken together, these analyses will reveal more about signalling cascades and factors influencing the differentiation of certain progenitors during endoderm-derived organ development.

To unravel the epigenetic mechanisms that regulate early embryogenesis, we have additionally analysed the role of the Elongator complex during post-implantation development and in the ESC system. This analysis revealed that deletion of the Elongator protein 4 is sufficient for loss of Elongator complex function confirming the requirement of all subunits for Elongator activity in mammals. *Elp4*-deficient embryos are growth retarded, delayed in their development and die between E10.5-11.5. Although only a slight delay of marker gene expression was observed during gastrulation and early somite

stage, the mRNA profile revealed that mutant embryos are severely affected on diverse levels such as metabolism and immune response. Since cells of the immune system are generated later in development, these changes emerge from inappropriate activation of genes and loci. *In vitro*, mutant ESCs expressed pluripotency markers and showed self-renewal capacity. However, mRNA profiling revealed an up-regulation of genes involved in cell differentiation suggesting that pluripotency conditions are compromised. In addition, the differentiation of ESCs to endoderm is impaired which was confirmed by mRNA profiling. Moreover, the profile points to an epigenetic function of the Elongator complex. In the following, the different result parts will be discussed in the context of the state-of-the-art.

5.2 The *Sox17^{CreERT2}* knock-in mouse line displays spatio-temporal activation of Cre recombinase in distinct Sox17 lineage progenitors

5.2.1 Effects of allelic combinations for *Sox17^{CreERT2}* and Cre reporters

The transcription factor Sox17 plays a crucial role during endoderm formation and is a key regulator of cell-lineage decisions during embryonic and fetal development (Choi et al., 2012; Clarke et al., 2013; Engert et al., 2013b; Engert et al., 2009; Kanai-Azuma et al., 2002; Kim et al., 2007; Lange et al., 2009; Liao et al., 2009; Morris et al., 2010; Park et al., 2006; Sakamoto et al., 2007; Spence et al., 2009). Since Sox17⁺ progenitor contribution is not restricted to a single cell population, genetic-lineage tracing and genetic manipulation within the Sox17 lineage are limited in their application. Therefore, we generated a hormone-inducible Sox17Cre line to activate Cre-mediated recombination in distinct Sox17⁺ progenitor populations.

The *Sox17^{CreERT2}* allele does not interfere with Sox17 function as a transcription factor. Although mice homozygous for *Sox17^{CreERT2}* are underrepresented (12% out of 25%

expected) and show reduced fertility, no phenotypic differences were observed among wild-type, heterozygous and homozygous embryos during embryonic development. Loss of Sox17 function in the endoderm results in developmental defects and embryonic lethality at E10.5 (Kanai-Azuma et al., 2002; Viotti et al., 2012). Since homozygous embryos were obtained at Mendelian ratio between E8.5 and E15.5, it is unlikely that the T2A-tag disrupts Sox17 function. However, the tag could influence Sox17 mRNA stability, resulting in reduced protein synthesis. As the T2A-tag is fused to the C-terminus of the Sox17 coding region, protein stability should not be affected according to the N-end rule pathway (Varshavsky, 1997). In contrast, the tag could interfere with protein-protein interaction. Subtle changes in transcription factor levels or impaired interactions could affect lineage specification and therefore interfere with tissue homeostasis at later stages of development.

The EST profile, which illustrates approximate expression patterns inferred from EST sources (<http://www.ncbi.nlm.nih.gov/UniGene>), suggests that Sox17 is expressed in the testis, oviduct, lung and pancreas amongst others. Interestingly, Sox17 expression in the lung influences lung epithelial progenitor cell behaviour (Lange et al., 2009). In the adult pancreas, Sox17 expression is required for β -cell homeostasis and function (Jonatan, unpublished data). Sox17 expression in the arteries was suggested to induce arterial specification and maintenance in the mature vasculature (Corada et al., 2013). These data support the idea that Sox17 regulates progenitor cell behaviour and lineage specification in different tissues (Lange et al., 2009). Therefore, altered Sox17 expression e.g. by reduced mRNA stability could affect differentiation and tissue homeostasis. Nevertheless, for most analyses heterozygous *Sox17^{CreERT2}* mice will be used, so that side effects in the homozygous state are ruled out.

Recombination characteristics of CreERT2 were analysed using two different Cre reporter lines, namely the *R26* and the *mT/mG* reporter (Muzumdar et al., 2007; Soriano, 1999). The analysis revealed differences in recombination efficiency between both reporter lines. Varying staining intensity between lacZ and GFP might be due to the comparison of whole organs to organ sections, homozygous reporter alleles to heterozygous alleles or differences in the recombination ability of distinct Cre reporter lines. Analysis of various

allelic combinations for CreERT2 and Cre reporters are necessary to definitely explain the described observations. Besides the differences in recombination efficiency, both Cre reporters are active in the same cell types and tissues demonstrating the specificity of *Sox17^{CreERT2}*.

5.2.2 The inducible *Sox17^{CreERT2}* mouse line allows lineage-restricted cell fate analysis and genetic modifications

Lineage analysis demonstrated that *Sox17^{CreERT2}* is inducible upon tamoxifen treatment in the expected cell lineages. Induction of Cre activity in progenitors of the extra-embryonic or embryonic endoderm resulted in the labelling of VE or DE cells. Activation of Cre in the embryonic compartment led to lineage labelling of all endoderm-derived epithelia. Induction of Cre activity between E9.0 to E9.5 resulted in lineage labelling of vascular endothelial cells, hematopoietic cells and cells of the ventral pancreas.

However, differences in lacZ staining intensity in endothelial cells and VP progenitors were observed depending on the allelic combination of *Sox17^{CreERT2}*. Presence of two *Sox17^{CreERT2}* alleles did not change the recombination pattern but the recombination seemed to be more homogenous and less mosaic and resulted in an approximately two fold increase in lacZ staining. The equivalent increase in Cre levels and staining intensity reflects the linear recombination efficiency from one allele to two alleles, which can be also observed in other Cre lines. Therefore, recombination of reporter alleles might not occur in early *Sox17⁺* progenitor cells if only one copy of Cre is present. In this case, not the whole progeny would be labelled. For CKO studies this would mean that gene deletion could be mosaic resulting in phenotypes with different severities complicating the interpretation of the data. In the endoderm, no differences in staining intensity were observed. This might be due to an early recombination event in endoderm progenitors or stronger expression of *Sox17* in the endodermal lineage compared to the vascular lineage. The difference in recombination efficiency, in particular in the endothelial lineage, should be taken in account for further studies.

Nevertheless, the analysis confirmed that Cre can be activated in the reported domains of *Sox17* expression (Burtscher et al., 2012; Choi et al., 2012; Clarke et al., 2013; Kanai-Azuma et al., 2002; Sakamoto et al., 2007; Spence et al., 2009). Therefore, the *Sox17^{CreERT2}* mouse line is a valuable tool to study *Sox17* lineage contribution in a tissue and time resolved manner. In addition, this mouse line can be used for tissue-specific genetic modifications.

5.2.3 Using *Sox17^{CreERT2}* to investigate VE cell fate

Prior to gastrulation the epiblast is surrounded by extra-embryonic endoderm which was long thought to contribute invariably to extra-embryonic tissues. Formation of the DE as the outer most cell layer supported the idea that the VE was replaced by DE during gastrulation. The combination of live cell imaging and genetic labelling demonstrated that VE cells in the embryonic compartment are not replaced by DE but dispersed (Kwon et al., 2008). This finding suggests that extra-embryonic cells contribute to the formation of the embryo proper. Since the VE and DE express the same set of markers, it is not possible to distinguish between these two cell populations. Therefore, the cell fate and function of dispersed VE cells within the DE is unknown.

Using the new *Sox17^{CreERT2}* line, we can induce reporter activity solely in VE cells and follow their fate over time. Short-term lineage tracing revealed that VE cells remain in the gut endoderm until E8.5 which is in line with previous findings (Kwon et al., 2008). It was suggested that incorporation of VE cell in the DE displays an alternative to increase surface area to keep up with the fast growth of the mouse embryo (Kwon et al., 2008). This suggests that VE cells adopt an embryonic fate to facilitate endoderm formation. Since VE-derived endoderm cells differ in their morphology and cellular organisation compared to epiblast-derived endoderm cells (Kwon et al., 2008) rather suggests that the VE displays a specialised subpopulation within the DE. In favour of this idea, genetic labelling revealed that VE cells preferentially organise around signalling centres such as the primitive streak (PS), node and axial mesoderm (Kwon et al., 2008). Interestingly,

subpopulations of the VE hold signalling function itself during body axis formation (Beddington and Robertson, 1998; Rivera-Perez and Magnuson, 2005; Tam and Beddington, 1992). In the anterior side, the VE displays head organizer activity whereas in the posterior the VE constitutes tail organizer activity. The distinct morphology, cellular composition and localisation of VE-derived endoderm cells during gastrulation and axis elongation suggests that these VE cells remain in the endoderm as a specialised cell population. The close proximity to the PS, node and axial mesoderm suggests an interaction between endoderm-derived and extra-embryonic endoderm-derived signalling centres to initiate organ formation along the AP axis. During organ formation, incorporated VE cells could be involved in further patterning by providing signals comparable to their function during gastrulation or by defining cellular compartments due to their special cellular architecture. If VE cells are maintained during adult hood or only serve as transient organizer cell population that is lost in late development is currently not known.

The *Sox17^{CreERT2}* line provides a convenient tool to investigate whether VE cells contribute to the endoderm and endoderm-derived organs in the long run and whether VE cells organise at specific domains/structures to interact with neighbouring tissue and to continue with their signalling function.

5.2.4 Using *Sox17^{CreERT2}* to investigate the pancreatic composition

In mice, pancreas development becomes apparent at E9.0 when two buds emerge from the foregut endoderm on the opposing side. The buds increase in size, change their morphology and start to form tubular structures. This early phase of remodelling is referred to as the primary transition. The epithelial pancreatic buds are not differentiated at this stage. Cell fate analysis revealed that Carboxypeptidase A1 (Cpa1)⁺ tip progenitors give rise to all pancreatic lineages before E14.0 (Zhou et al., 2007). During further development, the buds fuse and form one single organ at E12.5. Now, the secondary transition is initiated involving expansion, further branching into a complex tubular

network in parallel with differentiation of tip and trunk cells which give rise to exocrine and endocrine or ductal cells, respectively. After the secondary transition, the pancreas consists of clusters of acinar cells at the tip of the duct branches and endocrine cell clusters which are scattered throughout the organ. The acinar cells together with the ductal cells constitute the exocrine pancreas. Acinar cells synthesise and secrete digestive enzymes via the duct into the duodenum to digest the uptaken food. The endocrine pancreas consists of five different cells types residing in the islets of Langerhans. The endocrine cells secrete hormones into the blood to regulate glucose homeostasis. Pancreas development and lineage specification is reviewed in Shih et al., 2013 (Shih et al., 2013).

Understanding pancreas development and differentiation of multipotent progenitors to the exocrine and endocrine lineages is the basis for development of better treatments of pancreas-associated disease such as diabetes mellitus. Genetic lineage tracing of different cell populations represents a valuable tool to investigate the development from multipotent progenitors to lineage-restricted specialised cells as demonstrated by the study of Zhou et al., in 2007.

Interestingly, Cre-mediated recombination of reporter alleles in Sox17⁺ ventral pancreas around E9.5 seems to label exocrine acinar but not endocrine or ductal cells, which needs to be confirmed. Since the previous model suggests that ventral and dorsal pancreas equipotentially contribute to all pancreatic lineage (Beger et al., 2009; Gu et al., 2003; Zhou et al., 2007), likewise Sox17⁺ VP cells should give rise to all lineages if the whole ventral pancreas expresses Sox17 at E9.0. Lineage labelling of only the acinar cells would therefore suggest that ventral pancreas in general contributes only to the exocrine compartment of the mature pancreas. If Sox17 is expressed in a subset of VP cells, which give rise to acinar cells only, this would suggest that Sox17 marks an acinar progenitor pool that arises from the VP. To distinguish these possibilities, a detailed analysis of Sox17 expression in the ventral pancreatic bud will be important to test if all VP progenitors are labelled uniformly. Nevertheless, solely labelling of acinar cells might suggest that lineage specification occurs separately in the dorsal and the ventral pancreas and already during primary transition when the buds receive different signals from distinct neighbouring

tissues. This might have further implication in choosing the right signalling factor cocktail for deriving exocrine and endocrine cell populations from ESCs for β -cell replacement therapy.

5.2.5 Using *Sox17^{CreERT2}* to investigate hemangioblast specification

The *Sox17^{CreERT2}* mouse line can also be used to investigate the fate of Sox17 lineage⁺ epiblast progenitors which were previously identified using the constitutively active *Sox17-2A-iCre* line (Diploma thesis). The presence of Sox17 lineage⁺ cells in the epiblast at E6.0 indicates that Sox17 is expressed much earlier at the blastocyst stage. Later, it was shown, that Sox17 is up-regulated in cells of the ICM during the transition from the 16- to the 32-cell stage (Morris et al., 2010). During further development, Sox17⁺ cells become restricted to the primitive endoderm (PrE) lineage (Morris et al., 2010). The Sox17⁺ PrE then gives rise to Sox17⁺ parietal and visceral endoderm which surrounds the epiblast.

The observation that approximately 50% of the *Sox17^{2AiCre/+}* embryos show Sox17 lineage⁺ cells in the epiblast as well as in the VE suggests that Cre levels need to reach a certain threshold to label not only the PrE lineage but also ICM-derived epiblast cells. This explains the expression of β -galactosidase in the epiblast whereas the fate of these cells remains unknown. Lineage analysis at later stages revealed that Sox17-expressing cells give rise to the endoderm, vascular endothelial cells and hematopoietic stem cells (Burtscher et al., 2012; Choi et al., 2012; Clarke et al., 2013; Engert et al., 2009; Kanai-Azuma et al., 2002; Kim et al., 2007; Liao et al., 2009; Matsui et al., 2006; Sakamoto et al., 2007). Since endoderm progenitors originate from the anterior primitive PS during gastrulation, the intriguing question arises whether these Sox17 lineage⁺ epiblast cells are already specified to become progenitors of the endothelial and/or hematopoietic lineage. Therefore, we aim to induce reporter gene recombination in Sox17⁺ ICM cells at E3.5-4.5 and trace their fate over time. Since tamoxifen displays anti-implantation action (Pugh and Sumano, 1982), blastocysts need to be isolated and cultured in tamoxifen and transferred back to pseudo-pregnant females (Takaoka et al., 2011), which we will do in

future experiments. This approach allows us to investigate whether Sox17 lineage⁺ epiblast cells are committed to become the hemangioblast.

The hemangioblast represents a bipotential progenitor which gives rise to hematopoietic and vascular cells. Detailed mapping revealed that hemangioblasts reside in the posterior region of the PS and are defined by expression of T and Flk1 (Huber et al., 2004). During further development the hemangioblast emigrates into extra-embryonic sites (ExE, yolk sac, allantois) and intra-embryonic sites (ectoderm) thereby getting restricted to the hematopoietic or angiogenic lineage (reviewed in Coultas et al., 2005).

Anigoblasts aggregate along the AP axis to form the dorsal aorta and cardinal vein. From here, further sprouting of vessels form the ramified vascular network work (Coultas et al., 2005). Vascularisation of the neural tube occurs by sprouting of the perineural vascular plexus between E9.0-10.0 (Nagase et al., 2005). Interestingly, genetic lineage tracing using the *Sox17-2A-iCre* line revealed lacZ⁺ cells in the neural tube as early as E8.5 (Engert et al., 2009). At E10.5, lacZ⁺ cells were observed additionally around the neural tube. The presence of Sox17 lineage⁺ cells in the neural tube before sprouting of the perineural vascular plexus occurs, suggests that endothelial cells of the neural tube arise from distinct precursors. The endothelial cells of the neural tube would be in the perfect position to colonise the whole embryonic body along the AP axis to form the vascular network.

Definitive hematopoiesis occurs in endothelial cells at the para-aortic splanchnopleural region, called the hemogenic endothelium. The close connection of endothelial and hematopoietic stem cells further supports the idea of the hemangioblast. It is interesting to note, that Sox17 is not only expressed in endothelial cells of the vasculature but also in the hemogenic endothelium and in hematopoietic stem cells (Choi et al., 2012; Clarke et al., 2013). The *Sox17^{CreERT2}* line represents an appropriate tool to investigate whether Sox17 lineage⁺ epiblast cells are committed to the vascular and/or hematopoietic lineage before appearance of T⁺/Flk1⁺ hemangioblasts in the PS region. This would imply that specification of the vascular and hematopoietic lineage occurs in distinct progenitors at an earlier time point than assumed up to now.

5.3 Wnt/ β -catenin signalling regulates Sox17 expression and is essential for organizer and endoderm formation in the mouse

5.3.1 Conditional knock-out of β -catenin in the Sox17 lineage

Deletion of β -catenin in the Sox17⁺ extra-embryonic endoderm, namely the AVE and PVE, resulted in failure of head and tail organizer formation in β -catenin CKO embryos. The anterior head and posterior neural tube truncations demonstrate a non-cell autonomous requirement of Wnt/ β -catenin signalling in the AVE and PVE for anterior and posterior organizer formation, respectively. In the embryonic endoderm, β -catenin is required cell-autonomously for Sox17-dependent lateral and posterior endoderm formation and loss of β -catenin impairs mid- and hindgut development. Expression of Sox17 in the endoderm in turn depends on Wnt/ β -catenin signalling in both *in vitro* and *in vivo*. Since no defects in the vasculature can be observed in β -catenin CKOs, vascular endothelial cell formation seems to be independent of β -catenin signalling.

Besides its function in canonical Wnt signalling, β -catenin is a component of the cell-cell adhesion complex. However, there is strong evidence that the observed phenotype of β -catenin CKOs is caused by loss of β -catenin signalling rather than impaired cell-cell adhesion. The cell adhesion molecule E-cadherin is still localised to the basolateral membrane of VE and DE in CKO embryos from E5.5 to E7.5, implying that adherens junctions are normally formed. In addition, vascular endothelial cells seem to form normal tubular structures indicating that cell-cell adhesion can be established and maintained in the absence of β -catenin. Furthermore, epithelial integrity of the endoderm is maintained up to E8.5. At this stage, loss of organizer induction has already led to head and tail truncations and impaired DE formation has caused mid- and hindgut defects. The observed rupturing of VE in mid- and hindgut region is likely caused by failure of generating the appropriate amount of DE cells to form the epithelium of the mid- and hindgut. Moreover, we identified *Sox17* as a downstream target of Wnt/ β -catenin signalling in endoderm differentiation culture. Loss of Sox17 protein in the AVE, PVE and

DE, which represent regions of active Wnt signalling, suggests direct or indirect regulation of *Sox17* in VE and DE. Since target gene activation and/or maintenance is affected before a morphological phenotype is observed, the CKO phenotype is most probably caused by loss of β -catenin signalling function. Above all, it was previously demonstrated that Plakoglobin can substitute for β -catenin to maintain cell-cell adhesion (Haegel et al., 1995; Huelsken et al., 2000; Lickert et al., 2002). Thus, loss of β -catenins signalling function and target gene activation accounts for all phenotypes observed in β -catenin CKOs.

5.3.2 Wnt/ β -catenin signalling is essential for head and tail organizer formation

Loss of β -catenin in the VE results in AVE migration defects rather than failure of DVE specification. Although β -catenin is deleted in the entire VE by E5.5, DVE marker genes are induced in CKO embryos, which is consistent with previous findings in β -catenin KO embryos (Huelsken et al., 2000). Absence of β -catenin throughout the VE suggests that β -catenin is already deleted in the PrE. Although it was previously shown that asymmetric localized Lefty1⁺ PrE cells give rise to DVE at E5.5 (Takaoka et al., 2011), the signals which regulate the translocation of PrE progenitors to the future DVE region are not known. Further movement of DVE cells to the prospective anterior side was suggested to be initiated by Wnt morphogen gradients subsequently to DVE induction (Kimura-Yoshida et al., 2005). As β -catenin deletion in PrE cells does not affect DVE formation but AVE migration, the results suggest that tightly balanced levels of Wnt activity is important for VE patterning and AVE migration but not for DVE induction.

The deletion of β -catenin leads to severe anterior and posterior axis truncation at E8.5. The anterior truncation can be explained by AVE defects. As previously shown, KO of AVE-specific genes and tissue ablation demonstrated the importance of the AVE for neural induction and maintenance of anterior epiblast identity (Beddington and Robertson, 1998; Perea-Gomez et al., 2001; Thomas and Beddington, 1996). However, deletion of AVE-specific genes, such as *Hex* and *Dkk1* (Martinez-Barbera et al., 2000; Mukhopadhyay et al., 2001) only affects anterior but not posterior axis development whereas deletion of

β -catenin in the VE affects both. Therefore, impaired posterior axis development implicates that PVE is important for posterior axis formation.

Lack of PVE identity leads to non-cell autonomous failure of organizer gene induction in the epiblast of β -catenin CKOs. The absence of the Wnt/ β -catenin target gene *Foxa2* in the PVE and loss of *Sox17* throughout the VE suggests that PVE identity is impaired. Dysfunctional PVE fails to induce the gastrula organizer gene *Foxa2* in the neighbouring epiblast. However, replacement of PVE by wild-type VE rescues *Foxa2* expression. These results indicate that Wnt/ β -catenin signalling in the PVE is required for proper organizer gene induction. Further support for this idea comes from studies demonstrating that *Wnt3* is expressed in the PVE and that lack of *Wnt3* or β -catenin leads to failure of AP axis formation (Huelsenken et al., 2000; Rivera-Perez and Magnuson, 2005). In addition, Wnt signalling was shown to be active in the PVE region at the time of PD axis conversion (Ferrer-Vaquer et al., 2010). Interestingly, the PVE remains a coherent epithelial sheet which overlies the PS from E6.5 to E8.5. In contrast, newly formed DE cells intercalate in a distal position into the VE and migrate to lateral and anterior regions (Burtscher et al., 2012; Burtscher and Lickert, 2009; Viotti et al., 2012). Additionally, DE as well as mid- and hindgut seems to have little effect on posterior axis formation as the tail truncation phenotype can be rescued by wild-type PVE in the absence of mid- and hindgut formation. Since the PVE overlies the PS region, it is perfectly positioned and in direct contact with the posterior medial epiblast to secrete paracrine factors that induce and maintain organizer gene expression. We speculate that these secreted factors are downstream of the Wnt/ β -catenin signalling cascade and *Sox17*, as both β -catenin CKO and *Sox17* KO embryos exhibit posterior truncations. Taken together, these observations indicate that the PVE secretes paracrine factors that induce gastrula organizer genes in the adjacent epiblast, analogous to the Nieuwkoop centre in *Xenopus* and the posterior marginal zone in chick embryos (Bachvarova et al., 1998; Harland and Gerhart, 1997; Nieuwkoop, 1969).

5.3.3 Wnt/ β -catenin signalling via Sox17 is required for DE formation

Besides the important function of Wnt/ β -catenin signalling in patterning and organizer gene induction, canonical Wnt signalling is also required for DE formation. It was previously shown that failure of Wnt/ β -catenin-mediated gene induction in the epiblast progenitors leads to ectopic cardiac mesoderm formation in expense of DE formation (Lickert et al., 2002). This suggests that Wnt/ β -catenin signalling is important to induce and specify mesendoderm epiblast progenitors to become DE (Huelsenken et al., 2000; Lickert et al., 2002). As no fate switch to the cardiac lineage occurred in the β -catenin CKO mutants, Sox17⁺ cells are already specified for the DE lineage. Furthermore, loss of *Sox17* expression in the endoderm and impaired endoderm formation indicates that Wnt/ β -catenin signalling regulates *Sox17* expression and an endoderm program. Interestingly, we identified several TBEs in the *Sox17* up- and downstream regulatory region. These TBEs were occupied by Tcf4 and β -catenin only in ESCs differentiated to endoderm. This result demonstrates that in presence of Wnt ligands, β -catenin and Tcf4 translocate to the nucleus to activate *Sox17* expression. Sox17 further activates an endoderm program for DE formation. The similarity of mid- and hindgut defects in β -catenin and Sox17 KO embryos implies that all Wnt activity is mediated by activation of *Sox17* (Kanai-Azuma et al., 2002; Viotti et al., 2012). This also shows that the Cre-mediated recombination is very efficient, as only very few, if any, Sox17⁺ cells escape genetic deletion of β -catenin. Since β -catenin CKO and Sox17 KO still form ADE and foregut endoderm, Wnt/ β -catenin signalling via Sox17 activation is essential for lateral and posterior endoderm formation.

5.3.4 Wnt/ β -catenin is required for epithelia formation of endoderm-derived organs

To circumvent embryonic lethality of CKO embryos in order to investigate Wnt signalling during organogenesis, we analysed the contribution of β -catenin CKO ESCs to endodermal organs of low-percentage diploid chimera. Loss of β -catenin impaired the formation of

endoderm-derived epithelia which is in line with the observation that Sox17⁺ DE cells solely give rise to the epithelial compartment of endoderm-derived organs (Engert et al., 2009). Since definitive endoderm is not formed in β -catenin CKO embryos and mutant ESCs fail to contribute to endoderm-derived epithelia, it is likely that lack of definitive endoderm directly results in the failure of epithelia formation. Lack of lateral and posterior endoderm results in absence of mid- and hindgut endoderm and consequentially leads to lack of mutant ESC-derived epithelia. Although anterior endoderm formation seems to be independent of Wnt signalling, no β -catenin CKO ESCs were found in epithelia of foregut-derived organs. Since it was shown, that different levels of Wnt signalling are required for endoderm-organ specification (McLin et al., 2007), this might suggest that this process was not initiated. Alternatively, further differentiation of endoderm cells could be impaired.

The sole contribution of wild-type ESCs to organ and epithelia formation demonstrates that wild-type ESCs had competitive advantage and substituted for loss of mutant endoderm cells. This indicates that differentiation of foregut endoderm to distinct epithelia of endoderm-derived organs is affected whereas initial foregut formation still occurs in absence of Wnt signalling. Further support comes from the observation that Wnt signalling is involved in cell proliferation and differentiation. This strongly suggests that differentiation and/or proliferation of foregut endoderm cells is defective preventing formation of epithelia.

5.4 The Elongator complex is required for proper differentiation of the early mouse embryo

5.4.1 The function of the Elongator complex during early mouse embryogenesis

The analysis of β -catenin function during endoderm development demonstrates how a signalling cascade integrates signals from the environment to activate specific

transcription factors, which in turn pattern the whole embryo and specify defined cell types. Regulation of gene expression on a higher level is controlled by the accessibility of DNA for transcription. This is regulated by chromatin remodelling enzymes, DNA modifying enzymes and the state of the compacted chromatin. One complex which is supposed to be involved in modification of DNA is the Elongator complex. It was previously shown that this complex is required for active DNA demethylation of the paternal pronucleus to erase paternally inherited methylation patterns (Okada et al., 2010). However, the function of the Elongator complex was not analysed during later development leaving the question which effects active DNA demethylation plays during gastrulation, neurulation and organogenesis. In this study, we demonstrate that the deletion of the *Elp4* subunit impairs embryonic development. Mutant embryos are growth retarded and delayed in development between gastrulation and neurulation. *In vitro* endoderm differentiation exhibited that mutant ESCs fail to differentiate or show abnormal differentiation abilities which might be caused by inaccurate expression of pluripotency- and differentiation-associated genes. Deregulated gene expression impairs development further than E10.5-11.5.

Although the multi-locus deletions also affect *Elp4* neighbouring genes, we strongly believe that the observed phenotype is caused solely by loss of Elongator function for several reasons: 1. *Pax6* is not expressed at the time when the phenotype is evident. In addition, it was previously shown that the *Pax6* KO leads to postnatal and not embryonic lethality (Hogan et al., 1986; Roberts, 1967). 2. Although *Rcn1* and *Immp1L* are expressed in the embryo between E7.5 and E7.75, the KO of *Rcn1* as well as the KO of the *Immp1L* family member *Immp2L* does not affect viability (Lu et al., 2008; Vega et al., 2003). Since *Immp1L* and *Immp2L* together form the mitochondrial inner membrane peptidase (IMP) complex it is unlikely that loss of *Immp1L* cause such a severe phenotype. 3. Embryos heterozygous for either *H9* or *Tcm2* and embryos homozygous for both deletions show identical phenotypes. Last: Embryos deficient for *Ikbkap*, which encodes for IKAP/Elp1, exhibit the same phenotype as homozygous *H9*, *Tcm2* or compound heterozygous *H9/Tcm2* embryos. This strongly suggests that loss of *Elp4* alone accounts for the observed phenotype. Moreover, the same phenotype of *Ikbkap* and *Elp4* mutants

demonstrate the requirement of all subunits for Elongator function during early mouse development. In future, rescue of *Elp4* in ESCs will be performed to confirm specificity of the observed phenotype.

5.4.2 Loss of *Elp4* leads to embryonic delay and reduced body size

Elp4-deficient embryos are approximately one day delayed in development compared to heterozygous or wild-type controls but show comparable features to developmentally equivalent controls. The delay can be observed already at late gastrula to head fold stage and is obvious at beginning of neurulation at E8.5 where mutants show features of late gastrula embryos. Besides the delay, the mutants are strongly reduced in their body size.

The predominant phenotype of delayed embryonic development was also observed in mice deficient for *Ikbkap*, which encodes for the Elongator subunit *Elp1*. Besides delayed entry into midgastrulation, Chen et al. proposed that vascular and neural development is disturbed resulting in lethality (Chen et al., 2009b) whereas Dietrich et al. suggested that impaired cardiovascular and forebrain development leads to lethality (Dietrich et al., 2011). This discrepancy of both analyses resulted from the comparison of littermates or developmentally matched controls to the *Elp1* mutants. Nevertheless, both research groups investigated the mutants shortly before death at E10.5, although the phenotype becomes apparent much earlier as it is for *Elp4*, and therefore likely analysed secondary complications of *Elp1* loss-of-function. Whether *Elp4* mutants show the same malformations shortly before death remains to be investigated. However, the early onset of the phenotype and the observations that all germ layers are affected does not support a direct role of Elongator in cardiovascular or forebrain development.

The delayed and stunt phenotype of *Elp4*-deficient mice is also similar to *Dnmt1* KO and *Dnmt3a/Dnmt3b* double KO phenotypes. While maintenance of DNA methylation marks is affected in the *Dnmt1* KO, de novo DNA methylation is altered in the *Dnmt3a/Dnmt3b* double KO (Li et al., 1992; Okano et al., 1999). The similar phenotypes of both KOs illustrate the importance of tightly controlled DNA modifications and chromatin dynamics

for proper development. The common features of Dnmt and Elp mutants also suggest that the Elongator complex is involved in chromatin modification rather than in anterior and cardiovascular development.

Interestingly, it was recently shown that maternal imprinted control regions (ICRs), DNA methylated regulatory sequences of imprinted genes, have a vital effect on developmental pathways related to the mother-to-fetus exchanges (Schulz et al., 2010). Maternal imprint-free and completely imprint-free embryos develop until 20 somite stage, the time where embryonic development becomes dependent on maternal resource allocation through placental exchanges (Schulz et al., 2010). At E9.5 the embryos exhibit growth retardation, swollen pericardial sac, lack of embryonic blood cells in the yolk sac, open neural tube, reduced head size and abnormal craniofacial features. The authors state that lack of maternal imprints causes defective placentation which results in embryonic lethality at mid-gestation (Schulz et al., 2010). Interestingly, the described phenotype of imprint-free embryos resembles the phenotype of *Ikbkap*-deficient (Chen et al., 2009b; Dietrich et al., 2011) and *Elp4*-deficient embryos. Moreover, the mRNA profile of *Elp4* mutant ESCs revealed deregulation of several imprinted genes (see section “*Elp4*-deficient ESCs reveal abnormalities during maintenance and differentiation”). Since ICRs escape the global demethylation at the zygote stage (Hajkova et al., 2002; Reik and Walter, 2001), differential expression of imprinted genes indicates that the Elongator complex is important for the correct methylation status of the genome.

Interestingly, the predominant phenotype of slow or delayed growth was also observed in other species. Whereas this phenotype does not interfere with viability in *Arabidopsis thaliana*, yeast and *Caenorhabditis elegans* (Chen et al., 2009b; Nelissen et al., 2005; Otero et al., 1999), loss of Elongator function results in larval/embryonic lethality in *Drosophila melanogaster* and mouse (Chen et al., 2009b; Dietrich et al., 2011; Walker et al., 2011). Additionally, mRNA or protein profiling of different Elongator-deficient species identified various sets of genes which are predominantly deregulated. In yeast and *Caenorhabditis elegans* it was proposed that Elongator-deficiency impairs certain wobble uridine tRNA modification resulting in reduced translation efficiency (Chen et al., 2009a; Esberg et al., 2006) of proteins whose translation depend on Elongator modified tRNAs (Bauer et al.,

2012). Whether defective tRNA modification accounts for all phenotypes in other species remains to be determined.

However, different sets of genes are affected by loss of Elongator function depending on the species analysed. Interestingly, Elongator-deficiency in *Drosophila melanogaster* and mouse does not only result in lethality, in contrast to the deletion in yeast and *Caenorhabditis elegans* but also affects similar processes. Micro array analysis in *Elp3* mutant *drosophila* larvae revealed an up-regulation of stress-induced genes and induction of genes involved in aberrant activation of larval immune system (Walker et al., 2011). Similarly, transcriptome and GO term analysis of E7.5 mutant embryos showed significant enrichment of genes involved in processes controlling defence response, immune response and inflammation. Additionally, GO terms were identified in the profile of *Elp3* mutant larvae which are associated with chemical reactions and pathway similar to the *Elp4* mutant embryos. Although different developmental stages, subunits and species were compared, similarities can be observed. Interestingly, the phenotype and mRNA profile of *Elp3* mutant larvae is similar to mutants lacking the *domino* gene. *Domino* encodes a SWI/SNF-like ATP dependent chromatin remodelling enzyme (Ruhf et al., 2001). The resemblance of phenotypes and gene expression profiles points to a function of Elongator in transcriptional regulation via interaction with chromatin.

More detailed investigation of the *Elp4* mutant phenotype by IHC revealed a slight delay in differentiation of epiblast cell. This suggests that cell lineage differentiation of epiblast progenitors is slower compared to controls. It was shown before that active proliferation of the epiblast to provide a sufficient cell number or tissue volume is crucial for initiation of gastrulation (Tam and Behringer, 1997). Since the epiblast of *Elp4*-deficient embryos is smaller compared to developmentally matching controls, this might lead to delayed onset of gastrulation. The delay could further shorten the time window which is required for mesoderm and endoderm progenitor recruitment. Alternatively, reduced cell proliferation during progenitor commitment and progenitor expansion could reduce the tissue volume of all germ layers leading to an overall reduction in embryonic growth. Since the progenitors of the mid- and hindgut endoderm arise at late bud to early head fold, extensive expansion of these progenitors is required to form the mid- and hindgut

(Tam et al., 2007). The shifted expression of *Foxa2* and *Sox17* to midgut endoderm in *Elp4* mutants could emanate from a shortened recruitment phase due to the delay or reduced proliferation of endoderm progenitors. This could result from persisting repressive DNA modifications which were not immediately erased in mutants due to loss of Elongator complex function. Since different models for DNA demethylation were suggested, it is possible that other factors were able to compensate for loss of Elongator complex function but with delay. As a consequence, the differentiation phase would be shortened leading to reduced tissue mass which impairs organ formation and growth and causes embryonic lethality during organogenesis.

5.4.3 *Elp4*-deficient ESCs reveal abnormalities during maintenance and differentiation

The difficulties in generating *Elp4*-deficient ESCs and spontaneous differentiation under normal pluripotency-conditions suggested that pluripotency or self-renewal is affected. Although core pluripotency markers were present and ESCs could be maintained, mRNA profiling revealed drastic changes upon *Elp4* deletion. These changes affect predominantly RNA metabolic process, regulation of transcription and several GO terms associated with chromosome organisation, DNA binding and DNA metabolic process. Significant enrichment of genes associated with RNA metabolic process and transcriptional regulation supports the suggested role of the Elongator complex in tRNA modification and transcriptional elongation (Bauer et al., 2012; Esberg et al., 2006; Gilbert et al., 2004; Huang et al., 2005; Mehlgarten et al., 2010; Otero et al., 1999; Wittschieben et al., 1999). However, we did not observe deregulation of genes involved in specific developmental processes as observed for yeast and worm (Bauer et al., 2012; Nelissen et al., 2005). The fact that all germ layers are equally affected by loss of *Elp4* rather suggests a general requirement for the Elongator complex for controlled gene expression.

The accumulation of GO terms associated with DNA organisation points towards an epigenetic function of the Elongator complex. Interestingly, *Dnmt* KO ESCs demonstrated

that in the ESC state, stem cell and proliferation properties are maintained, comparable to the *Elp4*-deficient ESCs. However, differentiation is affected in *Dnmt1* KO or *Dnmt1/3a/3b* triple KO ESCs suggesting that DNA methylation is required for effective differentiation and/ or proliferation (Lei et al., 1996; Tsumura et al., 2006). Similar observations were made for *Elp4*-deficient ESCs. Mutant cells show reduced or abnormal differentiation abilities. Interestingly, almost all of the 20 Yamanaka factors associated with pluripotency were strongly up-regulated in the female mutant line 46 whereas expression levels in the male mutant line 47 were in most cases not changed. High expression of pluripotency genes were kept during endoderm differentiation. The elevated levels could explain the impaired ability of mutant clone 46 to differentiate. In contrast, the rather normal expression levels of pluripotency-associated genes in the mutant ESC clone 47 enabled efficient differentiation comparable to wild-type clones. However, the differentiation tendency of clone 47 is aberrant. Impaired or aberrant differentiation ability is also reflected in the mRNA profile for endoderm differentiated cells suggesting that transcriptional silencing of pluripotency genes and/or delayed activation of differentiation genes could be affected. These results are in line with the *in vivo* phenotype of delayed differentiation of epiblast cells to the primary germ layers.

Interestingly, among the deregulated genes we found several imprinted genes. It was previously reported that methylation is globally reduced in female ESCs due to the presence of two active X chromosomes (Zvetkova et al., 2005). The study demonstrates that hypomethylation affects repetitive and unique sequences including imprinted genes. To be sure that differential expression of imprinted genes in *Elp4*-deficient ESCs is not caused by general hypomethylation, the transcriptome analysis needs to be completed by including female control ESCs. However, up- and down-regulation of imprinted genes in the mutant female ESC line suggests that the deregulation is not caused by a general hypomethylation of imprinted gene. In addition, we observe deregulation of some imprinted genes, even though less, in the male mutant ESC line.

Controlled expression of imprinted genes was shown to be crucial for embryonic development (Schulz et al., 2010). Maternal imprint-free and completely imprint-free embryos develop until 20 somite stage but exhibit growth retardation and stunt

development similar to *Elp1* KO and *Elp4*-deficient embryos (Chen et al., 2009b; Dietrich et al., 2011). This supports the idea that the Elongator complex functions in adequate expression of genes via DNA modification. This will be proven experimentally by the analysis of the methylation status of developmentally and imprinted genes by using bisulfite sequencing and 5mC ChIP.

6 Material and methods

6.1 Material

6.1.1 Equipment

Agarose gel chamber	Midi 450 (Harnischmacher, Kassel) Typ Mini (neoLab, Heidelberg)
Balances	Scout™ Pro (OHAUS) Sartorius
Cameras	AxioCam MRC5 (Carl Zeiss AG, Göttingen) AxioCam HRm (Carl Zeiss AG, Göttingen)
Centrifuges	5417 R (Eppendorf AG, Hamburg) 5417 C (Eppendorf AG, Hamburg) 5804 R (Eppendorf AG, Hamburg) Haereus Rotanta 460R (Thermo Fisher Scientific Inc., Waltham) Hettich Universal 30F (Andreas Hettich GmbH & Co. KG, Tuttlingen) 1-14 (Sigma Laborzentrifugen GmbH, Osterode am Harz) Galaxy Mini (VWR International GmbH, Darmstadt) Sprout™ (Kisker Biotech GmbH, Steinfurt) Avanti J-E centrifuge (Beckman Coulter)
Counting chamber (cells)	Neubauer (LO-Laboroptik GmbH, Friedrichsdorf)
Cryotome	Leica CM 3050S
Developing machine	AGFA Curix 60 developing machine (AGFA HealthCare GmbH, Bonn)
Electroporation system	BioRad Gene Pulser Xcell (BioRad Laboratories, München)

Film cassettes	Hypercassette (Amersham, GE Healthcare GmbH, München)
Freezer	-20 °C (Liebherr Hausgeräte Ochsenhausen GmbH, Ochsenhausen) -80 °C (New Brunswick Scientific)
Fridge	4 °C (Liebherr Hausgeräte Ochsenhausen GmbH, Ochsenhausen)
Gel documentation system	UV-Transilluminator (Biorad, München) Gene Flash (Syngene Bio Imaging, Synoptics Ltd, Cambridge)
Glassware	Schott-Duran (Schott, Mainz)
Heating plate	RCT basic (IKA® -Werke GmbH, Staufen)
Hybridisation tubes	Hybridizer HB 100 (ThermoHybaid, Thermo Fisher Scientific Inc., Waltham)
Icemaschine	Ziegra Eismaschinen
Incubation systems/ovens	Shaking incubator; 37 °C bacteria (Shel Lab, Sheldon Manufacturing, Cornelius) TH-30 and SM-30; 32 °C bacteria (Edmund Bühler GmbH, Hechingen) 65 °C Southern Blot (Thermo Electron Corporation) Thermomixer comfort (Eppendorf AG, Hamburg) Shake'n'Stack (ThermoHybaid, Thermo Fisher Scientific Inc., Waltham)
Microscopes	Axiovert 200 M (Carl Zeiss AG, Göttingen) Lumar.V12 (Carl Zeiss AG, Göttingen) MS5, MZ75 (Leica Microsystems GmbH, Wetzlar) TCS SP5 (Leica Microsystems GmbH, Wetzlar)
Microtome	Microm HM 355 S rotation microtome (Thermo Fisher Scientific Inc., Waltham)
Microwave	700 W (Severin Elektrogeräte GmbH, Sundern)

PCR machines	Personal Thermocycler (Biometra, Goettingen) Px2 ThermoHybaid (Thermo Fisher Scientific Inc., Waltham) PXE0.2 Thermo Cycler (Thermo Fisher Scientific Inc. Waltham)
pH meter	pH211 Microprocessor pH Meter (HANNA instruments Deutschland GmbH, Kehl am Rhein)
Photometer	BioPhotometer (Eppendorf) ND-1000 Spectrophotometer NanoDrop, (Thermo Fisher Scientific Inc., Waltham)
Pipettes (2 ml /5 ml/10 ml)	Greiner Bio-One GmbH, Frickenhausen
Pipette tips	Eppendorf AG, Hamburg
Pipette Filtertips	TipOne (Starlab GmbH, Hamburg)
Pipettboy	accu-jet and accu-jet® pro (Brand GmbH & Co. KG, Wertheim)
Plastic ware	VITLAB GmbH, Großostheim
Polyacrylamid gel chamber	Mini Trans-Blot® Cell (BioRad GmbH, Heidelberg)
Polyacrylamid gel preparation	BioRad
Power suppliers	Power Pack Basic (BioRad Laboratories, München) EC105 (Thermo Electron Corporation)
Pumps	LABOPORT ® (neoLab Migge Laborbedarf-Vertriebs GmbH, Heidelberg)
Radiation monitor	Berthold LB122 radiation monitor (BERTHOLD TECHNOLOGIES GmbH & Co. KG, Bad Wildbach)
Roller Mixer	SRT1 (Bibby Scientific (Stuart), Staffordshire, GB)
Rotator/tumbler	VSR 23 (Grant BOEKEL, VWR international GmbH,Darmstadt) SHAKER DOS-10L (neoLab, Heidelberg)
Sonificator	Elmasonic UW 2070 (Bandelin electronics, Berlin)

Stirrer	STIR (VWR international GmbH, Darmstadt)
Water bath	VWR GFL, Burgwedel
Western Blot semi-dry system	Trans-Blot® SD, Semi-Dry Transfer cell (Biorad, Heidelberg) Trans-Blot Turbo (Biorad)
Vortexer	Vortexer (VWR international GmbH, Darmstadt)

6.1.2 Consumables

50 ml/ 15 ml tubes	Becton and Dickinson and Company, Franklin Lakes; Sarstedt, Nürnbergrecht
14 ml tubes	BD Labware (Becton Dickinson GmbH, Heidelberg)
safe-lock reaction tubes	Eppendorf AG, Hamburg
dishes	nunc (Thermo Scientific Fisher, Wiesbaden)
4-well plates	nunc (Thermo Scientific Fisher, Wiesbaden)
6-/ 12-/ 24-/ 48-well plates	Falcon
96-well plates (straight/conical)	nunc (Thermo Scientific Fisher, Wiesbaden)
10 cm bacterial plates	BD Falcon™ (Becton Dickinson GmbH, Heidelberg)
Cover slips	VWR
Cell scraper	Starstedt
DNA Ladder (100 bp)	NEB
Embedding cassettes	Carl Roth GmbH & Co. KG, Karlsruhe
Embedding moulds	Carl Roth GmbH & Co. KG, Karlsruhe
Plastic pipettes	Greiner bio-one, Frickenhausen
Glas slide, Superfrost Plus	Thermo Scientific
Glas vials (ISH)	A. Hartenstein

Pasteur pipettes, plastic	transfer pipettes (Carl Roth GmbH & Co. KG, Karlsruhe)
Pasteur pipettes, glass	15cm/23cm (LABOR-BRAND, Gießen; Hirschmann Laborgeräte GmbH & Co. KG, Eberstadt)
Parafilm	Parafilm (Pechiney Plastic Packaging, Menasha)
PCR Tubes	Eppendorf AG, Hamburg
PVDF membrane	Immun-Blot PVDF-Membrane (BioRad Laboratories, Hercules)
Nitrocellulose membrane	GE Healthcare Buchler GmbH & Co. KG, München
Blotting paper	Whatman paper (GE Healthcare Buchler GmbH & Co. KG, München)
Scalpels	surgical disposable scalpels B/Braun (Aesculap AG & Co. KG, Tuttlingen)
Films	Kodak BioMax MS (Sigma-Aldrich GmbH, Hamburg) Amersham Hyperfilm ECL (GE Healthcare Buchler GmbH & Co. KG, München)

6.1.3 Kits

QIAquick PCR Purification Kit (Qiagen Holding, Hilden)
QIAquick Gel Extraction Kit (Qiagen Holding, Hilden)
QIAGEN Plasmid Maxi Kit (Qiagen Holding, Hilden)
QIAprep Spin Miniprep (Qiagen Holding, Hilden)
miRNeasy Mini Kit (Qiagen Holding, Hilden)
QIAamp DNA Blood Mini Kit (Qiagen Holding, Hilden)
PCR Master (Roche Diagnostics)
In Situ Cell Death Detection Kit Fluorescein (Roche Diagnostics)
ECL Detection Kit (Millipore Cooperation, Billerica, MA)

6.1.4 Chemicals

(Sigma-Aldrich GmbH, Hamburg, Merck KGaA, Darmstadt, Carl Roth GmbH & Co. KG, Karlsruhe)

- A** Acetic acid (glacial; Merck KGaA, Darmstadt)
Acetic Anhydride (Sigma-Aldrich A6404-200ML)
Activin A, human (R&D Systems, Minneapolis)
Acrylamide/bisacrylamide (Rotiphorese® Gel 30 (37,5:1), Roth 3029.2)
Agarose (Biozym Scientific GmbH, Hess. Oldendorf)
Aluminium Sulphate (Sigma-Aldrich A-0843)
Ampicillin (Roche 10835269001)
Ammonium peroxodisulfate (APS; Roth A3678-25G)
Anti-Digoxigenin-AP Fab fragments (Roche Diagnostics, Mannheim)
Antifade (Invitrogen P36930, Oregon)
Aqua Poly/Mount (Polyscience Inc., Warrington)
- B** Blocking reagent (Roche Diagnostics, 11096176001, Mannheim)
Big Dye/ Big Dye Buffer (Life Technologies 4337457 or Lager 5000986)
BM purple AP Substrate (Roche Diagnostics, Mannheim)
BSA
Bradford reagent (Sigma-Aldrich)
Bromophenol Blue (Roth A512.1)
- C** Calcium chloride (Roth CN93.1)
Chemiluminescent HRP Substrate (Millipore, WBKLS0500)
Chloroform, 99+ % (Sigma-Aldrich)
CI (Chloroform-Isoamylalcohol: 24:1)
Citric acid monohydrate (Roth)
Corn Oil (Sigma-Aldrich)

- CT 99021 (Gsk3 β , 1386; Axon Medchem BV, Groningen)
- D** D-EMEM (+) 4.5 Glucose (+) Pyrovate (Gibco®, Invitrogen™ Cooperation, Carlsbad, CA)
- Dextranulphate (Roth 5956.2)
- Diethylpyrocarbonate (DEPC), approx. 97 % (Sigma-Aldrich)
- Dimethylsulfoxide (DMSO), >99.9 % (Sigma-Aldrich D5879-100ML)
- Disodium phosphate dehydrate (Roth)
- Dithiothreitol (DTT; Sigma D0632-10G)
- dNTPs (Fermentas GmbH, St. Leon-Rot)
- DPBS (-)MgCl₂, (-) CaCl₂ (Gibco®, Invitrogen™ Cooperation, Carlsbad, CA)
- E** EDTA (Roth 8043.2)
- EGTA (Roth)
- Enhanced chemiluminescence (ECL) solution (Millipore Corporation)
- Ethanol 100 % (Merck KGaA, Darmstadt)
- Ethidiumbromide (Roth)
- F** FBS (heat inactivated, Gibco®, Invitrogen™ Cooperation, Carlsbad, CA)
- Formaldehyde (>37 %; Roth 7398.1)
- Formamide (>99,5 %; Roth 6749.1)
- G** Gelatine (Applichem A1693,0500)
- Glutaraldehyde (25 %; Sigma-Aldrich G6257-1L)
- Glycerol (Sigma G9891-25G)
- Glycine (Sigma G8898-1KG)
- G418 (Geneticin, 50mg/ml, Gibco, Invitrogen™ Cooperation, Carlsbad, CA)
- H** HCl (0,5 M; Roth P708.1), (1 M; Roth K025.1)
- HCl (2 M; Roth T134.1)
- Heparin (Sigma-Aldrich H3393-100KU)
- HEPES (200 mM, Gibco, Invitrogen™ Cooperation, Carlsbad, CA)

- H₂O₂ 30 % (Roth)
- I** Isopropanol, 100 % (Merck KGaA, Darmstadt)
- K** Kanamycin (Sigma K-1377)
- L** LB-Agar: (LB Agar, Miller (Luria-Bertani) from BD 244520)
Levamisole hydrochloride (AppliChem)
L-glutamine (200 mM, Gibco, Invitrogen™ Cooperation, Carlsbad, CA)
LIF
- M** Magnesium chloride (VWR Prolabo 25108.260)
Magnesium Sulphate 7 hydrate (Roth)
Maleic acid (Sigma-Aldrich M0375-250G)
MEMs non essential amino acids (100x, Gibco, Invitrogen™ Cooperation, Carlsbad, CA)
Methanol, 100 % (Merck 1.06009.2500)
Mek1 (PD98059, Cell Signalling Technology, Frankfurt am Main)
Milk powder (Roth)
Mitomycin C (Sigma-Aldrich)
MOPS (AppliChem A2947,0500)
β-mercaptoethanol (50 mM, Gibco, Invitrogen™ Cooperation, Carlsbad, CA)
- N** N-laurolysarcosine sodium salt (Sigma-Aldrich L5777-50G)
Nitrogen(I) (Linde AG, München)
NP-40 (Roche Diagnostics, Mannheim)
Nuclear Fast Red (NFR; Fluka 60700)
- O** Oligo-dT-primer (Promega GmbH, Mannheim)
Orange G (AppliChem, Darmstadt)
- P** PAA (PAA Laboratories GmbH/GE Healthcare, Pasching)
PAN (PAN-Biotech GmbH „Pansera ES“)
Paraformaldehyde (Sigma-Aldrich)

- Paraplast X-Tra (Sigma-Aldrich)
- PBS (Gibco, Invitrogen™ Cooperation, Carlsbad, CA)
- PCI (Phenol-Chloroform-Isoamylalcohol: 25:24:1; Carl Roth GmbH + Co. KG, Karlsruhe)
- Penicillin/Streptomycin (Gibco, Invitrogen™ Cooperation, Carlsbad, CA)
- Polyacrylamide/Rotiphorese Gel 30 (Roth)
- Ponceau S solution (Sigma P7170-1L)
- Potassium acetate (Roth)
- Potassium chloride (Roth)
- Potassium hexacyanoferrate(III) (Sigma-Aldrich)
- Protease Inhibitor (Sigma, P8340)
- Proteinase K (Roche)
- Proteinmarker (Fermentas SM1811)
- Q** Q-Solution (Qiagen Holding, Hilden)
- R** RNaseZAP (Sigma-Aldrich)
- Rotihistol (Roth 6640.1)
- Roti-Phenol/C/I (Roth)
- S** Sheep serum (ISH, Sigma Aldrich S-2263)
- Sodium chloride (Merck 1.06404.1000)
- Sodium desoxycholate (97 %; Sigma D6750-100G)
- Sodiumdodecylsulphate (SDS) (Roth N071.1)
- Sodium Dihydrogen Phosphate (Roth)
- Sodium hydrogenic phosphate (Roth)
- Sodium hydroxide (Roth)
- Sodium acetate trihydrate (Roth)
- T** Tamoxifen (Sigma-Aldrich)
- TEMED (Roth, 2367.3)

Triethanolamine (Sigma T1377-500ML), (>99 %; Roth 6300.1)

Tris (Merck 1.08382.2500)

Tri-sodium-citrat (>99 %, Roth 3580.2)

Triton X-100 (Roth)

Trizol Reagent (Gibco, Invitrogen™ Cooperation, Karlsruhe)

0-05 % Trypsin/EDTA (Gibco, Invitrogen™ Cooperation, Carlsbad, CA)

Tryptone (Roth 8952.2)

TWEEN-20 (Sigma P2287-500ML; Karl Roth GmbH, Karlsruhe)

V Vectashield (Vector Laboratories, Burlingame)

X Yeast extract (Roth)

Xylene (Merck 8.08691.2500)

6.1.5 Buffer and solutions

6.1.5.1 Isolation of genomic DNA

Proteinase K lysis buffer: 100 mM Tris, pH 8.0-8.5, 5 mM EDTA, pH 8.0, 2 % SDS, 200 mM Sodium chloride

Yolk sac lysis buffer: 50 mM KCl, 10 mM Tris-HCl, pH 8.3, 2 mM MgCl₂, 0.45 % NP-40, 0.45 % Tween-20

Lysis buffer 96-well: 2.5 ml 1M Tris pH 7.5, 5.0 ml 0.5 EDTA, 0.5 ml 5M NaCl
Set pH to 7.0 and autoclave, add 0.5 % N-laurolysarcosine sodium salt and 0.4 mg/ml Proteinase K before use

6.1.5.2 DNA/RNA agarose gels

TAE buffer (50x stock): 2 M Tris, 50 mM Glacial acetic acid, 50 mM EDTA

Loading buffer DNA: 100 mM EDTA, 2 % SDS, 60 % Glycerol, 0.2 % Bromophenol blue

Loading buffer RNA (2x): 95 % Formamide, 0.025 % SDS, 0.025 % Bromophenol blue, 0.025 % Xylene cyanol FF, 0.025 % Ethidium bromide, 0.5 mM EDTA

6.1.5.3 Southern blot

Depurination

(fragments ≥ 10 kb): 11 ml HCl in 989 ml H₂O

Denaturation (all gels): 87.66 g Sodium chloride, 20.00 g NaOH in 800 ml H₂O, fill up to 1 l H₂O

Neutralization (all gels): 87.66 g Sodium chloride, 60.50 g Tris in 800 ml H₂O, adjust pH 7.5 with HCl conc. (approx. 11 ml), fill up to 1 l H₂O

Transfer, 20x SSC (all gels): 88.23 g Tri-sodium-citrat, 175.32 g Sodium chloride in 800 ml H₂O, check pH 7-8, fill up to 1000 ml H₂O

Hybridisation buffer: 1 M Sodium chloride, 50 mM Tris, pH7.5 (at 37 °C), 10 % Dextran sulphate, 1 % SDS, 250 µg/ml Salmon Sperm DNA sonificated, store aliquots à 30 ml at -20 °C

Washing buffers:

- a) 2x SSC / 0.5 % SDS
- b) 1x SSC / 0.5 % SDS
- c) 0.1 % SSC / 0.5 % SDS

Stock solutions:

- a) 20x SSC 175.3 g Sodium chloride, 88.2 g sodium citrate, pH7.0
- b) 20 % SDS 200 g SDS, 1 l H₂O (final volume)

6.1.5.4 Western blot

4x SDS-loading dye: 200 mM Tris-HCl, pH 6.8, 8 % SDS, 40 % Glycerol, 0.4 % Bromophenol blue, store aliquots à 320 µl at -20 °C, add 80 µl 2 DTT before use

2 M DTT: dissolve 3,085 g DTT powder in 10 ml H₂O, store aliquots à 80 µl at -20 °C, add 320 µl 4x SDS loading buffer before use

10 % APS: dissolve 5 g Ammonium peroxodisulfate powder in 45 ml H₂O, store aliquots à 2 ml at -20 °C

Lysisbuffer (RIPA):	50 mM Tris-HCl, pH 7.4, 150 mM Sodium chloride, 0.5 % sodium deoxycholate, 1 % Nonidet P-40, 0.1 % SDS, filtrate sterile and add Proteinase Inhibitor 1:200 before use
4x Tri.HCl/SDS buffer:	100 ml: 6.05 g Tris, add 40 ml H ₂ O, adjust pH to 6.8 with conc. HCl, add H ₂ O to a total volume of 100 ml, filter sterile through a 0.45 µm filter, add 0.4 g SDS, store at RT
4x Tris-HCl/SDS buffer:	500 ml: 91 g Tris base, add 300 ml H ₂ O, adjust pH to 8.8 with conc. HCl, add H ₂ O to total volume of 500 ml, filter sterile through a 0.45 µm filter, add 2 g SDS, store at RT
10x Running Buffer:	60.6 g Tris, 288.2 g Glycine, 100 ml 20 %SDS, add H ₂ O up to a volume of 2 l, store at RT
10xTBST:	171.4 g NaCl (final conc. 150 mM), 150,0 g Tris (final conc. 50 mM), dissolve in 1 l H ₂ O, adjust pH 7.5, add H ₂ O up to a volume of 2 l, autoclave, store at RT
KP-Buffer:	3 g Tris-HCl, 3 g Glycine, 100 ml Methanol, add H ₂ O to a final volume of 1 l, store at RT
AP I –Buffer:	36.3 g Tris-HCL, 100 ml Methanol, add H ₂ O to a final volume of 1 l, store at RT
AP II-Buffer:	3 g Tris-HCL, 100 ml Methanol, add H ₂ O to a final volume of 1 l, store at RT
Ponceau-solution:	0.2 % PonceauS, 3 % TCA
Blocking solution:	milk powder 1:10 in 1x TBST
ECL-solution:	mix directly before usage Solution A and B mix: 1:1

6.1.5.5 Immunostainings

Permeabilisation:	0.1 % TritonX-100, 100 mM Glycine in H ₂ O
Blocking solution:	10 % FCS, 1 % BSA, 3 % serum (donkey) in PBST (0.1 % Tween-20 in PBS)

6.1.5.6 TUNEL

Permeabilisation:	1 % BSA, 0.1 % Triton X-100, .1 % 1 M Sodium citrate in H ₂ O
DNase I treatment:	300 U/ml DNase I, 1 mg/ml BSA in 50 mM Tris-HCl, pH 7.5

6.1.5.7 LacZ-staining

Fixation buffer:	0.02 % NP-40, 5 mM EGTA, pH 8.0, 2 mM MgCl ₂ x 6H ₂ O, 1 % Formaldehyde, 0.2 % Glutaraldehyde in PBS
Washing buffer:	0.02 % NP-40 in PBS
Staining buffer:	0.02 % NP-40, 2 mM MgCl ₂ x 6H ₂ O, 5 mM K ₃ [Fe(CN) ₆], 5 mM K ₄ [Fe(CN) ₆] x 6H ₂ O, 0.01% Sodium desoxycholat, 1 mg/ml X-Gal (add freshly before use) in PBS

6.1.5.8 *In situ* hybridization

DEPC-H ₂ O:	add DEPC 1:1000 to H ₂ O, stir overnight, autoclave
PBS:	1.15 g Disodium Phosphate, 8 g Sodium Chloride, 0.2 g Monopotassium Phosphate, 0.2 g KCl in 1 l DEPC-H ₂ O, add 0.1 g MgCl ₂ x 6H ₂ O and 0.1 g CaCl ₂ x 2H ₂ O, adjust pH to 7.2-7.3, filtrate sterile
PBT:	0.1 % Tween-20 in PBS
Heparin:	50 mg/ml in DEPC-H ₂ O
tRNA:	20 mg/ml in DEPC-H ₂ O
SDS:	dissolve 10 g SDS in DEPC-H ₂ O
20 x SSC:	175 g Sodium Chloride, 88.2 g Sodium citrate in 1 l DEPC-H ₂ O, adjust pH to 4.5 with citric acid
Hybridisation buffer:	1 µg RNA probe per ml prehybridisation buffer
Prehybridisation buffer:	50 % Formamide, 5 x SSC, pH 5.4, 1 % SDS, 50 µg/ml yeast tRNA, 50 µg/ml Heparine, store at -20 °C
Solution I:	50 % Formamide, 5 x SSC, pH 5.4, 1 % SDS in MiliQ H ₂ O, store at -20 °C

Solution II:	50 % Formamide, 2 x SSC, pH 5.4, 0.2 % SDS in MiliQ H ₂ O, store at -20 °C
MAB:	100 mM Maleic acid, 150 mM Sodium Chloride, 2 mM Levamisole; 0.1 % Tween-20 in MiliQ H ₂ O, adjust pH to 7.5 with Sodium hydroxide, prepare solution fresh
MAB/Block	2 % Boehringer Mannheim blocking reagent in MAB
Antibody solution:	dissolve 10 mg embryo powder in 5 ml MAB/Block in a 50 ml falcon tube, vortex and incubate at 70 °C for 30 min, cool down on ice. Add 50 µl sheep serum, 4 µl α-Dig Alkaline Phosphatase (1:5000) and incubate at 4°C for 1 h. Centrifuge at 5000 rpm for 10 min at 4 °C. Decant supernatant to new falcon, add 154 µl sheep serum and dilute to 20 ml with MAB/Block. Prepare solution fresh.
TNT:	10 mM Tris pH 7.5, 0.5 M Sodium Chloride, 0.1 % Tween-20 in MiliQ H ₂ O
NTMT:	100 mM Tris, pH 9.5, 50 mM MgCl ₂ , 100 mM Sodium Chloride, 0.1 % Tween-20, 100 µl Levamisole in MiliQ H ₂ O

6.1.5.9 *In situ* hybridization on slides (additional solutions)

0.2 N HCl:	dilute 2 M HCl solution 1:10 with DEPC-H ₂ O
0.1 M Glycine:	dilute 2 M Glycine stock solution 1:20 with DEPC-PBS
10 x PBS:	75.97 g Sodium Chloride, 1.46 g Disodium Phosphate, 4.80 g Sodium Dihydrogen Phosphate, dissolve in 800 ml ddH ₂ O, adjust pH to 7.0 with 5 M Sodium hydroxide, fill up to 1 l, add 0.1 % DEPC, stir overnight, autoclave
1 x PBS:	add 100 ml 10 x PBS to 900 ml ddH ₂ O, add 0.1 % DEPC, stir overnight, autoclave
1 M Tris_HCl pH 7.5:	121 g Tris in 800 ml ddH ₂ O, adjust pH to 7.5 with conc. HCl, fill up to 1 l with ddH ₂ O, autoclave
1 M Triethanolamine	2.8 ml Triethanolamine, 193.2 ml DEPC-H ₂ O, stir vigorously, adjust pH to 8.0 with 4 ml 2 M HCl, add 500 µl Acetic anhydride immediately before use
1 M MgSO ₄ :	12.3 g MgSO ₄ in 50 ml DEPC-H ₂ O

0.5 M EGTA:	4.75 g in 25 ml DEPC-H ₂ O, adjust pH to 8.0 with Sodium Hydroxide
10 x MOPS:	83.7 g MOPS, 13.6 g Sodium acetate trihydrate, 3.7 g EDTA in 800 ml DEPC-H ₂ O, adjust pH to 7.0, fill up to 1 l with DEPC-H ₂ O, autoclave, protect from light
MEMFA buffer:	100 mM MOPS, 2 mM EGTA, 1 mM MgSO ₄ , 3.2 % Formamide in DEPC-H ₂ O

6.1.5.10 Nuclear Fast Red staining

NFR:	25 g Aluminium sulphate in 500 ml dH ₂ O, add 0.5 g NFR, heat up to solve, cool down and filter
------	--

6.1.6 Enzymes

Proteinase inhibitors	Sigma-Aldrich GmbH, Seelze
Superscript II	Fermentas GmbH, St. Leon-Rot
RNase inhibitors	Fermentas GmbH, St. Leon-Rot
Restriction enzymes	NEB GmbH, Frankfurt a. M.; Fermentas GmbH, St. Leon-Rot
DNA-Polymerases	<i>Taq</i> DNA Polymerase recombinant (Fermentas GmbH, St. Leon-Rot) <i>Taq</i> DNA Polymerase (Qiagen, Hilden) <i>Pfu</i> DNA Polymerase (Stratagene, La Jolla)
RNA-Polymerases	Sp6 (Roche Diagnostics, Mannheim) T7 (Roche Diagnostics, Mannheim) T3 (Roche Diagnostics, Mannheim)
RNase A	Qiagen Holding, Hilden
RNase A	Roche Diagnostics, Mannheim
RNase-free DNase I	Promega GmbH, Mannheim
Ligase	T4 DNA ligase (NEB GmbH, Frankfurt a. M.; M0202)

Phosphatase

T4 Polynucleotide Kinase (NEB GmbH, Frankfurt a. M.);
Antarctic phosphatase (NEB GmbH, Frankfurt a. M.)

6.1.7 Antibodies and Sera

6.1.7.1 Primary antibodies:

A list of primary antibodies used in this thesis. Abbreviations: WB: Western Blot, IC: immunohistochemistry

ID	name	species	dilution	company
1	Actin Ab-5	mouse IgG1	WB 1:5000	BD
5	E-Cadherin	mouse IgG2a	IC 1:2000	BD
9	anti-RFP	rabbit polycl.	IC 1:1000	Biotrend
22	anti-beta-catenin	rabbit antiserum	IC 1:2000	Sigma
23	HNf-3 β (Foxa2) M-20	goat polycl.	IC 1:1000	Santa Cruz
25	Brachyury (N-19)	goat polycl.	IC 1:1000	Santa Cruz
48	chicken anti-GFP	chicken	IC 1:1000	Aves Labs
53	rat anti-mouse CD31/PECAM1	rat IgG2a,K	IC 1:500	BD
56	Foxa2	rabbit polycl.	IC 1:1000	abcam
59	Oct-3/4 (C-10)	mouse monocl.	IC 1:1000	Santa Cruz
84	Ep-CAM (G8.8-c)	rat hybridoma	IC 1:500	DSHB Hybridoma
99	Sox17	goat polycl.	IC 1:500 WB 1:5000	Acris/Novus
102	Oct-3/4 (N-19)	goat polycl.	IC 1:500-1:1000	Santa Cruz
103	GATA-4 (C-20)	goat polycl.	IC 1:100	Santa Cruz
104	GATA-6	goat polycl.	IC 1:100	R+D
121	mouse anti-beta-Catenin	mouse monocl.	IC 1:1000	BD
206	Anti-GAPDH	mouse monocl.	WB 1:6000	Merck Biosciences
216	Ki67	rabbit polycl.	IC 1:1000	abcam

Table 1: List of primary antibodies

6.1.7.2 Secondary antibodies:

List of secondary antibodies used in this thesis. Abbreviations: WB: Western Blot, IC: immunohistochemistry, HRP: Horseredish Peroxidase

ID	name	conjugated	dilution	company
15	goat ant-mouse IgG	HRP	WB 1:200.000 IC 1:500	Dianova
16	rabbit anti-goat IgG	HRP	WB 1:200.000 IC 1:500	Dianova
18	donkey anti-goat IgG 633	fluorescent	IC 1:800	Invitrogen
23	donkey anti-mouse IgG 488	fluorescent	IC 1:800	Invitrogen
24	donkey antirabbitt IgG 555	fluorescent	IC 1:800	Invitrogen
25	donkey anti-goat IgG 488	fluorescent	IC 1:800	Invitrogen
26	donkey anti-rabbit IgG 488	fluorescent	IC 1:800	Invitrogen
28	donkey anti-chicken IgY	Cy2	IC 1:800	Dianova
37	donkey anti-mouse IgG 473	fluorescent	IC 1:800	Dianova
41	donkey anti-rat IgG 549	Cy3	IC 1:800	Dianova
43	rabbit anti-rat IgG	HRP	WB 1: 10.000	abcam
45	donkey anti-rat IgG 649	Dy light 649t	IC 1:800	Dianova

Table 2: List of secondary antibodies

6.1.7.3 Sera:

Sheep serum (Sigma-Aldrich GmbH, Hamburg)

Goat serum (Sigma-Aldrich GmbH, Hamburg)

Donkey serum (Sigma-Aldrich GmbH, Hamburg)

6.1.8 Vectors and BACs

Vectors: 2A-RFP-2A-CreERT2 pMA (gift of Mr. Gene)

pL254-Sox17 (Liao et al., 2009)

pBKS-Ex5 HR (Engert et al., 2009)

pL451 Δ loxP (Liu et al., 2003)

pBKS-Ex5 HR-2A-CreERT2 (Engert et al., 2013b)

pBKS-Ex5 HR-2A-CreERT2-FRT-neo-FRT (Engert et al., 2013b)

pCAG H2B-Td-Tomato (E032; Engert *et al.*, 2013)

BACs: BAC-RP23-285G23 Gene: *Sox17*

6.1.9 Oligonucleotides

6.1.9.1 Oligonucleotides for cloning

Restriction enzyme sites are underlined and indicated; the oligonucleotides are displayed in 5' to 3' direction.

EP039: 5'-GCTATTACGCCAGCTGGCGAAAGGGGGATGTG-3'

EP333: 5'-GGCCGC^{NotI}ACGCGT^{MluI}TTGAAGGTAGAGGCTCTTTACTAACATGCGGCGACGTT
GAGGAAAACCCAGGACC-3'

6.1.9.2 Oligonucleotides for Southern probe

Sox17 5' Southern probe (744 bp)

Primer for generation:

Sox17 5' probe reverse primer: 5' NNNACCGGTCGGGAATGTTTC-3'

Sox17 5' probe forward primer: 5'-NNNAAGCTTTGGAAGCTAAATTAGGTTC-3'

Sequence:

5'-

AAGCTTTGGAAGCTAAATTAGGTTCAGGTTAGAAATCTGTTATGCTTGAAGCGCATAACAGGA
GGTAATGAGTGCTGTCAGGAGTGGCAAGTCCTATTTAACTTTGATCATTTCCATGATCACAG
AGCACATACTTGGCCTAACCAACAATCTGGCGCCATGCAGTTAATCCTGATAGGGGATCTTG
GGAGCAGAGTTTTCTGGATGGAAAGGCACCTATTGCCTCTGCTACAAAACCAAAGCAAACCTCA
ACGAAACAACCTCAATGTGCTTGACCCACTGTGTAGTCATCATCACTTTCACAGTCCAGGAACG
GAGTATTACAGGATCATAGACTGAGCTGGATATTAATAAATCAGAGAAGAAGACTAAGGATG
CCACACTGGGCATCCTGGGAAGCAGTCCTACCCAGTTTGCTCTCTGGAGAGAGTGCAAGTGCT
CTGCTCACAGTGACAGGCCAGACTGCAAGGCGAGGATTGCCTTTCTCCAAGGAAGCCCGTCTT
CCCTAGGGTGTGGTACTACTAGGCTACAGCAGCCATCACCTTTATAAAAACCCAAGCCATATT

TGAATTGTCTTTAAATTTCAAGGAAGAGGACAAAGAAATGTGAGCAAGGCTTCATTCCTACT
 CTCAGACTACCGTCCCAAGAGAACCTGAGGTTCCATGGAGCAGGAATAAAGAGGAGTCCTTAC
 TTCGTCTGGGGAACACAGATGGGGTATGGGTCTAAGAAACATTCCCGACCGGT-3'

6.1.9.3 Oligonucleotides for genotyping

List of oligonucleotides used for genotyping; all oligonucleotides are displayed in 5' to 3' direction.

Name	Sequence
EP064	CATGCTCCAGACTGCCTTGG
EP176	CTAATGTTGTGGGAAATTGGAGC
EP177	CTCGAGGATAACTTGTATTATGC
EP308	AAAGTCGCTCTGAGTTGTTAT
EP309	GCGAAGAGTTTGTCTCAACC
EP310	GGAGCGGGAGAAATGGATATG
EP400	GTGTATAAGCCCGAGATGG
EP401	CTCAACTGTTCAAGTGGCAG
EP482	AAGGTAGAGTGATGAAAGTTGTT
EP483	CACCATGTCCTCTGTCTATTC
EP484	TACACTATTGAATCACAGGGACTT
EP564	GATCTATGGTGCCAAGGATGAC
EP692	CTGCTAACCATGTTTCATGCC
EP693	GGTACATTGAGCAACTGACTG
EP980	TCCCACATTAGGCACATGAG
EP990	TGACTGGGATGCAGTAGTTC
EP991	TGTGCTAGAGAGAAACCCTG
EP1302	CTCTGCTGCCTCTGGCTTCT
EP1303	CGAGGCGGATCACAAGCAATA
EP1304	TCAATGGGCGGGGGTCGTT
8C14 27L	TCAGTGTTCCAAGGAGGGCTGTG
Elp4 170R	CGTTCCTGGGTCGCTAAACTTGG
8C14 K 1L	ACAAAGTGTGTCCCTGCCCTTCC
8C14 K 1R	GCAAGGGATTCTAAATTACAGCCTTGG
431C3 65L	GTCCAGGCATCTCCGGTGTC
146D23 34R	CAAACCTCAGCCAAACATCAAATTCC
431C3 K 1L	GGCCTGAGTCCTTTCCTTCCCAC
431C3 K 1R	TGAGTGTGTTTCGCCTTGACACC

Table 3: Oligonucleotides for genotyping

6.1.10 Molecular weight markers

DNA ladder:	100 bp ladder; 1 kb ladder (NEB GmbH, Frankfurt a. M.)
Protein ladder:	SeeBlueR Plus2 Pre-Stained Standard (Gibco, Invitrogen™ Cooperation, Carlsbad, CA)
RNA ladder:	RNA ladder high range (Fermentas GmbH, St. Leon-Rot)

6.1.11 Bacteria and culture media

6.1.11.1 Bacteria

<i>E.coli</i> K12 EL350	(Lee et al., 2001)
<i>E.coli</i> K12 DH5 α	F-. lacI-recA1, endA1, D(lacZY A-argF), U169, F80dlacZDM15, supE44, thi-1, gyrA96, relA1 (Hanahan, 1985)

6.1.11.2 Culture media

Ampicillin:	dissolve 1 g Ampicillin powder in 10 ml H ₂ O (final conc. 100 mg/ml), sterile filtration, prepare 1 ml aliquots and store at -20 °C
Kanamycin:	dissolve 300 mg Kanamycin powder in 10 ml sterile H ₂ O (final conc. 30 mg/ml), prepare 1 ml aliquots and store at -20 °C
LB-Agar:	dissolve 16 g in 400 ml H ₂ O, boil for 1 min until it is completely dissolved, autoclave and store at RT or 4 °C
LB-Agar-plates:	cook LB-Agar in the microwave or water bath, cool down to 50-55 °C, add antibiotics, fill Agar into 10 cm dishes and store at 4 °C
LB-Medium:	dissolve 10 g Tryptone, 10 g Yeast extract, 5 g Sodium chloride in 1 l H ₂ O, autoclave and store on 4 °C

6.1.12 Cell lines

IDG3.2	murine ESC line (F1); genetic background 129S6/SvEvTac x C57BL/6J (Hitz et al., 2007)
MEF	primary murine embryonic fibroblasts isolated on E13.5
β -catenin CKO	(Engert et al., 2013b)

β -catenin Ctrl	(Engert et al., 2013b)
H9/Tcm2	murine ESC line (F1); genetic background 129/C3HJ
H9/Tcm2 Ctrl	murine ESC line (F1); genetic background 129/C3HJ

6.1.13 Culture media

MEF	DMEM (Gibco, Invitrogen™ Cooperation, Carlsbad, CA), supplemented with 2 mM L-glutamine (200 mM Gibco, Invitrogen™ Cooperation, Carlsbad, CA), 15 % FCS (PAN Biotech GmbH, Aidenbach), 0.1 mM β -mercaptoethanol (50 mM, Gibco, Invitrogen™ Cooperation, Carlsbad, CA), 1x MEM (non-essentiell amino acids, 100x; Gibco, Invitrogen™ Cooperation, Carlsbad, CA)
ESC lines	DMEM (Gibco, Invitrogen™ Cooperation, Carlsbad, CA), supplemented with 2 mM L-glutamine (200x, Gibco, Invitrogen™ Cooperation, Carlsbad, CA), 15 % FCS (PAN Biotech GmbH, Aidenbach), 0.1 mM β -mercaptoethanol (50 mM, Gibco, Invitrogen™ Cooperation, Carlsbad, CA), ESGRO® (LIF) (107 U/ml; Chemicon, Millipore, Schwalbach), 1x MEM (non-essential amino acids, 100x; Gibco, Invitrogen™ Cooperation, Carlsbad, CA), 2 mM HEPES (200 mM, Gibco, Invitrogen™ Cooperation, Carlsbad, CA)
Freezing Medium 1x:	5ml FCS (PAN/PAA), 4 ml D-MEM (or ESC medium), 1 ml DMSO
Freezing Medium 2x:	8 ml FCS, 2 ml DMSO

6.1.14 Solutions for cell culture

1x PBS without Mg^{2+}/Ca^{2+}	Gibco, Invitrogen™ Cooperation, Carlsbad, CA
1x trypsin-EDTA	0.05 % Trypsin, 0.53 mM EDTA•4Na, (Gibco, Invitrogen™ Cooperation, Carlsbad, CA)

6.1.15 Mouse lines

<i>C57BL6</i>	inbred strain (Helmholtz Zentrum München)
<i>CD1</i>	outbred strain (Helmholtz Zentrum München)
<i>C3H/J</i>	inbred strain (Helmholtz Zentrum München)
<i>Pax611Neu (H9)</i>	(Favor et al., 2009); background: C3HJ
<i>Pax613Neu (Tcm2)</i>	(Favor et al., 2009); background: C3HJ
<i>Flp-e</i>	(Dymecki, 1996); background: <i>C57BL6</i>
<i>R26R</i>	(Soriano, 1999); background: <i>C57BL6</i>
<i>β-catenin F/F</i>	(Brault et al., 2001); background: <i>C57BL6</i>
<i>β-catenin FD/+</i>	(Brault et al., 2001); background: <i>C57BL6</i>
<i>Sox17^{2A-iCre}</i>	(Engert et al., 2009); background: two generations <i>C57BL6</i>
<i>Sox17^{CreERT2}</i>	(Engert et al., 2013a); background: mixed
<i>mT/mG</i>	(Muzumdar et al., 2007); background: <i>C57BL/6J</i>

6.2 Methoden

6.2.1 Cell culture

6.2.1.1 Embryonic stem cell culture

6.2.1.1.1 Expansion of mouse embryonic fibroblasts

One aliquot of mouse embryonic feeders (MEFs) passage 2 was thawed on 5 x15 cm dishes in 20 ml Feeder medium. MEFs were fed every second day with fresh feeder medium. Depending on growth abilities and density, MEFs were split 3 to 4 days after seeding in a ratio of 1:5. For splitting, cells were washed two times with 10 ml DPBS (-MgCl₂), 4 ml 0.05 % trypsin/EDTA were added per plate and incubated at 37 °C for 4 min. Trypsin was neutralized with 6 ml medium, cells were resuspended and transferred to 50 ml falcon tube. Cells were centrifuged at 1200 rpm for 4 min. The pellet was resuspended in

medium and passage 3 MEFs were thawed on new 15 cm dishes. To obtain passage 4, MEFs were handled and treated as described before.

6.2.1.1.2 Treatment of MEFs with mitomycin

5 x 15 cm dishes of MEFs were expanded to passage 4 as described above. MEFs at passage 4 were grown till they were confluent. 5 x 15 cm dishes were washed two times with 15 ml DPBS (-MgCl₂), 4 ml 0.05 % trypsin/EDTA were added per plate and incubated at 37 °C for 4 min. Trypsin was neutralized with 6 ml medium, cells were resuspended and transferred to a 50 ml falcon tube. Cells were centrifuged at 1200 rpm for 4 min. The pellet was resuspended in 20 ml feeder medium containing 10 µg/ml mitomycin (MMC). The falcon tube was put with loose cap at 37 °C for 20 min. After 20 min, the closed tube was inverted several times. The tube was put with loose cap at 37 °C for another 20 min. The process was repeated and finished after 1 h of MMC treatment. The cells were centrifuged at 1200 rpm for 4 min and washed three times with 20 ml DPBS. MMC-treated MEFs were seeded or frozen.

6.2.1.1.3 Freezing/thawing of MEFs

MEFs of 5 x 15 cm dishes were resuspended in 2.5 ml 1 x feeder freezing medium and 5 x 500 µl aliquots were frozen. Before thawing feeder aliquots, dishes were coated with 0.1 % gelatine and dried. ESCs were defrosted in a water bath for 1 min at 37 °C. ESCs were transferred to a 15 ml falcon tube prefilled with ESC medium. Cells were centrifuged at 1200 rpm for 4 min and the cell pellet was resuspended in the according amount of ESC medium. ESCs were cultured on MMC-treated MEFs at 5-7 % CO₂ in a humidified incubator.

6.2.1.1.4 Cryopreservation of ESCs

For long-term storage, ESCs were trypsinized as described above and the cell pellet was resuspended in 500 µl cooled 1 x ESC freezing medium. Cells were transferred to cryovials which were put into pre-cooled freezing boxes. Freezing boxes were kept at -80 °C for at least 4 h to cool the cells slowly down to -80 °C before vials were transferred to N₂ tank.

6.2.1.1.5 Snap freezing of ESCs

ESCs were washed twice with DPBS. Trypsin/EDTA was added and cells were incubated for 4 min at 37 °C. Afterwards, the cell suspension was neutralized with ESCs medium, centrifuged at 1200 rpm for 4 min and the pellet washed once with DPBS. After centrifugation, the pellet was resuspended in 1 ml DPBS, transferred to an Eppendorf tube and the cells were pelleted using a table centrifuge. The DPBS was removed and the cells directly put into liquid nitrogen. The pellets were stored at -80 °C.

6.2.1.2 Homologous recombination in ESCs

Homologous recombination in IDG3.2 ESCs were used to generate the *Sox17^{CreERT2}* mouse line.

6.2.1.2.1 Transformation of ESCs by electroporation

For each electroporation half a 10 cm dish of IGD3.2 ESCs was used. ESCs were trypsinized as described before. Single cell suspension was washed with 10 ml DBPS centrifuged at 1200 rpm for 4 min and the cell pellet was resuspended in 1.5 ml ice-cold DPBS and put on ice. 0.7 ml of the single cell suspension was mixed with 0.1 ml of the *Swal*-linearized pL254 *Sox17^{CreERT2}* targeting vector. The suspension was transferred to a pre-cooled cuvette. The electroporation was performed as followed:

2 pulses, stored on ice in between for 1 min
Program: 220 V
500 μ F
Resistance: ∞

After electroporation, the cuvette was kept 5 min on ice. Cells were transferred to pre-warmed dish containing MMC-treated MEFs and supplemented with ESC medium. One electroporation provides material for two 10 cm dishes. Medium was changed every day. After 24 h, selection of cells was started with geneticin (G418) at a concentration of 300 μ g/ml. Colonies were picked after 6 to 8 days.

6.2.1.2.2 *Picking of ESC clones*

For picking, two conical 96-well plates were pre-filled with 60 μ l DPBS. Two normal 96-well plates, coated with 0.1 % gelatine and two others containing MMC-treated MEFs, were pre-filled with 100 μ l ESC medium containing G418. After discarding the medium, 10 ml DPBS was added to the 10 cm dishes containing the cell colonies. Colonies that looked compact and round were picked under a stereo microscope in 20 μ l DPBS. Single colonies were transferred to a pre-filled conical 96-well plate without contaminating with single floating cells. After picking, 30 μ l of trypsin/EDTA was added to the wells and the plates were incubated at 5-7 % CO₂ in a humid incubator for 15 min at 37 °C. After trypsinization, the cell suspension was resuspended several times by pipetting up and down. 50 μ l were transferred to each of the two prepared 96-well plates (one with feeder layer which is the master plate for freezing, one with gelatin which is the template for DNA preparation).

6.2.1.2.3 *Cryopreservation of ESC clones in 96-well plates*

To cryopreserve the ESCs within the 96-well plate, 2 x freezing medium was prepared and cooled down to 4 °C.

2 x freezing medium (10 ml per 96-well plate)

4 ml ES cell medium

4 ml FCS (PAN)

2 ml DMSO

After 2 to 4 days incubation at 6 % CO₂ in a humidified incubator, the ESCs on the master plate were frozen. After discarding the medium, the cells were washed once with 200 μ l DPBS per well. To detach the cells, 40 μ l of trypsin/EDTA were added to each well and the plate was incubated at 37 °C for 5 min. After incubation, 60 μ l of cold ESC medium were added to each well and cells were resuspended by pipetting up and down. 100 μ l of 2 x ESC freezing media was added to the single cell suspension und resuspended two times. The plates were sealed with parafilm and put in napkins to store them at -80 °C for 6 to 8 weeks. Freezing of cells needs to be fast to prevent cell death. ESCs in the template plate were grown until the medium changed to yellow within one day. Afterward the DNA was isolated to perform Southern Blot analysis.

6.2.1.2.4 *Thawing of ESCs in the 96-well plate*

48-well plates with feeders were prepared prior to thawing. The frozen 96-well plates from -80 °C were thawed with the help of a pre-warmed metal block in a humidified incubator at 37 °C. Cells within the 96-wells were transferred to the 48-well plate. Medium was changed at the end of the day. During the following days the ESCs were expanded stepwise from 48-well to 10 cm dish. The cells were frozen in 5 x 1/5 of a 10 cm dish.

6.2.1.3 Establishment of ESC lines from blastocysts

ESC medium:

500 ml of DMEM (high glucose + sodium pyruvate), 75 ml FCS (tested PAN), 9 ml L-glutamine (200 mM), 12 ml Hepes (1 M), 6 ml MEM non-essential amino acids (100 x), 1.2 ml β -mercaptoethanol, 100 μ l LIF (1.500 U/ml), 6 ml penicillin/streptomycin (100 x)

Stock solution:

50 mM stocks of PD98059 (MEK1) and 10 mM stocks of CT 99021 (Gsk3 β) were prepared. Stock solutions and ESC medium were warmed up in a waterbath at 37 °C before adding the inhibitors to the medium, to prevent precipitation. The MEK1 inhibitor was used in a working concentration of 50 μ M, Gsk3 β in a working concentration of 3 μ M. For establishment of β -catenin CKO and control ESC lines, only MEK1 was added to the medium, while for generating Elp4 ESC lines, MEK1 as well as Gsk3 β were used.

96-well feeder plates were prepared one day before the experiment. For establishing ESC lines, one aliquot of MMC-treated feeders was thawed on half a 96-well plate to provide a dense feeder cell layer. The 96-well plate was pre-filled with 0.2 ml ESC medium containing MEK1 (and Gsk3 β).

Blastocyst production:

Male mice of the favoured strain were mated with superovulated females. The next day, the female mice were checked for presence of a vaginal plug and separated. At E3.5, the

uteri of plugged females were dissected and collected in a tube with PBS. The forceps and mouth pipette were cleaned with 70 % EtOH and washed with PBS. The uteri were washed with PBS. Each uterus horn was flushed with 0.5 ml ESC medium in a 6 cm dish. Under a laminar flow hood, the embryos were washed once in a drop of ESC medium. Each embryo was placed into one well of the prefilled 96-well plate.

Blastocyst culture:

Blastocysts were cultured for 3 days without disturbance at 7.5 % CO₂ in a humid incubator at 37 °C. At day 3 of culturing, when most of the embryos have attached to the feeder layer, medium was changed. Culture was continued up to day 5-6.

ICM dissociation:

After 5 to 6 days of culturing, the blastocyst outgrowth was trypsinised and plated on freshly seeded 96-well feeder plates. The medium was aspirated and each well was washed with 100 µl DPBS. After adding 30 µl DPBS, the plate was incubated for 10 min at 37 °C. Afterwards 30 µl 0.05 % trypsin/EDTA were added to each well, mixed and the plate was incubated another 10 min at 37 °C. Immediately after trypsinisation, the outgrowth was disaggregated by strongly pipetting up and down. 100 µl ESC medium were added and disaggregation continued. The cell suspension was transferred into a new 96-well feeder plate pre-filled with 40 µl ESC medium containing MEK1 (and Gsk3β). Cells were fed the next day with fresh medium.

After 6 days, grown ESC colonies were marked and labeled with passage number 1. ESC were fed daily with ESC medium without MEK1 (in the case of Elp4 ESCs, inhibitors were added during the whole process of ESC expansion).

ESC line expansion:

Upon expansion of ESC colonies (5-6 days) in the 96-well plate, each well was washed once with DPBS and 50 µl of 0.05% trypsin/EDTA were added. The plates were incubated for 5 to 10 min at 37 °C and neutralized with 50 µl ESC medium. Depending on the cell density, the cells were transferred to one or two wells of a 48-well feeder plate pre-filled with 0.5 ml ESC medium and carefully mixed. In case of very few colonies, the cells were transferred to a new 96-well feeder plate. ESC were labeled with passage number 2.

Culturing was continued for about 3 days until ESC colonies expanded. Cells were fed on a daily basis. ESC lines were expanded to 10 cm dishes. During expansion, ESCs were additionally splitted on 0.1 % gelatine-coated plates for genotyping.

6.2.2 Generation of the Sox17^{CreERT2} targeting vector

The knock-in construct was designed as shown in Fig. 35. The codon usage of the CreERT2 sequence was changed in order to eliminate restriction sites within the gene resulting in the 2A-RFP-2A-CreERT2 pMA (gift of Mr. Gene). To generate the pBKS-Ex5 HR-2A-CreERT2 vector, the 2A-CreERT2 sequence was generated by PCR (fwd: 5'-GCTATTACGCCAGCTGGCGAAAGGGGATGTG-3', rev: *NotI* 5'-GGCCGCACGCGTTTGAAGGTAGAGGCTCTTTACTAACATGCGGCGACGTTGAGGAAAACCCAGGACC-3') using the 2A-RFP-2A-CreERT2 pMA as template and cut with *MluI*. The 5'/3' overhangs were filled with Klenow, and digested with *HindIII*. The sequence was subcloned between the *XbaI*-blunt/*HindIII* sites of the pBKS-Ex5 HR (Engert et al., 2009). In the next step, the PGK promoter-driven neomycin resistance gene flanked by *FRT* sites, was cloned from pL451ΔloxP (Liu et al., 2003), cut with *HindIII* and *SmaI* and subcloned into the pBKS-Ex5 HR-2A-CreERT2, cut with *ClaI*, filled with Klenow and digested with *HindIII* resulting in pBKS-Ex5 HR-2A-CreERT2-FRT-neo-FRT. The cassette was cut out with *SacII* and *XhoI* and introduced into pL254-Sox17 (Liao et al., 2009) via bacterial homologues recombination in EL350 bacteria, resulting in the final targeting vector (Fig. 36a), which was confirmed by sequencing.

6.2.3 Identification of TBE binding elements

TCF/LEF binding elements were identified using genomatrix. For targeting sequence and genomic position see Table 4.

Name	Forward primer	Reverse primer	Genomic position mm9
TBE1	CCCCACATCTCAAGTGCTG	TGGTGATCGAGCTCAGTTTG	chr1:4484862-4484967
TBE2	CCGCTACTGTTTTCAATCGTC	CCCTCACCTCCACAGTGAC	chr1:4485823-4485971
TBE3	GGCTTTGATAACGTCGTGAG	GTGAGTGGGCCATATTTTCAG	chr1:4486458-4486528
negative	GGATGGAAAGGCACCTATTG	ACAGTGGGTCAAGCACATTG	chr1:4488145-4488223
TBE4-7	TAACTTCCAGGGCAGTTGTG	GTCTGTCTTTAGGGCATTGG	chr1:4488882-4488998
TBE4-7	TGTGGCGTTAAGTCACTGAGTC	ACTGCCCTGGAAGTTACTGAAG	chr1:4488983-4489067
TBE 8-10	AGTCTGAGAGAACATGGCACAC	GGCAAATTCTAATTCATCTGAGC	chr1:4489550-4489658
TBE 11	GTAGTGCACACCTTCAAAGAGG	AATGGCAGCTCACAATCATC	chr1:4490552-4490631
TBE 12-13	CTTCAGCAAAGGACTGTGAGTG	GTGTGTGGCCATGTAACCAG	chr1:4492173+449232

Table 4: TCF/LEF binding elements

6.2.4 Chromatin immunoprecipitation (ChIP) assays

Preparation and immunoprecipitation of chromatin was done according to published methods with modifications (Kagey et al.). For ChIP 5 µg anti-β-Catenin (#9652 Cell Signalling) antibody or anti-Tcf4 (Ab #2565 Cell Signalling) respectively were used. Quantitative PCR (qPCR) was performed with Fast SYBR Green Master Mix qPCR kit (Applied Biosystems) using 10 µl of total reaction and analyzed on the Light Cycler 480 real-time PCR system (Roche Applied Bioscience). For qPCR primers see Table 5.

Tcf/Lef binding elements	Target sequence	Genomic position mm9
TBE 1	5' CATTCTTTGAGTTTTTC 3'	chr1: 4484854
TBE 2	5' GAGATCTTTGAAAAGAT 3'	chr1: 4485876
TBE 3	5' GCTGGCTTTGATAACGT 3'	chr1: 4486521
TBE 4	5' TGAATTATTGAAGGAGA 3'	chr1: 4488741
TBE 5	5' CTTCGATAAAAAGCATT A 3'	chr1: 4488812
TBE 6	5' TTAATTTCAAAGATAAC 3'	chr1: 4488911
TBE 7	5' AGAACCTTTGTTATGTG 3'	chr1: 4489071
TBE 8	5' CAGATATCAAAATAAAT 3'	chr1: 4489533
TBE 9	5' TCCATCTTTGAACCTT 3'	chr1: 4489588
TBE 10	5' AGTTCATCAAAGCTAAC 3'	chr1: 4489676
TBE 11	5' ACACCTTCAAAGAGGTG 3'	chr1: 4490617
TBE 12	5' TAGAAAACAAAGAAACA 3'	chr1: 4492229
TBE 13	5' CCTTCAGCAAAGGACTG 3'	chr1: 4492314

Table 5: Oligonucleotides for ChIP analysis

6.2.5 Endoderm differentiation

Stocks of ESCs were generated in order to increase reproducibility of differentiation experiments. ESCs were expanded to 10 cm dishes on a feeder layer in ESC medium containing PAA instead of PAN. ESCs from one 10 cm dish were splitted in ratio of 1:2 on a gelatine-coated 15 cm dish. Depending on the growth characteristics, ESCs from one 15 cm dish were splitted to 5 x 15 gelatine-coated dishes (p2 gelatine). After two days, two aliquots of ESCs were frozen from one 15 cm dish.

Prior to endoderm differentiation, one aliquot of ESCs was thawn on one gelatine-coated 10 cm dish (p3) in ESC medium with PAA. After incubation at 6 % CO₂ in a humified incubator at 37 °C for one to two days, depending on density, the dishes were washed two times with DPBS, trypsinised, neutralized and centrifuged at 1200 rpm for 4 min. The cell pellet of one 10 cm dish was resuspended in 5 ml endoderm differentiation medium and

cells were counted using a Neubauer chamber. Depending on their growth characteristics, 50000 to 80000 cells per 96 well were seeded in endoderm differentiation medium containing Activin A and Wnt3a. Cells were harvested at day 0 to day 3.

6.2.6 Generation of expression vectors

The cDNA encoding td-tomato fluorescent protein (Shaner et al., 2004) was amplified by PCR using the following primers: Tomato fwd (5'-*Xba*I), 5' TCTAGAATGGTGAGCAAGGGCGAGGAG; Tomato rev (5'-*Spe*I), 5' ACTAGTTTACTTGTACAGCTCGTCCATGCCG. *Xba*I/*Spe*I- digested PCR product was cloned into the pBKS vector. The gene encoding histone 2B (H2B) was amplified by PCR using following primers: H2B fwd (5' *Not*I-Kozak- ATG-H2B), 5' GCGGCCGCGCCACCATGCCAGAGCCAGCG; H2B rev (5' *Xba*I-H2B), 5' TCTAGACTTAGCGCTGGTGTACTTGGTGATGG. The amplified sequence was digested with *Not*I/*Xba*I and subcloned in front of the td-tomato cDNA in the pBKS vector. The *Not*I/*Spe*I-digested H2B-td-tomato fluorescent marker was subcloned into the *Not*I/*Nhe*I sites of the eukaryotic expression vector pCAGGS (Niwa et al., 1991).

6.2.7 Generation of fluorescent β -catenin CKO and control ESCs cell lines

The pCAGGS vector containing H2B-td-tomato was linearized with *Eco*RV over night. Linearization was confirmed by loading digested DNA on a gel. The DNA was precipitated using isopropanol and resuspended in DPBS on the day of experiment. 15 μ g of plasmid DNA was used per electroporation per ESC clone. β -catenin CKO and control ESCs were grown on 6 cm feeder dishes until they were subconfluent. ESCs were fed in the morning of the electroporation. ESCs were washed twice with DPBS and trypsinized until single cell suspension was achieved (~ 6 min). After neutralization with ESC medium and centrifugation, cells were resuspended in 10 ml DPBS and counted. Cells were centrifuged and resuspended in DPBS for a final concentration of 7.5×10^6 cells/ml. 700 μ l of cell suspension was mixed with 16 μ g of plasmid DNA and incubated for 5 min at RT. Suspension was transferred to a cuvette and a single pulse was applied with following

parameter: 230 V, 500 μ F, Resistance: ∞ . Cells were selected on puromycin MEFs (6 cm dish). Several colonies were picked and expanded. Cell clones were screened for ubiquitous reporter expression *in vivo* using embryos derived from ESCs.

6.2.8 Molecular biology

6.2.8.1 DNA extraction

a) Plasmid preparations were performed according to QIAGEN Plasmid kits

b) BAC mini preparation according to Copeland:

Preparation of BAC DNA is analogous to plasmid DNA preparation. The used protocol was adopted from a published protocol (Warming et al., 2005). Approximately 1 to 1.5 μ g can be obtained by using this protocol.

Inoculate 5 ml LB medium supplemented with 25 μ g/ml chloramphenicol overnight. The bacterial culture was centrifuged in a 15 ml falcon tube at 5000 rpm for 5 min. Supernatant was discarded and the pellet dissolved in 250 μ l P1 buffer (QIAGEN Mini Kit). The solution was transferred to an Eppendorf reaction tube, 250 μ l P2 buffer was added and the tube inverted carefully. The solution was incubated at RT for a maximum of 5 min. After incubation, 250 μ l P3 buffer was added, mixed and incubated on ice for 5 min. The proteins were precipitated by centrifugation at 13500 rpm for 5 min and the DNA containing supernatant transferred to a new Eppendorf tube. Centrifugation was repeated to completely eliminate the precipitate. For BAC precipitation, 750 μ l isopropanol was added, mixed and incubated on ice for 10 min. The DNA was pelleted by centrifugation at 13500 rpm for 10 min. The supernatant was discarded and the pellet was washed with 1 ml of 70 % ethanol and centrifuged at 13500 rpm for 5 min. The pellet was dried up to 10 min at RT and dissolved in 50 μ l TE at 37 °C on a shaker (500 rpm) for 1 h. Restriction digest was performed in a volume of 60 μ l.

c) BAC maxi preparation was done according to the NucleoBond BAC Purification Max Kit.

d) Isolation of genomic DNA from 96-well plate:

Before starting, the lysis buffer was supplemented with proteinase K in a working concentration of 100 µg/ml to avoid self-digestion over time. The medium was aspirated and the cells washed twice with PBS – Mg²⁺/Ca²⁺. PBS was removed and 50 µl lysis buffer was added per well. The plate was sealed with parafilm and incubated at 55 °C in a humidified chamber overnight. The next day, 150 µl sodium chloride were mixed with 10 ml ice-cold ethanol. For DNA precipitation, 100 µl of the mixture was added to each well and incubated at RT for 30 min without moving the plate. To remove the liquid, the plate was carefully and slowly inverted. Remaining liquid was removed by putting it on a paper towel upside-down. The DNA was washed three times with 150 µl of 70 % ice-cold ethanol. Ethanol was removed by inversion of plate as described above. The DNA can be stored in 70 % ethanol at -20 °C. After the last washing step, the DNA was dried for 10 to 15 min at RT and the DNA was dissolved in 25 µl H₂O overnight at 4 °C or 1 h at 37 °C in a humid chamber while shaking.

e) DNA extraction for *in vitro* transcription:

Digestion of the vector was carried out in a volume of 40 µl. 1 µl was used to check for proper linearization on a gel. The remaining 39 µl were filled up to 100 µl by adding TE. The same volume of phenol/chloroform/isoamylalcohol was added. The mixture was vortexed and centrifuged at 14000 rpm for 5 min. The supernatant was transferred to a new Eppendorf tube and 10 µl 3 M sodium acetate as well as 250 µl 100 % ice-cold ethanol was added. The mixture was put on -20°C for 30 min and afterwards centrifuged at 14000 rpm at 4 °C for 15 min. The pellet was washed once with 70 % cold ethanol and centrifuged at 4 °C for 10 min. The pellet was dried and resuspended in 20 µl of DEPC-H₂O. The DNA was stored at -20 °C.

f) Phenol-chloroform extraction to purify DNA:

The same volume of phenol was added to the dissolved DNA, vortexed and centrifuged at 13000 rpm for 5 min. The aqueous upper phase (avoid interphase) was transferred to new Eppendorf tube and one volume of chloroform was added. The mixture was vortexed, centrifuged and the aqueous upper phase transferred to a new Eppendorf tube. A tenth of

the total volume of ammonium acetate (10 M) and 2.5 volume of 100 % ethanol were added and incubated at least for 2 h at -20 °C. Higher incubation times at -20 °C will yield higher concentrations of DNA. The sample was centrifuged at 13000 rpm at 4 °C for 20 min. The pellet was washed in 200 µl 70 % ethanol and centrifuged again at 4 °C for 15 min. Supernatant was discarded and the pellet resuspended in 6 µl H₂O. DNA concentration was determined with Nanodrop by taking out 0.5 µl and diluting in 9.5 µl H₂O.

6.2.8.2 RNA extraction

Extraction of RNA was done according to QIAGEN miRNeasy kit.

6.2.8.3 *In vitro* transcription and generation of *in situ* probes

Prior to transcription the vector containing the favoured cDNA is linearized with restriction enzyme at the future 3' end to exclude transcription of the vector DNA sequence. The DNA was extracted according to "DNA extraction for *in vitro* transcription".

A typical reaction scale for IVT is as followed:

- 6 µl DEPC-H₂O
- 1 µl 10 x transcription buffer
- 1 µl 10 x Dig Mix
- 0.5 µl RNase inhibitor
- 0.5 µl Sp6/T7 or T3 polymerase
- 500 ng DNA

The mixture was incubated at 37 °C for 2 h. After the IVT, 1 µl of DNase I was added to the mixture to digest the vector DNA. The mixture was incubated at 30 °C for 15 min. to precipitate the RNA, 100 µl of DEPC-H₂O, 10 µl of 4 M LiCl and 300 µl of 100 % ethanol were added and the mixture was incubated on dry ice for 15 min. Afterwards the mixture was centrifuged at 14000 rpm at 4 °C for 10 min. The pellet was washed once with 70 %

ethanol, centrifuged and dried at RT for 5 min. The pellet was resuspended in 55 μ l DEPC-H₂O. 5 μ l were used to check the RNA probe on a 1 % RNA gel.

6.2.8.4 Determination of DNA or RNA concentration in solution

The concentration of DNA and RNA can be determined by measuring the extinction 260 ($E_{260\text{nm}}$) nm with a photometer (NanoDrop). The NanoDrop allows measurement of concentrations in small amounts of solution. The quotient of $E_{260\text{nm}}$ and $E_{280\text{nm}}$ indicates the purity of nucleic acid and should be between 1.9 to 2.0 for RNA solutions and 1.8 to 1.9 for clean DNA solutions.

6.2.8.5 Restriction analysis of DNA

Analytical or preparative restriction digestions for BAC or plasmid DNA

a) A typical scale for a restriction digestion is as followed:

DNA from mini preparation (ca. 500-100 ng)	5.0 μ l
10x buffer	2.0 μ l
10x BSA (optional)	2.0 μ l
enzyme (5.000 U)	0.5 μ l
<u>dist. H₂O</u>	<u>10.5 μl</u>
Σ	20.0 μ l

The digestion was incubated in a 1.5 Eppendorf tube at 37 °C or 25 °C for 1.5 h to overnight.

b) Restriction digestion of genomic DNA

I. Restriction digestions of genomic DNA from ESCs for Southern blot analysis

A typical mix for restriction digestion is as followed:

25 µl genomic DNA
1x restriction buffer
(1x BSA)
1x spermidine (1 mM)
50-100 µg/ml RNaseH
H₂O to fill up
approx. 50 U of restriction enzyme

The digestion was incubated at the designated enzyme-dependent temperature overnight.

II. Restriction digestion of genomic DNA from ESCs in a 96-well pate for Southern blot analysis

25.0 µl DNA (whole DNA preparation of one well)	
0.40 µl 100x BSA	C _{end} = 1x BSA
0.40 µl 100 mM spermidine	C _{end} = 1 mM spermidine
0.25 µl RNase A 1 mg/ml	C _{end} = 6.25 µg RNase
4.00 µl 10x enzyme buffer	C _{end} = 1x enzyme buffer
2.50 µl enzyme (10 U/µl)	C _{end} = 25 U enzyme/reaction
7.45 µl H ₂ O	
<hr/>	
40.0 µl	

A mix of all components except DNA was added to each well of the 96-well plate using a multi-pipette and incubated overnight at 37 °C or 25 °C, depending on the working temperature of the enzyme. To avoid evaporation, the plate was sealed with parafilm and incubated in a humidified chamber.

6.2.8.6 Gel electrophoresis

a) Analytical agarose gel electrophoresis

The agarose gel was prepared according to the expected fragment size with 0.8 % to 2 % agarose in TAE buffer. The agarose was dissolved by heating using a microwave. The solution was cooled down and ethidiumbromide (EtBr; $c_{\text{EtBr}} = 1 \text{ mg}/\mu\text{l}$, end concentration 0.005 %) was added, the solutions mixed and poured in a gel chamber without bubbles. The gel was run at approximately 100 V (higher voltage for RNA gels to speed up the process) for 45 min. The fragment pattern was documented under UV light.

b) Preparative agarose gel electrophoresis

The electrophoresis was performed analogous to the analytical electrophoresis, but the bands with the correct size were cut out and documented with less UV intensity to avoid UV-light induced mutations.

6.2.8.7 Isolation of DNA fragments from agarose gels

After separation, the appropriate DNA fragment was cut out and transferred to an Eppendorf tube. The DNA was isolated according QIAquick Gel Extraction Kit.

6.2.8.8 Dephosphorylation of linearized DNA

A typical mixture to dephosphorylate linearized DNA is as followed:

1.0 μg DNA	
1.0 μl 10x enzyme buffer	$c_{\text{end}} = 1\text{x enzyme buffer}$
1.0 μl alkaline phosphatase (1 U/ μl)	$c_{\text{end}} = 1 \text{ U enzyme/reaction (1 } \mu\text{g DNA)}$
7.0 μl H ₂ O	
<hr/>	
10.0 μl	

6.2.8.9 Ligation

A typical scale for ligation of vector and insert DNA is as followed:

1.0 µl vector DNA (e.g.; see below)	
0.5 µl insert DNA (e.g.; see below)	
1.0 µl 10x T4 ligation buffer	cond = 1x enzyme buffer
0.5 µl T4 ligase (10 U/µl; NEB)	cond = 5 U enzyme/reaction
7.0 µl dist. H ₂ O (add at 10 µl with dist. H ₂ O)	
<hr/>	
10.0 µl	

The following formula can be used to calculate the amount of vector and insert

Ratio: vector/insert = 1/3

vector concentration:	$c(v) [\text{ng}/\mu\text{l}] = x \text{ ng}/\mu\text{l}$	size (v) [bp] = y bp
insert concentration:	$c(i) [\text{ng}/\mu\text{l}] = a \text{ ng}/\mu\text{l}$	size (i) [bp] = b bp
used amount of vector-DNA:	100-400 ng	> used for ligation: $v \text{ ng} / w \mu\text{l}$
used amount of insert-DNA:	$\text{intron} [\text{ng}] = 3 * (b \text{ bp} / y \text{ bp}) * w \mu\text{l}$	> intron DNA [μl]

Ligation is carried out between 14 to 16 °C for one to several hours. For ligation of sticky ends, 1 h at RT is sufficient. Ligation of blunt ends is more difficult due to the low efficiency. The ligation is incubated for 4 to 18 h at 16 °C or overnight at 4 °C.

6.2.8.10 Generation of competent bacteria

Generation of electro-competent bacteria (E. coli K-12 XL1-Blue) recA1 endA1 gyrA96 thi-1 hsdR17 supE44 relA1 lac [F' proAB lacIqZΔM15 Tn10 (Tetr)]

Out of a 2 ml pre-culture, bacteria were plated on LB plates with kanamycin (30 µg/ml), tetracycline, ampicillin (40 µg/ml), and with antibiotics as controls and incubated at 37 °C overnight. The following day, if the control plates have proven that there cannot be found any adapted resistance, a 50 ml preculture was set up for the next day using a single colony and incubated overnight at 37 °C while shaking. All material that will be used should be washed carefully with clean water. Any detergent that is left will reduce the efficiency of competence. The following day 500 ml LB medium were inoculated with 5 ml bacterial preculture at 37 °C until OD₆₀₀ = 0.5 (~3 h).

The following steps were all carried out on ice or at 4 °C to prevent the bacteria from warming. Every material used should be precooled. First the bottles with the bacterial

suspension were put in ice water for at least 15 min to cool down. The bacteria were then pelleted in clean centrifugation bottles (2x 250 ml) by spinning them for 15 min at 4.000 x g in the precooled centrifuge. The pellets were resuspended in 250 ml ice-cold water each and pelleted at 6.000 x g for 15 min. Increasing g is necessary to avoid losing a lot of bacteria. After centrifugation each pellet was again resuspended in 125 ml ice-cold water and centrifuged under latter conditions. After this centrifugation step the bacteria were resuspended in 5 ml pre-cooled 10 % glycerol solution per pellet and transferred to pre-cooled 30 ml Correx-tubes. The cells were centrifuged at 8.000 x g for 15 min. Finally, the pellets were resuspended in 0.5 ml fresh pre-cooled 10 % glycerol solution. Aliquots à 40 µl were made and immediately frozen down on dry ice. The bacteria were kept on -80 °C.

6.2.8.11 Transformation of bacteria

a) Transformation of bacteria using electroporation

For transformation one aliquot of electro-competent bacteria (50 µl) was used per construct. The bacteria were thawed on ice. 1 to 2 µl of DNA was incubated with the bacteria for 5 min on ice. The mixture was transferred to a pre-cooled electroporation cuvette (0.1 cm) avoiding bubbles. One pulse was given with a tension of $U = 2.5 \text{ kV}$, 25 µF, 200 to 400 Ω. The pulse should last around 4.5 to 5.0 ms. Immediately after the pulse, the mixture was transferred to an Eppendorf tube and 0.9 ml LB medium was added. The bacteria were incubated at 37 °C for 30 to 60 min while gently shaking (850 rpm) to allow the bacteria to regenerate. Afterwards a fraction of the bacteria were plated on selective LB dishes supplemented with the appropriate antibiotics. The plates were incubated overnight at 37 °C.

b) Transformation of rubidium chloride competent DHα5F' bacteria

One aliquot of competent bacteria (50 µl) per construct was thawed on ice. Approximately 1 ng of DNA was mixed with the bacteria and incubated for 30 min on ice. For the heat shock, the mixture was incubated at 42 °C for 90 sec. Immediately afterwards, the bacteria were put on ice for 5 min and 0.9 ml LB medium was added. The bacteria were incubated

at 37 °C for 60 min while shaking (850 rpm) for regeneration and plated on selective LB dishes. Plates were incubated overnight at 37 °C.

6.2.8.12 Homologous recombination in bacteria

H18-C (pL-254- New Sox17 retrieval) EL-350 bacteria from a glycerol stock were incubated in 5 ml LB medium overnight at 32 °C. The next day, the bacterial culture was diluted 1:50 to 1:100 and grown in 50 ml LB medium to an optical density (OD) of 0.6 measured at a wave length of 600 nm ($OD_{600} = 0.5$). If the OD was reached, the culture was split: 25 ml were kept in a falcon tube at RT (serves as recombineering control), the other 25 ml were incubated at 42 °C for 15 min in a water bath while shaking. Afterwards both cultures were incubated on ice for 5min and kept cool during the further procedure.

Bacteria were centrifuged in a 50 ml falcon tube at 5000 rpm at 4 °C for 5 to 10 min. The bacterial pellet was resuspended in 1.8 ml of ice-cold 10 % glycerol and transferred to 2 ml Eppendorf tubes. The suspension was centrifuged at 14000 rpm at 4 °C for 20 sec and again resuspended in 1.8 ml of ice-cold glycerol by vortexing. This step was repeated three more times. After the last step, the pellet was resuspended in 600 μ l 10 % glycerol and aliquots of 60 μ l were frozen. One aliquot of the bacterial suspension was used per electroporation (+/- construct). 15 ng of *SacII/XhoI* digested pBKS-Ex5 HR-2A-CreERT2-FRT-neo-FRT was mixed with 50 μ l of the competent cells, kept on ice for 5 min and was then electroporated (program: bacterial \rightarrow E.coli 1 mm). Immediately, 1 ml LB medium was added and the suspension was transferred to an Eppendorf tube. The cells were grown at 32 °C for 1 h, plated in two different dilutions (200 μ l = 1:5 and 20 μ l = 1:50) on selective LB dishes (canamycin) and incubated at 32 °C overnight.

6.2.8.13 Growth of bacteria

5 ml of LB medium supplemented with ampicillin in a final concentration of 0.1 mg/ ml was inoculated with a single bacterial colony by touching a sterile pipette tip to the colony and putting it into the tube. The tube was placed on a shaker at 37 °C until the culture is

saturated (at a density of $1-2 \times 10^6$ cells/ml, takes approximately 6 h). The inoculated 5 ml suspension was used to inoculate a larger medium (200 ml LB, 50 $\mu\text{g/ml}$ ampicillin) and incubate at 37 °C overnight while shaking.

6.2.8.14 DNA sequencing

a) Sequencing reaction:

The following mixture is used for one sequencing reaction

<u>Long sequence</u>	<u>short sequence</u>	
1.0 μl	0.5 μl	Big Dye containing the polymerase
1.0 μl	2.0 μl	Big Dye buffer
10 pM	10 pM	sense or antisense primer
<u>(n) bp/ 100 = x ng template DNA</u>		
Σ 5.0 μl		

Following PCR program was used to amplify the sequencing products:

96°C 1 min	} 35 x
96°C 10 s	
50°C 5 s	
60°C 4 min	
16°C ∞	

b) DNA preparation of sequencing:

For precipitating DNA, 0.5 μl of 125 mM EDTA is added to each sample of a size of 5.0 μl . 2.0 μl 3 M sodium acetate as well as 50 μl of 100 % ethanol were added. The solution was mixed well and incubated at RT for 15 min. Afterwards the DNA was pelleted by centrifugation at 11000 rpm at 4 °C for 30 min. The pellet was washed once with 70 % ethanol and centrifuged for 10 min at 4 °C. The ethanol was removed and the pellet was dried at RT. The DNA was resuspended in 15 to 25 μl HPLC- H_2O .

6.2.8.15 Southern blot

a) Gel electrophoresis:

The DNA was isolated according to “Isolation of genomic DNA from 96-well plate”. The DNA was digested according to “Restriction digestions of genomic DNA from ES cells for Southern blot analysis”. The digestion was completed by adding 5 µl Orange g loading buffer, applied to a 0.8 % agarose gel and separated slowly (35 V) overnight. The next day, the gel was documented under UV-light next to a fluorescent ruler serving as reference length. If the digestion was completed, repetitive sequences can be detected by a distinct band under UV light.

b) Blot:

After electrophoresis, the gel was depurinated by incubation in 989 ml H₂O supplemented with 11 ml concentrated HCl for 10 to 15 min while shaking. Afterwards the gel was shortly washed with H₂O. The depurination was followed by denaturation in 0.2 M sodium hydroxide and 0.6 M sodium chloride in H₂O for 30 to 60 min while shaking. After shortly washing with H₂O the gel was neutralized in 1.0 M Tris and 0.6 M sodium chloride in H₂O for 30 to 60 min while shaking. After quick washing with H₂O, the blot was built up in 20 x SSC and the transfer was carried out overnight.

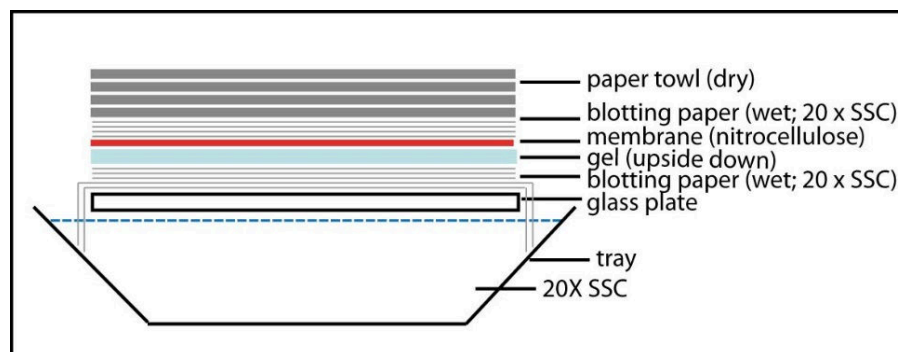


Figure 44: Southern Blot setup

The blot was set up in a tray filled with 20 x SSC. A glass plate was used as a carrier. Overhangs of blotting paper reached the 20 x SSC. The gel was put upside down on the

blotting paper. The membrane was soaked with 20 x SSC and placed on the gel. The membrane was covered by blotting paper and paper towels.

The next day, the blot setup was taken apart and the slots of the gel were marked with a ball pen. The membrane was dried between Whatman paper at RT. Afterwards the membrane between the Whatman paper was incubated at 80 °C for 30 min to cross-link the DNA to the membrane.

c) Hybridisation:

I. Prehybridisation

30 ml hybridisation solution per membrane was pre-heated to 65 °C in a water bath. The membrane was put into the hybridisation tube and the hybridisation solution was poured into the tube without bubbles between the membrane and the tube. The membrane was pre-hybridised at 65 °C while rotating for 1.5 to 3 h.

II. Radioactive labelling of the probe and hybridisation

While prehybridising, the radioactive labelling of the probe was performed. Approximately 25 ng of linearized DNA probe was filled up to 23 µl by adding H₂O to an Eppendorf tube. 10 µl of random oligonucleotides were added and the mixture was denatured at 100 °C for 5 min in a water bath. Afterwards the mixture was cooled down on ice, centrifuged to collect the liquid at the bottom of the tube and put back on ice. 10 µl of pre-cooled 5 x dCTP buffer was added. In the radioactive lab, P³² labelled dCTP (50 µCi) and 1 µl (5 U) Exo (-)Klenow-enzyme were added, the mixture carefully vortexed or well-mixed, shortly centrifugated and labelled at 37 °C for 30 to 60 min. For completion of the reaction 2 µl 0.2 M EDTA (pH 8.0) were added. EDTA binds Mg²⁺ and Ca²⁺ ions and thus inhibits the activity of the polymerase. 49 µl TE were added and the mixture was transferred to prepared micro-spin columns (centrifuged without sample for 2 min at 760 g) and centrifuged at 760 g (3000 rpm) for 2 min. Non-incorporated nucleotides remain on the column. The radioactive probe is kept on ice, shortly mixed and centrifuged before measuring the radioactivity. 1 µl of the probe transferred to a scintillation detector and measured 1 min (P³²). The probe is fine if it shows 300000 to 400000 counts/µl. For chemical denaturation, 500 µl salmon sperm (SS) DNA (10 mg/ml) were boiled at 100 °C for 10 min in a water bath. The SS-DNA was transferred to a 50 ml falcon tube and kept on ice. The radioactive labelled probe in a working concentration of 1x10⁶ counts/ml hybridisation solution was added (2x10⁷ per 20 ml). While carefully swirling, 50 µl of 10 N sodium hydroxyl were added to denature the sample then 300 µl 2 M Tris pH 8.0 and 475 µl 1 M HCl were pipetted drop wise into the tube for neutralization. After prehybridisation, the solution was decanted from the tube and discarded. The

radioactive-labelled probe was pipetted into the hybridisation tube and the tube was put back into the oven to 65 °C overnight while rotating.

III. Membrane washing

The hybridisation solution was discarded into P³² liquid waste. The membrane was washed with 2 x SSC/0.5 % SDS in a plastic bowl at RT for 5 min while shaking. Afterwards, the solution was discarded and the membrane washed with pre-warmed 2 x SSC/0.5 % SDS at 65 °C for 30 min in a water bath while shaking. The membrane was measured for intensity of radioactivity. If the signal was still too high but relatively weak (100-200x10² counts), the membrane was washed again in 2 x SSC/0.5 % SDS at 65 °C and measured every 5 min. If higher signals were measured (> 200x10² counts) the stringency of the washing steps could be increased by reducing the concentration of SSC (1 x SSC/ 0.5 % SDS). If the signal decreased to approximately 35x10² counts, the membrane was wrapped in saran foil and fixed in a film cassette. A film (Kodax, BioMax) was applied and the cassette was stored at -80 °C for 1 to 3 days depending on the signal intensity until developing.

6.2.9 Methods in protein biochemistry

6.2.9.1 Extraction of proteins

a) Protein extraction from whole cell lysate

The medium was aspirated of each 6-well plate and the cells were washed once with ice-cold PBS. The PBS was removed and the cells were lysed in 50 to 100 µl lysis buffer supplemented with proteinase inhibitor cocktail (1:200) on ice. The cells were abraded using a cell scraper and transferred to a 1.5 ml Eppendorf tube with a pipette. The cells were centrifuged at 14000 rpm at 4 °C for 10 min to pellet insoluble constituents such as nuclei and parts of the cell membrane. The supernatant containing the proteins was transferred to a new tube and stored at -80 °C if not used immediately.

b) Protein extraction from tissue

Mice were killed by cervical dislocation, the lung was dissected quickly and the weight was determined (~ 0.2 g). The tissue was immediately kept in PBS on ice. The tissue was cut with a scissor, transferred to a 15 cm falcon tube and 1 ml RIPA buffer supplemented with proteinase inhibitor (1:200) were added (one ice). The tissue was further homogenised and sonificated. Afterwards, the suspension was centrifuged at 14000 rpm for 10 min at 4 °C and the supernatant was transferred to Eppendorf tube. The protein concentration was measured and the suspension was frozen at -80 °C.

6.2.9.2 Determination of protein concentrations using Bradford assay

The Bradford assay is based on the absorbance shift of the coomassie dye when it binds to protein (from red to blue > 595 nm). Protein samples are measured at OD₆₀₀ relatively to each other. 1 µl protein sample was diluted 1:10 with distilled H₂O and 990 µl Bradford was added and the mixture was incubated at RT for 10 min. The mixture was measured against a blank value and the relative concentration was calculated according to the directly proportional absorbance measured.

6.2.9.3 Western Blot

a) Denaturing SDS-polyacrylamide gel electrophoresis

For 2 small 10 % separating gels the following composition was used:

- 5 ml acrylamide/bisacrylamide-mixture (ready-to-use)
- 3.75 ml 4x Tris.HCl/SDS buffer pH 8.8
- 6.25 ml H₂O
- 20 µl TEMED
- 150 µl 10 % APS

The mixture was immediately filled between two sealed glass plates and covered with isopropanol. After polymerisation the isopropanol was decanted and the sucked off with a paper towel.

For 2 small stacking gels the following composition was used:

650 μ l acrylamide/bisacrylamide-mixture (ready-to-use)
1.25 ml 4xTris/SDS pH 6.8
3.10 ml H₂O
10 μ l TEMED
50 μ l 10 % APS

The mixture was immediately filled between the two glass plates till the space was completely filled and the comb was put in.

4 x SDS loading buffer was mixed before use with dithiothreitol (DTT) and mixed with the protein sample in a ratio 1:3. The mixture was denatured at 95 °C for 5 min and kept on ice afterwards. The comb was removed and the gel was placed in the gel chamber filled with 1 x Tris glycine running buffer. The pockets of the stacking gel were cleaned using needle. The samples were applied to the pockets and a 5 μ l of a page ruler were used to later identify the weight of the proteins. The proteins were separated at 100 V for approximately 1 h.

Acrylamide concentration (in %) linear range of separation (kDa):

<u>%</u>	<u>kDa</u>
15.0	12 – 43
10.0	16 – 68
7.0	36 – 94
5.0	57 – 212

b) Semi-dry blot

After gel electrophoresis the gel was released from the glass plates and equilibrated in KP buffer for 10 min. The PVDF membrane was activated in methanol for 15 sec, washed in H₂O for 2 min and incubated in APII buffer for 5 min.

The blot was set up as followed:

Cathode (top)

3 x blotting paper soaked with KP buffer

gel

membrane

1 x blotting paper soaked with APII buffer

2 x blotting paper soaked with API buffer

Anode (bottom)

The gel was blotted at 0.22 A per gel for 30 min. After blotting the membrane was incubated in Ponceau S solution to confirm successful blotting. The membrane was washed with H₂O until the staining solution was vanished.

c) Immunostaining

The membrane was blocked with blocking solution (1 x TBST + 5 % milk powder) for 1 h. Afterwards, the membrane was incubated in the primary antibody solution (blocking solution with primary antibody) overnight at 4 °C while shaking. The next day, the membrane was washed 3 x with TBST for 10 min. Then the membrane was incubated in blocking solution containing the secondary antibody at RT for 1 to 2 h. The membrane was washed 4 x 15 min with TBST while shaking. After washing, the membrane was put on saran foil and incubated in mixed ECL solution 1 and 2. Solution was decanted and the membrane wrapped in foil and placed in a film cassette. In a dark room the film was added and exposed for 1s to 5 min. After exposure the film was developed.

6.2.9.4 Immunohistochemistry

a) Immunohistochemistry on whole mount embryos

Embryos were dissected in PBS+ (PBS containing Mg²⁺ and Ca²⁺) and fixed for 20 min with 2 % PFA in PBS+ at room temperature while shaking. Afterward the embryos were rinsed 2 x with PBS containing Mg²⁺, Ca²⁺ and 0.1 % Tween 20 (PBST+). They were permeabilised 10-20 min according to their developmental stages using 0.1 M Glycine and 0.1 % Triton X - 100 in PBS+.

E6.5-E7.5: 10 - 15 min

E8.5: 20 min

The embryos were rinsed again 2 x in PBST+ and transferred to the blocking solution containing 0.1 % Tween - 20, 10 % heat inactivated fetal calf serum (FCS), 0.1 % BSA and 3 % donkey serum in PBS+. They were incubated for 3 h or more at room temperature while shaking. The blocking solution was replaced by blocking solution containing the primary antibodies (for dilutions see 6.1.7 primary antibody list). Embryos were incubated overnight at 4 °C while gently rocking. The next day the embryos were incubated another 1-2 h at room temperature. Afterwards, they were rinsed 2 x in PBST+ and washed 3 x 10 min with PBST+. The secondary antibodies were diluted 1:800 in blocking solution and the embryos were incubated for minimum 3 h at room temperature. Secondary antibodies were discarded and replaced by DAPI in PBST+ in a dilution 1:500. After 20 min incubation at room temperature, the embryos were rinsed 2 x in PBST+ and washed 3 x 10 min with PBST+. Embryos between E6.0 and E7.5 were dehydrated in 15 % and 30% Glycerol in PBS, each 5 min. A 100 µm spacer with 3 holes was stuck to a coverslip and each embryo was transferred to a single space and oriented. The glycerol was removed with a pipette and replaced by antifade embedding medium. The embryos were covered with a second coverslip to be able to scan the embryos from both sides. Embedded embryos were stored at 4 °C in the dark. The documentation was carried using a Leica Sp5 confocal microscope. After scanning the embryos were removed from the coverslip and used for genotyping.

b) Immunohistochemistry on cryo sections

The frozen sections were dried for 1 h at room temperature. They were washed 3 x 15 min with PBS and permeabilised with 0.1 M glycerol and 0.1 % Triton X - 100 in PBS for 10 min. Afterwards they were washed 30 min in PBS + 0.1 % Tween-20 (PBST) at room temperature. The sections were blocked in PBST+ containing 10 % FCS, 3 % donkey serum and 10 % BSA for at least 1 h. The primary antibodies were diluted (see 6.1.7 primary antibody list) in blocking solution and the section were incubated overnight at 4 °C. The next day the sections were incubated another hour at room temperature before

washing 4 x 15 min with PBST. The secondary antibodies were diluted 1:800 in blocking solution. The sections were incubated for at least 2 h at room temperature. Afterwards they were washed 3 x 15 min in PBST. DAPI was diluted 1:500 in PBS and the sections were incubated 30 min at room temperature. Afterward, they were washed for 15 min in PBS and mounted using antifade embedding medium. Images were taken on the Leica SP5 confocal microscope.

c) Immunohistochemistry on cells

The medium was removed from the 384-well plates by inverting the plate. The wells were washed twice with PBS, fixed with 4 % PFA for 8 min at room temperature, rinsed twice with PBS and permeabilised with 1 % Triton X - 100, 1 % glycine in H₂O for 5 min. Cells were rehydrated for 10 min in PBST and blocked in blocking solution containing 0.1 % Tween-20, 10 % FCS, 0.1 % BSA and 3 % serum in PBS for more than 30 min. Primary antibodies were diluted in blocking solution and incubated overnight at 4 °C. The next day, the plates were rinsed twice with PBST and washed 3 x 10 min with PBST. The secondary antibodies were diluted in blocking/PBS (1:1) and cells were incubated 1 h at room temperature. Afterwards, the cells were incubated in PBST containing DAPI in a ratio 1:500 and incubated for 20 min at RT. The cells were rinsed twice with PBST and washed 3 x 10 min with PBST. After washing, the wells were covered with 50 to 100 µl PBS and stored at 4 °C in the dark.

d) Cell death analysis was done by using the “*In Situ* Cell Death Detection Kit”.

6.2.10 Embryology

6.2.10.1 Mouse husbandry and matings

The mice were kept in a day-night cycle (6.30 am-6.30 pm). For determination of the embryonic stages, bred female mice were checked in the morning for the presence of a vaginal plug. Noon of the day of the plug was considered as embryonic day 0.5 (E0.5).

6.2.10.2 Generation of mutant mice

a) Generation of β -catenin conditional knock-out mice:

The *Sox17^{2AiCre}* allele, the *β -catenin floxed (F)* and *β -catenin floxed deleted (FD)* alleles were previously described (Brault et al., 2001; Engert et al., 2009; Lickert et al., 2002). *Sox17^{2AiCre/+}* mice were mated to β -catenin FD mice to obtain mice heterozygous for both alleles. The mice were bred on a mixed CD1xC57Bl/6 background. To generate mutant embryos the *Sox17^{2AiCre/+}*; β -catenin FD mice were mated to β -catenin F/F mice carrying the *R26R* allele (Soriano, 1999). One quarter of the offspring was mutant for the *β -catenin* allele.

b) Generation of *Elp4* deficient mice

To generate mice with a homozygous deletion for the *Elp4* allele, mice heterozygous for *Pax6^{11Neu}* (here referred to as H9) or *Pax6^{13Neu}* (here referred to as Tcm2) were bred (Favor et al., 2009). The heterozygous mice were bred on C3H/HeJ background for 31 generations.

6.2.10.3 Genotyping of mice and embryos using PCR

Tail tips were digested in lysis buffer containing 0.1 M Tris - HCl pH 8.0 - 8.5, 5 mM EDTA pH 8.0, 0.2 % SDS, 0.2 M NaCl and proteinase K overnight at 55 °C. Digested tails were vortexed and centrifuged for 10 min at 14.000 rpm. Supernatant was transferred to a new tube and 500 μ l of 2-Propanol were added and mixed. After 10 min centrifugation, the supernatant was decanted and the pellet was washed once with 70 % ethanol, dried for 10 min at room temperature, dissolved in 200 μ l MilliQ water and incubated at 37 °C while shaking.

Embryonic material was digested in lysis buffer containing 50 mM KCL, 10 mM Tris - HCl, pH 8.3, 2 mM MgCl₂, 0.45 % NP - 40 and 0.45 % Tween 20. 20 μ l of a proteinase K stock (2 mg/ml) was added to 1 ml lysis buffer. Digestion was performed in 20 μ l of lysis buffer at 55 °C for 8 h. Proteinase K was inactivated for 10 min at 95 °C. Digested embryonic material was directly used for PCR genotyping.

A typical reaction scale for PCR is as followed:

2 μ l 10x Taq buffer with $(\text{NH}_4)_2\text{SO}_4$
2 μ l 25 mM MgCl_2
1 μ l 10 mM dNTPs
1 μ l 10 μ M primer a
1 μ l 10 μ M primer b
1 μ l 10 μ M primer c
0.2 μ l Taq polymerase
10.8 μ l nuclease-free water
1 μ l genomic DNA

a) PCR genotyping of *Sox17^{2AiCre/+}*; β -catenin FD mice was performed as previously described (Brault et al., 2001; Engert et al., 2009; Lickert et al., 2002).

The primer EP 400, EP 401 and EP 564 were used to distinguish the *Sox17^{2AiCre}* and wild-type allele. The wild-type allele shows a band size of 288bp, the *Sox17^{2AiCre}* allele a size of 470bp. EP 482, EP 483 and EP 484 were used to distinguish the *β -catenin FD* (500bp), *β -catenin F* (324bp) and wild-type (221bp) allele.

b) PCR genotyping of *Sox17^{CreERT2}* mice was performed as previously described (Engert et al., 2013a). The primer EP 400, EP 401 and EP 980 were used to distinguish the *Sox17^{CreERT2}* and wild-type allele. The wild-type allele shows a band size of 288bp, the *Sox17^{CreERT2}* allele a size of 470bp. EP 064, EP 401 and EP 980 were used to distinguish *Sox17^{CreERT2 Δ neo}* (470 bp) and *Sox17^{CreERT2neo}* (306 bp) allele.

c) PCR genotyping of Flp-e mice was performed as previously described (Dymecki, 1996). The primer EP 176 and EP 177 were used to detect the Flp-e band with a size of approximately 600 bp.

d) PCR genotyping of R26R mice was performed as previously described (Soriano, 1999). The primer EP 308, EP 309 and EP 310 were used to distinguish wild-type allele (~500 bp) and mutant allele (~250 bp). Genotyping of the R26R mice was previously described

e) PCR genotyping of mt/mG reporter was performed as previously described (Zong et al., 2005). The primer EP 1302, EP 1303 and EP 1304 were used to for genotyping. The wild-type allele has a band size of 330 bp, the mutant allele of 250 bp.

f) Genotyping of H9 and Tcm2 mice:

The primer pair 8C1427L and Elp4 170R was used to detect the H9 deletion (536 bp).

The primer pair 8C14K1L and 8C14K1R was used to detect the wild type allele (356 bp).

The primer pair 431C3 65L and 146D23 34R was used to detect the H9 deletion (625 bp).

The primer pair 431C3 K1L and 431C3 K1R was used to detect the wild-type allele (432bp).

For genotyping H9 and Tcm2 mice, the Kapa Robust PCR Kit was used:

PCR master mix

10 µl Master mix
4 µl nuclease-free water
0.4 µl primer a
0.4 µl primer b
1 µl DNA

PCR programm

94°C 4 min
94°C 1 min
57°C 1 min
72°C 1 min
72°C 7 min

} 30 cycles

g) Genotyping for Sry:

The primer EP 990 and EP 991 were used to genotype for the gender. Male mice show a band at 239 bp.

6.2.10.4 Tamoxifen administration

20 mg tamoxifen were dissolved in 1 ml corn oil and kept at 4 °C. 150 µl tamoxifen was applied either orally using a gavage or by intraperitoneal injection.

6.2.10.5 Isolation of embryos and organs

Dissection of embryos and organs were performed according to Nagy and Behringer („Manipulating the mouse embryo: a laboratory manual“). The stages were determined according to Downs and Davis (Downs and Davies, 1993).

6.2.10.6 X-gal (5 – bromo – 4 – chloro – 3 - indolyl β – D - galactoside) staining

Embryos and organs were dissected in PBS containing Ca^{2+} and Mg^{2+} and fixed in PBS containing 0.02 % NP-40, 5 mM EGTA, 2mM MgCl_2 , 1 % formaldehyde and 0.2 % glutaraldehyde at room temperature for 20-40 min, depending on the embryonic stages. Embryos and organs were washed 3 x 10 min in PBS containing 0.02 % NP-40 and stained in LacZ staining solution (PBS containing 0.02 % NP-40, 2 mM MgCl_2 , 5 mM $\text{K}_3[\text{Fe}(\text{CN})_6]$, 5 mM $\text{K}_4[\text{Fe}(\text{CN})_6] \times 6\text{H}_2\text{O}$, 0,01 % sodium deoxycholate, 1 mg/ml X-gal).

Staining was carried out overnight at room temperature while shaking. After staining, samples were washed 3 x 10 min in PBS containing 0.02 % NP-40 and postfixed in 4 % formaldehyde at 4 °C. Stained embryos and organs were washed in PBS and documented on a Zeiss Lumar.V12. MRc5 camera.

6.2.10.7 Whole mount *in situ* hybridisation (ISH)

Preparation of mouse embryos:

Embryos were dissected in DEPC-treated PBS, transferred to a glass tube and fixed in 4 % PFA for 1 h at 4 °C. Embryos were washed with PBT (DEPC - treated-PBS containing 0.1 % Tween-20) and dehydrated in 25 % methanol/ PBT, 50 % methanol/ PBT, 75 % methanol/ PBT and 100 % methanol, each for 5 min. Embryos were in 100 % methanol and kept at -20 °C.

Day 1: Pretreatment and Hybridisation

Embryos were rehydrated with 75 %, 50 % and 25 % methanol/ PBT each for 5 min and washed once with PBT for 5 min. Embryos were bleached with 3 % H_2O_2 in PBT for 20 min

in the dark. After bleaching, the embryos were washed 3 x 5 min with PBT and post-fixed with 4 % PFA containing 0.2 % glutaraldehyde for 20 min. After washing 3 x 5 min with PBT, 1 ml pre-heated prehybridisation buffer was added and swirled for 5 min. The prehybridisation buffer was changed and the embryos were incubated at 70 °C for at least 2 h with loose cap. After 2 h, 1 µg RNA/ml prehybridisation buffer was denatured at 80 °C for 5 min and the prehybridisation buffer was exchanged with the probe. The embryos were incubated at 70 °C overnight. Solution I and II were put on 70 °C overnight with loose cap.

Day 2: Post hybridisation washes and antibody incubation

The probe carefully removed and transferred back to an Eppendorf tube. The probe can be reused if stored at -20 °C. The embryos were quickly washed with prehybridisation buffer, and than 3 x 30 min with solution I at 70 °C. In the meanwhile, the MAB solution was prepared. After washing with solution I, the embryos were washed 3 x 5 min with TNT and treated with 100 µg/ml RNase in TNT at 37 °C for 1 h. After RNase treatment, the embryos were washed in TNT/solution II (1:1) for 5 min at room temperature, then 3 x 30 min with solution II at 65 °C and afterwards 3 x 5 min with MAB at room temperature. The embryos were blocked in 10 % sheep serum in MAB/2 % blocking reagent for 2 to 3 h at room temperature. The blocking solution was removed and 1 to 2 ml antibody solution were added. The embryos were incubated overnight at 4 °C.

Day 3: Post antibody washes

The next day, the embryos were washed 3 x 10 min with MAB at room temperature. Afterwards, the embryos were washed hourly with MAB all day long. The embryos were incubated in MAB at 4 °C overnight.

Day 4 and 5: Colour development

The embryos were washed 3 x 10 min with NTMT at room temperature. After washing, the embryos were incubated in 1 to 2 ml BM purple at room temperature and developed until a bright, specific signal was detected. If overnight staining was required, the embryos were put at 4 °C overnight and the next day incubation was continued at room

temperature. The staining reaction was stopped by washing the embryos 3 x with PBT. Embryos were documented on a Zeiss Lumar.V12. MRc5 camera.

6.2.10.8 *In situ* hybridization on slides

Preparation of mouse embryos:

Embryos were dissected in DEPC – treated PBS, transferred to a glass tube and fixed in 4 % PFA at 4 °C overnight. Embryos were washed 2 x 5 min in PBS at room temperature. Embryos were dehydrated in 40 %, 70 %, 95 % ethanol in PBS each for 5 to 10 min. Embryos were incubated 3 x 3 min in 100 % ethanol, 3 x 3 min in xylene and in paraffin at 65 °C overnight. Embryos were embedded in paraffin and sectioned.

Day 1: Pretreatment and Hybridisation

The slides were dewaxed in xylene 2 x 10 min at room temperature. Afterwards, the slides were incubated in 100 % ethanol for 5 min and rehydrated through an ethanol series by dipping the slides quickly into 95 %, 80 %, 70 % and 50 % ethanol. The slides were washed once with PBS and postfixed in 4 % PFA for 20 min at room temperature. The slides were washed twice with PBS and embryonic material was digested with 10 µg/ ml proteinase K in 0.1 M Tris pH 7.5 at 37 °C for 10 min. Digestion was stopped with 0.2 % glycine in PBS for 10 min. The slides were washed 2 x 5 min in PBS, once with 0.2 N HCl and 3 x 5 min with PBS. The slides were put in a dish with a stir bar in 0.1 M triethanolamine pH 8.0 under the hood. Acetic anhydride was added at a concentration of 0.25 % to the stirring triethanolamine (20 slides: 600 ml 0.1 M triethanolamine and 1.5 ml acetic anhydride) and stirred for 10 min. The slides were washed once with PBS for 5 min and once with H₂O for 5 min. Slides were incubated in prehybridisation buffer at 70 °C for 2 h (as an alternative, the prehybridisation solution can be directly put on the slides). Afterwards, the prehybridisation solution was removed and 240 ng RNA per 60 µl hybridisation solution were put on the slide. The slides were covered with a hybrid- slip, transferred to a humidified chamber (whatman paper soaked with prehybridisation solution), sealed with sticky tape and incubated at 70 °C overnight.

Day 2: Post hybridisation washes and antibody incubation

The hybrid-slips were removed and the slides were put in a copeland jar and washed 3 x 30 min with pre-warmed solution I at 70 °C. Afterwards, the slides were washed 3 x 5 min in TNT at room temperature and treated with 100 µg/ml RNase in TNT at 37 °C (RNase/TNT solution was added directly on the slide and covered with a hybrid-slip and put in a humidified chamber). Slides were put back in a copeland jar and washed with solution II/TNT (1:1) for 5 min at room temperature. Slides were washed 3 x 30 min with solution II at 65 °C and thereafter 3 x 5 min in MAB at room temperature. 200 µl of 10 % sheep serum/MAB/2% blocking reagent were put directly on the slides and the slides were incubated 2 to 3 h at room temperature. The blocking reagent was removed and replaced by 200 µl antibody solution. Slides were carefully put at 4 °C overnight.

Day 3: Post antibody washes

Slides were put in a Copeland jar and washed 3 x 10 min with MAB at room temperature and then hourly for 3 to 4 h. Slides were washed 3 x 10 min with NTMT and incubated in BM purple at room temperature. BM purple was added on a lid and sections were incubated upside down. Colour reaction was checked regularly. Reaction was stopped by washing the slides twice with PBS and post-fixation in MEMFA for 45 min at room temperature. Slides were washed twice with PBS for 5 min and mounted with Moviol. Sections were documented on a Zeiss Lumar.V12. MRc5 camera.

6.2.11 Histology

6.2.11.1 Paraffin sections

a) Embedding of embryos and organs for paraffin sections

PFA-fixed samples were washed in PBS at 4 °C overnight. The next day the samples were dehydrated.

E7.5-8.5: 70 % ethanol for 15 min to 2 h, 96 % ethanol for 5 min, 100 % ethanol for 5 min and xylene for 5 min.

Organs: 70 % ethanol, 96 % ethanol, 100 % ethanol and xylene each for 30 min

The embryos and organs were transferred to paraffin and incubated at 65 °C overnight. For sectioning, the tissue samples were put in plastic moulds, oriented and covered with fresh paraffin. After solidification, the embedding mould was removed and the paraffin block was fixed to an embedding grid by partially melting the paraffin block.

b) Paraffin sections

The paraffin block was placed in a microtome and oriented. Thickness of sections depended on the developmental stage and size.

E7.5-E8.5: 4 µm thickness

Organs: 8 µm thickness

The sections were transferred to a waterbath at 37 °C for spreading and put on a glass slide. The sections were dried on heating plate at 42 °C were put at 38 °C overnight before counter staining.

c) Counter staining with Nuclear Fast Red (NFR)

The sections were dewaxed for 20 min in xylene. Afterwards, the slides were rehydrated using 100 % ethanol, 96 % ethanol, 80 % ethanol and 70 % ethanol, each for 3 min, washed in tap water for 3min and stained for 45 sec with NFR. The slides were washed again in water and dehydrated using the same alcohol series for 2 min each dilution. Then the slides were incubated for 5 min in xylene and 5 min in rotihistol before embedding in mounting medium. The slides were dried and evaporated at room temperature overnight. The sections were documented using a Zeiss Lumar.V12 stereomicroscope connected to an AxioCam MRc5.

6.2.11.2 Cryo sections of lacZ stained embryonic organs

After lacZ staining, the organs were washed 3 x 10 min with 0.02 % NP-40 in PBS and fixed for 1 h in 4 % PFA at room temperature. Then the organs were washed with PBS and incubated in 15 % saccharose at 4 °C overnight. The next day, the organs were transferred

to 30 % saccharose for 3 h at room temperature and then to 30 % saccharose/OCT (1:1) for another hour at room temperature. The organs were incubated in OCT and transferred to an embedding mould and covered with OCT. The embedded organs were frozen on dry ice and stored at -80 °C. Embedded organs were put at -20 °C 1 h before sectioning.

The block was fixed to the cryostat using OCT and sectioned at a thickness of 10 µm. The sections were melted on cover slips and dried for 30 min at room temperature. Sections were stored at -20 °C.

7 References

- Ang, S.L., Conlon, R.A., Jin, O., Rossant, J., 1994. Positive and negative signals from mesoderm regulate the expression of mouse *Otx2* in ectoderm explants. *Development* 120, 2979-2989.
- Ang, S.L., Wierda, A., Wong, D., Stevens, K.A., Cascio, S., Rossant, J., Zaret, K.S., 1993. The formation and maintenance of the definitive endoderm lineage in the mouse: involvement of HNF3/forkhead proteins. *Development* 119, 1301-1315.
- Arkell, R.M., Tam, P.P., 2012. Initiating head development in mouse embryos: integrating signalling and transcriptional activity. *Open biology* 2, 120030.
- Arnold, S.J., Robertson, E.J., 2009. Making a commitment: cell lineage allocation and axis patterning in the early mouse embryo. *Nat Rev Mol Cell Biol* 10, 91-103.
- Arnold, S.J., Stappert, J., Bauer, A., Kispert, A., Herrmann, B.G., Kemler, R., 2000. Brachyury is a target gene of the Wnt/beta-catenin signaling pathway. *Mech Dev* 91, 249-258.
- Artus, J., Piliszek, A., Hadjantonakis, A.K., 2010. The primitive endoderm lineage of the mouse blastocyst: sequential transcription factor activation and regulation of differentiation by Sox17. *Dev Biol* 350, 393-404.
- Avilion, A.A., Nicolis, S.K., Pevny, L.H., Perez, L., Vivian, N., Lovell-Badge, R., 2003. Multipotent cell lineages in early mouse development depend on SOX2 function. *Genes Dev* 17, 126-140.
- Bachvarova, R.F., Skromne, I., Stern, C.D., 1998. Induction of primitive streak and Hensen's node by the posterior marginal zone in the early chick embryo. *Development* 125, 3521-3534.
- Barnes, J.D., Crosby, J.L., Jones, C.M., Wright, C.V., Hogan, B.L., 1994. Embryonic expression of *Lim-1*, the mouse homolog of *Xenopus Xlim-1*, suggests a role in lateral mesoderm differentiation and neurogenesis. *Dev Biol* 161, 168-178.
- Bauer, F., Hermand, D., 2012. A coordinated codon-dependent regulation of translation by *Elongator*. *Cell Cycle* 11, 4524-4529.
- Bauer, F., Matsuyama, A., Candiracci, J., Dieu, M., Scheliga, J., Wolf, D.A., Yoshida, M., Hermand, D., 2012. Translational control of cell division by *Elongator*. *Cell Rep* 1, 424-433.
- Beddington, R.S., Robertson, E.J., 1998. Anterior patterning in mouse. *Trends Genet* 14, 277-284.

- Beddington, R.S., Robertson, E.J., 1999. Axis development and early asymmetry in mammals. *Cell* 96, 195-209.
- Beger, H.G., Buchler, M., Kozarek, R., Lerch, M., Neoptolemos, J., Warshaw, A., Whitcomb, D., Shiratori, K., 2009. *The Pancreas: An Integrated Textbook of Basic Science, Medicine, and Surgery*. Wiley.
- Ben-Haim, N., Lu, C., Guzman-Ayala, M., Pescatore, L., Mesnard, D., Bischofberger, M., Naef, F., Robertson, E.J., Constam, D.B., 2006. The nodal precursor acting via activin receptors induces mesoderm by maintaining a source of its convertases and BMP4. *Dev Cell* 11, 313-323.
- Bird, A., 2002. DNA methylation patterns and epigenetic memory. *Genes Dev* 16, 6-21.
- Bowles, J., Schepers, G., Koopman, P., 2000. Phylogeny of the SOX family of developmental transcription factors based on sequence and structural indicators. *Dev Biol* 227, 239-255.
- Boyer, L.A., Mathur, D., Jaenisch, R., 2006. Molecular control of pluripotency. *Curr Opin Genet Dev* 16, 455-462.
- Brault, V., Moore, R., Kutsch, S., Ishibashi, M., Rowitch, D.H., McMahon, A.P., Sommer, L., Boussadia, O., Kemler, R., 2001. Inactivation of the beta-catenin gene by Wnt1-Cre-mediated deletion results in dramatic brain malformation and failure of craniofacial development. *Development* 128, 1253-1264.
- Brennan, J., Lu, C.C., Norris, D.P., Rodriguez, T.A., Beddington, R.S., Robertson, E.J., 2001. Nodal signalling in the epiblast patterns the early mouse embryo. *Nature* 411, 965-969.
- Burtscher, I., Barkey, W., Schwarzfischer, M., Theis, F.J., Lickert, H., 2012. The Sox17-mCherry fusion mouse line allows visualization of endoderm and vascular endothelial development. *Genesis* 50, 496-505.
- Burtscher, I., Lickert, H., 2009. Foxa2 regulates polarity and epithelialization in the endoderm germ layer of the mouse embryo. *Development* 136, 1029-1038.
- Carlson, L.L., Page, A.W., Bestor, T.H., 1992. Properties and localization of DNA methyltransferase in preimplantation mouse embryos: implications for genomic imprinting. *Genes Dev* 6, 2536-2541.
- Chambers, I., Colby, D., Robertson, M., Nichols, J., Lee, S., Tweedie, S., Smith, A., 2003. Functional expression cloning of Nanog, a pluripotency sustaining factor in embryonic stem cells. *Cell* 113, 643-655.
- Chazaud, C., Rossant, J., 2006. Disruption of early proximodistal patterning and AVE formation in *Apc* mutants. *Development* 133, 3379-3387.

- Chen, C., Tuck, S., Bystrom, A.S., 2009a. Defects in tRNA modification associated with neurological and developmental dysfunctions in *Caenorhabditis elegans* elongator mutants. *PLoS Genet* 5, e1000561.
- Chen, Y.T., Hims, M.M., Shetty, R.S., Mull, J., Liu, L., Leyne, M., Slaugenhaupt, S.A., 2009b. Loss of mouse *Ikbkap*, a subunit of elongator, leads to transcriptional deficits and embryonic lethality that can be rescued by human *IKBKAP*. *Mol Cell Biol* 29, 736-744.
- Chen, Z.X., Riggs, A.D., 2011. DNA methylation and demethylation in mammals. *J Biol Chem* 286, 18347-18353.
- Choi, E., Kraus, M.R., Lemaire, L.A., Yoshimoto, M., Vemula, S., Potter, L.A., Manduchi, E., Stoeckert, C.J., Jr., Grapin-Botton, A., Magnuson, M.A., 2012. Dual lineage-specific expression of *Sox17* during mouse embryogenesis. *Stem Cells* 30, 2297-2308.
- Clarke, R.L., Yzaguirre, A.D., Yashiro-Ohtani, Y., Bondue, A., Blanpain, C., Pear, W.S., Speck, N.A., Keller, G., 2013. The expression of *Sox17* identifies and regulates haemogenic endothelium. *Nat Cell Biol* 15, 502-510.
- Close, P., Gillard, M., Ladang, A., Jiang, Z., Papuga, J., Hawkes, N., Nguyen, L., Chapelle, J.P., Bouillenne, F., Svejstrup, J., Fillet, M., Chariot, A., 2012. *DERP6* (*ELP5*) and *C3ORF75* (*ELP6*) regulate tumorigenicity and migration of melanoma cells as subunits of *Elongator*. *J Biol Chem* 287, 32535-32545.
- Close, P., Hawkes, N., Cornez, I., Creppe, C., Lambert, C.A., Rogister, B., Siebenlist, U., Merville, M.P., Slaugenhaupt, S.A., Bours, V., Svejstrup, J.Q., Chariot, A., 2006. Transcription impairment and cell migration defects in *elongator*-depleted cells: implication for familial dysautonomia. *Mol Cell* 22, 521-531.
- Corada, M., Orsenigo, F., Morini, M.F., Pitulescu, M.E., Bhat, G., Nyqvist, D., Breviario, F., Conti, V., Briot, A., Iruela-Arispe, M.L., Adams, R.H., Dejana, E., 2013. *Sox17* is indispensable for acquisition and maintenance of arterial identity. *Nature communications* 4, 2609.
- Coultas, L., Chawengsaksophak, K., Rossant, J., 2005. Endothelial cells and VEGF in vascular development. *Nature* 438, 937-945.
- Creppe, C., Malinouskaya, L., Volvert, M.L., Gillard, M., Close, P., Malaise, O., Laguesse, S., Cornez, I., Rahmouni, S., Ormenese, S., Belachew, S., Malgrange, B., Chapelle, J.P., Siebenlist, U., Moonen, G., Chariot, A., Nguyen, L., 2009. *Elongator* controls the migration and differentiation of cortical neurons through acetylation of alpha-tubulin. *Cell* 136, 551-564.
- D'Amour, K.A., Agulnick, A.D., Eliazar, S., Kelly, O.G., Kroon, E., Baetge, E.E., 2005. Efficient differentiation of human embryonic stem cells to definitive endoderm. *Nat Biotechnol* 23, 1534-1541.

Dietrich, P., Yue, J., E, S., Dragatsis, I., 2011. Deletion of exon 20 of the Familial Dysautonomia gene *Ikbkap* in mice causes developmental delay, cardiovascular defects, and early embryonic lethality. *PLoS One* 6, e27015.

Donnelly, M.L., Hughes, L.E., Luke, G., Mendoza, H., ten Dam, E., Gani, D., Ryan, M.D., 2001a. The 'cleavage' activities of foot-and-mouth disease virus 2A site-directed mutants and naturally occurring '2A-like' sequences. *J Gen Virol* 82, 1027-1041.

Donnelly, M.L., Luke, G., Mehrotra, A., Li, X., Hughes, L.E., Gani, D., Ryan, M.D., 2001b. Analysis of the aphthovirus 2A/2B polyprotein 'cleavage' mechanism indicates not a proteolytic reaction, but a novel translational effect: a putative ribosomal 'skip'. *J Gen Virol* 82, 1013-1025.

Downs, K.M., Davies, T., 1993. Staging of gastrulating mouse embryos by morphological landmarks in the dissecting microscope. *Development* 118, 1255-1266.

Dymecki, S.M., 1996. Flp recombinase promotes site-specific DNA recombination in embryonic stem cells and transgenic mice. *Proc Natl Acad Sci U S A* 93, 6191-6196.

Engert, S., 2009. Charakterisierung der Sox17-2A-iCre Mauslinie. Diplomarbeit.

Engert, S., Burtscher, I., Kalali, B., Gerhard, M., Lickert, H., 2013a. The Sox17 knock-in mouse line displays spatiotemporal activation of Cre recombinase in distinct Sox17 lineage progenitors. *Genesis*.

Engert, S., Burtscher, I., Liao, W.P., Dulev, S., Schotta, G., Lickert, H., 2013b. Wnt/beta-catenin signalling regulates Sox17 expression and is essential for organizer and endoderm formation in the mouse. *Development* 140, 3128-3138.

Engert, S., Liao, W.P., Burtscher, I., Lickert, H., 2009. Sox17-2A-iCre: a knock-in mouse line expressing Cre recombinase in endoderm and vascular endothelial cells. *Genesis* 47, 603-610.

Esberg, A., Huang, B., Johansson, M.J., Bystrom, A.S., 2006. Elevated levels of two tRNA species bypass the requirement for elongator complex in transcription and exocytosis. *Mol Cell* 24, 139-148.

Favor, J., Bradley, A., Conte, N., Janik, D., Pretsch, W., Reitmeir, P., Rosemann, M., Schmahl, W., Wienberg, J., Zaus, I., 2009. Analysis of Pax6 contiguous gene deletions in the mouse, *Mus musculus*, identifies regions distinct from Pax6 responsible for extreme small-eye and belly-spotting phenotypes. *Genetics* 182, 1077-1088.

Feil, R., Brocard, J., Mascrez, B., LeMeur, M., Metzger, D., Chambon, P., 1996. Ligand-activated site-specific recombination in mice. *Proc Natl Acad Sci U S A* 93, 10887-10890.

- Feil, R., Wagner, J., Metzger, D., Chambon, P., 1997. Regulation of Cre recombinase activity by mutated estrogen receptor ligand-binding domains. *Biochem Biophys Res Commun* 237, 752-757.
- Fellows, J., Erdjument-Bromage, H., Tempst, P., Svejstrup, J.Q., 2000. The Elp2 subunit of elongator and elongating RNA polymerase II holoenzyme is a WD40 repeat protein. *J Biol Chem* 275, 12896-12899.
- Ferrer-Vaquer, A., Piliszek, A., Tian, G., Aho, R.J., Dufort, D., Hadjantonakis, A.K., 2010. A sensitive and bright single-cell resolution live imaging reporter of Wnt/ss-catenin signaling in the mouse. *BMC Dev Biol* 10, 121.
- Fichtner, L., Jablonowski, D., Schierhorn, A., Kitamoto, H.K., Stark, M.J., Schaffrath, R., 2003. Elongator's toxin-target (TOT) function is nuclear localization sequence dependent and suppressed by post-translational modification. *Mol Microbiol* 49, 1297-1307.
- Fichtner, L., Schaffrath, R., 2002. KTI11 and KTI13, *Saccharomyces cerevisiae* genes controlling sensitivity to G1 arrest induced by *Kluyveromyces lactis* zymocin. *Mol Microbiol* 44, 865-875.
- Frohloff, F., Fichtner, L., Jablonowski, D., Breunig, K.D., Schaffrath, R., 2001. *Saccharomyces cerevisiae* Elongator mutations confer resistance to the *Kluyveromyces lactis* zymocin. *EMBO J* 20, 1993-2003.
- Fuentes, J.J., Genesca, L., Kingsbury, T.J., Cunningham, K.W., Perez-Riba, M., Estivill, X., de la Luna, S., 2000. DSCR1, overexpressed in Down syndrome, is an inhibitor of calcineurin-mediated signaling pathways. *Hum Mol Genet* 9, 1681-1690.
- Gadue, P., Huber, T.L., Paddison, P.J., Keller, G.M., 2006. Wnt and TGF-beta signaling are required for the induction of an in vitro model of primitive streak formation using embryonic stem cells. *Proc Natl Acad Sci U S A* 103, 16806-16811.
- Gehring, M., Huh, J.H., Hsieh, T.F., Penterman, J., Choi, Y., Harada, J.J., Goldberg, R.B., Fischer, R.L., 2006. DEMETER DNA glycosylase establishes MEDEA polycomb gene self-imprinting by allele-specific demethylation. *Cell* 124, 495-506.
- Gilbert, C., Kristjuhan, A., Winkler, G.S., Svejstrup, J.Q., 2004. Elongator interactions with nascent mRNA revealed by RNA immunoprecipitation. *Mol Cell* 14, 457-464.
- Glatt, S., Letoquart, J., Faux, C., Taylor, N.M., Seraphin, B., Muller, C.W., 2012. The Elongator subcomplex Elp456 is a hexameric RecA-like ATPase. *Nat Struct Mol Biol* 19, 314-320.
- Glatt, S., Muller, C.W., 2013. Structural insights into Elongator function. *Curr Opin Struct Biol* 23, 235-242.

- Goldberg, A.D., Allis, C.D., Bernstein, E., 2007. Epigenetics: a landscape takes shape. *Cell* 128, 635-638.
- Goll, M.G., Bestor, T.H., 2005. Eukaryotic cytosine methyltransferases. *Annu Rev Biochem* 74, 481-514.
- Gong, Z., Morales-Ruiz, T., Ariza, R.R., Roldan-Arjona, T., David, L., Zhu, J.K., 2002. ROS1, a repressor of transcriptional gene silencing in Arabidopsis, encodes a DNA glycosylase/lyase. *Cell* 111, 803-814.
- Gorlach, J., Fox, D.S., Cutler, N.S., Cox, G.M., Perfect, J.R., Heitman, J., 2000. Identification and characterization of a highly conserved calcineurin binding protein, CBP1/calciressin, in *Cryptococcus neoformans*. *EMBO J* 19, 3618-3629.
- Grosschedl, R., Giese, K., Pagel, J., 1994. HMG domain proteins: architectural elements in the assembly of nucleoprotein structures. *Trends Genet* 10, 94-100.
- Gu, G., Brown, J.R., Melton, D.A., 2003. Direct lineage tracing reveals the ontogeny of pancreatic cell fates during mouse embryogenesis. *Mech Dev* 120, 35-43.
- Haegel, H., Larue, L., Ohsugi, M., Fedorov, L., Herrenknecht, K., Kemler, R., 1995. Lack of beta-catenin affects mouse development at gastrulation. *Development* 121, 3529-3537.
- Hajkova, P., Erhardt, S., Lane, N., Haaf, T., El-Maarri, O., Reik, W., Walter, J., Surani, M.A., 2002. Epigenetic reprogramming in mouse primordial germ cells. *Mech Dev* 117, 15-23.
- Hajkova, P., Jeffries, S.J., Lee, C., Miller, N., Jackson, S.P., Surani, M.A., 2010. Genome-wide reprogramming in the mouse germ line entails the base excision repair pathway. *Science* 329, 78-82.
- Hanahan, D., 1985. Techniques for transformation of *E.coli*. In *DNA cloning techniques: a practical approach*, D. M. Glover, Ed (IRL Press, Oxford).
- Harland, R., Gerhart, J., 1997. Formation and function of Spemann's organizer. *Annu Rev Cell Dev Biol* 13, 611-667.
- Hawkes, N.A., Otero, G., Winkler, G.S., Marshall, N., Dahmus, M.E., Krappmann, D., Scheidereit, C., Thomas, C.L., Schiavo, G., Erdjument-Bromage, H., Tempst, P., Svejstrup, J.Q., 2002. Purification and characterization of the human elongator complex. *J Biol Chem* 277, 3047-3052.
- Hermesz, E., Mackem, S., Mahon, K.A., 1996. Rpx: a novel anterior-restricted homeobox gene progressively activated in the prechordal plate, anterior neural plate and Rathke's pouch of the mouse embryo. *Development* 122, 41-52.
- Hitz, C., Wurst, W., Kuhn, R., 2007. Conditional brain-specific knockdown of MAPK using Cre/loxP regulated RNA interference. *Nucleic Acids Res* 35, e90.

- Hogan, B.L., Horsburgh, G., Cohen, J., Hetherington, C.M., Fisher, G., Lyon, M.F., 1986. Small eyes (Sey): a homozygous lethal mutation on chromosome 2 which affects the differentiation of both lens and nasal placodes in the mouse. *J Embryol Exp Morphol* 97, 95-110.
- Holmberg, C., Katz, S., Lerdrup, M., Herdegen, T., Jaattela, M., Aronheim, A., Kallunki, T., 2002. A novel specific role for I kappa B kinase complex-associated protein in cytosolic stress signaling. *J Biol Chem* 277, 31918-31928.
- Huang, B., Johansson, M.J., Bystrom, A.S., 2005. An early step in wobble uridine tRNA modification requires the Elongator complex. *RNA* 11, 424-436.
- Huber, T.L., Kouskoff, V., Fehling, H.J., Palis, J., Keller, G., 2004. Haemangioblast commitment is initiated in the primitive streak of the mouse embryo. *Nature* 432, 625-630.
- Huelsken, J., Vogel, R., Brinkmann, V., Erdmann, B., Birchmeier, C., Birchmeier, W., 2000. Requirement for beta-catenin in anterior-posterior axis formation in mice. *J Cell Biol* 148, 567-578.
- Ito, S., D'Alessio, A.C., Taranova, O.V., Hong, K., Sowers, L.C., Zhang, Y., 2010. Role of Tet proteins in 5mC to 5hmC conversion, ES-cell self-renewal and inner cell mass specification. *Nature* 466, 1129-1133.
- Ito, S., Shen, L., Dai, Q., Wu, S.C., Collins, L.B., Swenberg, J.A., He, C., Zhang, Y., 2011. Tet proteins can convert 5-methylcytosine to 5-formylcytosine and 5-carboxylcytosine. *Science* 333, 1300-1303.
- Jaenisch, R., Bird, A., 2003. Epigenetic regulation of gene expression: how the genome integrates intrinsic and environmental signals. *Nat Genet* 33 Suppl, 245-254.
- Johansson, B.M., Wiles, M.V., 1995. Evidence for involvement of activin A and bone morphogenetic protein 4 in mammalian mesoderm and hematopoietic development. *Mol Cell Biol* 15, 141-151.
- Kagey, M.H., Newman, J.J., Bilodeau, S., Zhan, Y., Orlando, D.A., van Berkum, N.L., Ebmeier, C.C., Goossens, J., Rahl, P.B., Levine, S.S., Taatjes, D.J., Dekker, J., Young, R.A., 2010. Mediator and cohesin connect gene expression and chromatin architecture. *Nature* 467, 430-435.
- Kamachi, Y., Uchikawa, M., Kondoh, H., 2000. Pairing SOX off: with partners in the regulation of embryonic development. *Trends Genet* 16, 182-187.
- Kanai-Azuma, M., Kanai, Y., Gad, J.M., Tajima, Y., Taya, C., Kurohmaru, M., Sanai, Y., Yonekawa, H., Yazaki, K., Tam, P.P., Hayashi, Y., 2002. Depletion of definitive gut endoderm in Sox17-null mutant mice. *Development* 129, 2367-2379.

- Kanai, Y., Kanai-Azuma, M., Noce, T., Saido, T.C., Shiroishi, T., Hayashi, Y., Yazaki, K., 1996. Identification of two Sox17 messenger RNA isoforms, with and without the high mobility group box region, and their differential expression in mouse spermatogenesis. *J Cell Biol* 133, 667-681.
- Kim, I., Saunders, T.L., Morrison, S.J., 2007. Sox17 dependence distinguishes the transcriptional regulation of fetal from adult hematopoietic stem cells. *Cell* 130, 470-483.
- Kim, J.H., Lane, W.S., Reinberg, D., 2002. Human Elongator facilitates RNA polymerase II transcription through chromatin. *Proc Natl Acad Sci U S A* 99, 1241-1246.
- Kimura-Yoshida, C., Nakano, H., Okamura, D., Nakao, K., Yonemura, S., Belo, J.A., Aizawa, S., Matsui, Y., Matsuo, I., 2005. Canonical Wnt signaling and its antagonist regulate anterior-posterior axis polarization by guiding cell migration in mouse visceral endoderm. *Dev Cell* 9, 639-650.
- Kinder, S.J., Tsang, T.E., Wakamiya, M., Sasaki, H., Behringer, R.R., Nagy, A., Tam, P.P., 2001. The organizer of the mouse gastrula is composed of a dynamic population of progenitor cells for the axial mesoderm. *Development* 128, 3623-3634.
- Kingsbury, T.J., Cunningham, K.W., 2000. A conserved family of calcineurin regulators. *Genes Dev* 14, 1595-1604.
- Koopman, P., 2005. Sex determination: a tale of two Sox genes. *Trends Genet* 21, 367-370.
- Koopman, P., Gubbay, J., Vivian, N., Goodfellow, P., Lovell-Badge, R., 1991. Male development of chromosomally female mice transgenic for Sry. *Nature* 351, 117-121.
- Kriaucionis, S., Heintz, N., 2009. The nuclear DNA base 5-hydroxymethylcytosine is present in Purkinje neurons and the brain. *Science* 324, 929-930.
- Krogan, N.J., Greenblatt, J.F., 2001. Characterization of a six-subunit holo-elongator complex required for the regulated expression of a group of genes in *Saccharomyces cerevisiae*. *Mol Cell Biol* 21, 8203-8212.
- Kurimoto, K., Yabuta, Y., Ohinata, Y., Ono, Y., Uno, K.D., Yamada, R.G., Ueda, H.R., Saitou, M., 2006. An improved single-cell cDNA amplification method for efficient high-density oligonucleotide microarray analysis. *Nucleic Acids Res* 34, e42.
- Kwon, G.S., Viotti, M., Hadjantonakis, A.K., 2008. The endoderm of the mouse embryo arises by dynamic widespread intercalation of embryonic and extraembryonic lineages. *Dev Cell* 15, 509-520.
- Lange, A.W., Keiser, A.R., Wells, J.M., Zorn, A.M., Whitsett, J.A., 2009. Sox17 promotes cell cycle progression and inhibits TGF-beta/Smad3 signaling to initiate progenitor cell behavior in the respiratory epithelium. *PLoS One* 4, e5711.

- Lee, E.C., Yu, D., Martinez de Velasco, J., Tessarollo, L., Swing, D.A., Court, D.L., Jenkins, N.A., Copeland, N.G., 2001. A highly efficient *Escherichia coli*-based chromosome engineering system adapted for recombinogenic targeting and subcloning of BAC DNA. *Genomics* 73, 56-65.
- Lee, J., Inoue, K., Ono, R., Ogonuki, N., Kohda, T., Kaneko-Ishino, T., Ogura, A., Ishino, F., 2002. Erasing genomic imprinting memory in mouse clone embryos produced from day 11.5 primordial germ cells. *Development* 129, 1807-1817.
- Lei, H., Oh, S.P., Okano, M., Juttermann, R., Goss, K.A., Jaenisch, R., Li, E., 1996. De novo DNA cytosine methyltransferase activities in mouse embryonic stem cells. *Development* 122, 3195-3205.
- Li, E., Bestor, T.H., Jaenisch, R., 1992. Targeted mutation of the DNA methyltransferase gene results in embryonic lethality. *Cell* 69, 915-926.
- Li, Q., Fazly, A.M., Zhou, H., Huang, S., Zhang, Z., Stillman, B., 2009. The elongator complex interacts with PCNA and modulates transcriptional silencing and sensitivity to DNA damage agents. *PLoS Genet* 5, e1000684.
- Li, Y., Takagi, Y., Jiang, Y., Tokunaga, M., Erdjument-Bromage, H., Tempst, P., Kornberg, R.D., 2001. A multiprotein complex that interacts with RNA polymerase II elongator. *J Biol Chem* 276, 29628-29631.
- Liao, W.P., Uetzmann, L., Burtscher, I., Lickert, H., 2009. Generation of a mouse line expressing Sox17-driven Cre recombinase with specific activity in arteries. *Genesis* 47, 476-483.
- Lickert, H., Domon, C., Huls, G., Wehrle, C., Duluc, I., Clevers, H., Meyer, B.I., Freund, J.N., Kemler, R., 2000. Wnt/(beta)-catenin signaling regulates the expression of the homeobox gene *Cdx1* in embryonic intestine. *Development* 127, 3805-3813.
- Lickert, H., Kutsch, S., Kanzler, B., Tamai, Y., Taketo, M.M., Kemler, R., 2002. Formation of multiple hearts in mice following deletion of beta-catenin in the embryonic endoderm. *Dev Cell* 3, 171-181.
- Lin, F.J., Shen, L., Jang, C.W., Falnes, P.O., Zhang, Y., 2013. *Ikbkap/Elp1* deficiency causes male infertility by disrupting meiotic progression. *PLoS Genet* 9, e1003516.
- Lindsley, R.C., Gill, J.G., Kyba, M., Murphy, T.L., Murphy, K.M., 2006. Canonical Wnt signaling is required for development of embryonic stem cell-derived mesoderm. *Development* 133, 3787-3796.
- Liu, P., Jenkins, N.A., Copeland, N.G., 2003. A highly efficient recombineering-based method for generating conditional knockout mutations. *Genome Res* 13, 476-484.

- Liu, P., Wakamiya, M., Shea, M.J., Albrecht, U., Behringer, R.R., Bradley, A., 1999a. Requirement for Wnt3 in vertebrate axis formation. *Nat Genet* 22, 361-365.
- Liu, P., Wakamiya, M., Shea, M.J., Albrecht, U., Behringer, R.R.K.-A., 2002 #317}, Bradley, A., 1999b. Requirement for Wnt3 in vertebrate axis formation. *Nat Genet* 22, 361-365.
- Lu, B., Poirier, C., Gaspar, T., Gratzke, C., Harrison, W., Busija, D., Matzuk, M.M., Andersson, K.E., Overbeek, P.A., Bishop, C.E., 2008. A mutation in the inner mitochondrial membrane peptidase 2-like gene (*Immp2l*) affects mitochondrial function and impairs fertility in mice. *Biol Reprod* 78, 601-610.
- Mao, B., Wu, W., Li, Y., Hoppe, D., Stannek, P., Glinka, A., Niehrs, C., 2001. LDL-receptor-related protein 6 is a receptor for Dickkopf proteins. *Nature* 411, 321-325.
- Martinez-Barbera, J.P., Rodriguez, T.A., Beddington, R.S., 2000. The homeobox gene *Hesx1* is required in the anterior neural ectoderm for normal forebrain formation. *Dev Biol* 223, 422-430.
- Martinez Barbera, J.P., Clements, M., Thomas, P., Rodriguez, T., Meloy, D., Kioussis, D., Beddington, R.S., 2000. The homeobox gene *Hex* is required in definitive endodermal tissues for normal forebrain, liver and thyroid formation. *Development* 127, 2433-2445.
- Matsui, T., Kanai-Azuma, M., Hara, K., Matoba, S., Hiramatsu, R., Kawakami, H., Kurohmaru, M., Koopman, P., Kanai, Y., 2006. Redundant roles of *Sox17* and *Sox18* in postnatal angiogenesis in mice. *J Cell Sci* 119, 3513-3526.
- Mayer, W., Niveleau, A., Walter, J., Fundele, R., Haaf, T., 2000. Demethylation of the zygotic paternal genome. *Nature* 403, 501-502.
- McKnight, K.D., Hou, J., Hoodless, P.A., 2010. *Foxh1* and *Foxa2* are not required for formation of the midgut and hindgut definitive endoderm. *Dev Biol* 337, 471-481.
- McLin, V.A., Rankin, S.A., Zorn, A.M., 2007. Repression of Wnt/beta-catenin signaling in the anterior endoderm is essential for liver and pancreas development. *Development* 134, 2207-2217.
- Mehlgarten, C., Jablonowski, D., Wrackmeyer, U., Tschitschmann, S., Sondermann, D., Jager, G., Gong, Z., Bystrom, A.S., Schaffrath, R., Breunig, K.D., 2010. Elongator function in tRNA wobble uridine modification is conserved between yeast and plants. *Mol Microbiol* 76, 1082-1094.
- Meissner, A., Mikkelsen, T.S., Gu, H., Wernig, M., Hanna, J., Sivachenko, A., Zhang, X., Bernstein, B.E., Nusbaum, C., Jaffe, D.B., Gnirke, A., Jaenisch, R., Lander, E.S., 2008. Genome-scale DNA methylation maps of pluripotent and differentiated cells. *Nature* 454, 766-770.

- Mitsui, K., Tokuzawa, Y., Itoh, H., Segawa, K., Murakami, M., Takahashi, K., Maruyama, M., Maeda, M., Yamanaka, S., 2003. The homeoprotein Nanog is required for maintenance of pluripotency in mouse epiblast and ES cells. *Cell* 113, 631-642.
- Monaghan, A.P., Kaestner, K.H., Grau, E., Schutz, G., 1993. Postimplantation expression patterns indicate a role for the mouse forkhead/HNF-3 alpha, beta and gamma genes in determination of the definitive endoderm, chordamesoderm and neuroectoderm. *Development* 119, 567-578.
- Morgan, H.D., Dean, W., Coker, H.A., Reik, W., Petersen-Mahrt, S.K., 2004. Activation-induced cytidine deaminase deaminates 5-methylcytosine in DNA and is expressed in pluripotent tissues: implications for epigenetic reprogramming. *J Biol Chem* 279, 52353-52360.
- Morris, S.A., Teo, R.T., Li, H., Robson, P., Glover, D.M., Zernicka-Goetz, M., 2010. Origin and formation of the first two distinct cell types of the inner cell mass in the mouse embryo. *Proc Natl Acad Sci U S A* 107, 6364-6369.
- Mukhopadhyay, M., Shtrom, S., Rodriguez-Esteban, C., Chen, L., Tsukui, T., Gomer, L., Dorward, D.W., Glinka, A., Grinberg, A., Huang, S.P., Niehrs, C., Izpisua Belmonte, J.C., Westphal, H., 2001. Dickkopf1 is required for embryonic head induction and limb morphogenesis in the mouse. *Dev Cell* 1, 423-434.
- Muzumdar, M.D., Tasic, B., Miyamichi, K., Li, L., Luo, L., 2007. A global double-fluorescent Cre reporter mouse. *Genesis* 45, 593-605.
- Nagase, T., Nagase, M., Yoshimura, K., Fujita, T., Koshima, I., 2005. Angiogenesis within the developing mouse neural tube is dependent on sonic hedgehog signaling: possible roles of motor neurons. *Genes Cells* 10, 595-604.
- Nagy, A., Rossant, J., Nagy, R., Abramow-Newerly, W., Roder, J.C., 1993. Derivation of completely cell culture-derived mice from early-passage embryonic stem cells. *Proc Natl Acad Sci U S A* 90, 8424-8428.
- Nelissen, H., Fleury, D., Bruno, L., Robles, P., De Veylder, L., Traas, J., Micol, J.L., Van Montagu, M., Inze, D., Van Lijsebettens, M., 2005. The elongata mutants identify a functional Elongator complex in plants with a role in cell proliferation during organ growth. *Proc Natl Acad Sci U S A* 102, 7754-7759.
- Niakan, K.K., Ji, H., Maehr, R., Vokes, S.A., Rodolfa, K.T., Sherwood, R.I., Yamaki, M., Dimos, J.T., Chen, A.E., Melton, D.A., McMahon, A.P., Eggan, K., 2010. Sox17 promotes differentiation in mouse embryonic stem cells by directly regulating extraembryonic gene expression and indirectly antagonizing self-renewal. *Genes Dev* 24, 312-326.

- Nichols, J., Zevnik, B., Anastassiadis, K., Niwa, H., Klewe-Nebenius, D., Chambers, I., Scholer, H., Smith, A., 1998. Formation of pluripotent stem cells in the mammalian embryo depends on the POU transcription factor Oct4. *Cell* 95, 379-391.
- Nieuwkoop, P.D., 1969. The formation of the mesoderm in urodelean amphibians. *Development Genes and Evolution* 162, 341-373.
- Niwa, H., 2007. How is pluripotency determined and maintained? *Development* 134, 635-646.
- Niwa, H., Yamamura, K., Miyazaki, J., 1991. Efficient selection for high-expression transfectants with a novel eukaryotic vector. *Gene* 108, 193-199.
- Nowotschin, S., Hadjantonakis, A.K., 2010. Cellular dynamics in the early mouse embryo: from axis formation to gastrulation. *Curr Opin Genet Dev* 20, 420-427.
- Okada, Y., Yamagata, K., Hong, K., Wakayama, T., Zhang, Y., 2010. A role for the elongator complex in zygotic paternal genome demethylation. *Nature* 463, 554-558.
- Okano, M., Bell, D.W., Haber, D.A., Li, E., 1999. DNA methyltransferases Dnmt3a and Dnmt3b are essential for de novo methylation and mammalian development. *Cell* 99, 247-257.
- Okano, M., Xie, S., Li, E., 1998. Cloning and characterization of a family of novel mammalian DNA (cytosine-5) methyltransferases. *Nat Genet* 19, 219-220.
- Otero, G., Fellows, J., Li, Y., de Bizemont, T., Dirac, A.M., Gustafsson, C.M., Erdjument-Bromage, H., Tempst, P., Svejstrup, J.Q., 1999. Elongator, a multisubunit component of a novel RNA polymerase II holoenzyme for transcriptional elongation. *Mol Cell* 3, 109-118.
- Paraskevopoulou, C., Fairhurst, S.A., Lowe, D.J., Brick, P., Onesti, S., 2006. The Elongator subunit Elp3 contains a Fe4S4 cluster and binds S-adenosylmethionine. *Mol Microbiol* 59, 795-806.
- Park, K.S., Wells, J.M., Zorn, A.M., Wert, S.E., Whitsett, J.A., 2006. Sox17 influences the differentiation of respiratory epithelial cells. *Dev Biol* 294, 192-202.
- Perea-Gomez, A., Rhinn, M., Ang, S.L., 2001. Role of the anterior visceral endoderm in restricting posterior signals in the mouse embryo. *Int J Dev Biol* 45, 311-320.
- Pevny, L.H., Lovell-Badge, R., 1997. Sox genes find their feet. *Curr Opin Genet Dev* 7, 338-344.
- Phillips, T., Shaw, K., 2008. Chromatin Remodeling in Eukaryotes, *Nature Education*.

- Piccolo, S., Agius, E., Leyns, L., Bhattacharyya, S., Grunz, H., Bouwmeester, T., De Robertis, E.M., 1999. The head inducer Cerberus is a multifunctional antagonist of Nodal, BMP and Wnt signals. *Nature* 397, 707-710.
- Pinson, K.I., Brennan, J., Monkley, S., Avery, B.J., Skarnes, W.C., 2000. An LDL-receptor-related protein mediates Wnt signalling in mice. *Nature* 407, 535-538.
- Plusa, B., Piliszek, A., Frankenberg, S., Artus, J., Hadjantonakis, A.K., 2008. Distinct sequential cell behaviours direct primitive endoderm formation in the mouse blastocyst. *Development* 135, 3081-3091.
- Popp, C., Dean, W., Feng, S., Cokus, S.J., Andrews, S., Pellegrini, M., Jacobsen, S.E., Reik, W., 2010. Genome-wide erasure of DNA methylation in mouse primordial germ cells is affected by AID deficiency. *Nature* 463, 1101-1105.
- Pradhan, S., Bacolla, A., Wells, R.D., Roberts, R.J., 1999. Recombinant human DNA (cytosine-5) methyltransferase. I. Expression, purification, and comparison of de novo and maintenance methylation. *J Biol Chem* 274, 33002-33010.
- Pugh, D.M., Sumano, H.S., 1982. The anti-implantation action of tamoxifen in mice. *Archives of toxicology. Supplement. = Archiv fur Toxikologie. Supplement* 5, 209-213.
- Rahl, P.B., Chen, C.Z., Collins, R.N., 2005. Elp1p, the yeast homolog of the FD disease syndrome protein, negatively regulates exocytosis independently of transcriptional elongation. *Mol Cell* 17, 841-853.
- Reik, W., 2007. Stability and flexibility of epigenetic gene regulation in mammalian development. *Nature* 447, 425-432.
- Reik, W., Walter, J., 2001. Evolution of imprinting mechanisms: the battle of the sexes begins in the zygote. *Nat Genet* 27, 255-256.
- Rivera-Perez, J.A., Magnuson, T., 2005. Primitive streak formation in mice is preceded by localized activation of Brachyury and Wnt3. *Dev Biol* 288, 363-371.
- Roberts, R.C., 1967. *Small eyes*-a new dominant eye mutant in the mouse. *Genetics Research* 9, 121-122.
- Rougier, N., Bourc'his, D., Gomes, D.M., Niveleau, A., Plachot, M., Paldi, A., Viegas-Pequignot, E., 1998. Chromosome methylation patterns during mammalian preimplantation development. *Genes Dev* 12, 2108-2113.
- Ruhf, M.L., Braun, A., Papoulas, O., Tamkun, J.W., Randsholt, N., Meister, M., 2001. The domino gene of *Drosophila* encodes novel members of the SWI2/SNF2 family of DNA-dependent ATPases, which contribute to the silencing of homeotic genes. *Development* 128, 1429-1441.

- Sakamoto, Y., Hara, K., Kanai-Azuma, M., Matsui, T., Miura, Y., Tsunekawa, N., Kurohmaru, M., Saijoh, Y., Koopman, P., Kanai, Y., 2007. Redundant roles of Sox17 and Sox18 in early cardiovascular development of mouse embryos. *Biochem Biophys Res Commun* 360, 539-544.
- Sasaki, H., Hogan, B.L., 1993. Differential expression of multiple fork head related genes during gastrulation and axial pattern formation in the mouse embryo. *Development* 118, 47-59.
- Sawada, A., Nishizaki, Y., Sato, H., Yada, Y., Nakayama, R., Yamamoto, S., Nishioka, N., Kondoh, H., Sasaki, H., 2005. Tead proteins activate the Foxa2 enhancer in the node in cooperation with a second factor. *Development* 132, 4719-4729.
- Schulz, R., Proudhon, C., Bestor, T.H., Woodfine, K., Lin, C.S., Lin, S.P., Prissette, M., Oakey, R.J., Bourc'his, D., 2010. The parental non-equivalence of imprinting control regions during mammalian development and evolution. *PLoS Genet* 6, e1001214.
- Shaner, N.C., Campbell, R.E., Steinbach, P.A., Giepmans, B.N., Palmer, A.E., Tsien, R.Y., 2004. Improved monomeric red, orange and yellow fluorescent proteins derived from *Discosoma* sp. red fluorescent protein. *Nat Biotechnol* 22, 1567-1572.
- Shawlot, W., Behringer, R.R., 1995. Requirement for Lim1 in head-organizer function. *Nature* 374, 425-430.
- Shih, H.P., Wang, A., Sander, M., 2013. Pancreas organogenesis: from lineage determination to morphogenesis. *Annu Rev Cell Dev Biol* 29, 81-105.
- Simeone, A., Acampora, D., Gulisano, M., Stornaiuolo, A., Boncinelli, E., 1992. Nested expression domains of four homeobox genes in developing rostral brain. *Nature* 358, 687-690.
- Simeone, A., Acampora, D., Mallamaci, A., Stornaiuolo, A., D'Apice, M.R., Nigro, V., Boncinelli, E., 1993. A vertebrate gene related to orthodenticle contains a homeodomain of the bicoid class and demarcates anterior neuroectoderm in the gastrulating mouse embryo. *EMBO J* 12, 2735-2747.
- Singh, N., Lorbeck, M.T., Zervos, A., Zimmerman, J., Elefant, F., 2010. The histone acetyltransferase Elp3 plays an active role in the control of synaptic bouton expansion and sleep in *Drosophila*. *J Neurochem* 115, 493-504.
- Soriano, P., 1999. Generalized lacZ expression with the ROSA26 Cre reporter strain. *Nat Genet* 21, 70-71.
- Spence, J.R., Lange, A.W., Lin, S.C., Kaestner, K.H., Lowy, A.M., Kim, I., Whitsett, J.A., Wells, J.M., 2009. Sox17 regulates organ lineage segregation of ventral foregut progenitor cells. *Dev Cell* 17, 62-74.

- Stirnimann, C.U., Petsalaki, E., Russell, R.B., Muller, C.W., 2010. WD40 proteins propel cellular networks. *Trends Biochem Sci* 35, 565-574.
- Stolt, C.C., Schlierf, A., Lommes, P., Hillgartner, S., Werner, T., Kosian, T., Sock, E., Kessar, N., Richardson, W.D., Lefebvre, V., Wegner, M., 2006. SoxD proteins influence multiple stages of oligodendrocyte development and modulate SoxE protein function. *Dev Cell* 11, 697-709.
- Tada, S., Era, T., Furusawa, C., Sakurai, H., Nishikawa, S., Kinoshita, M., Nakao, K., Chiba, T., Nishikawa, S., 2005. Characterization of mesendoderm: a diverging point of the definitive endoderm and mesoderm in embryonic stem cell differentiation culture. *Development* 132, 4363-4374.
- Tahiliani, M., Koh, K.P., Shen, Y., Pastor, W.A., Bandukwala, H., Brudno, Y., Agarwal, S., Iyer, L.M., Liu, D.R., Aravind, L., Rao, A., 2009. Conversion of 5-methylcytosine to 5-hydroxymethylcytosine in mammalian DNA by MLL partner TET1. *Science* 324, 930-935.
- Takaoka, K., Yamamoto, M., Hamada, H., 2011. Origin and role of distal visceral endoderm, a group of cells that determines anterior-posterior polarity of the mouse embryo. *Nat Cell Biol* 13, 743-752.
- Tam, P.P., Beddington, R.S., 1992. Establishment and organization of germ layers in the gastrulating mouse embryo. *Ciba Found Symp* 165, 27-41; discussion 42-29.
- Tam, P.P., Behringer, R.R., 1997. Mouse gastrulation: the formation of a mammalian body plan. *Mech Dev* 68, 3-25.
- Tam, P.P., Khoo, P.L., Lewis, S.L., Bildsoe, H., Wong, N., Tsang, T.E., Gad, J.M., Robb, L., 2007. Sequential allocation and global pattern of movement of the definitive endoderm in the mouse embryo during gastrulation. *Development* 134, 251-260.
- Tam, P.P., Rossant, J., 2003. Mouse embryonic chimeras: tools for studying mammalian development. *Development* 130, 6155-6163.
- Tamai, K., Semenov, M., Kato, Y., Spokony, R., Liu, C., Katsuyama, Y., Hess, F., Saint-Jeannet, J.P., He, X., 2000. LDL-receptor-related proteins in Wnt signal transduction. *Nature* 407, 530-535.
- Thomas, P., Beddington, R., 1996. Anterior primitive endoderm may be responsible for patterning the anterior neural plate in the mouse embryo. *Curr Biol* 6, 1487-1496.
- Tortelote, G.G., Hernandez-Hernandez, J.M., Quaresma, A.J., Nickerson, J.A., Imbalzano, A.N., Rivera-Perez, J.A., 2013. Wnt3 function in the epiblast is required for the maintenance but not the initiation of gastrulation in mice. *Dev Biol* 374, 164-173.

- Tsumura, A., Hayakawa, T., Kumaki, Y., Takebayashi, S., Sakaue, M., Matsuoka, C., Shimotohno, K., Ishikawa, F., Li, E., Ueda, H.R., Nakayama, J., Okano, M., 2006. Maintenance of self-renewal ability of mouse embryonic stem cells in the absence of DNA methyltransferases Dnmt1, Dnmt3a and Dnmt3b. *Genes Cells* 11, 805-814.
- Varshavsky, A., 1997. The N-end rule pathway of protein degradation. *Genes Cells* 2, 13-28.
- Vega, R.B., Rothermel, B.A., Weinheimer, C.J., Kovacs, A., Naseem, R.H., Bassel-Duby, R., Williams, R.S., Olson, E.N., 2003. Dual roles of modulatory calcineurin-interacting protein 1 in cardiac hypertrophy. *Proc Natl Acad Sci U S A* 100, 669-674.
- Viotti, M., Niu, L., Shi, S.H., Hadjantonakis, A.K., 2012. Role of the gut endoderm in relaying left-right patterning in mice. *PLoS Biol* 10, e1001276.
- Walker, J., Kwon, S.Y., Badenhorst, P., East, P., McNeill, H., Svejstrup, J.Q., 2011. Role of elongator subunit Elp3 in *Drosophila melanogaster* larval development and immunity. *Genetics* 187, 1067-1075.
- Wang, S.C., Frey, P.A., 2007. S-adenosylmethionine as an oxidant: the radical SAM superfamily. *Trends Biochem Sci* 32, 101-110.
- Warming, S., Costantino, N., Court, D.L., Jenkins, N.A., Copeland, N.G., 2005. Simple and highly efficient BAC recombineering using galK selection. *Nucleic Acids Res* 33, e36.
- Winkler, G.S., Petrakis, T.G., Ethelberg, S., Tokunaga, M., Erdjument-Bromage, H., Tempst, P., Svejstrup, J.Q., 2001. RNA polymerase II elongator holoenzyme is composed of two discrete subcomplexes. *J Biol Chem* 276, 32743-32749.
- Wittschieben, B.O., Otero, G., de Bizemont, T., Fellows, J., Erdjument-Bromage, H., Ohba, R., Li, Y., Allis, C.D., Tempst, P., Svejstrup, J.Q., 1999. A novel histone acetyltransferase is an integral subunit of elongating RNA polymerase II holoenzyme. *Mol Cell* 4, 123-128.
- Wodarz, A., Nusse, R., 1998. Mechanisms of Wnt signaling in development. *Annu Rev Cell Dev Biol* 14, 59-88.
- Yamaguchi, T.P., Takada, S., Yoshikawa, Y., Wu, N., McMahon, A.P., 1999. T (Brachyury) is a direct target of Wnt3a during paraxial mesoderm specification. *Genes Dev* 13, 3185-3190.
- Yamamoto, M., Saijoh, Y., Perea-Gomez, A., Shawlot, W., Behringer, R.R., Ang, S.L., Hamada, H., Meno, C., 2004. Nodal antagonists regulate formation of the anteroposterior axis of the mouse embryo. *Nature* 428, 387-392.
- Yasunaga, M., Tada, S., Torikai-Nishikawa, S., Nakano, Y., Okada, M., Jakt, L.M., Nishikawa, S., Chiba, T., Era, T., Nishikawa, S., 2005. Induction and monitoring of definitive and visceral endoderm differentiation of mouse ES cells. *Nat Biotechnol* 23, 1542-1550.

Ying, Q.L., Wray, J., Nichols, J., Battle-Morera, L., Doble, B., Woodgett, J., Cohen, P., Smith, A., 2008. The ground state of embryonic stem cell self-renewal. *Nature* 453, 519-523.

Zhou, Q., Law, A.C., Rajagopal, J., Anderson, W.J., Gray, P.A., Melton, D.A., 2007. A multipotent progenitor domain guides pancreatic organogenesis. *Dev Cell* 13, 103-114.

Zong, H., Espinosa, J.S., Su, H.H., Muzumdar, M.D., Luo, L., 2005. Mosaic analysis with double markers in mice. *Cell* 121, 479-492.

Zorn, A.M., Wells, J.M., 2009. Vertebrate endoderm development and organ formation. *Annu Rev Cell Dev Biol* 25, 221-251.

Zvetkova, I., Apedaile, A., Ramsahoye, B., Mermoud, J.E., Crompton, L.A., John, R., Feil, R., Brockdorff, N., 2005. Global hypomethylation of the genome in XX embryonic stem cells. *Nat Genet* 37, 1274-1279.

8 List of abbreviations

- A: ADE: anterior definitive endoderm
AID: activin-induced deaminase
AME: anterior mesendoderm
AO: aorta
AP: anterior-posterior
APC: adenomatous polyposis coli
Apobec-1: apolipoprotein B RNA-editing catalytic component-1
AVE: anterior visceral endoderm
- B: BER: base excision repair
bp: base pair
BV: bloodvessels
- C: caC: carboxycytisine
Cer1: Cerberus-like protein 1
Chrd: Chordin
ChIP: chromatin immunoprecipitation
CKO: conditional knock-out
Cre: Causes recombination/ Cyclization recombinase
Ctrl: control
Cv: cardinal vein
- D: D0: Day 0
D4: Day 4
DA: dorsal aorta
DE: definitive endoderm
Dkk1: Dickkopf homologue 1
DME: Demeter
Dnmt1: DNA methyltransferase 1

- DP: dorsal pancreas
- DVE: distal visceral endoderm
- E: E: embryonic day
- Ect: ectoderm
- EGO: early gastrula organizer
- Elp3: Elongator protein 3
- Elp4: Elongator protein 4
- emb: embryonic
- embVE: embryonic visceral endoderm
- EMT: epithelial-to-mesenchymal transition
- Epi: epiblast
- ES: embryonic stem
- ER: estrogen receptor
- ex: extra-embryonic
- ExE: extra-embryonic ectoderm
- exVE: extra-embryonic visceral endoderm
- F: F: floxed
- fC: formylcytosine
- FD: flox deleted
- FDR: false discovery rate
- Fe-S: iron-sulphur
- FG: foregut
- Flp: flippase
- FRT: flippase recognition target
- G: Gadd45: Growth arrest and DNA-damage-inducible protein 45
- GO: Gene Ontology
- Gsk3 β : glycogen synthase kinase 3 beta

- Gsc: Goosecoid
- GR: gut region
- H: HAT: histonacetytransferase
- HG: hindgut
- hmC:-hydroxymethycytosine
- HMG: high mobility group
- HSP: heatshock protein
- HT: heart
- I: ICM: inner cell mass
- ICR: imprinted control region
- IHC: Immunohistochemistry
- Imp1L: inner mitochondrial membrane peptidase-like
- IMP: inner membrane peptidase
- ISH: In situ hybridization
- J: JAK: Janus kinase
- K: kb: kilo base
- kD: kilo Dalton
- KO: knock-out
- L: LEF: Lymphoid enhancer factor
- Lefty1: left-right determination factor 1
- LB: limb bud
- LGO: late gastrula organizer
- LIF: leukemia inhibitory factor
- loxP: locus of X-over P1
- M: MBD4: methylated DNA binding protein
- mC: methylcytosine
- MEK: mitogen-activated protein kinase enzyme MEK1

- Mes: mesoderm
- MG: midgut
- MGO: mid gastrula organizer
- N: NER: nucleotide excision repair
- neo: neomycin
- NeoR: neomycin resistant cassette
- Nog: Noggin
- NT: neural tube
- P: pA: polyadenylation signal
- Pax6: paired box gene 6
- PGCs: primordial germ cells
- PGK: phosphor-glycerate-kinase
- PH3: phospho histone H3
- PP2A: protein phosphatase 2A
- PrE: primitive endoderm
- PS: primitive streak region
- PT: pulmonary trunk
- PVE: posterior visceral endoderm
- R: Rcn1: reticulocalbin 1
- RFP: red fluorescent protein
- Ros1: Repressor of Silencing
- R26R: Rosa26 reporter
- S: SAM: S-adenosylmethionine
- SO: somites
- ST: stomach
- STAT: signal transducer and activator of transcription
- StIP1: Stat3-interacting protein

- T: T: Brachyury
TM: tamoxifen/4-hydroxytamoxifen
TBE: Tcf/Lef-binding elements
TCF: T-cell factor
TDG: Thymine DNA glycosylase
TE: trophectoderm
TET: ten eleven translocation
TH: thymus
TR: trachea
- U: UTR: untranslated region
- V: V: vascular system
VE: visceral endoderm
VP: ventral pancreas
- W: WISH: whole mount in situ hybridization
WT: wild-type
Wt1: Wilms tumor 1 homolog
- Y: YFP: yellow fluorescent protein

9 Appendix

9.1 Curriculum Vitae

Name: Silvia Engert
Geburtsdatum: 15.05.1983
Geburtsort: Reutlingen
Nationalität: Deutsch

Promotion

2009 – 2013: Promotion am WZW der technischen Universität München
Doktorvater: Prof. Dr. Martin Hrabě de Angelis
Experimentelle Genetik, Helmholtz Zentrum München

Studium

2008 - 2009: Diplomarbeit "*Charakterisierung der Sox17-2A-iCre Mauslinie*",
Betreuerin: Prof. Dr. Magdalena Götz
Insitut für Stammzellforschung, Helmholtz Zentrum München,
2003 – 2009: Diplomstudiengang Biologie, Julius-Maximilians-Universität
Würzburg

Praktika

2002 – 2003: Praktikum am Naturwissenschaftliches und Medizinisches Institut,
Tübingen und in der Pathologie des Kreiskrankenhauses
Reutlingen

Ausbildung

1993 – 2002: Friedrich-List-Gymnasium Reutlingen
1990 – 1993: Jos-Weiß-Schule, Grundschule Reutlingen

9.2 List of publications and conference contributions

9.2.1 Publications

Ingo Burtscher, [Silvia Engert](#), Stefan Hasenöder, Daniela Padula, Heiko Lickert

Steuerungsmechanismen der Entodermentwicklung in der Maus (Biospektrum; 5/2011; non-peer reviewed)

[Engert S](#), Burtscher I, Liao WP, Dulev S, Schotta G, Lickert H

Wnt/ β -catenin signalling regulates Sox17 expression and is essential for organizer and endoderm formation in the mouse. Development. 2013 Aug;140(15):3128-38

[Engert S](#), Burtscher I, Kalali B, Gerhard M, Lickert H

The Sox17CreERT2 knock-in mouse line displays spatiotemporal activation of Cre recombinase in distinct Sox17 lineage progenitors. Genesis. 2013 Aug 26

9.2.2 Conference contributions

Munich, Germany, 2009, 2010, 2011: **Interact- The Munich Life Science Symposium for PhD Students**

Gesellschaft für Entwicklungsbiologie, Dresden, Germany, 2011: **Joint Meeting of the German and Japanese Societies of Developmental Biologists**

EMBO Workshop, Leuven, Belgium, 2011: **Lineage Commitments: Emphasis on Extraembryonic-Embryonic Interfaces**

(Poster prize)

Hong Kong Society for Developmental Biology Symposium, Hong Kong, China, 2012: **From Embryology to Disease Mechanisms**

(Talk)

9.3 Danksagung

Zuerst möchte ich mich bei meinem Doktorvater Prof. Dr. Martin Hrabě de Angelis bedanken, der es mir ermöglichte meine Doktorarbeit am WZW anzufertigen.

Herzlich danken möchte ich Prof. Dr. Heiko Lickert, für die Möglichkeit meine Leidenschaft für die Embryologie in vollen Zügen während meiner Diplom- und Doktorarbeit ausleben zu dürfen. Ich hoffe, dass du dieses Feld nie ganz verlassen wirst. Denn mal ehrlich, was gibt es denn spannenderes als die Frage nach der Entstehung des Lebens? Ich danke dir für die zahlreichen Diskussionen und Anregungen und für deinen ausgleichenden Optimismus.

Herrn Prof. Dr. Langosch danke ich herzlich für die Übernahme des Vorsitzes der Prüfungskommission.

Dr. Ingo Burtscher möchte ich für die Einführung in sämtliche Mikroskopieverfahren und Techniken danken. Danke, dass du immer ein offenes Ohr für meine Fragen hast und meist auch deren Antwort.

Perry Liao möchte ich für die Betreuung, die über die Diplomarbeit hinausging, bedanken und für seinen herrlichen nüchternen Humor.

Ich danke allen TAs für ihre hervorragende Arbeit und Unterstützung während der letzten Jahre, ebenso wie den Tierpflegern für die Versorgung zahlreicher Mauslinien.

Natürlich möchte ich mich herzlich bei all meinen ehemaligen und jetzigen Kollegen für ihre Hilfe und Ratschläge und für eine angenehme Atmosphäre innerhalb und außerhalb des Labs bedanken. Ganz besonders danke ich Alexander Korostylev für die Unterstützung beim Elp-Projekt.

Meinen Kooperationspartnern, vor allem Gunnar Schotta, Martin Irmeler und Jack Favor, danke ich für die erfolgreiche Zusammenarbeit und Bereitstellung von Ressourcen und Materialien.

Lena Uetzmann danke ich für die liebevolle Aufnahme in die AG Lickert und der daraus resultierenden Freundschaft.

Mein allergrößter Dank geht natürlich an meine Familie, die immer für mich da ist, auf mich achtgibt, mich unterstützt und hinter mir steht.

Ich danke meinen Freunden, dass sie trotz der Distanz immer bei mir sind.

Ich danke dir, Stephan, für deine Liebe, dein Verständnis, dein Vertrauen und deine Unterstützung - ich danke dir dass es dich für mich gibt.